82-249-10314.

CONDUCTIVITY SURVEY
ON THE
NITHI MOUNTAIN MOLYBDENUM PROPERTY
FRASER LAKE, BRITISH COLUMBIA

MOM GROUP
(MOLLY 1-14, 17, 18 Mineral Claims)
OMINECA MINING DIVISION

N.T.S. MAP SHEETS 93 F/15, 93 K/2
Latitude 53°57'24" to 54°00'07"
Longitude 124°47'48" to 124°53'07"

for
ROCKWELL MINING CORPORATION
Vancouver, British Columbia

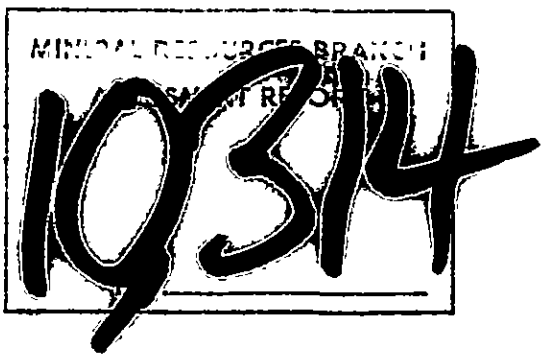

by
T. B. Millinoff, B.Sc.
TAIGA CONSULTANTS LTD.
Calgary, Alberta

APRIL 1982

TABLE OF CONTENTS

LIST OF TABLES

Table

LIST OF FIGURES

LIST OF APPENDICES

Appendix

INTRODUCTION (Location, Property Description)

The Nithi Mountain molybdenum property is located about 8 km (5 mi.) south of the village of Fraser Lake, which is 158 km (98 mi.) west of the city of Prince George in central British Columbia (Figure 1). The property lies almost entirely within N.T.S. 93 F/15 with the northern margin extending into the southern part of N.T.S. 93 K/2. The top of Nithi Mountain is located at approximately 124°50' West longitude and 53°58' North latitude, near the central part of the property, at an elevation of 1,352 metres (4,435 feet) ASL, Figure 1a.

The Nithi Mountain property consists of 17 old-style two-post claims and about 110 claim units staked under the modified grid system, within the Omineca Mining Division. As is shown in Figure 2, these claims cover and surround Nithi Mountain and its flanks. This contiguous block of claims is held under option by Rockwell Mining Corporation from three different owners. The Molly 1-14, 17 and 18 are optioned from Andrew Robertson (Fraser Lake Mines); the MJM 1-5 claims from Nithex Explorations Ltd.; and the Strep and Strep 79 claims from P. Ogryzlo and Don Young. In addition, the DB 1-4 claims were staked in the summer of 1980 for Rockwell Mining Corporation. The total area under option is 2,850 hectares (7,042 acres). These claims have been grouped for purposes of assessment into the MOM group (consisting of the MOLLY 1-14, 17, 18, MJM 3-5 claims), and the SMID group (consisting of the DB 1-4, MJM 1-2, STREP, STREP 79 claims). A summary of relevant claim data is presented in Table 1.1 and the claims are shown in Figure 1b.

Assessibility

The Nithi Mountain property is accessible from Fraser Lake by four-wheel-drive vehicles via the Chowsunkit logging road and secondary roads. The main electrical power line for the Endako Mine is only four miles north of the property. The village of Fraser Lake is located along the Yellowhead Highway (B.C. Highway 16) and the main Canadian National rail line through central British Columbia to Prince Rupert. A small airfield is located about 1 km south of Fraser Lake, which is capable of accommodating light aircraft. Thus, there exists an excellent transportation and mining infrastructure within a relatively short distance from the property which would allow rapid development of any mineral deposits found in the vicinity.

TABLE 1.1

SUMMARY OF CLAIM DATA

	Claim Name	Claim Units	Record Number	Record Date	Expiry Date *
MOM Group	MOLLY 1	2-post claims	15166	June 27/62	June 27/83
	MOLLY 2		14167	"	"
	MOLLY 3		15168	"	"
	MOLLY 4		14169	"	"
	MOLLY 5		15170	"	"
	MOLLY 6		15171	"	"
	MOLLY 7		15172	"	"
	MOLLY 8		15173	"	"
	MOLLY 9		15174	"	"
	MOLLY 10		15175	"	"
	MOLLY 11		15176	"	"
	MOLLY 12		15177	"	"
	MOLLY 13		15178	"	"
	MOLLY 14		15179	"	"
	MOLLY 17		15182	June 29/62	June 27/82
	MOLLY 18		15183	"	"
	MJM 3	20	837	Oct. 17/77	Oct. 17/89
	MJM 4	20	838	"	Oct. 17/87
	MJM 5	10	839	"	"
SMID Group	DB 1	14	3132	Aug. 27/80	Aug. 27/93
	DB 2	2	3133	"	"
	DB 3	7	3134	"	"
	DB 4	3	3556	Feb. 4/81	Feb. 4/93
	MJM 1	20	835	Oct. 17/77	Oct. 17/93
	MJM 2	20	836	"	"
	STREP	9	801	Sep. 26/77	Sep. 27/93
	STREP 79	2-post claim	2394	Dec. 14/77	Dec. 14/93

* as at August 1981

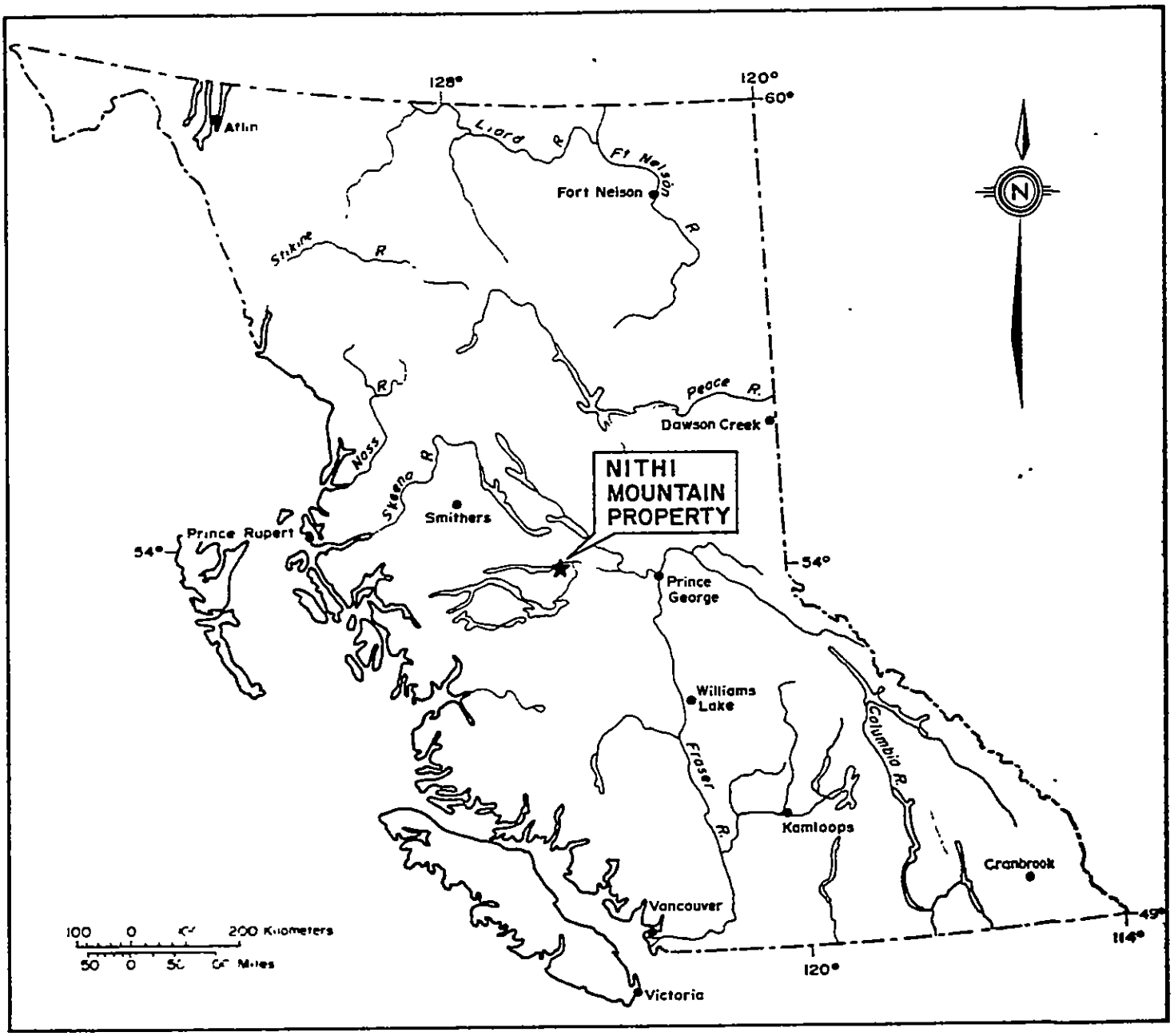

FIGURE 1a

REGIONAL LOCATION MAP

NITHI MOUNTAIN MOLYBDENUM PROPERTY

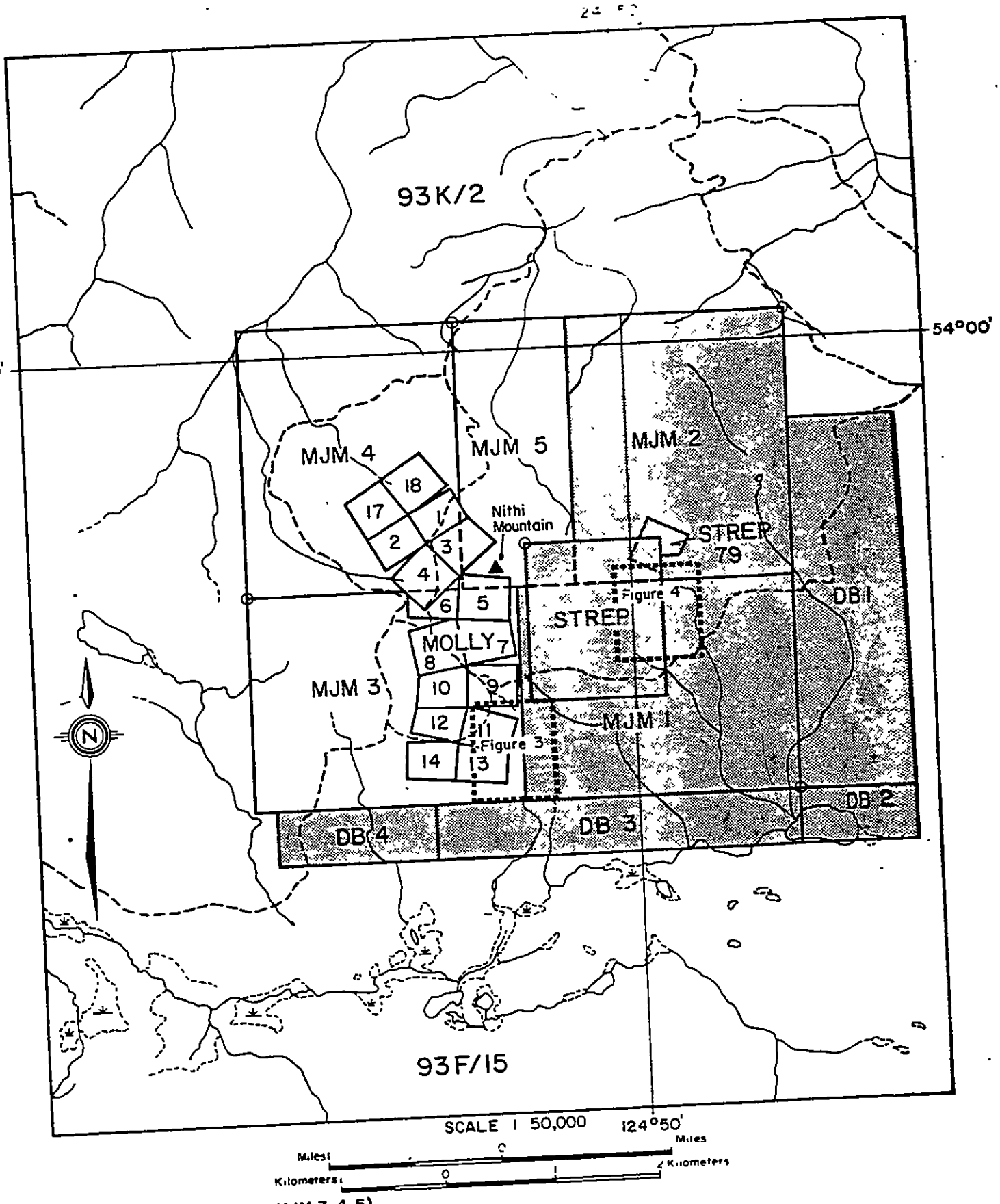

FIGURE 1b

PROPERTY LOCATION MAP

PROPERTY HISTORY

The original claims staked on Nithi Mountain were staked during the period 1952-1955 for uranium. Mineralization in the form of the secondary uranium minerals was found in a fractured rhyolite prophyry dyke within Topley granite. The showing was located at an elevation of 1,070m (3,500 feet) on the northwestern slope of Nithi Mountain. The dyke had a length of 185m (600 feet) and a width of about 30m (100 feet), and trended north-south.

Work on these original claims included trenching and drilling. Four drill holes were completed in 1956 by American Standard Mines who optioned the original claims. In all, a total of 100m (333 feet) of drilling was completed. This uranium mineralization was found to have no depth extension and the claims were subsequently dropped.

With the discovery of the Endako Mine in 1962, there was renewed exploration in the area for molybdenite. This exploration resulted in the staking of Nithi Mountain by various junior mining companies including R & P Metals Ltd. (Fraser Lake Mines), Fort Reliance Minerals, Dundee Mines, Jodee Explorations, and New Indian Mines. Trenching, soil sampling, and diamond drilling were completed during this period. Although molybdenum mineralization was discovered, both in surface workings and in subsequent diamond drilling, little effort was directed towards a systematic evaluation of these properties. Interest gradually declined in the late 1960's and most claims were allowed to lapse.

In 1970, Nithex Exploration restaked the area and carried out an exploration program of trenching and diamond drilling. Nithex drilled a total of four diamond drill holes, one of which encountered significant molybdenite mineralization.

In 1975, Amex Potash Limited optioned the claims held by Nithex and Fraser Lake Mines on Nithi Mountain and subsequently acquired additional claims in the same area in order to complement their land position. Exploration carried out in 1975 by Amex included geologic mapping, soil sampling, magnetic surveying, and induced polarization surveying. In the summer of 1976, a percussion drilling program was completed by Amex on their Nithi Mountain properties. Twelve holes totalling 975m (3,200 feet) were drilled on the property. Subsequently, Amex dropped their option on the property.

In 1980, Rockwell Mining Corporation optioned the various mineral properties on Nithi Mountain and contracted Taiga Consultants Ltd. to carry out an exploration program on these properties. This exploration program consisted of soil and rock geochemical sampling, geological mapping, and prospecting, carried out during the summer of 1980. Based on the encouraging results obtained from this program, a further program was initiated in the fall of 1980 consisting of road building, drill-site preparation, trenching, and rock geochemical sampling. In early 1981, additional road building was undertaken to open up a second access road and to complete a sump hole on the Chris Showing.

From April 24 to June 1, 1981, a diamond drilling program was completed on the property. Work carried out on the claims consisted of diamond drilling of 1,818 m (5,963') of NQ core at ten locations on the property, as shown on Map 1 in the back pocket of this report. Four of these drill holes were on the Chris Showing and the remaining six drill holes were on the Terri Showing.

All drill core was geologically logged, split and assayed for molybdenum, with the results reported as MoS_2. These results were presented in a series of drill logs that accompanied a drilling report by Taiga Consultants Ltd. in July 1981. A series of cross-sections accompany the drilling report and these illustrate the grade and structural attitude of the molybdenite mineralization that was encountered.

PURPOSE OF THE STUDY AND SUMMARY OF WORK DONE

Exploration methods used in the search for a molybdenite orebody at Nithi Mountain, British Columbia were, to this date, conventional prospecting and mapping, geochemical soil surveys and an induced polarization survey. This study proposes that the conductivity of soils may reduce the target area and serve as an ore guide in a manner equivalent to or superior to the use of soil geochemistry as an exploration technique.

Results based on 1,867 soil samples from the entire study area proved that the correlation between manganese, iron, zinc, and conductivity with molybdenum was very weak due to the large sample size and the mixture of the barren earth material population with the mineralized population. Correlation coefficients increased significantly when two profiles of smaller areas were examined. One profile crossed known molybdenum mineralization at the surface and the other crossed an area with no mineralization at surface but the soils contained anomalous concentrations of molybdenum. In the first case, conductivity proved to have the strongest correlation with molybdenum mineralization. In

the second profile, neither manganese, iron, zinc, or conductivity were found to correlate with molybdenum. Also, conductivity values across the unmineralized profile were lower than the mineralized profile. It is believed that conductivity is detecting alteration that is characteristic of quartz-molybdenite veins in the study area. Conductivity appears to be a useful technique to reduce the target area and compared to other elements in the geochemical survey, has the best correlation with molybdenum concentrations in the soil, over known mineral occurrences.

A 1:5,000 scale conductivity contour map is supplied in the back pocket of this report. Values above 1263 $\mu mhos^{-1}$ are considered anomalous (Map 2).

TOPOGRAPHY AND GLACIATION

The Endako-Fraser Lake area lies within a glacially dissected part of the Nechako Plateau. Major east trending valleys separate broken upland ridges (Carr, 1965). According to Tipper (1971), piedmont glaciers from the Coast Mountains of British Columbia advanced across the Nechako Plateau in a northeast direction during Pleistocene time. Ice also moved into the area from the Omineca and Skeena Mountains from the northwest. The ice masses coalesced over the Nechako Plateau then moved east and northeast until meeting the Rocky Mountain barrier. Glacial striations that trend east have been observed at the summit of Nithi Mountain (Davis, 1980). The retreat of the ice, in this area was along the Fraser river (Tipper, 1971). According to Carr (1965), Francois Lake was dammed by stagnant ice at the southern foot of Nithi Mountain, in late glacial time. Francois Lake emptied into Fraser Lake through a rock-cut canyon, in its present spillway, the Stellako River. Carr (1965) sites as evidence for this, the existence of, residual patches of glacial lake silts and gravels that rest on bedrock at low elevations along

the shore of Francois Lake. Moreover, Carr (1965) also states that, although the topography has been strongly influenced by the east trending Pleistocene ice movement, the bedrock structure, joint and fault systems have a more pronounced effect on the topography.

REGIONAL GEOLOGY

The following description for the regional geology of the Endako-Fraser Lake area, which includes Nithi Mountain, is based on Davis (1980), Carr (1965), and Bright (1967). The stratigraphy was originally described by Tipper (1959), then modified by Davis (1980).

The geology of the area is dominated by a batholith composed of numerous individual plutons belonging to the Topley Intrusives, (Bright, 1967).

The Topley Intrusives are Mesozoic in age and range in composition from diorite to alaskite, but 75% of the batholith is quartz monzonite and granodiorite. The Topley Intrusives cover an area, approximately 259 km^2, centred around Endako, as shown in Fig. 1d. They form part of a composite body that lies in a northwest trending belt of granitic plutons, extending from Babine Lake to Quesnel, a distance of 290 km (Bright, 1967). The Topley Intrusives range in age from Middle Jurassic to Lower Cretaceous (Tipper, 1963). Symons (1973) has obtained an age of 139 $\pm$ 4 m.y. for the Topley Intrusives, based on a paleomagnetic study of 114 samples.

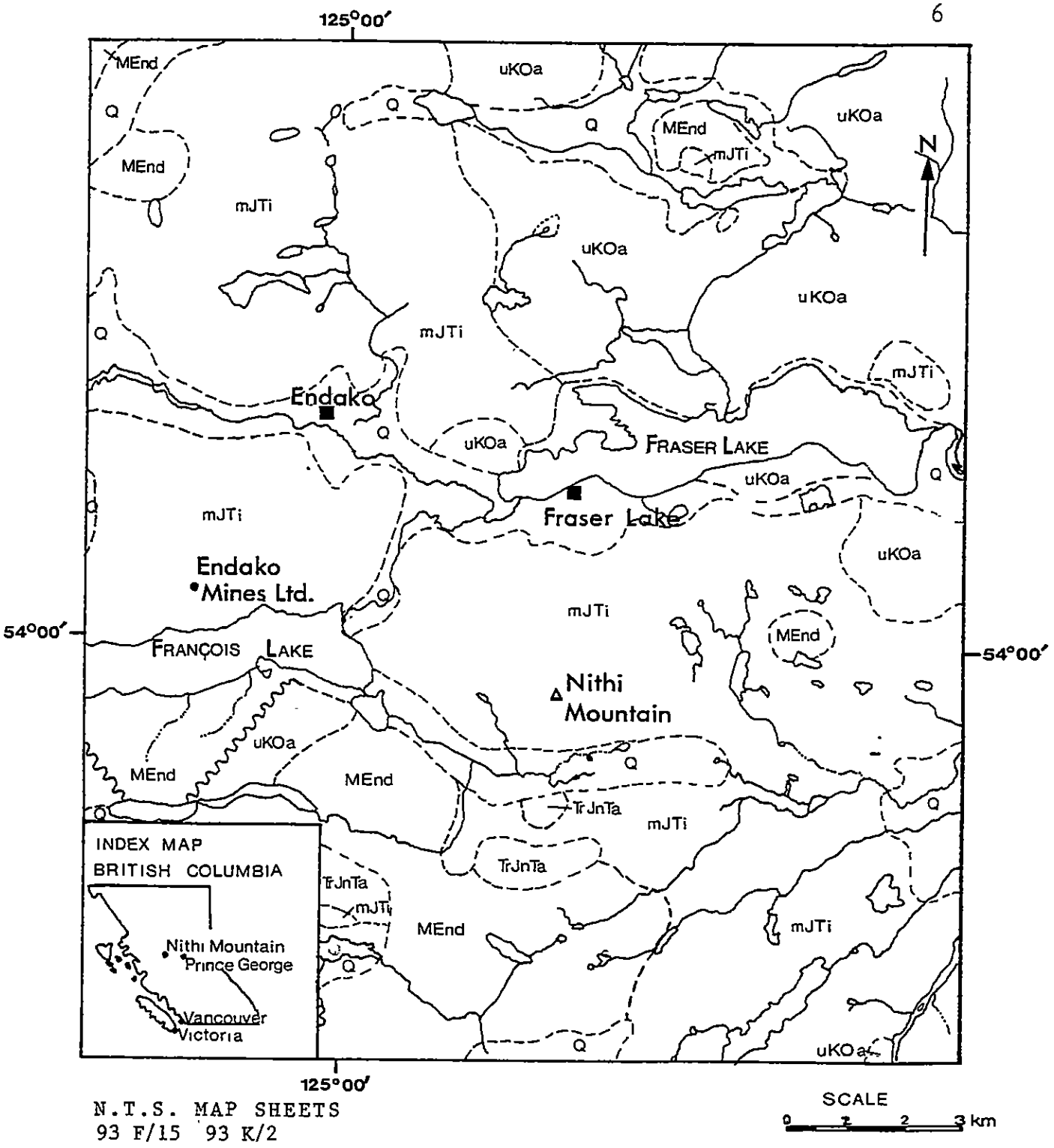

Figure 1c

REGIONAL GEOLOGY NITHI MOUNTAIN

BRITISH COLUMBIA

Q	Quaternary	mJTi	Topley Intrusions
MEnd	Endako Group	TrJnTa	Takla Group
uKOa	Ootsa Lake Group		Fault

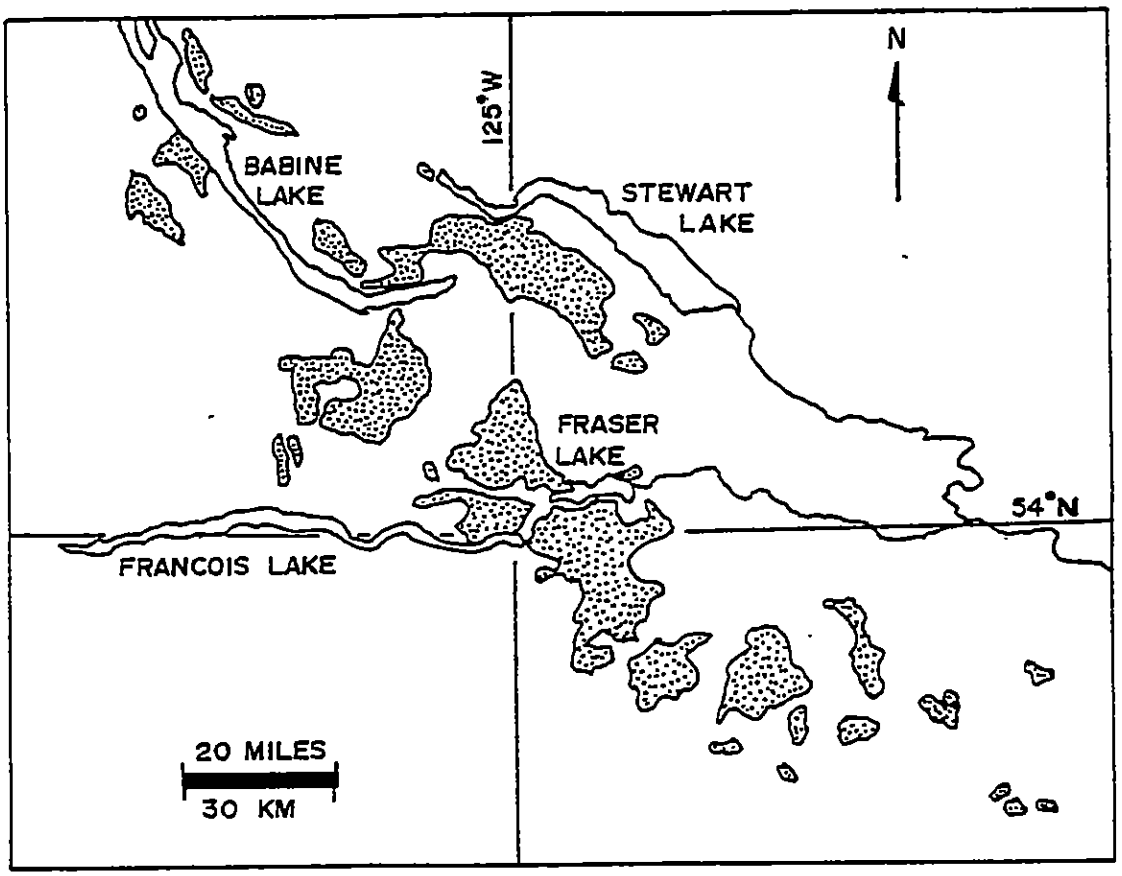

Figure 1d. The Topley Batholith, Nechako Plateau, central British Columbia. After Symons (1972).

Tipper (1959) has subdivided the Topley Intrusives into 9 lithological units, as shown in Table 1. According to Carr (1965), there are more than 12 individual plutons of Topley Intrusives in the area. Five of these plutons occur within the study area as shown in Figure 2. The most significant of these plutons are the Simon Bay diorite Complex, the Nithi quartz monzonite, and Casey alaskite as these contain Molybdenum mineralization. The mineralization is localized in fractures and veins, containing molybdenum and quartz and as disseminations.

According to Davis (1980), the Nithi quartz monzonite is equivalent in age and composition to the Endako quartz monzonite, which is the host rock for the Endako Molybdenum deposit. However, there is some conflict as to the age relation of the Endako and Nithi plutons. Carr (1965) states that the Nithi quartz monzonite superficially resembles the Endako quartz monzonite in composition and grain size but unlike the Endako quartz monzonite, these rocks contain oscillatory zoned plagioclase. Bright (1967) states that the Nithi quartz monzonite is younger than the Endako quartz monzonite since he believes that the Nithi

TABLE 1.2

REGIONAL STRATIGRAPHIC SUCCESSION

Era	Period or Epoch	Formation	Lithology
Cenozoic	Recent		Stream and lake deposits, talus, soil
	Pleistocene		Glacial and glacio-fluvial deposits
	Erosion interval		
	Oligocene and Miocene	Endako Group	Basalt, andesite; related tuff and breccia; minor shale and greywacke
Angular unconformity			
Mesozoic and Cenozoic	Upper Cretaceous and Paleocene	Ootsa Lake Group	Rhyolitic and dacitic tuff and breccia; shale, sandstone, conglomerate
			Rhyolite, dacite, trachyte, andesite; minor basalt; related tuff and breccia
			Basalt, andesite; minor rhyolite, sandstone, and conglomerate
Erosion interval			
Mesozoic	Lower and Middle Jurassic	Hazelton Group	Greywacke, argillite, conglomerate tuff, breccia, andesite, and arkose; minor rhyolite
			Andesite, related tuffs and breccias, chert-pebble conglomerate, shale, and sandstone
	Unconformity; erosional interval		
	Middle Jurassic to Lower Cretaceous	Topley Intrusions:	Granite, granodiorite, diorite, and quartz diorite
		Fraser quartz monzonite	Pink biotite-hornblende quartz monzonite. Small circular stock.
		Stellako intrusions	Pink biotite quartz monzonite, pink-grey hornblende-biotite granodiorite. Discordant, north-northeast trend
		Francois granite	Red porphyritic biotite granite. Miarolytic, chilled margins. No molybdenum deposits.
		Casey alaskite	Leucogranite and quartz monzonite. Discordant stocks and satellitic dykes. Molybdenum deposits at Owl Lake, Tatin Lake, Nithi Mountain, and Endako.
		Glenannan complex	Zoned pluton north of Endako. Pink porphyritic granite, quartz monzonite, granodiorite. No molybdenum deposits.
		Nithi quartz monzonite	Pink-grey subporphyritic biotite-hornblende quartz monzonite. Resembles Endako quartz monzonite and may be equivalent. Molybdenum deposit at Nithi Mountain
		Quartz feldspar porphyry, porphyritic granite, aplite	Brown-pink porphyry dykes up to 45 metres wide, abundant at mine. Porphyritic pink potash feldspar granite dykes up to 15 metres wide. Pink sugary aplite up to 1.2 metres wide
		Endako quartz monzonite	Pink subporphyritic biotite-hornblende quartz monzonite. Host rock at Endako mine
		Simon Bay diorite complex	Coarse-grained, foliated hornblende diorite, quartz diorite, granodiorite, gabbro. Mesozonal, concordant pluton. Oldest Topley unit. No molybdenum deposits
	Intrusive contact with lower part of Takla Group		
	Upper Triassic and Lower Jurassic	Takla Group	Red and brown shale, conglomerate, and greywacke
			Andesitic and basaltic flows, tuffs, and breccias; interbedded argillite and minor limestone
Intrusive contact between Topley Intrusions and Cache Creek Group			
Paleozoic	Pennsylvanian and Permian	Cache Creek Group	Limestone, chert, argillite

(After Tipper, 1959. Modified by Davis, 1980).

quartz monzonite is part of the Glennanan Complex which intrudes the Simon Bay Complex and the Endako quartz monzonite.

According to Tipper (1959), the oldest rocks in the area consist of Permian and Pennsylvanian limestone, chert, and argillite of the Cache Creek Group. These are intruded by the Topley Intrusives. Next in the stratigraphic succession are Upper Triassic and Lower Jurassic volcanics, shale, conglomerate, and greywacke of the Takla Group which are also intruded by the Topley Intrusives.

The Topley batholith is unconformably overlain by Lower to Middle Jurassic volcanics, chert-pebble conglomerate, shale, sandstone, greywacke, argillite, and arkose of the Hazelton Group. The Hazelton Group is unconformably overlain by Upper Cretaceous and Paleocene volcanics, shale, and sandstone of the Ootsa Lake Group. The Ootsa Lake Group is unconformably overlain by Oligocene and Miocene volcanics, shale, and greywacke of the Endako Group. The Pleistocene glacial deposits are glacio-fluvial deposits. Recent deposits are fluvial and lacustine sediments (Tipper, 1959).

Locally, in the Endako area, the Topley Intrusives are unconformably overlain by flat-lying Tertiary volcanic flows of the Endako Group (Carr, 1965).

According to Carr (1965), there is a major northeast trending fault system south of Francois Lake that separates the Takla and Hazelton Groups from younger Ootsa Lake Group rocks to the east. All three groups contain small intrusions consisting of dacite to granite which are Cenozoic in age and are in the form of dykes, sill-like bodies, and agglomeratic necks (Carr, 1965). Carr (1965) also states that these intrusions are highly fractured and faulted and are often mineralized with specular hematite and pyrite as sparse disseminations or in fractures.

GEOLOGY OF NITHI MOUNTAIN

Five members of the Topley Intrusives are present within the study area at Nithi Mountain, Fig. 2. Three contain molybdenite: the Simon Bay Complex, Nithi quartz monzonite, and Casey alaskite. There are also many granitic dykes that are phases of the Topley Intrusives and there are also mafic dykes of the younger Endako Group.

The following description of the geology of the study area is based on Davis (1980), Carr (1966) and Bright (1967). A brief description of the rock units is given by Tipper (1959), Table 1.

Bright (1967) has chronologically divided the intrusive bodies for the Topley batholith into 5 units, as follows:

oldest	(1)		Simon Bay (diorite) Complex
	(2)	(i)	Endako Quartz Monzonite
		(ii)	Francois Granite
	(3)		Glennanan Complex
	(4)		Casey Quartz Monzonite
youngest	(5)		Stellako Quartz Monzonite

Bright (1967) describes the Nithi quartz monzonite as part of the Glennanan Complex and suggests that it was emplaced while in a highly fluid state into the epizonal environment. Bright (1967) also suggests that the intrusion of the Glennanan Complex, (which includes the Nithi quartz

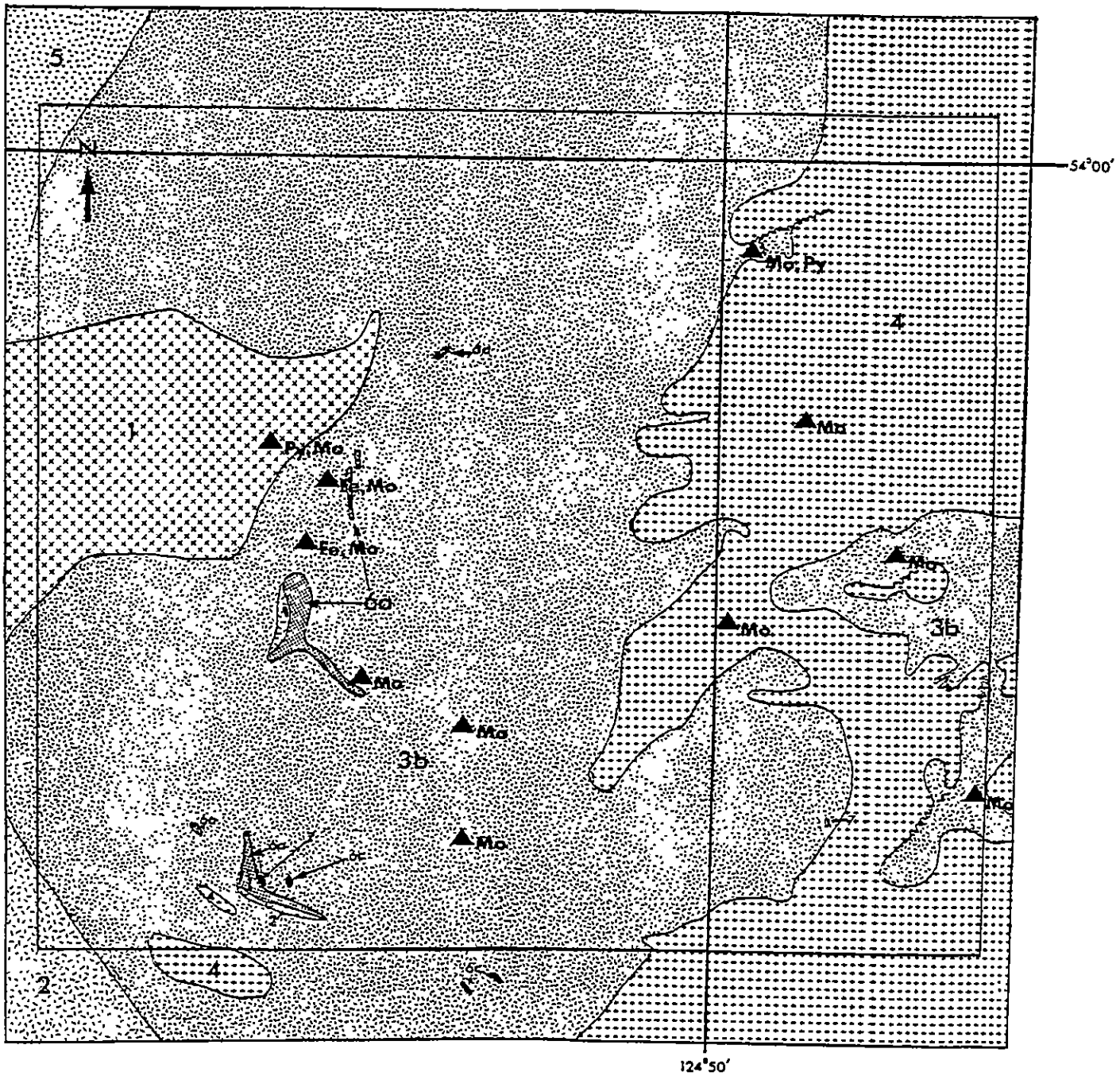

FIGURE 2 NITHI MOUNTAIN, BRITISH COLUMBIA GEOLOGIC COMPILATION MAP

LEGEND

TOPLEY INTRUSIVES

1 Simon Bay diorite

2 Caledonia quartz monzonite

3A Nithi quartz monzonite, m.gr.

3B Nithi quartz monzonite, c.gr.

4 Casey Alaskite

5 Stellako quartz monzonite

6 – FELSIC DYKES

6A Quartz porphyry

6B Quartz feldspar porphyry

6C Aplite

ENDAKO GROUP

7 Mafic dykes

Showing, mineralization

SCALE

0 500 1000

METERS

monzonite) subjected the earlier intrusives, especially the Endako quartz monzonite, to intense fracturing and local block faulting.

Moreover, Bright (1967) states that Topley stages 2 to 5 represent a continuous period of epizonal intrusion following the emplacement of the more deep seated Simon Bay Complex. Apparently, northwest and northeast trending fracture zones controlled the structural evolution of the Topley complex in the study area (Bright, 1967).

Simon Bay (diorite) Complex

According to Bright (1967), the Simon Bay Complex is the southeast extension of a discontinuous belt of foliated diorite and amphibolite, trending northwest along the periphery of the Topley intrusions. Bright (1967) states that the foliation of the Simon Bay Complex conforms to the regional northwest trend of the Topley batholith.

Carr (1965) describes these rocks as greenish, fine to medium grained, equigranular quartz diorites, consisting of moderate amounts of quartz and orthoclase or microcline and abundant plagioclase, biotite, and hornblende. According to Bright (1967), the diorite is sheared and altered and

contains minor lenses of amphibolite, gneiss, and gabbro which accentuate the foliation of the Simon Bay Complex. Where the diorite is unsheared, the character of the foliation suggests a primary origin produced during the emplacement of the magma (Bright, 1967).

Endako Quartz Monzonite

This intrusive does not occur on Nithi Mountain but it may be equivalent to the Nithi quartz monzonite (Davis, 1980). It outcrops in a belt containing the Endako Molybdenum deposit and extends from the Stellako River west northwest for approximately 14.5 km. It is bounded by a younger intrusive to the south, the Casey quartz monzonite, which occurs at Nithi Mountain.

This rock type consists of pink-grey, medium-grained, porphyritic quartz monzonite. Red phenocrysts of perthitic orthoclase account for 1/3 of the composition, and these phenocrysts range from .5 cm to 1 cm in length (Carr, 1965). There are also paler coloured phenocrysts of plagioclase and quartz. The remainder of the rock consists of 1 to 2 mm crystals of the same composition with biotite and some hornblende accounting for 5% of the rock (Carr, 1965).

Nithi Quartz Monzonite

The Nithi quartz monzonite forms the summit and the north and south flanks of Nithi Mountain. It is bounded on the east flank of the mountain by the younger Casey alaskite and it intrudes the older Simon Bay diorite on the western flank of the mountain. To the northwest, it is intruded by the younger Stellako quartz monzonite and to the southwest, it is intruded by another younger intrusion, the Caledonia quartz monzonite.

The Nithi quartz monzonite consists of 2 phases: (1) a medium-grained, pink-grey rock with abundant biotite and a granular texture which is subporphyritic, and (2) a lighter coloured pink rock, strongly porphyritic, coarse-grained with phenocrysts of perthitic orthoclase and aggregated quartz, but also of plagioclase that together account for 1/3 of the rock.

According to Carr (1965), the subporphyritic variety consists of 35% quartz, 21% orthoclase, 35% plagioclase, 7% biotite, and 1% hornblende.

The porphyritic variety consists of 40% quartz, 30% orthoclase, 23% plagioclase, 7% biotite, hornblende and accessory minerals.

Carr (1965), unlike Bright (1967), does not classify the Nithi quartz monzonite as part of the Glennanan quartz monzonite, but specifies that the only difference between these two intrusives is that the Nithi quartz monzonite contains phenocrysts and medium sized crystals of orthoclase and plagioclase that reach lengths of 2 cm and 5 cm respectively. The quartz phenocrysts contain feldspar inclusions.

Caledonia Quartz Monzonite

The Caledonia quartz monzonite occurs on the southwest flank of Nithi Mountain and it also intrudes the Endako quartz monzonite. This is a pink-grey porphyritic, medium-grained rock containing equivalent amounts of quartz, plagioclase and potassium feldspar, and 5 to 10% biotite. Phenocrysts of subhedral potassium feldspar up to 16 mm long account for 10% of the rock (Carr, 1966).

Casey Alaskite - Quartz Monzonite

The Alaskite variety of this intrusive is found at the margins of the body as dykes and veins. It consists of 33% quartz, 40% orthoclase, 25% plagioclase, and 2% biotite (Carr, 1965). Pink or white coarser-grained quartz monzonites are also classified with this intrusive.

Weathering is either white or brown. These rocks are found in the stock or the north arm of the stock on Nithi Mountain. Coarser-grained quartz monzonites may contain large phenocrysts of orthoclase and quartz up to 1 cm in length, and they may account for 30% of the rock. These varieties consist of quartz 36%, orthoclase 30%, plagioclase 30%, biotite 3%, and accessories 1% (Carr, 1965).

Stellako Quartz Monzonite

This intrusive body is found at the northwest corner of the study area. It is one of the youngest of the Topley intrusives and consists of grey, finely crystalline, massive quartz monzonite with approximately 5% biotite and 2% hornblende (Davis, 1980).

Minor Intrusions

According to Davis (1980), aplite dykes occur with granitic pegmatite in the study area, as shown in Figure 2. The aplite is pink, fine-grained, and consists of quartz, orthoclase, plagioclase, and biotite. Rhyolitic porphyry dykes, quartz latite, dacite, and andesite dykes also occur. Dyke rocks are generally pre-mineral in age (Davis, 1980).

Dykes with quartz, orthoclase, and plagioclase phenocrysts are found on the west side of Nithi Mountain within the Nithi quartz monzonite. Mineralization in this type is unique to Nithi Mountain and the Endako ore deposit in the Endako quartz monzonite (Davis, 1980).

Small lamprophyre dykes, associated with shear zones and joints, also occur on Nithi Mountain and at the Endako ore body, and they are post-ore in age (Davis, 1980).

REGIONAL STRUCTURAL GEOLOGY

According to Carr (1965), the majority of the Topley Intrusives are tabular in shape and steeply inclined, but there is not enough evidence to describe the structure of the batholith in detail. Faulting appears to have been the dominant component of structural control for all the intrusive episodes. Repeated conditions of tension would be necessary to allow successive emplacement of the intrusions (Carr, 1965).

The Topley Intrusives intrude the southwest flank of the Pinchi geanticline which is an elongate, northwest trending, fault bounded belt of Cache Creek Group rocks (Davis, 1980). According to Davis (1980), the Pinchi geanticline was uplifted, folded, and faulted in Late Triassic time and the peripheral faults along the flanks of the geanticline may have controlled emplacement of the Topley batholith. Davis (1980) cites that the Topley Intrusives are intrusive into the Takla and Hazelton Groups to the southwest of Nithi Mountain.

Carr (1965) suggests that the uneven granular texture of the Casey quartz monzonite may be due to crushing and

milling prior to the final stages of crystallization. Carr (1965) also suggests that the primary foliation in many of the intrusive bodies, such as the Simon Bay Complex, are due to external stress.

Topographic lineaments, other than the east trending lineaments associated with glaciation, may coincide with faults (Carr, 1965). These lineaments trend west northwest, northeast, and north.

STRUCTURAL GEOLOGY OF THE ENDAKO MOLYBDENUM DEPOSIT AND OF THE NITHI MOUNTAIN AREA

According to Davis (1980), the Endako Molybdenum deposit is a mineralized elongate stockwork. The structural geology of this deposit, described by Drummond and Kimura (1976), is as follows:

Four major fault trends occur in the mine area; these are local representatives of regionally developed fault systems. The local fault trends are represented by the easterly trending South Boundary fault, northwesterly trending Casey fault, northerly trending Tailings Creek fault, and north-easterly trending West Basalt Fault, Fig. 2b. The former three faults form conspicuous topographic lineaments.

Relative movement and displacement along the South Boundary fault is unknown. It is considered that this fault acted as a major control for development of the Endako stockwork. Relative horizontal movement along the Casey and Tailings Creek faults is indicated by the apparent offsets of the Endako quartz monzonite and Casey alaskite. The West Basalt fault offsets the ore deposit

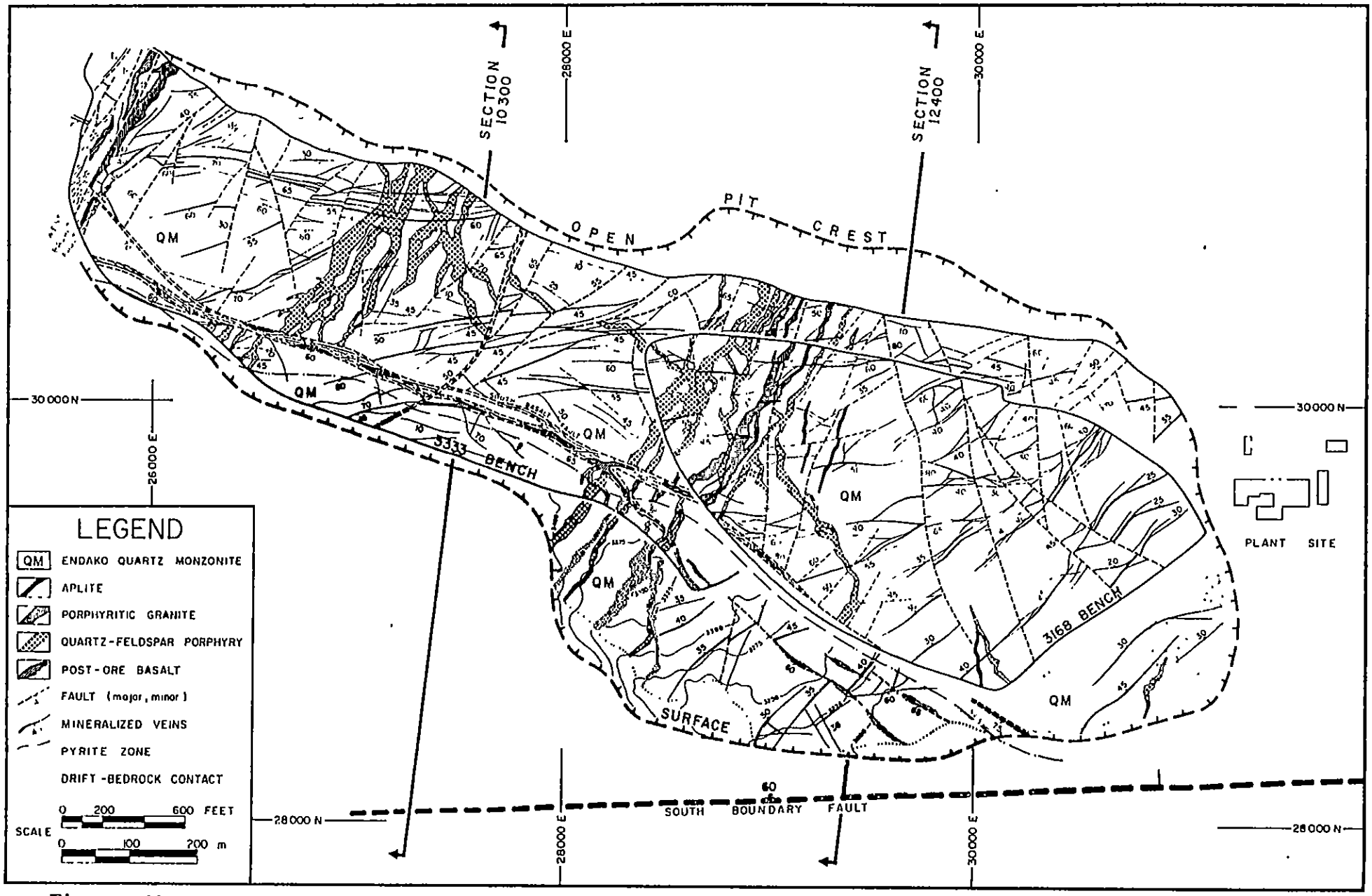

Figure 2b. Composite geological map of 3168 Bench, 3333 Bench and surface, Endako Molybdenum Mine, British Columbia. After Dawson and Kimura (1972).

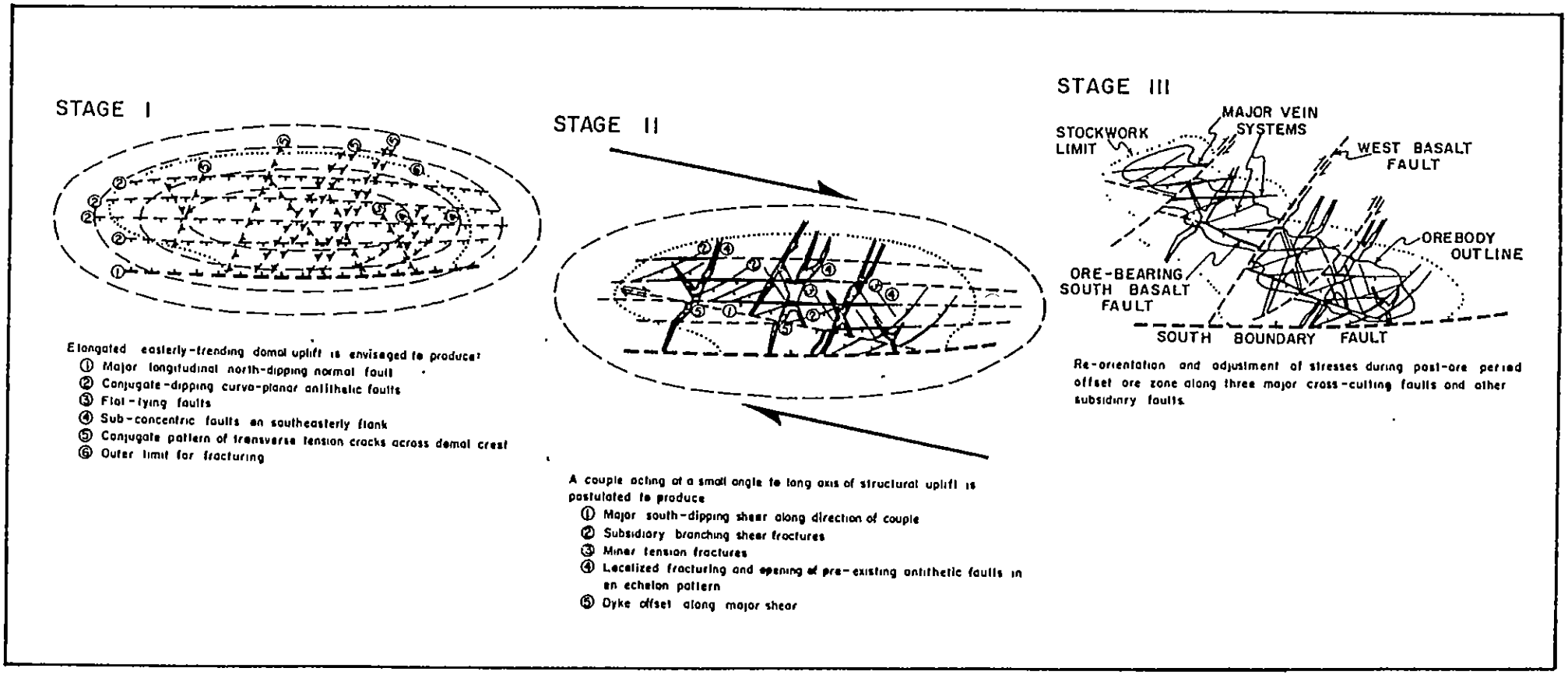

Figure 2c. Schematic diagram depicting the formation of the Endako Molybdenum deposit in central British Columbia. After Dawson and Kimura (1972).

150 m relative right-hand movement.

According to Dawson and Kimura (1972), the formation of the Endako Molybdenum deposit was influenced by three related events: the emplacement and crystallization of the Endako quartz monzonite; intrusion of residual granitic magma as pre-ore dykes; and the ascent of hydrothermal fluids through the localized zone of intense fracturing related to wrench faulting and doming. Dawson and Kimura (1972) suggest that early compressional stress during the emplacement and cooling of the Endako quartz monzonite, generated localized doming and fracturing in the vicinity of the mine at the regional intersection of eastwest, northwest, and northeast fracture systems, as shown in Fig. 2c. Pre-ore dykes followed the emplacement of the pluton. The major structural adjustments of the pluton consisted of wrench faulting along principal orebody faults and secondary shears, doming of the orebody area, and antithetic faulting along conjugate south and northwest dipping fractures (Dawson and Kimura, 1972).

Many large veins and smaller stockwork veinlets follow the predominant eastwest and northeast fracture directions

(Dawson and Kimura, 1972).

According to Davis (1980), the structure of Nithi Mountain is similar to the Endako mine in that the major fault zones south and southwest of Nithi Mountain are similar to the regional fault set which controlled the initial development of the Endako stockwork. Davis (1980) states that the general eastwest trend of quartz molybdenite veins on Nithi Mountain is similar to the trend of mineralized veins at the Endako deposit. Furthermore, Davis (1980) suggests that the northwest fracture pattern on Nithi Mountain is a first order shear direction related to left-lateral movement along the major eastwest trending fault zone, located south of Nitni Mountain. The northeast trending set of fractures would then represent a conjugate shear direction of the northwest set. It is concluded by Davis (1980) that the conditions necessary to develop a stockwork, similar to the Endako stockwork, appear to be present in the Nithi Mountain area.

REGIONAL MOLYBDENUM MINERALIZATION

Molybdenum mineralization is found at the Endako Molybdenum deposit in Endako quartz monzonite. Several surface occurrences are also found on Nithi Mountain and south of Owl Lake. At the latter two sites, molybdenite occurs in narrow quartz veins, in fractures, and as disseminations in stockwork. On Nithi Mountain there are short lenses of mineralized banded quartz up to 0.6 m thick and approximately 6 m in length that strike northeast and dip both south and north (Carr, 1965).

At Nithi Mountain and at Owl Lake there is widespread rock alteration that is partly strongly sericitic and partly weakly chloritic, and also a type of alteration, found at the Endako deposit, that results in green coloured plagioclase and the introduction of biotite and orthoclase (Carr, 1965). Molybdenum has also been found in drill holes and trenches.

According to Carr (1965), the mineralization at Nithi Mountain is similar to that found at Endako for the following reasons: (1) It is in an older, medium-grained quartz monzonite adjacent to the younger Casey intrusion,

(2) porphyry dykes found near mineralization are the same as some of those at the Endako Mine, and (3) strong chloritic faults occur near some showings.

MINERALIZATION AT THE ENDAKO MOLYBDENUM DEPOSIT

The following description of the mineralization at Endako, from Drummond and Kimura (1976), is as follows:

The primary ore minerals in the orebody are molybdenite, pyrite, and magnetite with minor amounts of chalcopyrite, traces of bornite, bismuthinite, scheelite and specularite, and all of these minerals are associated with quartz veins. Ore minerals occur in large quartz molybdenite veins and in fine fracture fillings and veinlets in the form of a stockwork.

Major ore bearing veins are 15 cm to 1 m wide, and occur in subparallel and complementary sets. Veins within the economic stockwork are spaced from 1 cm apart to several meters apart.

A pyrite zone bounds the orebody to the south. This zone consists of fine quartz and pyrite, minor magnetite, and rare molybdenite mineralization as fracture fillings in a poorly developed stockwork. The zonal boundary between molybdenite and pyrite mineralization is the hanging wall of the South Basalt fault, as shown in Figure 2b.

Three phases of hydrothermal alteration have been noted at the Endako deposit within the ore zone:

(1) K-feldspar envelopes on veins and fractures.

(2) Quartz-sericite-pyrite envelopes on veins.

(3) Pervasive kaolinization of the Endako quartz monzonite.

Within the orebody, K-feldspar-bearing envelopes are more commonly developed on quartz-molybdenite veins, and the frequency of this occurrence increases towards the footwall of the orebody.

There is no correlation between intensity of pervasive kaolinization and vein mineralogy. However, within the stockwork, the most common alteration type would lie between weak and moderate kaolinization. Intense kaolinization occurs as bounding zones around major vein systems and fault zones.

MOLYBDENUM MINERALIZATION ON NITHI MOUNTAIN

According to Davis (1980), there are 10 major molybdenite showings found in outcrops or in trenches on Nithi Mountain. Minor occurrences exposed on the surface are scattered throughout the study area. The location of each showing is given by the claim map, Fig. 2d.

Description of Molybdenite Occurrences

North Showing

The North Showing is located within the MJM claim. Molybdenite is found in quartz-molybdenite veins and fracture fillings within Nithi quartz monzonite. The veins strike N65°E and N70°E. Secondary ferromolybdenite is also present. This area is surrounded by Casey granite on three sides. To the west and south, the Nithi quartz monzonite is found in intrusive contact with the Casey granite and to the north, a fault separates the two rock units. Argillic alteration is moderate to intense. There is minor potassic alteration adjacent to some fractures.

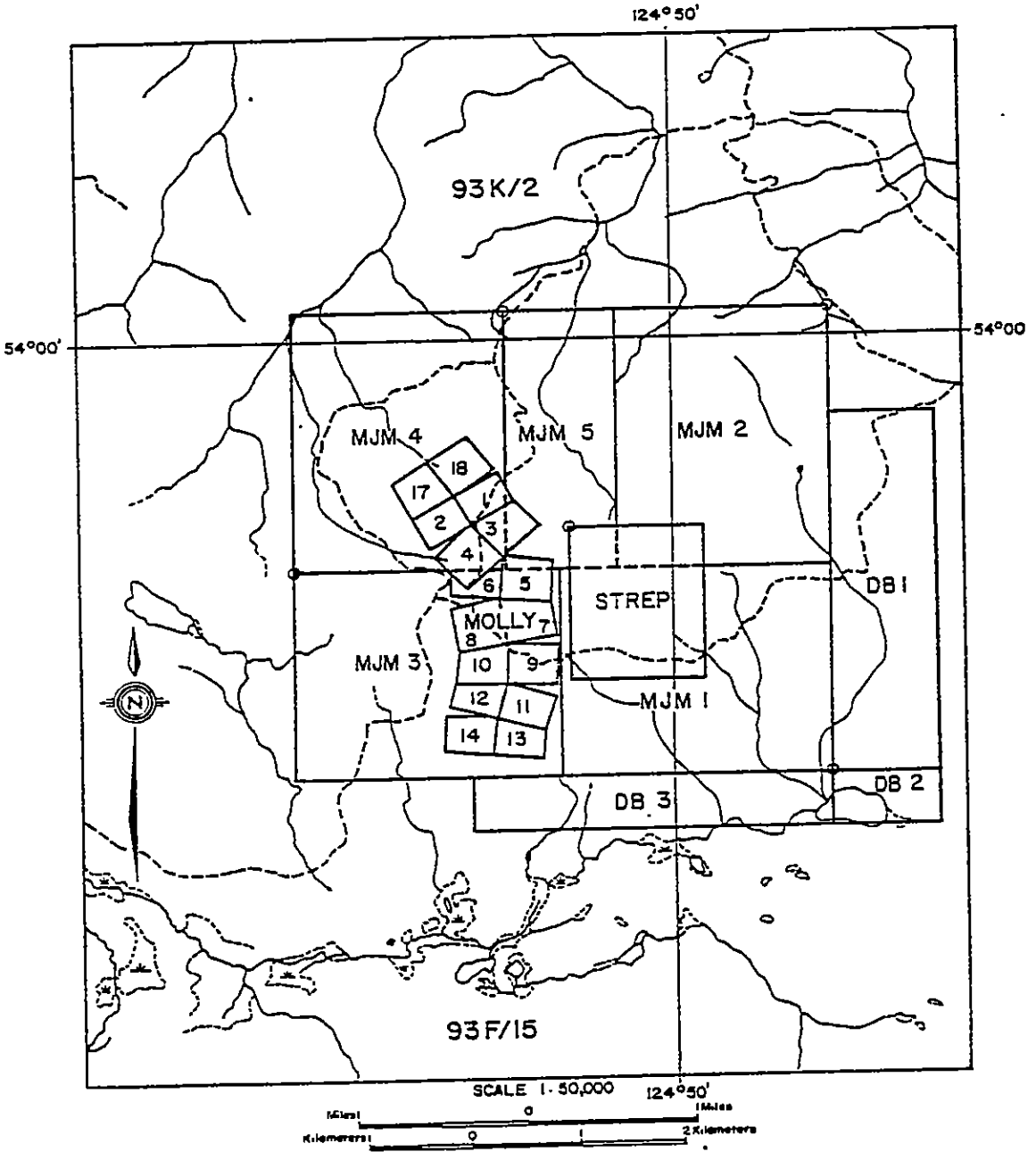

PROPERTY LOCATION MAP

Figure 2d. Property location map of Nithi Mountain, British Columbia. Molybdenite occurrences are given by claim locations, as described in the text.

Tan Showing

The Tan Showing is found within the MJM2 claim. Coarsely disseminated molybdenite and quartz-molybdenite veins are found within an area of orthoclase-rich Casey granite. There is weak argillic alteration and minor potassic alteration.

Central Showing

The Central Showing is located at the boundary of the MJM1 and MJM2 claims. Quartz-molybdenite veins and fracture fillings are hosted by Casey granite which is surrounded by Nithi quartz monzonite. Argillic alteration is weak to strong and very strong along faults. Drilling into a vein at this showing was stopped at 27 m depth because a fault zone was encountered. The drilling intersected a quartz-molybdenite vein striking N65°E.

South Showing

The South Showing is found within the east-central section of the MJM1 claim. Molybdenite is found as disseminations within highly altered Nithi quartz monzonite. There is strong argillic alteration and narrow

seams of potassic alteration adjacent to joint surfaces. Intrusive contacts with Casey granite occur on three sides.

Terri Showing

The Terri Showing, which was discovered by the writer, is located within the east-central section of the Strep claim. Quartz-molybdenite veins trending N65°E and fracture fillings and disseminations are found in frost-heaved boulders and outcrop of Casey granite. Intrusive contacts with Nithi quartz monzonite are found nearby to the north, northeast, and south. Mild argillic alteration is present.

Chris Showing

The Chris Showing is located within the south-central part of the MJM3 claim. Quartz-molybdenite veins and fracture fillings strike N60°E and N70°E within Nithi quartz monzonite. One vein is 20 cm wide. Argillic alteration is moderate to intense. There is minor phyllic and potassic alteration adjacent to fracture surfaces. Two drill holes were completed in this area. One intersected only low grade quantities of molybdenite. The other intersected a combined thickness of 170 m of

molybdenite mineralization.

Southwest Showing

The Southwest Showing is found within the south central section of the MOLLY 9 claim. Nithi quartz monzonite hosts many narrow quartz-molybdenite veins that strike N65°E, scattered over a 400 m X 600 m area. Argillic alteration is moderate to strong. There is also minor potassic alteration.

West Showing

The West Showing is located on the main access road within the MOLLY 8 claim. A 15 cm wide, quartz-molybdenite vein, striking N67°E is found within Nithi quartz monzonite. Secondary ferromolybdenite is present.

A-Line Showing

The A-Line Showing is located in the south part of the MJM4 claim. A 1 m wide quartz-molybdenite vein striking N45°E and dipping 27°N is exposed for 9 m along the strike. It is hosted by Nithi quartz monzonite and the vein appears to diverge into smaller veins towards the east. The Nithi quartz monzonite has been subject to intense argillic alteration, Drilling completed in

this area intersected low grade quartz-molybdenite veins.

Molly Showing

The Molly Showing is found within the MOLLY 1 and MOLLY 2 claims. Nithi quartz monzonite hosts a quartz-molybdenite vein that is 30 cm thick and 80 m long, exposed in 3 trenches. Ferromolybdenite and secondary uranium minerals are present. Rhyolite porphyry dikes nearby also host secondary uranium minerals. Intense argillic alteration is present and minor K-feldspar alteration is also present.

Northwest Showing

The Northwest Showing is found within the Molly 17 claim. Molybdenite and pyrite occur as fine disseminations in quartz filled fractures and gossaned shears within the Simon Bay diorite. The intrusive contact with Nithi quartz monzonite is to the west.

THEORY OF ELECTROCHEMICAL DISPERSION

The use of conductivity as an exploration method is based on a model of electrochemical dispersion by Govett (1973) and Bolviken and Logn (1975). This model is based upon the existence of self-potential anomalies associated with ore deposits (Bolviken and Gleeson, 1977). Vertical redox potential gradients in the upper lithosphere cause orebodies to conduct electrons and the area around the orebody acts as a galvanic cell (Fig. 2e). The current flow is carried by electrons in the orebody and ions in the groundwater (Bolviken and Gleeson, 1977). Overburden tends to have better electrical conductivity than bedrock. Therefore, the current flows more vertically in bedrock and more horizontally in the overburden. For the overburden, the current density tends to be highest above the subcrop of the hanging wall of the orebody.

Bolviken and Gleeson (1977) state that ions will move along the current paths and, if during their migration they meet retaining agents such as fine-grained overburden, Fe-Mn hydroxides, or humus, they may be absorbed or complexed and interchanged for more mobile

ions which in turn are released to the electrolyte.

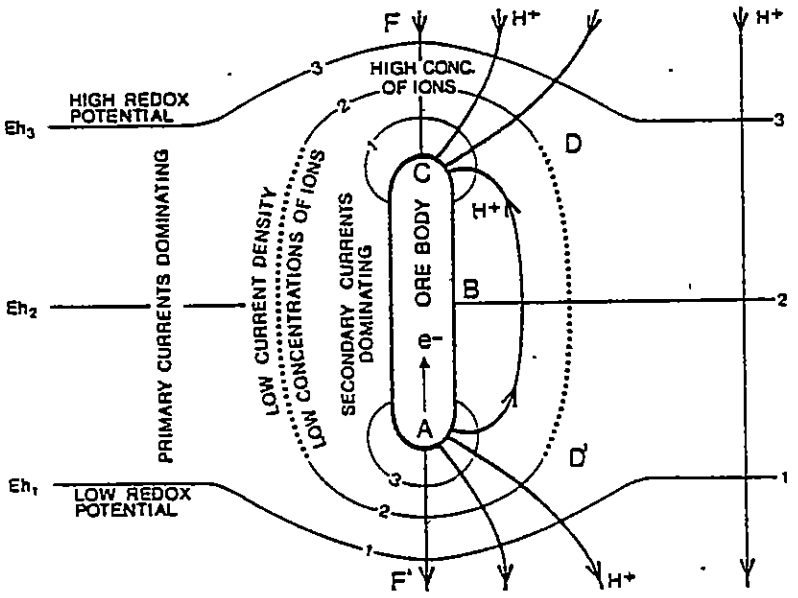

Fig. 2e. Schematic model of an ore body as electrode in a primary redox potential field. Eh_1, Eh_2, and Eh_3: selected equipotential surfaces. Heavy lines indicate path of primary and secondary currents, arrows indicate direction of positive electricity (cations) in the electrolyte. Arrow inside ore body: direction of electron flow in the ore. A = anode; B = electrical symmetry point at country rock/ore interface; C = cathode; D = limit of zone where secondary currents counteract primary currents; F = extension of the ore. (Bolviken and Logn, 1975).

Govett (1972) states that the presence of pyrite is important in increasing the dissolution of sulphides more electronegative in character than itself. Molybdenite is more electronegative than pyrite. The resultant conductivity dispersion pattern is governed by the rate of dissolution at the orebody-host rock interface, the solubility of the dissolved species, and the mechanism

of movement. Govett (1973) suggests that the ongoing electrochemical processes that occur around ore deposits may control the amount and kinds of ions released from a sulphide and play a major role in the dispersion of elements into the surrounding rocks and soils. Sulphides that are less massive in character and deeply buried deposits produce profile patterns that are small in amplitude and of long wavelength. Major lithological changes may produce the same effect, but generally on a smaller scale (Fig. 2f).

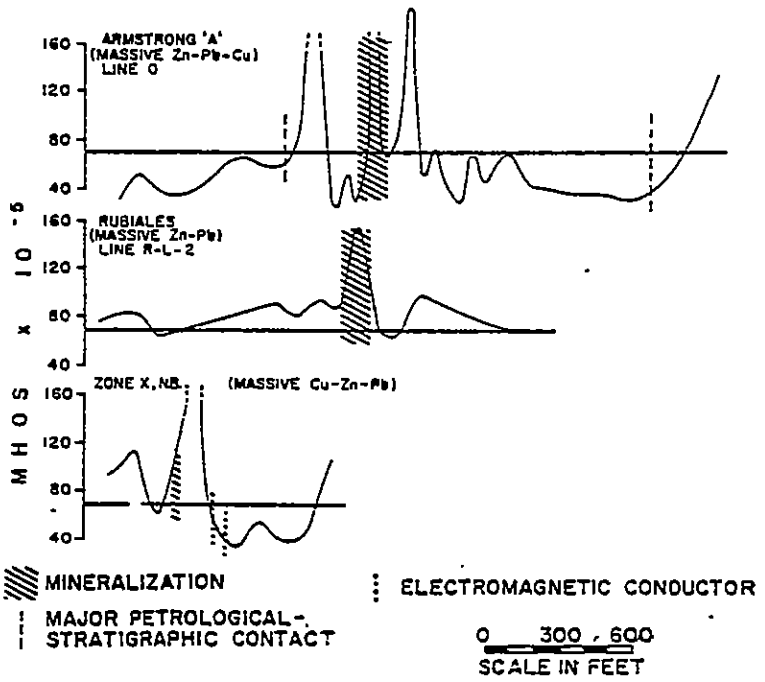

Fig. 2f. Case studies done by Govett (1975) of massive sulphide deposits and the relation of conductivity in soils over these deposits to the mineralized areas.

RESULTS AND DISCUSSION

Molybdenum, manganese, iron, and zinc determinations were carried out by a custom lab for Taiga Consultants Ltd., on minus 100-mesh B horizon soils. The same samples were subsequently used for measurements of conductivity. The method is that of Govett (1974). The procedure used is as follows: 1 gram of sample was weighed out into a 150 ml beaker, to this was added 100 ml of triple distilled water and then the contents of the beaker was stirred for 1 minute, using a magnetic bar stirrer. Conductivity was measured immediately using a Barnstead Model PM-70 CB conductivity bridge and a dip-type conductivity cell having a cell constant of 1.0. The conductivity of the water was measured for each group of samples and substracted from the resultant readings. The results of the molybdenum, manganese, iron, and zinc determinations and conductivity measurements are compiled in Appendix A. The thresholds and statistical parameters for the entire population is given in Table 2.1. Comparing the anomalous values of elements in soils

Table 2.1

Statistical parameters of the entire population, Nithi Mountain Area.

Variable	Number of Samples	Mean	Standard Deviation	Minimum Value	Maximum Value	Threshold*
Mo(ppm)	1869	13.81	23.62	1.0	400.0	61.05
Mn(ppm)	1869	400.83	371.77	28.0	3860.0	1144.37
Fe(%)	1869	2.4	0.74	0.2	6.0	3.88
Zn(ppm)	1869	101.26	89.53	2.0	1260.0	280.32
Conductivity ($umhos^{-1}$)	1488	6.07	3.28	0.85	47.15	12.63

*Threshold = Mean + 2 (Standard Deviation)

within the study area to the abundances, as shown in Table 2.2, it is obvious that molybdenum, manganese, and zinc have a higher concentration than the average abundances. However, iron and manganese are within the normal range of abundance for soils. Exceptionally high values, shown in Figures 5, 6, and 7 for manganese, iron, and zinc, occur in low, swampy, organic rich terrain, particularly at the southwest corner of the study area.

Figure 3 shows the distribution of anomalous conductivity in soils, for the study area. The threshold is 12.63 $umhos^{-1}$. Conductivity anomalies coincide with molybdenum anomalies (Fig. 4) in the southeast portion of the study area. The conductivity anomalies are much smaller than the molybdenum anomalies. High conductivity in soils appears to coincide with anomalous regions of manganese, iron, and zinc in the southeast portion of the study area, as shown in Figures 3, 5, 6, and 7. However, this is not found to be true on a smaller scale over known mineral occurrences.

The correlation between the 5 variables is given

Table 2.2

Geochemical abundances and characteristics of Mo, Mn, Fe and Zn. From Hawkes and Webb (1962).

ELEMENT	IGNEOUS ROCKS			SOILS		MOBILITY
	Av.	Av. Umaf.	Av. Fel.	Av.	Range	
Mo (ppm)	1.7	0.4	1.9	2	0.2-5.0	moderate to extremely high limited by: 1) rate of solution of primary MoS_2, 2) sorbtion on limonite to form ferrimolybdenite at pH 2.5-7.0. 3 ppt. in CO_3 rich environments.
Mn (ppm)	1000	1300 Mafic: 2200	600	850	200-3000	low, unless in an acid environment, then mobile as Mn^{2+}.
Fe (%)	4.65	9.85 Mafic: 8.56	2.7		1.4-4	Fe^{2+} moderate Fe^{3+} low } limited by ppt. of limonite
Zn (ppm)	80	50 Mafic: 130	60	50	10-300	moderately high, limited by organic activity and coprecipitation with limonite.

in Table 3 as a correlation matrix. At the 99.9% level of confidence, all the correlation coefficients are significant even though they appear as small numbers. This is because the sample size is large (n = 1,867). The highest correlation (r = .473) between manganese and zinc is followed by conductivity and manganese (r = .325), then molybdenum and manganese (r = .284). Thus, when considering the value of one element versus another as an exploration tool for the entire study area, no single element takes precedence over any others. Furthermore, the weak correlation between conductivity and molybdenum is also due to the large sample size which produces a dilution effect. This is the result of mixing of two populations, one representing the barren earth material population and the other being caused by mineralization. Diagrams and statistics showing the relationships between the elements and conductivity for the entire study area are in Appendix B. The correlation coefficients for the same X-Y plots using log transformations are generally higher than for untransformed data. For example, molybdenum versus

Table 3

Correlation matrix for the entire sample population.

Variable	MO(ppm)	Mn(ppm)	Fe(%)	Zn(ppm)	Conductivity ($umbos^{-1}$)
Mo(ppm)	1				
Mn(ppm)	.284	1			
Fe(%)	.122	.120	1		
Zn(ppm)	.257	.473	.149	1	
Conductivity ($umhos^{-1}$)	.138	.325	.186	.130	1

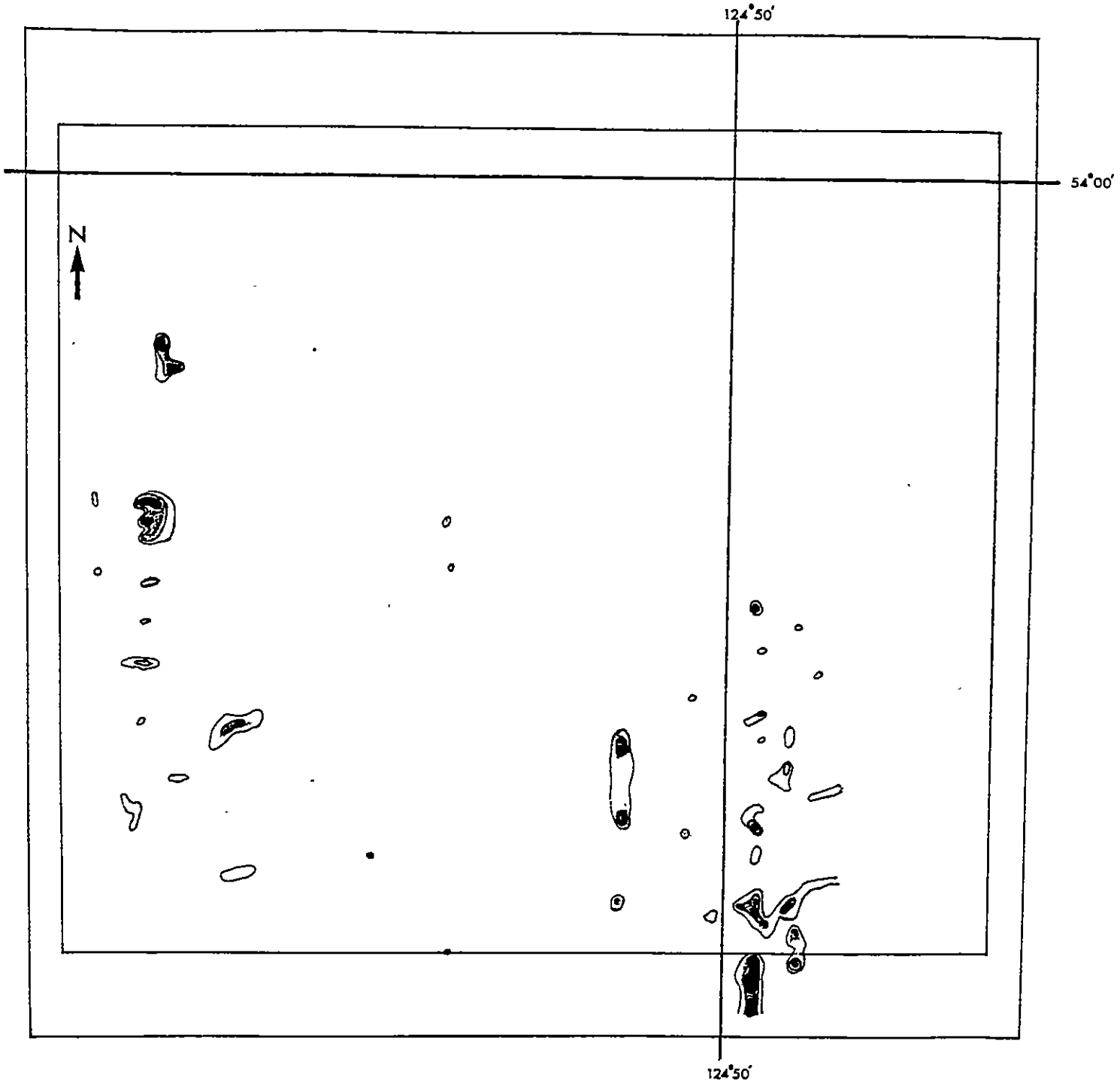

FIGURE 3

CONDUCTIVITY MAP

NITHI MOUNTAIN, BRITISH COLUMBIA

Note: Conductivity anomalies in the east-central area, coincide with known molybdenite occurrences at the surface. Anomalies in the northwest area coincide with known pyrite occurrences at the surface.

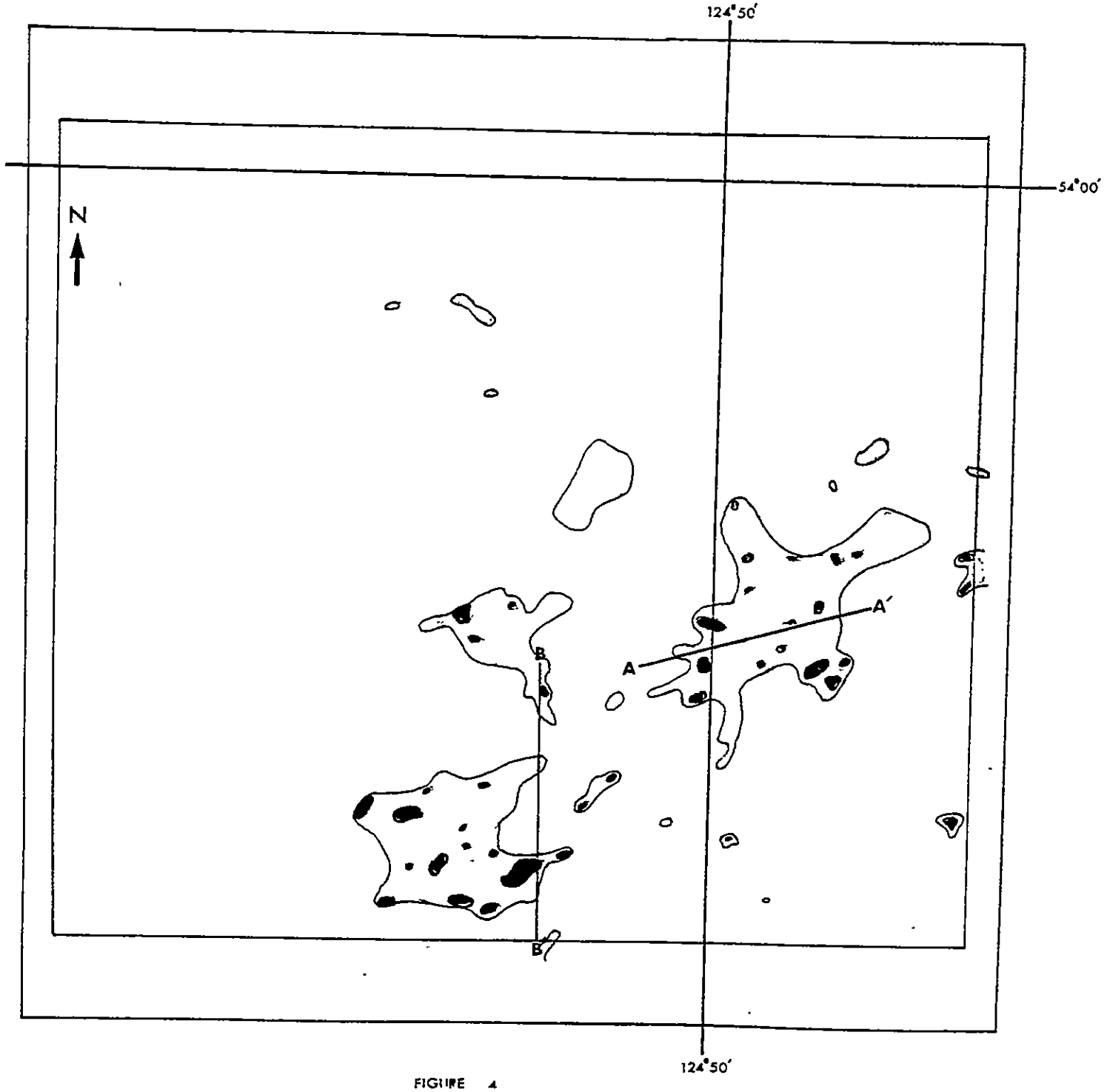

FIGURE 4

DISTRIBUTION OF MOLYBDENUM IN SOILS

NITHI MOUNTAIN, BRITISH COLUMBIA

LEGEND

ppm

50-75

75-100

> 100

SCALE

0 500 1000

METERS

Note: Anomalies cross the Chris, Southwest, Terri, Central and Tan showings. Profiles A-A' and B-B' are plotted in Figure 8 with conductivity.

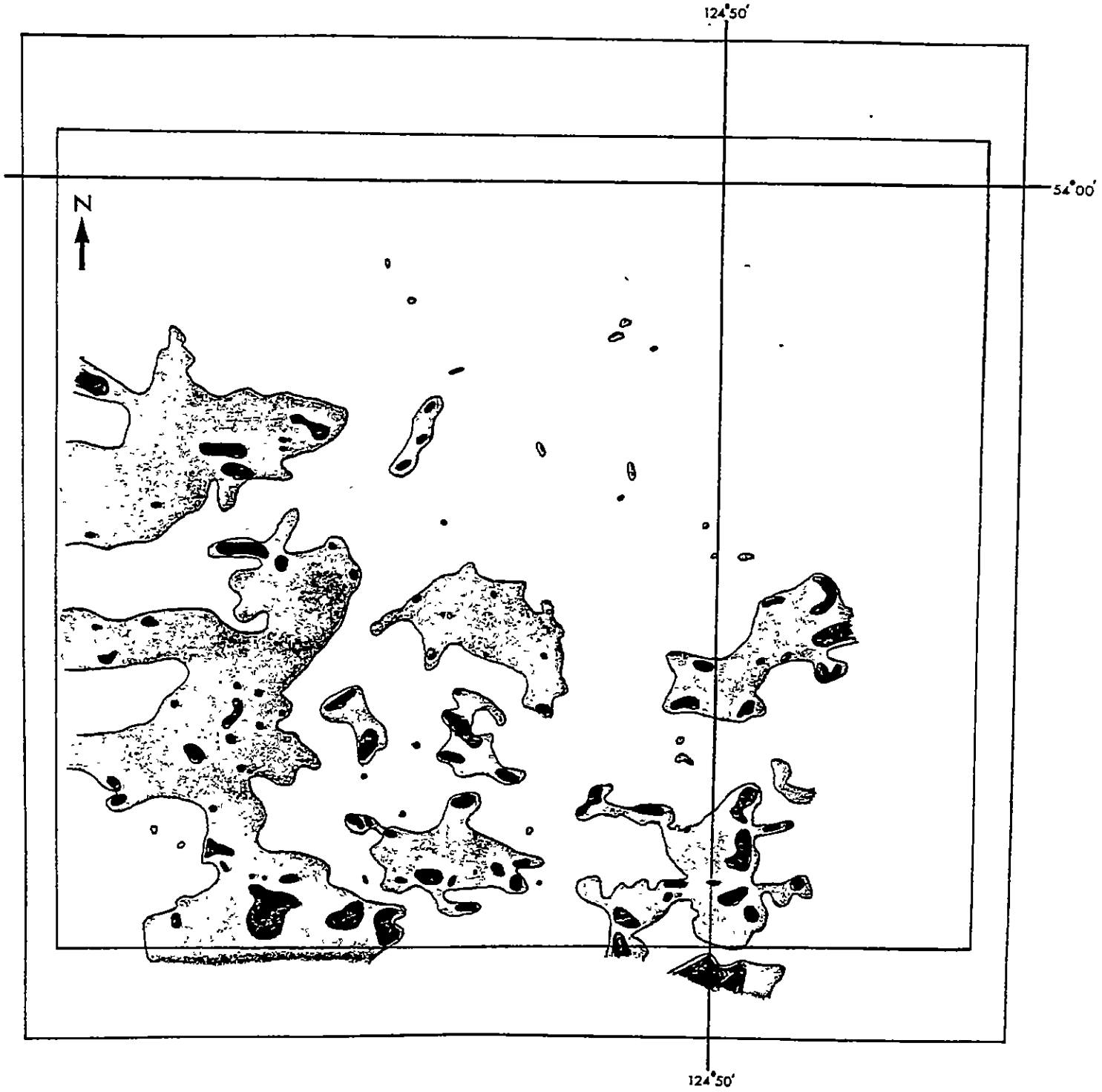

FIGURE 5

DISTRIBUTION OF MANGANESE IN SOILS

NITHI MOUNTAIN, BRITISH COLUMBIA

LEGEND

ppm

500–1000

1000–3000

3000–5000

>5000

SCALE

0 500 1000

METERS

Note: The distribution of manganese anomalies covers too great an area, therefore, it is not useful for pinpointing smaller target areas.

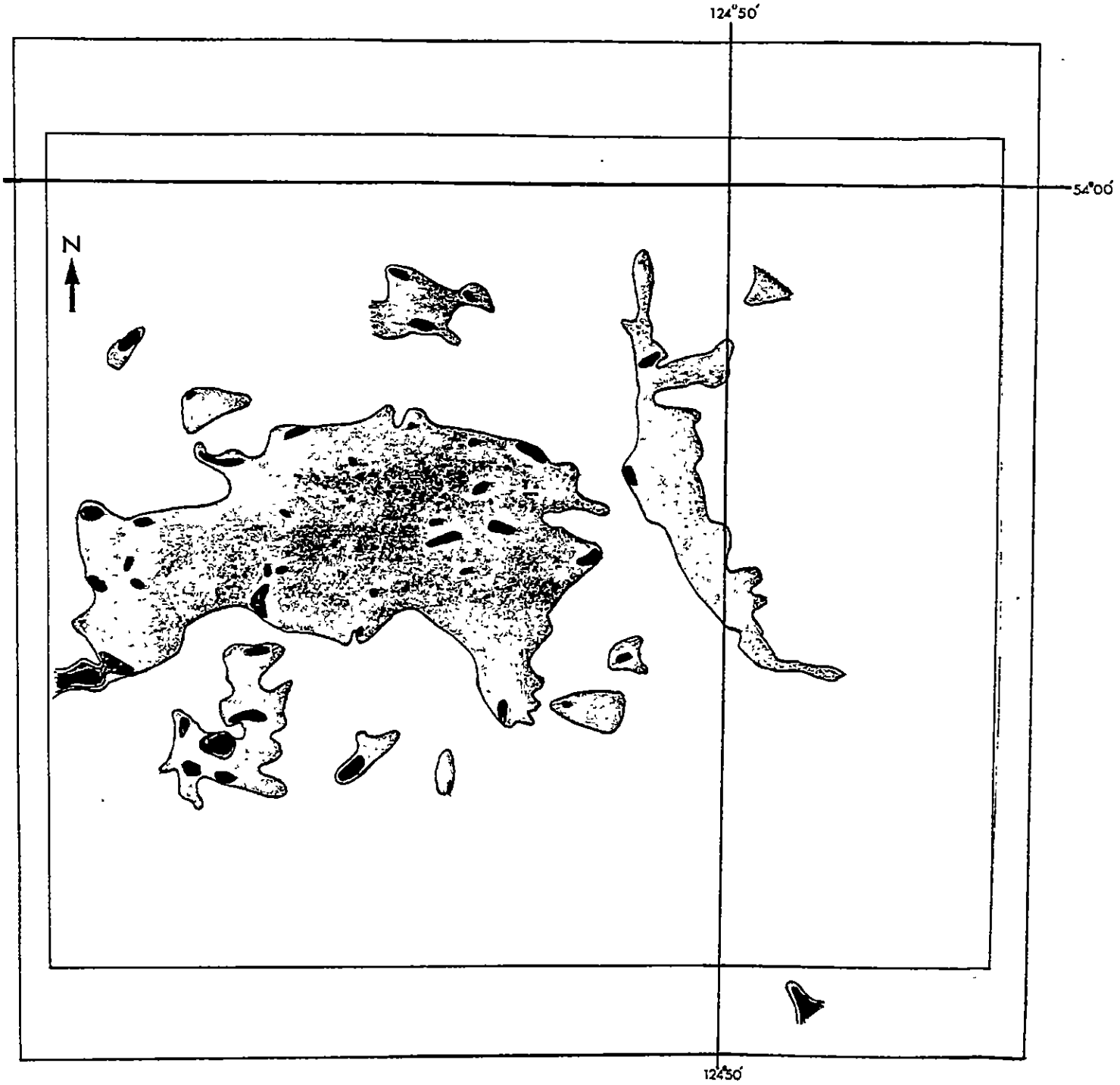

FIGURE 6

DISTRIBUTION OF IRON IN SOILS

NITHI MOUNTAIN, BRITISH COLUMBIA

LEGEND

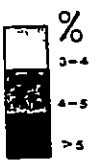

SCALE

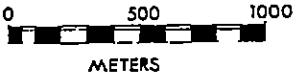

Note: Anomalous iron values are concentrated south and downslope from the Simon Bay diorite and known pyrite occurrences.

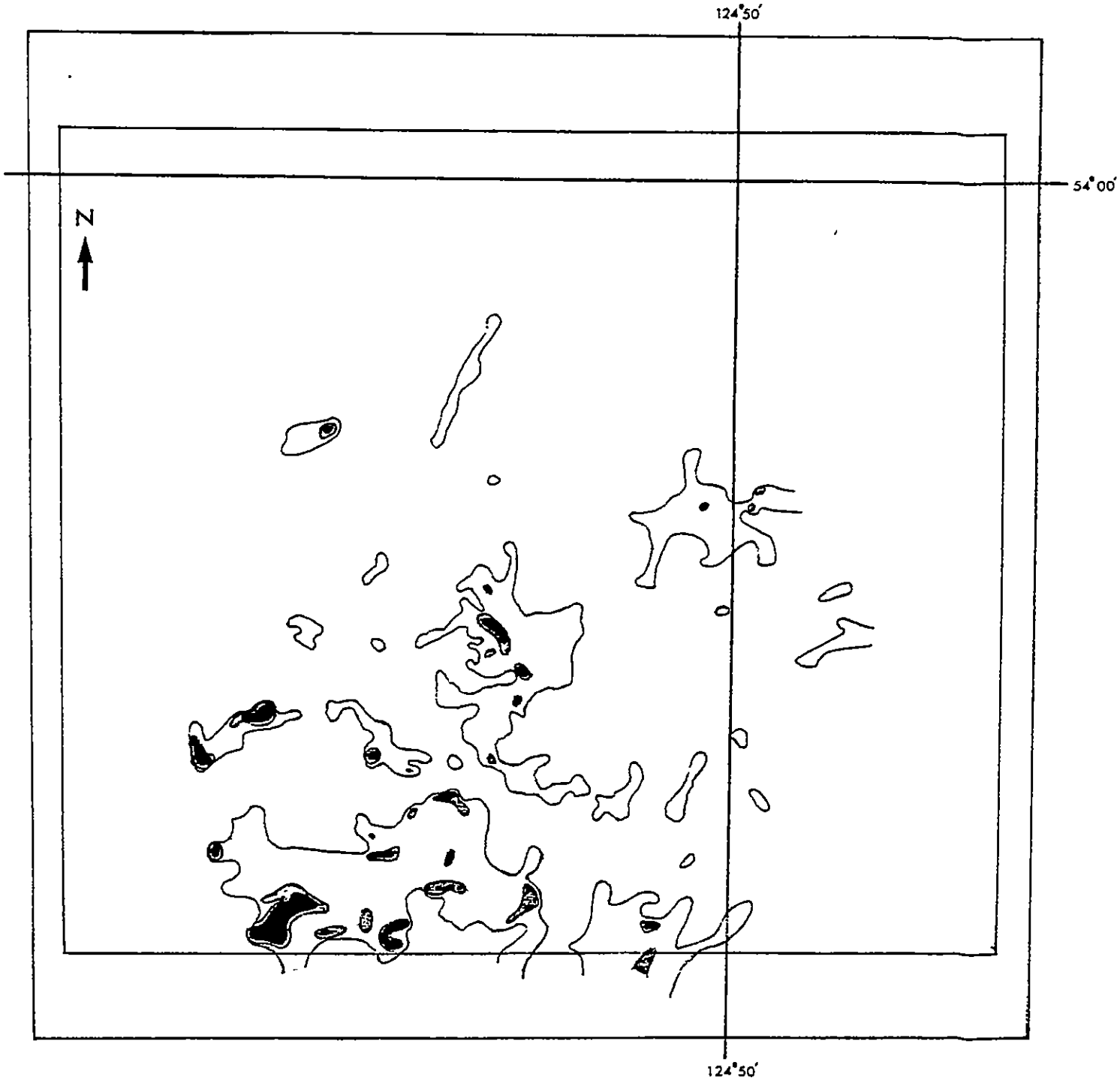

FIGURE 7

DISTRIBUTION OF ZINC IN SOILS

NITHI MOUNTAIN, BRITISH COLUMBIA

LEGEND

ppm

200 – 400

400 – 500

> 500

SCALE

0 500 1000

METERS

Note: Highest zinc correlations are found in low-lying areas.

conductivity, r = .138; while for log molybdenum and log conductivity, r = .146. This is because the concentrations of elements is log normally distributed, as typical of trace element data in geochemistry, while conductivity is normally distributed. However, the differences are minor.

In order to study the behaviour of the elements as a function of conductivity, two profiles of small areas were examined. The location of two profiles is shown in Figure 4. Profile A-A' crosses the Terri showing and is 50 to 70 m downslope from the central showing. Profile B-B' crosses an area barren of mineralization at the surface. However, the soils contain 50 to 100 ppm molybdenum, which compared to average abundances (Table 2.2) are still anomalous.

Table 4 shows the correlation relations between the elements and conductivity for the profile A-A' which is 1,100 m in length. The correlation between manganese, iron, and zinc with molybdenum are not statistically significant. The correlation of molybdenum and conductivity is very significant. Iron and

Table 4

Correlation matrix for the profile A-A'. This profile crosses outcrops of molybdenite and areas of 75 ppm Mo in soils.

Variable	MO(ppm)	Mn(ppm)	Fe(%)	Zn(ppm)	Conductivity ($umhos^{-1}$)
Mo(ppm)	1				
Mn(ppm)	.072	1			
Fe(%)	-.274	.784	1		
Zn(ppm)	-.302	.708	.915	1	
Conductivity ($umhos^{-1}$)	.687	.176	.073	.098	1

manganese, zinc and manganese, and iron and zinc correlate well. Conductivity does not correlate to iron, manganese, or zinc. By taking the logs of the elements and plotting them against one another, there is an increase between the correlation of manganese, iron, and zinc with molybdenum but this correlation is negative, thus when molybdenum increases, the others decrease.

The correlation between conductivity and molybdenum as log values decreases slightly, but it is still statistically significant. Data for this profile is compiled in Appendix C. The pattern of conductivity over this profile is shown in Figure 8. The conductivity peaks over the mineralized areas and increases towards the east northeast along the profile. The molybdenum content in the soil peaks just to the left of the mineralized area, to the west southwest, which is generally downslope. Mineralization occurs in mild argillically altered Casey granite. Argillic alteration tends to be moderate to intense around quartz-molybdenite veins that outcrop at other showings on

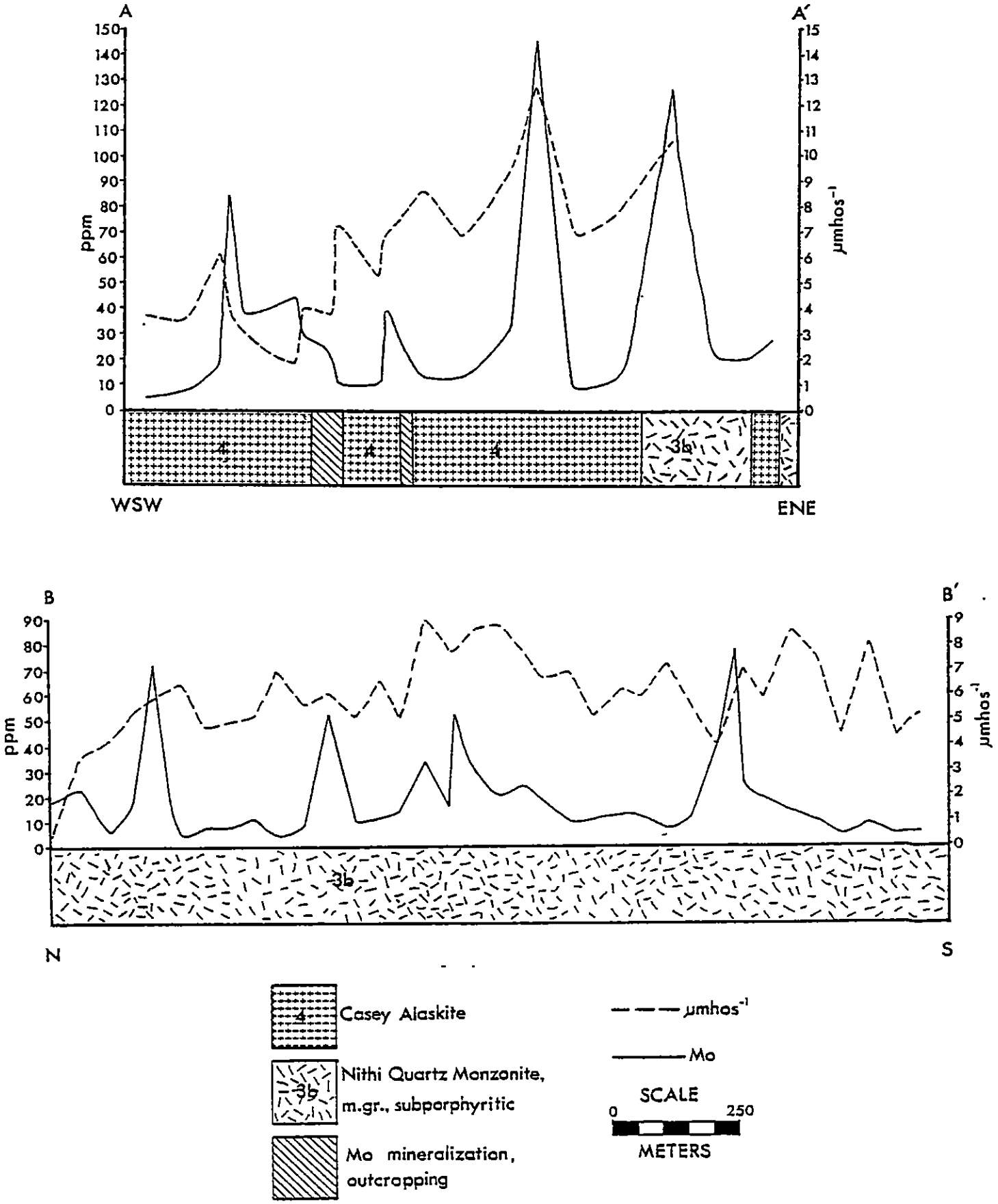

Figure 8. Profiles across mineralized and unmineralized zones on Nithi Mountain, British Columbia. The locations of these profiles are given in Figure 4.

Nithi Mountain. The conductivity peak that increases upslope from the mineralization at surface may be detecting stronger alteration around mineralized veins within the granite. Further to the east northeast, both conductivity and molybdenum peak simultaneously along the profile. This strong correlation suggests that mineralization subcrops in this area.

Table 5 is the correlation matrix for molybdenum manganese, iron, zinc, and conductivity for the profile B-B' which crosses an unmineralized area, 1,750 m in length. This area is located on the south-central slope of Nithi Mountain and it contains soils that have 50-100 ppm Mo. As can be seen from the matrix, none of the elements correlate with molybdenum; they are negative and statistically insignificant. Furthermore, conductivity does not correlate with molybdenum in this profile. Iron has a statistically significant correlation with manganese and zinc. Manganese correlates strongly with zinc. Data for Profile B-B' is compiled in Appendix D.

Profile B-B' is shown in Figure 8 and Figure 4.

Table 5

Correlation matrix for the profile B-B', which does not cross over any known mineral occurrences.

Variable	Mo(ppm)	Mn(ppm)	Fe(%)	Zn(ppm)	Conductivity ($umhos^{-1}$)
Mo(ppm)	1				
Mn(ppm)	-.150	1			
Fe(%)	-.122	.430	1		
Zn(ppm)	-.028	.671	.475	1	
Conductivity ($unhos^{-1}$)	.131	-.166	-.255	-.207	1

While there is no direct correlation of conductivity with molybdenum, peaks of conductivity occur to the south of anomalous molybdenum concentrations. This is likely due to downslope dispersion.

SUMMARY AND CONCLUSION

In examining the geochemical data for the entire study area, which is an 1,867 X 5 matrix, all 5 variables show a significant relation to each other. Thus conductivity measurement would be just as good as either manganese, iron, and zinc as indicators of mineralization. Conductivity is a relatively simple and inexpensive measurement and could be done in the field. Furthermore, iron, manganese, and zinc give too many anomalies.

Conductivity measures the readily soluble ions. It is known that in this region, the molybdenum mineralization is characterized by strong argillic alteration. Such alteration is characterized by high sodium, potassium, calcium, etc., and least by iron, manganese, and zinc. Thus, conductivity should pick up the alteration zones which should be characteristic of molybdenum mineralization of the Endako type.

In trying to prove that conductivity could be used as a pathfinder for molybdenum in the initial test of the hypothesis, the data for all 1,867 samples was used and this did not show a very high r value between molyb-

denum and conductivity. This is because the sample size is too large and too heterogeneous, and is a mixture of a large background population and a small population related to molybdenum mineralization. To overcome this effect of dilution, two random sections were drawn.

Section A-A' was picked to evaluate molybdenum and conductivity relations over 3 known occurrences of molybdenum mineralization. This is shown in Fig. 8. It is apparent from this that there is a direct, positive correlation between molybdenum and conductivity. The r value for this correlation is .687. Also, molybdenum versus manganese, iron, and zinc gives r values of .072, -.274, -.302, respectively (Table 4).

The section B-B' was drawn over the Nithi quartz monzonite in an area which does not contain any known molybdenite mineralization (Figure 8). It should be noted, however, that the soil here runs 50 to 100 ppm molybdenum and is anomalous. The correlation between molybdenum and conductivity is 0.131 and between molybdenum and manganese, iron and zinc is -.150, -.122, and -.028 respectively (Table 5).

It is therefore clear that molybdenite mineralization in this area produces significant conductivity anomalies. The high conductivity values are a measure of the alteration associated with the quartz-molybdenite veins. Moreover, there appears to be little merit in measuring iron, manganese, and zinc for the purposes of locating molybdenite mineralization in this setting.

Also, conductivity is more selective in identifying anomalous areas. For example, manganese (Fig. 5), iron (Fig. 6), and zinc (Fig. 7) show large anomalous areas. On the other hand, the conductivity (Fig. 3) shows, perhaps, 5% of the area as anomalous.

It is therefore concluded that conductivity is a better indicator for molybdenite mineralization than iron, manganese, and zinc and is better for pinpointing smaller target areas for further prospecting and exploration in this area.

REFERENCES

Armstrong, J. E.
1949: Fort St. James Map-Area, Cassiar and Coast District, British Columbia; Geological Survey of Canada, Memoir 252.

Bolviken, B. and Gleeson, C. F.
1979: Focus on the use of soils for geochemical exploration in glaciated terrain; in Geophysics and Geochemistry in the Search for Metallic Ores; Peter J. Hood, editor; Geological Survey of Canada, Economic Geology Report 31, p. 295-326.

Bolviken, B. and Logn, O.
1975: An electrochemical model for element distribution around sulphide bodies; in Geochemical Exploration 1974. J.L. Elliot and W.K. Fletcher (Eds.); Elsevier Publ. Co., p. 631-648.

Bright, E. M.
1967: Geology of the Topley Intrusives in the Endako Area, British Columbia; M.Sc. Thesis, Department of Geology, University of British Columbia, pp. 111.

Carr, M. J.
1965: The geology of the Endako Area; in Lode Metals in British Columbia, 1965; British Columbia Department of Mines and Petroleum Resources, p. 114-138.

Davis, J. W. and Aussant, C. H.
1980: Geochemical Report on the Nithi Mountain molybdenum project; unpublished report, Taiga Consultants Ltd.; for Rockwell Mining Corporation.

Dawson, K. M. and Kimura, E. T.
1972: Endako Report; in XXIV International Geological Congress, Copper and Molybdenum Deposits of the Western Cordillera, pp. 36-37, 40-45.

Drummond, A. D. and Kimura, E. T.
1969: Geology of the Endako Molybdenum Deposit; in Canadian Institute of Mining and Metallurgy Transactions, Vol. LXII, p. 183-192.

Govett, G.J.S.
1973: Differential secondary dispersion in transported soils and post-mineralization rocks: an electrochemical interpretation; in Geochemical Exploration 1972. M. J. Jones (Ed.); Institute of Mining and Metallurgy, p. 81-91.

1975: Soil conductivities: assessment of an electrochemical exploration technique; in Geochemical Exploration 1974. I.L. Elliott and W.K. Fletcher (Eds.); Elsevier Publishing Co., Amsterdam, p. 101-118.

Govett, G.J.S. and Chork, C. Y.
1977: Detection of deeply-buried sulphide deposits by measurement of organic carbon, hydrogen ion and conductance of surface soils; in Prospecting in areas of glaciated terrain 1977. G.R. Davis (Ed.); Institute of Mining and Metallurgy, p. 49-55.

Harris, F. R. and Lebel, J. L.
1975: Geological, geophysical, and geochemical report on the Nithi Mountain property; for Amax Potash Ltd.; British Columbia Dept. of Mines, Assessment Report 5714.

Hawkes, H. E. and Webb, J. S.
1962: Geochemistry in mineral exploration; Harper and Row, New York, 415p.

Ractliffe, J. F.
1962: Elements of mathematical statistics; Oxford University Press, Toronto, 202p.

Rise, H.M.A.
1948: Geological information, Placer deposits, Map 971A, Smithers and Fort St. James, British Columbia; British Columbia Department of Mines and Petroleum Resources.

Tipper, H. W.
1959: Revision of the Hazelton and Takla Group of Central British Columbia, Geol. Survey of Canada, bulletin 47.

1968: Nechako River Map Area, British Columbia; Geological Survey of Canada, Memoir 324

Tipper, H. W.
1973: Glacial geomorphology and Pleistocene history of central British Columbia; Geological Survey of Canada, bulletin 196.

Tipper, H. W., Campbell, R. B., Taylor, G. S., Stott, D.F.
1974: Geological compilation, Parsnip River, British Columbia; Geological Survey of Canada, Map 1424A.

APPENDIX A

Sample number, Mo(ppm), Mn(ppm), Fe(%), Zn(ppm) and conductivity($umhos^{-1}$) for the entire study area.

SAMPLE NUMBER	MO	MN	FE	ZN	CONDUCTIVITY
[illegible]	13.	1150.	1.7	132.	11.17
[illegible]	11.	320.	2.3	58.	23.48
[illegible]	25.	430.	4.3	166.	9.77
[illegible]	67.	2200.	2.0	360.	8.63
2+00N	15.	520.	3.0	102.	6.39
2+50N	3.	360.	2.0	150.	7.53
3+00N	12.	640.	2.1	78.	5.06
3+50N	140.	120.	0.2	22.	12.76
4+00N	62.	200.	2.6	76.	13.00
4+50N	17.	520.	2.0	82.	6.21
5+00N	12.	500.	2.7	88.	8.01
5+50N	25.	160.	0.9	28.	4.15
6+00N	13.	560.	2.0	186.	5.21
6+50N	6.	200.	2.3	184.	6.49
7+00N	13.	220.	2.1	116.	6.01
7+50N	22.	280.	2.1	104.	9.24
8+00N	30.	280.	2.6	320.	11.16
8+50N	37.	240.	2.1	308.	7.16
9+00N	6.	200.	2.7	184.	5.44
0+00S	5.	180.	1.7	50.	4.07
1+00S	8.	200.	1.9	78.	5.63
1+50S	5.	320.	1.9	78.	6.79
2+00S	11.	300.	1.9	34.	7.45
2+50S	3.	180.	1.9	50.	6.03
3+00S	25.	200.	2.0	90.	11.49
3+50S	8.	200.	2.4	182.	13.93
4+00S	13.	200.	2.0	50.	7.10
4+50S	23.	200.	2.2	90.	7.42
5+00S	45.	1240.	2.3	124.	16.19
6+00S	10.	400.	1.8	72.	13.65
6+50S	13.	440.	1.6	62.	12.39
7+00S	11.	340.	1.8	114.	7.34
7+50S	5.	200.	1.5	10.	5.72
8+00S	5.	300.	1.8	92.	7.04
8+50S	9.	320.	1.8	54.	5.65
9+00S	7.	300.	1.7	52.	6.17
9+50S	9.	300.	1.7	146.	8.06
10+00S	7.	210.	1.9	92.	7.74
10+50S	4.	200.	1.5	96.	5.01
11+00S	6.	450.	1.5	94.	8.18
11+50S	5.	430.	1.9	176.	10.21
12+00S	28.	900.	4.4	102.	17.00
12+50S	7.	450.	3.4	50.	8.16
13+00S	7.	540.	2.1	52.	7.70
13+50S	8.	420.	2.3	44.	9.01
14+00S	8.	490.	2.4	46.	8.79
14+50S	9.	320.	2.2	42.	9.42
15+00S	5.	510.	2.4	66.	11.23
0+50N	12.	200.	2.1	234.	5.11
1+00N	8.	440.	2.9	130.	5.24
1+50N	10.	300.	2.3	136.	5.07
2+00N	19.	140.	2.2	96.	6.34
2+50N	32.	190.	0.7	20.	9.47
3+00N	35.	720.	2.2	144.	7.01
3+50N	32.	160.	2.0	94.	8.31
4+00N	55.	200.	3.4	118.	7.26
4+50N	28.	280.	2.9	74.	8.55
5+00N	41.	340.	2.5	124.	5.41
5+50N	19.	240.	2.3	106.	4.20
6+00N	7.	140.	2.0	92.	5.47
[illegible]	4.	300.	2.5	106.	4.06
[illegible]	5.	320.	2.4	132.	4.27
[illegible]	23.	160.	1.0	120.	6.34
[illegible]	7.	400.	2.0	234.	5.80
[illegible]	[illegible]	[illegible]	[illegible]	[illegible]	7.46
[illegible]	[illegible]	740.	[illegible]	166.	7.36
[illegible]	[illegible]	240.	[illegible]	58.	8.65
[illegible]	[illegible]	280.	[illegible]	42.	7.39
[illegible]	13.	190.	2.1	64.	5.49
[illegible]	[illegible]	440.	2.1	64.	6.91
[illegible]	22.	200.	2.3	80.	6.64
[illegible]	28.	300.	1.5	42.	5.73

22+15E	4+50N	22.	150.	1.9	35.	7.38
22+15E	5+00N	34.	130.	2.8	54.	9.12
22+15E	5+50N	25.	440.	2.8	164.	10.68
22+15E	6+00N	19.	420.	2.5	176.	8.49
22+15E	6+50N	10.	250.	2.3	95.	5.96
22+15E	7+00N	14.	320.	2.7	192.	5.94
22+15E	7+50N	10.	360.	2.2	242.	7.17
22+15E	8+00N	5.	180.	1.9	73.	7.60
22+15E	8+50N	14.	110.	1.4	105.	6.18
22+15E	8+75N	14.	240.	2.4	72.	4.83
22+15E	0+50S	11.	610.	1.8	70.	5.23
22+15E	1+00S	37.	210.	2.7	74.	10.79
22+15E	1+50S	12.	300.	2.4	85.	5.32
22+15E	2+00S	6.	190.	1.9	56.	3.68
22+15E	2+50S	8.	620.	1.7	56.	3.71
22+15E	3+00S	23.	270.	1.9	44.	5.34
22+15E	3+50S	15.	150.	2.5	93.	5.81
22+15E	4+00S	23.	240.	1.9	42.	5.96
22+15E	4+50S	11.	200.	2.3	33.	3.52
22+15E	5+00S	9.	420.	2.0	80.	5.07
22+15E	5+50S	10.	440.	1.7	60.	5.57
22+15E	6+00S	21.	290.	4.0	102.	13.35
22+15E	6+50S	7.	220.	1.3	84.	5.15
22+15E	7+00S	13.	1220.	1.9	90.	4.99
22+15E	7+50S	13.	460.	2.1	92.	5.74
22+15E	8+00S	14.	350.	2.1	50.	5.51
22+15E	8+50S	9.	410.	2.3	80.	5.81
22+15E	9+00S	15.	340.	2.1	54.	4.74
22+15E	9+50S	14.	470.	2.2	52.	4.62
22+15E	10+00S	9.	540.	1.8	44.	5.17
22+15E	10+50S	10.	520.	1.9	34.	9.40
22+15E	11+00S	5.	390.	1.8	45.	7.09
22+15E	11+50S	10.	540.	1.3	50.	3.68
22+15E	12+00S	3.	720.	2.0	53.	7.74
22+15E	12+50S	7.	1540.	1.6	264.	16.85
22+15E	13+00S	10.	740.	1.8	76.	15.65
22+15E	13+50S	12.	380.	1.9	37.	6.21
22+15E	14+00S	4.	420.	1.9	46.	9.31
22+15E	14+50S	4.	300.	1.8	54.	8.12
22+15E	15+00S	2.	590.	2.0	98.	10.59
22+15E	15+50S	4.	480.	1.8	66.	10.39
21+40E	1+50S	13.	220.	1.4	32.	4.11
21+40E	2+00S	11.	1100.	1.7	94.	5.61
21+40E	2+50S	23.	1320.	1.7	53.	16.95
21+40E	3+00S	12.	130.	1.4	44.	4.55
21+40E	3+50S	15.	160.	1.7	36.	4.83
21+40E	4+00S	39.	230.	2.0	124.	14.03
21+40E	4+50S	4.	130.	1.6	34.	3.89
21+40E	5+00S	1.	280.	1.9	53.	4.79
21+40E	5+50S	5.	940.	1.2	74.	8.94
21+40E	6+00S	3.	660.	1.0	62.	4.30
21+40E	6+50S	11.	650.	1.4	51.	6.06
21+40E	7+00S	21.	1280.	1.6	94.	6.97
21+40E	7+50S	25.	2420.	1.7	244.	14.35
21+40E	8+00S	6.	500.	1.9	114.	4.42
21+40E	8+50S	40.	1430.	3.5	152.	22.95
21+40E	9+00S	26.	3050.	1.6	90.	9.95
21+40E	9+50S	19.	1020.	1.4	54.	13.35
21+40E	10+00S	30.	1040.	1.2	50.	10.16
21+40E	10+50S	21.	1000.	1.6	94.	5.21
21+40	11+00S	4.	700.	1.8	40.	8.31
21+40E	11+50S	5.	1590.	1.6	64.	17.65
21+40E	12+00S	6.	830.	1.7	45.	19.45
21+40E	12+50S	15.	900.	2.4	58.	14.35
21+40E	13+00S	7.	570.	1.8	54.	9.62
21+40E	13+50S	1.	310.	1.9	134.	3.69
21+40E	14+00S	2.	540.	1.5	64.	6.75
21+40E	14+50S	13.	330.	2.9	98.	47.15

21+40E	15+00S	4.	1080.	1.5	90.	17.35
21+40E	15+50S	28.	3370.	1.6	190.	27.35
21+40E	0+50N	20.	740.	1.8	96.	8.21
21+40E	1+00N	14.	220.	2.7	78.	0.24
21+40E	1+50N	12.	200.	1.3	75.	11.76
21+40E	2+50N	13.	260.	2.5	40.	8.06

SAMPLE NUMBER	NI	MN	FE	ZN	CONDUCTIVITY
19+15E 8+00S	10.	320.	1.3	72.	9.74
19+15E 8+50S	14.	360.	1.9	48.	8.36
19+15E 9+00S	2.	240.	1.2	50.	5.23
19+15E 9+50S	4.	200.	1.4	76.	7.32
19+15E 10+00S	10.	180.	1.6	40.	4.67
19+15E 10+50S	9.	250.	1.0	94.	3.31
19+15E 11+00S	7.	220.	1.7	70.	5.34
19+15E 11+50S	12.	280.	1.4	46.	8.58
19+15E 12+00S	2.	200.	1.4	50.	4.47
19+15E 12+50S	3.	350.	1.3	46.	2.92
19+15E 13+00S	1.	640.	1.1	76.	5.64
19+15E 13+50S	24.	1000.	3.4	106.	14.90
19+15E 14+00S	3.	380.	1.0	220.	9.97
19+15E 14+50S	3.	320.	1.1	82.	5.80
19+15E 15+00S	2.	700.	1.1	46.	8.41
19+15E 15+50S	12.	1720.	1.7	96.	4.97
19+15E 0+50N	10.	190.	2.4	86.	3.08
19+15E 1+00N	44.	120.	0.2	20.	1.80
19+15E 1+50N	29.	100.	0.2	14.	3.35
19+15E 2+00N	15.	130.	3.1	112.	5.86
19+15E 2+50N	102.	160.	1.0	22.	2.71
19+15E 3+00N	9.	120.	2.4	76.	3.08
19+15E 3+50N	9.	280.	2.4	110.	3.35
19+15E 4+00N	31.	500.	2.1	144.	4.09
19+15E 4+50N	15.	200.	2.8	84.	2.61
19+15E 5+00N	3.	200.	1.8	116.	4.42
19+15E 5+50N	1.	150.	1.4	94.	6.09
19+15E 6+00N	3.	240.	1.9	112.	5.72
19+15E 6+50N	2.	520.	2.0	126.	5.57
19+15E 7+00N	4.	480.	1.2	128.	6.07
19+15E 7+50N	2.	200.	1.5	74.	5.05
19+15E 8+00N	17.	1400.	1.7	54.	5.27
19+15E 8+50N	18.	240.	2.5	74.	5.37
19+15E 9+00N	11.	220.	2.2	298.	4.31
19+15E 9+50N	8.	400.	2.8	308.	3.14
19+15E 10+00N	7.	220.	2.6	208.	4.49
19+15E 10+50N	4.	270.	2.5	70.	3.52
19+15E 11+00N	6.	200.	2.4	68.	3.29
19+15E 11+50N	6.	220.	1.8	74.	3.03
19+15E 12+00N	15.	190.	1.9	48.	2.72
19+15E 12+50N	7.	190.	1.1	32.	4.06
19+15E 13+00N	8.	180.	2.7	18.	1.96
19+15E 13+50N	5.	220.	2.6	122.	5.29
19+15E 14+00N	3.	160.	1.3	42.	5.36
19+15E 14+50N	13.	100.	2.1	2.	9.25
19+15E 15+00N	4.	220.	2.7	80.	3.70
19+15E 15+50N	1.	200.	2.5	49.	3.33
19+15E 16+00N	1.	200.	1.9	38.	3.81
19+15E 16+50N	1.	220.	1.8	24.	4.79
19+15E 17+00N	1.	260.	2.0	30.	2.32
19+15E 17+50N	9.	320.	3.0	54.	6.31
19+15E 18+00N	1.	260.	2.5	40.	3.51
19+15E 18+50N	1.	250.	2.2	44.	2.82
19+15E 19+00N	2.	200.	1.9	24.	4.31
17+65E 0+50S	10.	240.	2.2	54.	4.51
17+65E 1+00S	52.	560.	4.4	172.	3.58
17+65E 1+50S	3.	600.	3.0	172.	12.17
17+65E 2+00S	12.	1520.	2.6	132.	4.22
17+65E 2+50S	12.	160.	2.6	76.	4.94
17+65E 3+00S	10.	230.	2.4	58.	3.45
17+65E 3+50S	12.	360.	2.4	74.	2.72
17+65E 4+50S	12.	240.	2.3	154.	3.43
17+65E 5+00S	14.	1040.	2.0	304.	5.01
17+65E 5+50S	14.	280.	3.0	107.	6.29
17+65E 6+00S	16.	210.	1.4	64.	2.27
17+65E 6+50S	20.	710.	2.0	74.	3.90
17+65E 7+00S	20.	170.	1.4	30.	2.71
17+65E 7+50S	16.	160.	1.4	54.	1.76
17+65E 8+00S	74.	480.	2.0	102.	2.74
17+65E 8+50S	30.	340.	2.2	50.	5.70
17+65E 9+00S	70.	400.	2.0	50.	4.20
17+65E 9+50S	15.	240.	2.0	54.	4.21

13+85E	1+00N	9.	230.	3.1	46.	4.81
13+85E	1+50N	14.	240.	4.3	103.	7.21
13+85E	2+00N	16.	130.	3.3	111.	6.76
13+85E	2+50N	11.	140.	2.9	148.	6.03
13+85E	3+00N	25.	160.	2.0	44.	4.84
13+85E	3+25N	15.	180.	2.6	58.	6.75
13+85E	5+50N	45.	200.	4.2	162.	9.34
13+85E	8+75N	24.	440.	3.2	222.	5.70
13+85E	9+00N	29.	200.	3.0	110.	9.11
13+65E	0+50S	3.	200.	2.0	52.	4.15
13+65E	1+00S	21.	260.	3.7	155.	8.38
13+65E	1+50S	10.	240.	3.4	150.	8.81
13+65E	2+00S	65.	740.	3.8	122.	11.76
13+65E	2+50S	53.	320.	3.4	100.	11.96
13+65E	3+00S	8.	160.	3.2	100.	6.76
13+65E	3+50S	9.	200.	2.5	54.	5.91
13+65E	4+00S	10.	200.	3.4	142.	3.65
13+65E	4+50S	15.	220.	3.7	172.	11.66
13+65E	5+00S	13.	240.	2.7	126.	9.12

SAMPLE	NUMBER	MO	MN	FE	ZN	CONDUCTIVITY
21+40E	2+00N	17.	430.	3.2	112.	10.35
21+40E	4+00N	12.	300.	2.2	94.	11.86
21+40E	4+50N	12.	240.	2.1	55.	24.26
21+40E	5+00N	75.	480.	4.3	120.	9.24
21+40E	5+50N	21.	230.	2.4	50.	9.69
21+40E	6+50N	33.	250.	3.1	150.	7.50
21+40E	7+50N	20.	290.	2.8	112.	4.01
21+40E	8+00N	10.	240.	2.7	118.	9.95
21+40E	8+50N	16.	220.	1.5	124.	5.56
21+40E	9+00N	41.	150.	1.6	216.	5.66
20+65E	0+50S	34.	220.	2.9	52.	7.25
20+65E	1+00S	72.	420.	3.0	98.	7.14
20+65E	1+50S	23.	320.	2.4	96.	7.24
20+65E	2+00S	6.	160.	1.8	42.	3.81
20+65E	2+50S	7.	280.	2.0	56.	5.49
20+65E	3+00S	116.	900.	3.9	126.	12.76
20+65E	3+50S	20.	180.	2.3	56.	6.22
20+65E	4+00S	10.	220.	2.0	62.	4.20
20+65E	4+50S	4.	160.	2.2	82.	4.76
20+65E	5+00S	8.	440.	2.3	70.	3.69
20+65E	5+50S	5.	180.	2.0	112.	5.84
20+65E	6+00S	5.	160.	1.4	112.	5.04
20+65E	6+50S	9.	360.	1.6	164.	5.23
20+65E	7+00S	10.	650.	1.7	230.	5.61
20+65E	7+50S	17.	400.	1.4	122.	5.81
20+65E	8+00S	42.	1160.	2.5	112.	14.56
20+65E	8+50S	16.	320.	1.5	90.	7.48
20+65E	9+00S	4.	180.	2.1	62.	4.69
20+65E	9+50S	9.	280.	1.7	62.	5.93
20+65E	10+00S	13.	300.	2.2	80.	7.31
20+65E	10+50S	32.	1440.	2.5	74.	8.54
20+65E	11+00S	7.	320.	2.4	48.	4.32
20+65E	11+50S	15.	320.	2.4	54.	6.60
20+65E	12+00S	17.	1920.	2.2	324.	19.86
20+65E	12+50S	1.	300.	1.9	152.	7.92
20+65E	13+00S	3.	300.	1.9	162.	7.92
20+65E	13+50S	7.	360.	2.8	72.	5.49
20+65E	14+00S	11.	600.	2.6	90.	11.86
20+65E	14+50S	5.	320.	2.8	82.	7.06
20+65E	15+00S	8.	360.	3.0	66.	10.81
20+65E	15+50S	14.	1170.	2.2	90.	11.26
20+65E	0+50N	79.	160.	3.0	110.	8.75
20+65E	1+00N	24.	120.	2.4	116.	4.63
20+65E	1+50N	25.	260.	2.6	110.	5.50
20+65E	2+00N	10.	160.	2.8	86.	5.29
20+65E	2+50N	39.	280.	3.2	30.	6.60
20+65E	3+00N	19.	200.	2.0	54.	2.77
20+65E	3+50N	14.	140.	3.2	90.	5.41
20+65E	4+00N	6.	220.	2.4	46.	4.08
20+65E	4+50N	12.	240.	2.9	62.	5.98
19+15E	3+50S	12.	130.	2.5	38.	6.11
19+15E	4+00S	5.	200.	1.2	59.	3.17
20+65E	5+00N	8.	240.	2.1	66.	5.07
20+65E	5+50N	41.	290.	3.6	74.	7.39
20+65E	6+00N	8.	200.	2.7	75.	6.47
20+65E	6+50N	9.	220.	2.3	52.	7.28
20+65E	7+00N	27.	140.	1.7	30.	[illegible]
20+65E	7+50N	51.	240.	2.5	335.	5.03
20+65E	8+00N	65.	120.	3.0	220.	7.73
20+65E	8+50N	21.	150.	1.3	90.	6.75

SAMPLE NUMBER	MG	MN	FE	ZN	CONDUCTIVITY
13+4[illegible] 5+[illegible]	2.	240.	2.4	94.	7.70
13+6[illegible] 6+[illegible]	14.	360.	2.1	93.	15.50
13+6[illegible] 6+[illegible]	554.	900.	3.3	284.	14.[illegible]
13+6[illegible] 7+[illegible]	337.	430.	2.1	194.	7.[illegible]
13+6[illegible] 7+[illegible]	27.	430.	2.0	142.	8.18
13+6[illegible] 8+[illegible]	28.	940.	2.1	302.	19.[illegible]
13+6[illegible] 8+[illegible]	41.	240.	2.7	58.	5.90
13+6[illegible] 9+[illegible]	10.	180.	1.8	114.	6.[illegible]
13+6[illegible] 9+[illegible]	4.	120.	1.4	34.	7.55
13+6[illegible] 10+[illegible]	15.	480.	1.9	74.	7.71
13+6[illegible] 10+[illegible]	18.	360.	1.9	100.	6.[illegible]
13+6[illegible] 11+[illegible]	31.	220.	2.0	64.	6.[illegible]
13+6[illegible] 11+[illegible]	15.	200.	1.4	70.	4.[illegible]
13+6[illegible] 12+[illegible]	3.	200.	1.2	54.	3.[illegible]
13+6[illegible] 12+[illegible]	26.	100.	2.[illegible]	212.	18.91
13+6[illegible] 13+[illegible]	144.	520.	2.2	84.	12.46
13+6[illegible] 13+[illegible]	8.	320.	1.9	44.	4.[illegible]
13+6[illegible] 14+[illegible]	5.	280.	1.5	64.	7.[illegible]
13+6[illegible] 14+[illegible]	3.	200.	2.2	54.	5.[illegible]
13+6[illegible] 15+[illegible]	6.	280.	2.[illegible]	64.	9.[illegible]
13+6[illegible] 15+[illegible]	5.	360.	1.[illegible]	86.	8.[illegible]
12+4[illegible] 9+SCN	3.	120.	3.0	66.	5.[illegible]
12+4[illegible] 10+[illegible]	10.	140.	2.7	66.	4.[illegible]
12+4[illegible] 10+SCN	17.	120.	1.8	36.	4.24
12+4[illegible] 11+[illegible]	4.	140.	2.0	44.	4.[illegible]
12+4[illegible] 11+SCN	5.	30.	1.6	30.	4.00
12+4[illegible] 12+[illegible]	5.	140.	2.2	52.	4.[illegible]
12+4[illegible] 12+[illegible]	5.	120.	2.0	92.	4.[illegible]
12+4[illegible] 13+[illegible]	5.	140.	1.9	36.	2.[illegible]
12+4[illegible] 13+SCN	1.	220.	2.7	60.	5.74
12+4[illegible] 14+[illegible]	4.	160.	2.5	56.	3.[illegible]
12+4[illegible] 14+SCN	1.	200.	2.8	50.	4.[illegible]
12+4[illegible] 15+[illegible]	1.	520.	2.9	78.	7.17
12+4[illegible] 15+[illegible]	1.	120.	2.1	52.	6.[illegible]
12+4[illegible] 16+[illegible]	1.	120.	2.0	56.	5.[illegible]
12+4[illegible] 17+[illegible]	1.	230.	2.5	60.	5.01
12+4[illegible] 17+[illegible]	1.	100.	1.7	48.	4.[illegible]
12+4[illegible] 17+[illegible]	1.	120.	2.1	102.	5.[illegible]
12+4[illegible] 18+[illegible]	1.	100.	2.6	86.	4.47
12+4[illegible] 18+[illegible]	1.	120.	2.1	44.	5.94
12+4[illegible] 19+[illegible]	1.	120.	2.5	90.	7.61
10+9[illegible] 0+SCN	4.	230.	2.6	94.	6.21
10+9[illegible] 1+[illegible]	8.	390.	2.5	120.	4.74
10+9[illegible] 1+SCN	6.	640.	4.5	172.	4.[illegible]
10+9[illegible] 2+[illegible]	11.	410.	3.4	86.	6.17
10+9[illegible] 2+SCN	4.	210.	2.2	78.	6.[illegible]
10+9[illegible] 3+[illegible]	3.	270.	2.6	150.	5.[illegible]
10+9[illegible] 3+SCN	38.	380.	2.5	114.	6.[illegible]
10+9[illegible] 4+[illegible]	10.	260.	2.3	72.	5.17
10+9[illegible] 4+SCN	11.	270.	2.3	84.	6.54
10+9[illegible] 5+[illegible]	31.	150.	1.4	38.	5.09
10+9[illegible] 5+SCN	33.	150.	1.3	40.	4.39
10+9[illegible] 6+[illegible]	15.	260.	2.6	180.	7.71
10+9[illegible] 6+SCN	40.	240.	2.5	113.	8.[illegible]
10+9[illegible] 7+[illegible]	20.	270.	2.5	118.	8.72
10+9[illegible] 7+SCN	24.	240.	2.6	116.	7.82
10+9[illegible] 8+[illegible]	14.	130.	2.3	68.	6.67
10+9[illegible] 8+SCN	10.	120.	1.6	76.	6.90
10+9[illegible] 9+[illegible]	11.	220.	1.8	46.	5.26
10+9[illegible] 9+SCN	13.	440.	1.6	62.	8.21

[illegible]	4.	[illegible]	1.[illegible]	144.	15.[illegible]
[illegible]	3.	300.	2.4	70.	10.[illegible]
[illegible]	4.	200.	1.7	74.	17.46
[illegible]	5.	220.	2.0	64.	12.[illegible]
[illegible]	[illegible]	[illegible]	[illegible]	100.	3.[illegible]
[illegible]	[illegible]	[illegible]	[illegible]	[illegible]	3.[illegible]
[illegible]	[illegible]	[illegible]	[illegible]	[illegible]	3.[illegible]
[illegible]	[illegible]	[illegible]	[illegible]	[illegible]	3.[illegible]

10+90E	10+COS	12.	160.	2.0	66.	5.49
10+90E	10+SOS	7.	320.	1.5	78.	7.12
10+90E	11+COS	12.	260.	1.4	74.	5.63
10+90E	11+SOS	42.	180.	1.7	34.	4.06
10+90E	12+COS	24.	200.	1.4	90.	7.09
10+90E	12+SOS	19.	160.	1.2	60.	5.98
10+90E	13+COS	14.	280.	1.6	70.	5.61
10+90E	13+SOS	10.	520.	2.1	76.	7.41
10+90E	14+COS	5.	240.	1.8	66.	4.41
10+90E	14+SOS	3.	850.	1.7	122.	8.02
10+90E	15+COS	5.	220.	1.9	44.	4.36
10+90E	15+SOS	6.	240.	1.6	122.	5.22
10+90E	0+50N	16.	680.	2.7	160.	5.30
10+90E	1+0CN	6.	340.	2.8	126.	4.21
10+90E	1+50N	23.	220.	2.9	142.	3.58
10+90E	2+0CN	18.	930.	2.9	530.	4.02
10+90E	2+50N	16.	180.	2.8	202.	3.26
10+90E	3+0CN	8.	190.	2.9	210.	3.64
10+90E	3+50N	13.	370.	2.9	242.	4.04
10+90E	4+0CN	5.	150.	2.7	94.	3.61
10+90E	4+50N	9.	160.	3.0	64.	4.03
10+90E	5+50N	5.	150.	2.8	174.	7.93
10+90E	6+0CN	17.	190.	2.3	66.	6.04
10+90E	6+50N	49.	280.	3.2	90.	5.26
10+90E	7+0CN	21.	410.	3.6	84.	5.32
10+90E	7+50N	13.	320.	3.1	62.	3.69
10+90E	8+0CN	30.	360.	2.9	70.	4.76
10+90E	8+50N	12.	340.	3.4	64.	4.17
10+90E	10+CON	14.	220.	2.4	58.	3.03
10+90E	10+50N	20.	260.	2.2	44.	2.40
10+90E	11+COS	14.	300.	2.6	64.	2.92
10+90E	11+50S	39.	230.	2.5	56.	2.53
10+90E	12+COS	4.	240.	2.6	58.	2.61
10+90E	12+50N	5.	260.	2.5	62.	6.02
10+90E	13+CON	7.	300.	2.3	46.	2.78
10+90E	13+50N	3.	250.	2.4	54.	2.66
10+90E	14+CON	1.	250.	2.5	67.	2.63
10+90E	14+50N	2.	300.	2.6	66.	1.78
10+90E	15+CON	5.	290.	2.2	54.	1.78
10+90E	15+50N	3.	320.	2.4	54.	2.29
10+90E	16+CON	3.	320.	2.4	38.	1.89
10+90E	16+50N	2.	260.	2.4	56.	2.56
10+90E	17+CON	2.	220.	2.0	64.	3.02
10+90E	17+50N	3.	240.	2.3	50.	4.10
10+90E	18+CON	2.	240.	1.9	42.	2.42
10+90E	18+50N	3.	300.	2.1	46.	1.92
10+90E	19+CON	1.	340.	2.5	110.	3.28
9+40E	0+50S	72.	270.	3.5	258.	5.04
9+40E	1+COS	22.	890.	2.9	148.	3.81
9+40E	1+50S	64.	320.	3.5	124.	5.02
9+40E	2+COS	39.	440.	1.9	124.	4.34
9+40E	2+50S	47.	300.	3.3	104.	4.79
9+40E	3+COS	14.	310.	2.7	74.	3.05
9+40E	3+50S	32.	410.	2.9	94.	3.82
9+40E	4+COS	7.	230.	2.0	60.	2.26
9+40E	4+50S	10.	220.	2.8	42.	2.96
9+40E	5+COS	15.	420.	2.5	274.	2.46
9+40E	5+50S	4.	230.	2.8	68.	2.65
9+40E	6+COS	8.	90.	1.1	44.	3.06
9+40E	6+50S	35.	310.	3.0	206.	5.12
9+40E	7+COS	24.	200.	2.9	64.	4.79
9+40E	7+50S	3.	220.	2.2	132.	3.17
9+40E	8+COS	20.	290.	2.2	54.	3.27
9+40E	8+50S	19.	220.	2.4	140.	3.38
9+40E	9+COS	18.	200.	2.3	110.	3.76
9+40E	9+50S	25.	370.	1.3	282.	3.89
9+40E	10+COS	19.	430.	1.8	500.	3.51
9+40E	10+50S	20.	290.	1.4	326.	3.49
9+40E	11+COS	33.	1690.	2.0	320.	11.21
9+40E	11+50S	110.	290.	1.2	130.	3.13
9+40E	12+COS	50.	560.	1.8	400.	5.15
9+40E	12+50S	101.	1080.	1.7	404.	5.22
9+40E	13+COS	4.	390.	1.1	424.	1.78
9+40E	13+50S	14.	490.	2.0	198.	5.37
9+40E	14+COS	19.	260.	2.2	96.	6.76
9+40E	14+50S	15.	540.	2.4	268.	3.75
9+40E	15+COS	7.	790.	1.3	322.	4.62
9+40E	15+50S	6.	330.	2.2	142.	4.61
9+40E	16+50N	24.	570.	3.1	294.	4.03
9+40E	17+CON	27.	180.	3.0	100.	4.91

SAMPLE NUMBER	MO	MN	FE	ZN	CONDUCTIVITY
4+70S 5+50S	17.	260.	3.3	146.	6.97
4+70E 6+00S	13.	280.	3.8	100.	7.12
4+70E 6+50S	33.	600.	3.5	347.	5.79
19+19S 4+50S	8.	200.	1.1	56.	3.50
19+19S 5+00S	10.	200.	1.7	80.	4.19
19+19S 5+50S	9.	240.	0.7	108.	4.68
4+70S 7+00S	48.	320.	2.0	500.	7.80
4+70E 7+50S	11.	320.	1.3	196.	10.18
4+70S 8+00S	9.	240.	4.4	160.	6.61
4+70S 8+50S	8.	320.	2.9	100.	11.55
4+70S 9+00S	9.	320.	1.4	124.	6.07
4+70E 9+50S	16.	240.	3.2	140.	6.40
4+70S 10+00S	12.	320.	3.0	418.	7.63
4+70E 10+50S	31.	360.	1.6	412.	7.94
4+70E 11+00S	10.	282.	1.2	162.	3.75
4+70E 11+50S	152.	640.	2.5	380.	11.19
4+70S 12+00S	30.	720.	3.0	330.	7.61
4+70E 12+50S	25.	540.	2.8	290.	5.56
4+70S 13+00S	7.	360.	1.8	230.	8.69
4+70E 13+50S	19.	560.	2.2	302.	6.60
4+70S 14+00S	9.	320.	2.1	142.	7.27
4+70S 14+50S	12.	480.	2.5	60.	6.20
4+70S 15+00S	5.	520.	2.2	108.	6.60
4+70E 15+50S	5.	240.	2.0	86.	7.50
4+70S 0+50N	25.	220.	2.3	190.	5.28
4+70E 1+00N	5.	300.	3.7	114.	3.56
4+70E 1+50N	4.	230.	2.3	66.	3.40
4+70E 2+00N	17.	190.	1.8	56.	4.00
4+70E 2+50N	18.	160.	1.6	96.	3.18
4+70E 3+00N	7.	1020.	2.9	306.	4.47
4+70E 3+50N	12.	360.	3.1	122.	4.69
4+70S 4+00N	12.	780.	2.6	230.	5.60
4+70S 4+50N	11.	280.	3.0	130.	5.47
4+70S 5+00N	5.	710.	2.6	254.	5.81
4+70E 5+50N	27.	200.	3.9	58.	13.75
4+70S 6+00N	8.	200.	3.1	100.	7.17
4+70E 6+50N	13.	170.	3.0	76.	2.32
4+70E 7+00N	23.	230.	2.5	220.	4.55
4+70E 7+50N	20.	140.	2.6	72.	12.05
4+70S 8+00N	7.	220.	3.5	64.	10.76
4+70S 8+50N	4.	320.	2.7	52.	2.22
4+70E 9+00N	6.	450.	2.4	150.	3.34
4+70E 9+50N	14.	210.	1.9	80.	3.66
4+70S 10+00N	24.	250.	3.3	78.	4.66
4+70S 10+50N	50.	300.	3.8	324.	3.97
4+70S 11+00N	10.	250.	2.4	54.	4.14
4+70S 11+50N	11.	430.	2.9	150.	5.45
4+70S 12+00N	7.	230.	2.9	140.	4.16
4+70S 12+50N	8.	750.	3.3	160.	2.46
4+70S 13+00N	13.	330.	3.1	104.	4.27
4+70S 13+50N	12.	230.	1.7	52.	7.58
4+70S 14+00N	11.	220.	2.7	68.	4.56
4+70S 14+50N	5.	220.	2.6	70.	6.21
4+70S 15+00N	8.	270.	3.4	104.	5.86
4+70S 15+50N	13.	230.	3.4	74.	8.79
4+70S 16+00N	11.	230.	2.0	44.	5.96
4+70S 16+50N	7.	320.	1.8	104.	5.91
4+70S 17+00N	18.	130.	2.4	48.	7.36
4+70S 17+50N	25.	140.	3.0	44.	8.42
4+70S 18+00N	11.	110.	1.3	24.	7.67

1+65E	1+00N	2.	270.	2.3	75.	3.10
1+65E	1+50N	3.	310.	2.5	80.	2.34
1+65E	2+00N	4.	410.	2.4	119.	4.13
1+65E	2+50N	5.	220.	2.2	60.	1.82
1+65E	3+00N	4.	290.	2.7	108.	3.53
1+65E	3+50N	2.	240.	1.9	40.	2.13
1+65E	4+00N	4.	380.	3.0	94.	4.42
1+65E	4+50N	2.	270.	2.5	54.	3.40
1+65E	5+00N	4.	310.	2.9	123.	4.40
1+65E	5+50N	15.	320.	2.8	236.	3.23
1+65E	6+00N	5.	250.	2.9	63.	2.42
1+65E	6+50N	5.	320.	2.6	122.	2.10
1+65E	7+00N	10.	410.	3.5	125.	4.93
1+65E	7+50N	9.	370.	2.5	84.	4.25
1+65E	8+00N	7.	470.	3.5	175.	6.13
1+65E	8+50N	6.	160.	1.9	39.	4.66
1+65E	9+00N	12.	140.	2.4	33.	8.55
1+65E	9+50N	10.	230.	2.7	52.	5.68
1+65E	10+00N	15.	140.	1.1	22.	4.04
1+65E	10+50N	12.	300.	2.9	52.	3.13
1+65E	11+00N	12.	150.	2.1	32.	3.26
1+65E	11+50N	5.	220.	2.3	42.	3.43
1+65E	12+00N	2.	250.	2.3	65.	5.59
1+65E	12+50N	2.	260.	2.7	72.	3.47
1+65E	13+00N	3.	230.	3.3	75.	3.06
1+65E	13+50N	[illegible]	200.	2.0	70.	2.87
1+65E	14+00N	5.	300.	3.3	70.	4.73
1+65E	14+50N	10.	340.	3.3	130.	6.54
1+65E	15+00N	11.	700.	3.6	159.	5.76
1+65E	15+50N	2.	230.	2.9	62.	4.43
1+65E	16+00N	2.	340.	2.6	54.	3.07
1+65E	16+50N	4.	210.	2.4	43.	3.73
1+65E	17+00N	3.	400.	2.3	102.	5.92
1+65E	17+50N	5.	330.	3.3	54.	3.38
1+65E	18+00N	[illegible]	370.	3.8	170.	4.54
1+65E	18+50N	2.	210.	2.8	102.	4.36
1+65E	19+00N	11.	310.	3.4	122.	4.65
1+65E	19+50N	9.	300.	4.2	62.	5.76
0+20E	0+50S	30.	130.	2.8	54.	6.26
0+20E	1+00S	21.	370.	1.4	116.	3.99
0+20E	1+50S	8.	300.	1.9	65.	4.40
0+20E	2+00S	22.	240.	1.3	70.	7.04
0+20E	2+50S	14.	1250.	2.0	100.	5.46
0+20E	3+00S	5.	340.	3.3	130.	5.49
0+20E	3+50S	8.	740.	2.7	84.	5.37
0+20E	4+00S	6.	1260.	2.7	125.	4.57
0+20E	5+00S	5.	2900.	2.5	346.	9.35
0+20E	5+50S	5.	430.	1.9	75.	4.04
0+20E	6+00S	5.	2900.	2.2	60.	2.68
0+20E	6+50S	2.	660.	2.2	50.	3.44
0+20E	7+00S	3.	300.	2.6	60.	2.82
0+20E	7+50S	3.	260.	2.4	55.	3.37
0+20E	8+00S	29.	410.	1.1	34.	7.64
0+20E	8+50S	73.	920.	1.3	290.	5.25
0+20E	9+00S	81.	950.	2.3	500.	4.45
0+20E	9+50S	11.	300.	2.5	106.	3.15
0+20E	10+00S	39.	1070.	1.5	560.	12.55
0+20E	10+50S	7.	0.	2.5	56.	4.52
0+20E	11+00S	6.	460.	2.0	46.	5.08
0+20E	11+50S	5.	340.	2.2	35.	3.07
0+20E	12+00S	14.	280.	2.1	92.	3.03
0+20E	12+50S	12.	320.	1.8	84.	[illegible]
0+20E	13+00S	37.	1040.	1.6	442.	[illegible]
0+20E	14+00S	18.	1410.	2.5	470.	10.55
0+20E	14+50S	7.	750.	2.3	292.	8.50
0+20E	0+50N	9.	240.	2.5	32.	2.57
0+20E	1+00N	6.	240.	2.5	114.	4.82
0+20E	1+50N	15.	230.	2.8	153.	3.19
0+20E	2+00N	9.	240.	2.4	108.	5.02
0+20E	2+50N	10.	260.	4.1	102.	5.38
0+20E	3+00N	10.	340.	3.6	94.	5.92
0+20E	3+50N	4.	240.	2.4	66.	4.82
0+20E	4+00N	13.	200.	3.3	64.	7.20
0+20E	4+50N	3.	130.	1.3	32.	11.85
0+20E	5+00N	12.	130.	1.6	31.	11.45
0+20E	5+50N	11.	390.	2.8	126.	7.18
0+20E	6+00N	9.	590.	2.6	228.	7.10
0+20E	6+50N	4.	1420.	2.8	256.	7.06
0+20E	7+00N	2.	340.	3.3	92.	5.23
0+20E	7+50N	2.	270.	2.1	42.	2.58

0+20E	8+00N	10.	560.	3.4	110.	7.69
0+20E	8+50N	26.	380.	3.3	36.	1.69
0+20E	9+00N	11.	200.	3.1	58.	4.30
0+20E	9+50N	8.	320.	2.9	68.	4.19
0+20E	10+00N	7.	220.	2.7	86.	4.00
0+20E	10+50N	6.	210.	2.5	64.	5.84
0+20E	11+00N	23.	150.	1.1	24.	7.56
0+20E	11+50N	5.	260.	2.7	62.	7.94
0+20E	12+00N	4.	190.	2.6	60.	6.23
0+20E	12+50N	6.	270.	2.3	106.	7.53
0+20E	13+00N	3.	410.	2.7	90.	8.49
0+20E	13+50N	3.	260.	2.7	60.	5.92
0+20E	14+00N	2.	210.	2.2	56.	6.00
0+20E	14+50N	3.	250.	2.8	80.	7.54
0+20E	15+00N	3.	380.	2.7	142.	8.91
0+20E	15+50N	2.	220.	2.2	44.	7.29
0+20E	16+00N	3.	290.	2.7	73.	4.73
0+20E	16+50N	4.	320.	2.8	90.	8.14
0+20E	17+00N	5.	170.	2.2	62.	5.92
7+00W	7+00S	1.	760.	2.6	88.	10.05
7+00W	7+50S	1.	800.	2.8	152.	8.41
7+00W	8+00S	1.	820.	3.0	316.	7.67
7+00W	8+50S	1.	420.	2.5	94.	4.27
7+00W	9+00S	3.	460.	2.8	80.	8.83
7+00W	9+50S	1.	300.	2.2	50.	8.67
7+00W	10+00S	4.	850.	3.6	92.	8.63
7+00W	10+50S	2.	460.	2.6	48.	1.09
7+00W	11+00S	3.	2400.	5.8	760.	8.71
7+00W	11+50S	1.	500.	2.8	88.	5.47
7+00W	12+00S	5.	640.	2.7	88.	6.90
7+00W	12+50S	1.	260.	2.6	46.	6.72
7+00W	13+00S	1.	540.	2.6	92.	8.32
7+00W	13+50S	1.	380.	2.2	58.	5.21
7+00W	14+00S	1.	510.	1.8	84.	5.61
7+00W	14+50S	1.	300.	2.2	43.	6.46
7+00W	15+00S	1.	580.	2.3	232.	9.34
7+00W	15+50S	1.	340.	2.0	84.	5.62
7+00W	16+00S	2.	840.	3.0	274.	11.49
7+00W	16+50S	2.	500.	2.1	70.	9.62
7+00W	17+00S	2.	1920.	2.6	128.	11.39
7+00W	17+50S	2.	820.	2.3	70.	11.20
7+00W	18+00S	2.	1340.	3.0	132.	14.77
7+00W	18+50S	3.	850.	2.3	54.	8.54
7+00W	19+00S	10.	1040.	2.2	70.	7.24
7+00W	19+50S	3.	800.	2.7	52.	8.21
7+00W	20+00S	3.	860.	2.7	90.	10.89
7+00W	20+50S	5.	480.	2.5	50.	5.65
7+00W	21+00S	2.	360.	2.2	58.	8.36
7+00W	21+50S	4.	880.	3.0	60.	10.09
9+50W	0+50S	3.	480.	2.8	82.	8.33
9+50W	1+00S	1.	280.	1.8	38.	5.36
9+50W	1+50S	3.	580.	2.6	72.	9.55
9+50W	2+00S	1.	340.	2.0	40.	6.66
9+50W	2+50S	2.	260.	2.5	44.	7.62
9+50W	3+00S	1.	300.	2.4	48.	7.14

SAMPLE NUMBER	MO	MN	FE	ZN	CONDUCTIVITY
9+50N 7+50S	3.	300.	2.9	68.	11.75
9+50N 8+00S	4.	240.	3.3	84.	11.48
9+50N 8+50S	4.	720.	2.0	136.	6.51
9+50N 9+00S	1.	380.	2.2	40.	4.56
9+50N 9+50S	1.	380.	3.7	86.	9.19
9+50N 10+00S	1.	640.	2.2	56.	9.10
9+50N 10+50S	1.	240.	2.6	42.	5.39
9+50N 11+00S	1.	700.	3.0	140.	5.44
9+50N 11+50S	1.	300.	2.0	58.	4.58
9+50N 12+00S	1.	300.	1.9	40.	4.60
9+50N 12+50S	1.	280.	2.1	38.	4.30
9+50N 13+00S	1.	300.	1.9	40.	5.68
9+50N 13+50S	2.	480.	2.3	60.	7.33
9+50N 14+00S	1.	300.	1.8	50.	7.29
9+50N 14+50S	1.	420.	1.9	70.	7.90
9+50N 15+00S	2.	340.	2.0	62.	5.98
10+00N 0+50S	6.	760.	2.0	90.	5.40
10+00N 1+00S	1.	420.	2.0	42.	7.09
10+00N 1+50S	7.	520.	2.0	90.	6.77
10+00N 2+00S	1.	240.	2.0	36.	5.38
10+00N 2+50S	1.	420.	2.1	76.	8.52
10+00N 3+00S	4.	360.	2.8	48.	4.23
10+00N 3+50S	2.	420.	2.8	64.	4.79
10+00N 4+00S	1.	300.	2.7	60.	5.17
10+00N 4+50S	1.	440.	2.8	70.	8.54
10+00N 5+00S	1.	300.	2.5	128.	5.87
10+00N 5+50S	1.	600.	2.9	72.	5.21
10+00N 6+00S	1.	260.	2.5	50.	5.71
10+00N 6+50S	4.	600.	3.7	74.	7.71
10+00N 7+00S	2.	340.	2.6	48.	8.00
10+00N 7+50S	3.	700.	2.7	78.	12.05
10+00N 8+00S	3.	300.	2.1	46.	2.78
10+00N 8+50S	3.	500.	2.8	82.	5.41
10+00N 9+00S	2.	320.	2.4	54.	4.96
10+00N 9+50S	2.	320.	2.1	40.	2.16
10+00N 10+00S	2.	300.	2.7	64.	3.73
10+00N 10+50S	2.	320.	2.3	54.	3.74
10+00N 11+00S	2.	320.	2.5	70.	4.48
10+00N 11+50S	3.	500.	2.2	38.	4.00
10+00N 12+00S	4.	380.	2.3	52.	4.34
10+00N 12+50S	7.	300.	2.2	66.	5.73
10+00N 13+00S	10.	300.	2.4	80.	6.54
10+00N 13+50S	5.	400.	2.3	74.	4.66
10+00N 14+00S	17.	400.	2.7	56.	3.58
10+00N 14+50S	2.	140.	2.2	70.	8.56
10+00N 15+00S	4.	620.	2.3	38.	4.06
10+00N 15+50S	5.	660.	2.6	250.	6.72
10+00N 16+00S	7.	520.	2.5	210.	7.71
10+00N 16+50S	2.	340.	2.4	62.	4.92
12+00N 0+00S	8.	700.	2.5	94.	8.37
12+00N 0+50S	5.	340.	2.4	68.	5.43
12+00N 1+00S	3.	420.	2.4	60.	7.82
12+00N 1+50S	5.	540.	2.8	109.	10.26
12+00N 2+00S	4.	180.	2.3	76.	9.51
12+00N 2+50S	4.	320.	2.6	116.	11.29
12+00N 3+00S	4.	340.	2.0	42.	8.32
12+00N 3+50S	3.	540.	2.4	73.	7.26
12+00N 4+00S	3.	400.	2.0	102.	8.77
12+00N 4+50S	3.	420.	2.4	62.	12.09
12+00N 5+00S	3.	260.	1.7	44.	6.75

12+	1+55	2.	220.	2.1	38.	8.06
12+	1+55	2.	220.	1.7	38.	6.25
12+	0+55	4.	440.	3.0	72.	10.79
12+	0+55	4.	720.	4.0	94.	18.99
12+	1+00	3.	420.	2.7	58.	7.31
12+	1+55	2.	230.	2.0	46.	5.98
12+	2+00	2.	220.	2.0	46.	7.41
12+	2+55	4.	1040.	3.7	92.	12.06
12+	3+00	2.	400.	2.7	66.	10.29
12+	3+55	1.	340.	2.2	40.	5.20
12+	4+00	1.	400.	2.6	54.	7.74
12+	4+55	2.	380.	2.5	48.	4.79
12+	5+00	4.	960.	4.5	120.	13.29
12+	5+55	3.	420.	3.0	62.	7.21
12+	6+00	3.	940.	2.9	70.	10.39
12+	6+55	2.	420.	3.2	70.	9.41
12+	7+00	2.	940.	3.1	68.	9.60
12+	7+55	2.	360.	2.7	54.	15.79
12+	8+00	1.	660.	3.4	82.	9.07
12+	8+55	3.	420.	4.1	96.	21.89
12+	9+00	4.	940.	2.5	58.	8.57
12+	9+55	6.	360.	2.7	54.	30.69
12+	10+00	4.	660.	2.7	72.	8.05
12+	10+55	4.	860.	2.6	70.	6.66
12+	11+00	4.	440.	2.3	62.	8.14
12+	11+55	1.	360.	2.1	66.	7.02
12+	12+00	1.	260.	2.1	86.	7.28
13+	12+55	2.	400.	2.0	64.	7.60
13+	13+00	1.	300.	2.2	56.	4.91
13+	13+55	4.	480.	2.4	82.	8.60
13+	14+00	2.	440.	2.5	72.	6.66
13+	14+55	1.	300.	2.4	60.	7.47
13+	15+00	2.	240.	2.2	68.	6.74
13+	15+55	5.	340.	1.8	56.	7.00
13+	16+00	1.	300.	2.3	140.	4.56
13+	16+55	1.	280.	2.0	100.	9.78
13+	17+00	2.	360.	2.1	38.	3.12
13+	17+55	1.	220.	1.9	38.	5.65
13+	18+00	1.	180.	1.5	30.	4.27
13+	18+55	1.	260.	2.0	38.	5.38
13+	19+00	1.	260.	1.9	38.	5.20
13+	19+55	1.	580.	2.8	114.	12.35
13+	20+00	1.	380.	2.8	54.	7.72
13+	20+55	6.	940.	2.3	90.	12.35
13+	21+00	4.	210.	1.5	38.	5.73
13+	21+55	3.	300.	1.9	64.	9.43
13+	22+00	3.	260.	1.8	42.	7.44
13+	22+55	2.	200.	1.5	44.	5.72
13+	23+00	1.	240.	1.9	66.	9.19
13+	23+55	1.	300.	2.1	54.	6.30
13+	24+00	1.	520.	2.6	82.	8.72
13+	24+55	1.	280.	2.1	44.	6.91
13+	25+00	1.	230.	1.7	34.	9.37
13+	25+55	3.	240.	1.7	34.	6.23
13+	26+00	1.	200.	1.5	30.	5.72
13+	26+55	1.	240.	1.3	28.	3.39
13+	27+00	3.	1220.	5.0	96.	8.66
13+	27+55	1.	400.	2.6	58.	2.30
13+	28+00	2.	920.	4.3	110.	10.35
13+	28+55	1.	320.	2.4	42.	4.78
13+	29+00	1.	460.	2.7	52.	4.56
13+	29+55	1.	240.	2.4	46.	4.47
13+	30+00	1.	320.	1.9	30.	2.69
13+	30+55	1.	280.	2.2	40.	3.38
13+	31+00	1.	420.	3.6	80.	3.73
13+	31+55	1.	480.	6.0	78.	9.17
13+	32+00	1.	280.	2.3	34.	3.12
13+	32+55	1.	280.	2.3	36.	5.57
13+	33+00	1.	520.	3.2	76.	3.46
13+	33+55	1.	480.	2.6	48.	8.24
13+	34+00	1.	860.	3.0	64.	6.36
13+	34+55	1.	360.	2.6	56.	5.14
13+	35+00	1.	240.	2.1	46.	8.22
13+	35+55	1.	330.	2.8	62.	5.46
13+	36+00	1.	240.	2.0	38.	3.36
13+	36+55	1.	400.	2.2	60.	6.35
13+	37+00	1.	240.	2.7	58.	6.49
13+	37+55	1.	240.	2.7	74.	9.51
13+	38+00	1.	260.	2.0	42.	4.17
13+	38+55	1.	920.	4.3	110.	10.96

SAMPLE NUMBER	MO	MN	FE	ZN	CONDUCTIVITY
26+15S 1+50N	74.	3160.	2.5	304.	0.00
26+15S 2N	14.	330.	2.0	42.	0.00
26+15S 2+50N	15.	720.	2.3	240.	0.000
26+15S 3N	20.	1120.	2.5	96.	0.000
26+15S 3+50N	14.	480.	2.6	154.	0.000
24+40S 0+50N	10.	240.	1.6	74.	0.000
23+65S 1S+00S	4.	440.	1.3	84.	0.000
21+40S 0+00S	24.	220.	2.0	60.	0.000
21+40S 1+00S	20.	360.	2.0	70.	0.000
19+00S 0+50N	19.	300.	2.7	94.	0.000
17+60S 1+00S	6.	150.	2.4	74.	0.000
16+40S 0+50S	4.	140.	1.6	44.	0.000
18+40S 1+00S	6.	190.	1.5	40.	0.000
18+40S 1+50S	10.	200.	1.3	44.	0.000
18+40S 2+00S	190.	2300.	4.4	190.	0.000
18+40S 2+50S	10.	640.	3.2	174.	0.000
18+40S 3+00S	10.	440.	2.3	94.	0.000
18+40S 3+50S	7.	280.	1.8	72.	0.000
18+40S 4+00S	6.	200.	1.5	56.	0.000
18+40S 4+50S	8.	240.	2.0	68.	0.000
18+40S 5+00S	8.	240.	2.5	90.	0.000
18+40S 5+50S	5.	1000.	1.1	94.	0.000
18+40S 6+00S	1.	600.	1.4	42.	0.000
18+40S 6+50S	13.	400.	1.8	50.	0.000
18+40S 7+00S	10.	140.	1.3	60.	0.000
18+40S 7+50S	11.	320.	1.3	72.	0.000
18+40S 8+00S	13.	240.	1.3	60.	0.000
18+40S 8+50S	7.	240.	1.7	52.	0.000
18+40S 9+00S	7.	180.	1.8	48.	0.000
18+40S 9+50S	10.	160.	2.1	36.	0.000
18+40S 10+00S	4.	120.	1.9	54.	0.000
18+40S 10+50S	11.	300.	1.2	44.	0.000
18+40S 11+00S	14.	400.	2.1	60.	0.000
18+40S 11+50S	26.	700.	4.0	114.	0.000
18+40S 12+00S	14.	560.	1.8	82.	0.000
18+40S 12+50S	9.	280.	1.3	70.	0.000
18+40S 13+00S	10.	1360.	1.3	168.	0.000
18+40S 13+50S	9.	720.	1.2	184.	0.000
18+40S 14+00S	5.	280.	1.4	54.	0.000
18+40S 14+50S	4.	540.	1.3	44.	0.000
18+40S 0+50N	36.	620.	2.0	66.	0.000
18+40S 1+00N	38.	240.	1.6	42.	0.000
18+40S 1+50N	11.	200.	1.6	54.	0.000
18+40S 2+00N	14.	580.	1.8	66.	0.000
18+40S 2+50N	34.	240.	1.7	58.	0.000
18+40S 3+00N	95.	220.	1.8	42.	0.000
18+40S 3+50N	22.	280.	1.9	104.	0.000
18+40S 4+00N	16.	190.	1.4	38.	0.000
18+40S 4+50N	27.	60.	1.1	58.	0.000
18+40S 5+00N	24.	140.	1.3	86.	0.000
18+40S 5+50N	20.	140.	2.0	78.	0.000
18+40S 6+00N	22.	160.	2.4	318.	0.000
18+40S 6+50N	12.	160.	2.0	46.	0.000
18+40S 7+00N	50.	200.	2.1	96.	0.000
18+40S 7+50N	26.	120.	1.2	34.	0.000
18+40S 8+00N	22.	160.	2.1	54.	0.000
18+40S 8+50N	44.	140.	2.0	208.	0.000
18+40S 9+00N	33.	240.	3.5	80.	0.000
18+40S 9+50N	5.	120.	1.9	52.	0.000
18+40S 10+00N	100.	1460.	3.8	62.	0.00

15+40S	13+50N	9.	260.	3.8	110.	0.000
15+40S	14+00N	5.	240.	3.7	94.	0.000
15+40S	14+50N	5.	360.	3.8	60.	0.000
15+40S	15+00N	4.	220.	3.5	152.	0.000
15+40S	15+50N	4.	300.	4.0	52.	0.000
15+40S	16+00N	4.	180.	3.0	62.	0.000
15+40S	16+50N	5.	290.	3.7	70.	0.000
15+40S	17+00N	10.	700.	4.7	80.	0.000
15+40S	17+50N	3.	220.	3.7	50.	0.000
15+40S	18+00N	1.	200.	3.1	43.	0.000
15+40S	18+50N	3.	240.	3.9	68.	0.000
15+40S	19+00N	4.	220.	3.2	64.	0.000
12+45S	0+50S	7.	240.	2.4	58.	0.000
12+45S	1+00S	6.	340.	3.4	72.	0.000
12+45S	1+50S	5.	400.	2.7	58.	0.000
12+45S	2+00S	6.	340.	2.4	48.	0.000
12+45S	2+50S	5.	480.	2.4	70.	0.000
12+45S	3+00S	12.	290.	1.8	48.	0.000
12+45S	3+50S	8.	320.	2.0	30.	0.000
12+45S	4+00S	11.	430.	2.4	58.	0.000
12+45S	4+50S	7.	200.	2.5	74.	0.000
12+45S	5+00S	8.	190.	2.2	44.	0.000
12+45S	5+50S	9.	200.	2.2	70.	0.000
12+45S	6+00S	11.	240.	1.6	48.	0.000
12+45S	6+50S	10.	160.	1.6	112.	0.000
12+45S	7+00S	27.	140.	1.0	44.	0.000
12+45S	7+50S	20.	230.	1.8	188.	0.000
12+45S	8+00S	118.	1390.	2.7	360.	0.000
12+45S	8+50S	14.	180.	1.6	86.	0.000
12+45S	9+00S	17.	200.	1.9	78.	0.000
12+45S	9+50S	7.	260.	2.0	102.	0.000
12+45S	10+00S	11.	240.	2.5	84.	0.000
12+45S	10+50S	25.	200.	1.4	43.	0.000
12+45S	11+00S	23.	260.	1.6	44.	0.000
12+45S	11+50S	13.	320.	2.0	142.	0.000
12+45S	12+00S	12.	300.	1.4	38.	0.000
12+45S	12+50S	7.	260.	1.6	54.	0.000
12+45S	13+00S	5.	320.	2.0	114.	0.000
12+45S	13+50S	2.	180.	1.4	142.	0.000
12+45S	14+00S	1.	200.	1.6	122.	0.000
12+45S	14+50S	2.	440.	2.4	186.	0.000
12+45S	15+00S	62.	940.	3.7	272.	0.000
12+45S	15+50S	29.	320.	1.9	84.	0.000
12+45S	0+50N	5.	190.	2.7	58.	0.000
12+45S	1+00N	6.	240.	3.7	94.	0.000
12+45S	1+50N	6.	180.	2.5	40.	0.000
12+45S	2+00N	11.	200.	2.3	130.	0.000
12+45S	2+50N	6.	180.	2.3	116.	0.000
12+45S	3+00N	9.	200.	2.4	50.	0.000
12+45S	3+50N	14.	300.	3.0	110.	0.000
12+45S	4+00N	12.	280.	2.9	100.	0.000
12+45S	4+50N	13.	320.	2.5	104.	0.000
12+45S	5+00N	7.	240.	2.7	106.	0.000
12+45S	5+50N	5.	160.	2.8	66.	0.000
12+45S	6+00N	10.	240.	3.3	74.	0.000
12+45S	6+50N	8.	300.	4.4	94.	0.000
12+45S	7+00N	13.	320.	4.3	76.	0.000
12+45S	7+50N	83.	260.	3.9	82.	0.000
12+45S	8+00N	8.	240.	2.9	62.	0.000
12+45S	8+50N	11.	120.	2.3	26.	0.000
12+45S	9+00N	8.	160.	2.8	44.	0.000
11+45S	9+00S	123.	220.	2.7	66.	0.000
11+45S	9+50S	92.	200.	3.2	178.	0.000
11+45S	10+00N	5.	220.	3.3	54.	0.000
11+45S	10+50N	11.	320.	2.9	62.	0.000
11+45S	11+00N	9.	260.	2.8	58.	0.000
11+45S	11+50N	8.	400.	4.9	90.	0.000
11+45S	12+00N	5.	28.	2.9	56.	0.000
11+45S	12+50N	1.	260.	2.8	46.	0.000
11+45S	13+00N	1.	220.	2.5	54.	0.000
11+45S	13+50N	1.	220.	2.4	44.	0.000
11+45S	14+00N	1.	260.	2.6	44.	0.000
11+45S	14+50N	13.	460.	2.8	72.	0.000
11+45S	15+00N	7.	180.	2.9	52.	0.000
11+45S	15+50N	1.	260.	2.8	52.	0.000
11+45S	16+00N	1.	240.	2.8	32.	0.000
11+45S	16+50N	1.	240.	2.6	52.	0.000
11+45S	17+00N	1.	260.	2.6	40.	0.000
11+45S	17+50N	1.	240.	2.9	30.	0.000
11+45S	18+00N	1.	200.	2.5	78.	0.000

11+65E	18+50N	7.	420.	4.4	215.	0.00
11+65E	19+00N	1.	720.	2.5	77.	0.00
7+70E	0+50S	3.	280.	4.4	108.	0.00
7+70E	1+00S	20.	240.	1.8	206.	0.00
7+70E	1+50S	10.	220.	5.2	300.	0.00
7+70E	2+00S	16.	390.	4.8	293.	0.00
7+70E	2+50S	5.	250.	5.6	32.	0.00
7+70E	3+00S	25.	1020.	2.6	394.	0.00
7+70E	3+50S	6.	330.	2.5	122.	0.00
7+70E	4+00S	12.	260.	2.3	53.	0.00
7+70E	4+50S	16.	230.	2.6	218.	0.00
7+70E	5+00S	28.	320.	2.3	180.	0.00
7+70E	5+50S	5.	420.	1.8	108.	0.00
7+70E	6+00S	50.	1620.	2.7	216.	0.00
7+70E	6+50S	43.	1760.	2.2	334.	0.00
7+70E	7+00S	24.	320.	2.3	94.	0.00
7+70E	7+50S	21.	300.	2.7	107.	0.00
7+70E	8+00S	38.	320.	2.0	75.	0.00
7+70E	8+50S	31.	280.	2.2	104.	0.00
7+70E	9+00S	52.	430.	2.5	110.	0.00
7+70E	9+50S	71.	320.	2.2	102.	0.00
7+70E	10+00S	60.	920.	1.3	173.	0.00
7+70E	10+50S	12.	240.	1.7	200.	0.00
7+70E	11+00S	100.	200.	0.9	102.	0.00
7+70E	11+50S	18.	1550.	1.6	1260.	0.00
7+70E	12+00S	162.	820.	2.3	156.	0.00
7+70E	12+50S	9.	300.	1.4	54.	0.00
7+70E	13+00S	13.	220.	1.5	36.	0.00
7+70E	13+50S	6.	260.	1.6	166.	0.00
7+70E	14+00S	400.	650.	4.4	330.	0.00
7+70E	14+50S	6.	500.	2.0	105.	0.00
7+70E	15+00S	3.	460.	1.7	32.	0.00
7+70E	15+50S	2.	330.	1.9	120.	0.00
7+70E	9+50N	25.	250.	3.4	82.	0.00
7+70E	10+00N	9.	130.	2.0	70.	0.00
7+70E	11+00N	34.	270.	3.1	109.	0.00
7+70E	11+50N	15.	620.	3.0	75.	0.00
7+70E	12+00N	5.	240.	2.4	43.	0.00
7+70E	12+50N	4.	340.	2.5	44.	0.00
7+70E	13+00N	4.	280.	2.9	63.	0.00
7+70E	13+50N	4.	300.	3.2	75.	0.00
7+70E	14+00N	16.	300.	2.4	52.	0.00
7+70E	14+50N	13.	230.	2.5	43.	0.00
7+70E	15+00N	59.	340.	2.6	90.	0.00
7+70E	15+50N	1.	200.	2.8	66.	0.00
7+70E	16+00N	1.	360.	2.8	76.	0.00
7+70E	16+50N	3.	360.	2.3	54.	0.00
7+70E	17+00N	10.	320.	2.2	64.	0.00
7+70E	17+50N	13.	420.	2.4	62.	0.00
7+70E	18+00N	37.	580.	2.8	90.	0.00
7+70E	18+50N	51.	340.	2.6	260.	0.00
7+70E	19+00N	15.	400.	2.5	104.	0.00
6+25E	0+50S	6.	280.	2.9	32.	0.00
6+25E	1+00S	34.	360.	2.9	204.	0.00
6+25E	1+50S	11.	260.	3.0	140.	0.00
6+25E	2+00S	12.	540.	2.6	146.	0.00
6+25E	2+50S	11.	330.	2.9	170.	0.00
6+25E	3+00S	13.	280.	2.7	256.	0.00
6+25E	3+50S	133.	500.	3.1	174.	0.00
6+25E	4+00S	14.	380.	3.3	232.	0.00
6+25E	4+50S	36.	1650.	2.7	284.	0.00
6+25E	5+00S	1.	300.	2.6	250.	0.00
6+25E	5+50S	2.	320.	2.6	68.	0.00
6+25E	6+00S	4.	520.	2.5	34.	0.00
6+25E	6+50S	4.	300.	2.0	76.	0.00
6+25E	7+00S	3.	290.	2.2	106.	0.00
6+25E	7+50S	12.	1500.	2.2	220.	0.00
6+25E	8+00S	20.	1030.	2.1	362.	0.00
6+25E	8+50S	22.	300.	2.0	253.	0.00
6+25E	9+00S	30.	250.	1.8	323.	0.00
6+25E	9+50S	108.	740.	2.6	226.	0.00
6+25E	10+00S	22.	240.	1.9	158.	0.00
6+25E	10+50S	157.	340.	2.5	132.	0.00
6+25E	11+00S	20.	900.	1.0	222.	0.00
6+25E	11+50S	23.	320.	1.9	118.	0.00
6+25E	12+00S	4.	200.	1.9	106.	0.00
6+25E	12+50S	5.	220.	1.4	115.	0.00
6+25E	13+00S	5.	320.	1.4	178.	0.00
6+25E	13+50S	364.	2000.	3.2	300.	0.00
6+25E	14+00S	2.	130.	3.3	52.	0.00

APPENDIX B

X-Y diagrams and correlation coefficients for the entire study area.

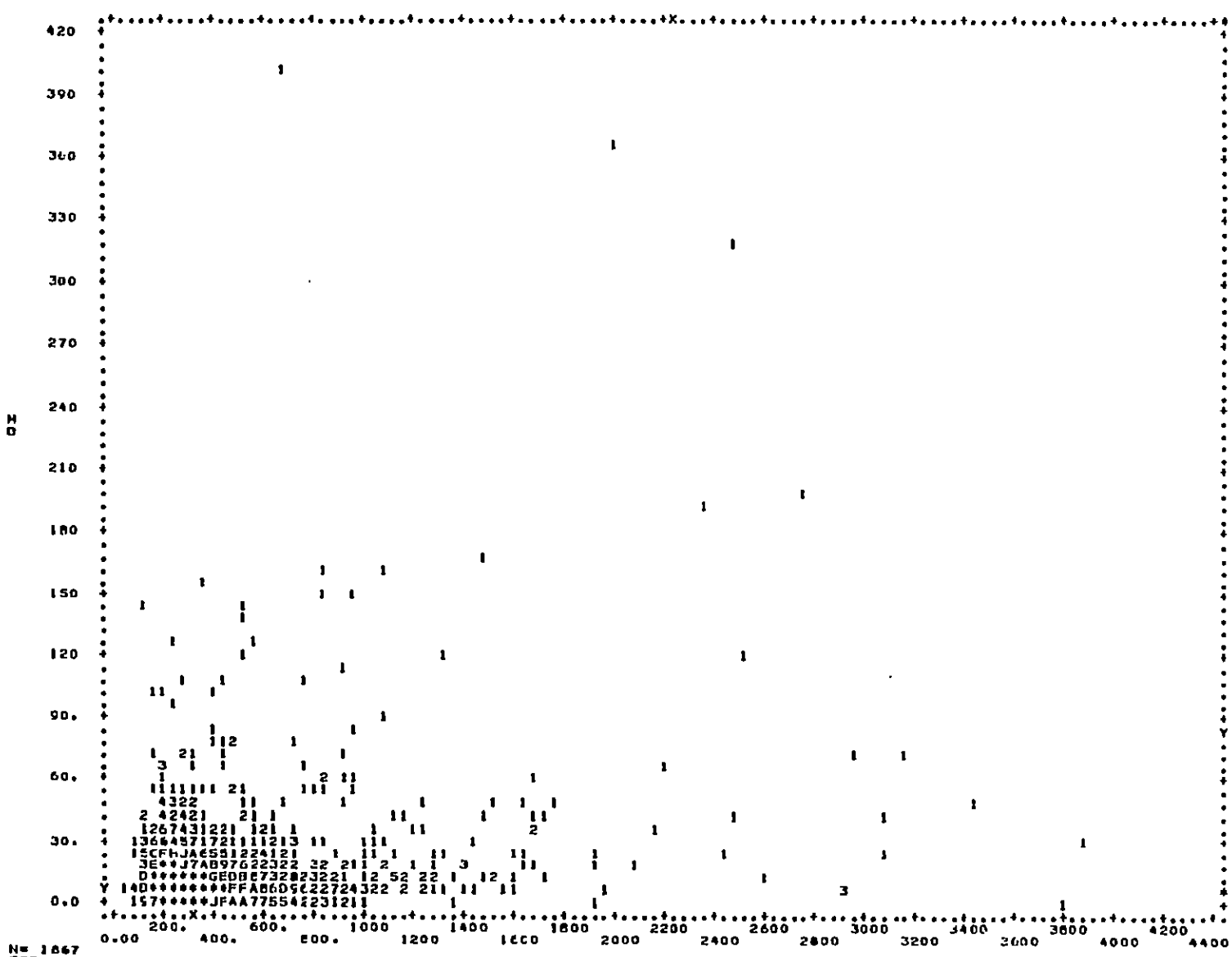

	MEAN	ST.DEV.	REGRESSION LINE	RES.MS.
X	400.70	371.86	Y= 4.4695*Y+ 338.95	127192
Y	13.816	23.635	Y= .01805*X+ 6.9811	513.79

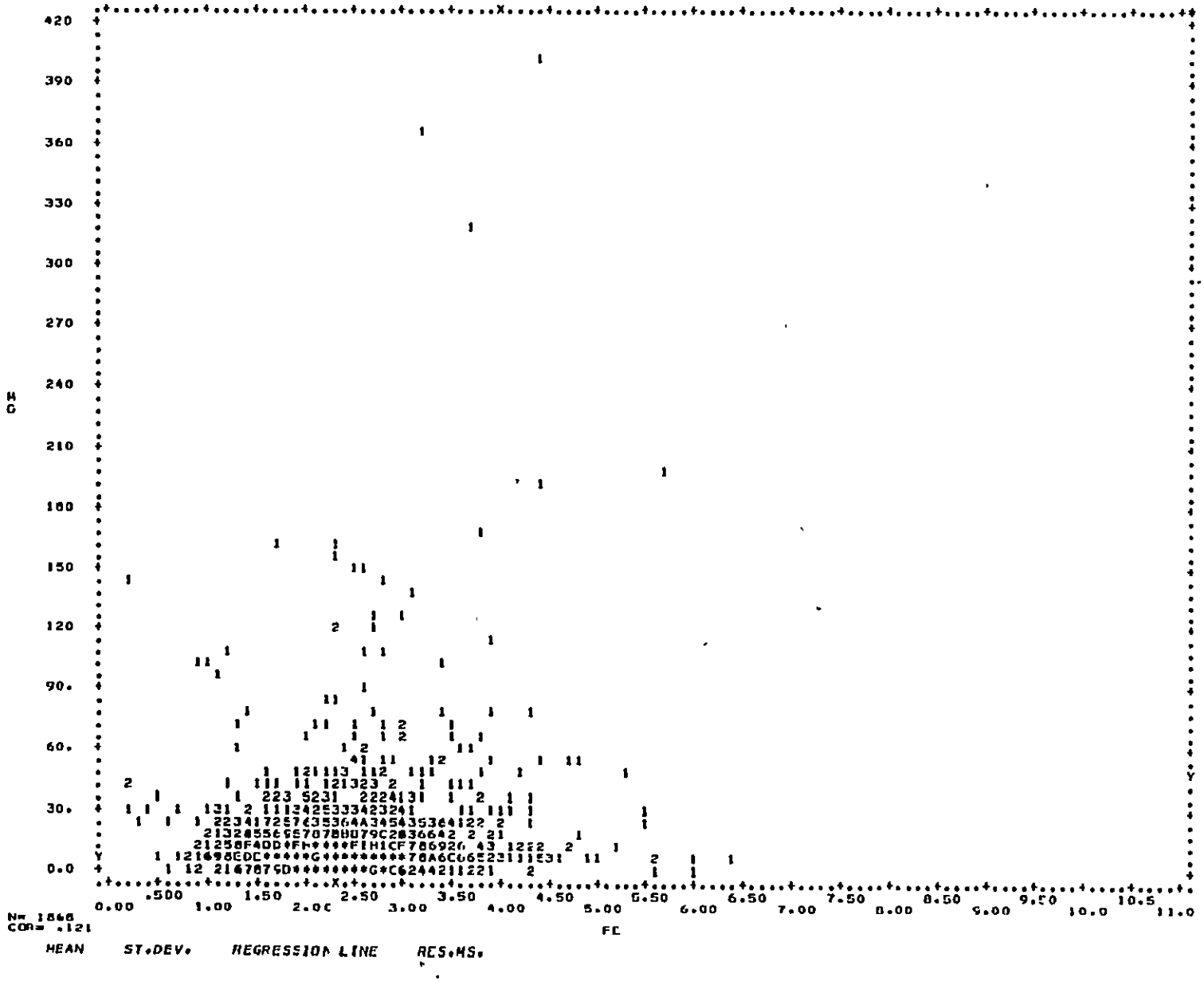
MC
FE
N= 1866
COR= .121
MEAN ST.DEV. REGRESSION LINE RES.MS.
X 2.4038 .74464 X= .00383*Y+ 2.3509 .54660
Y 13.812 23.629 Y= 3.8560*X+ 4.5455 550.38

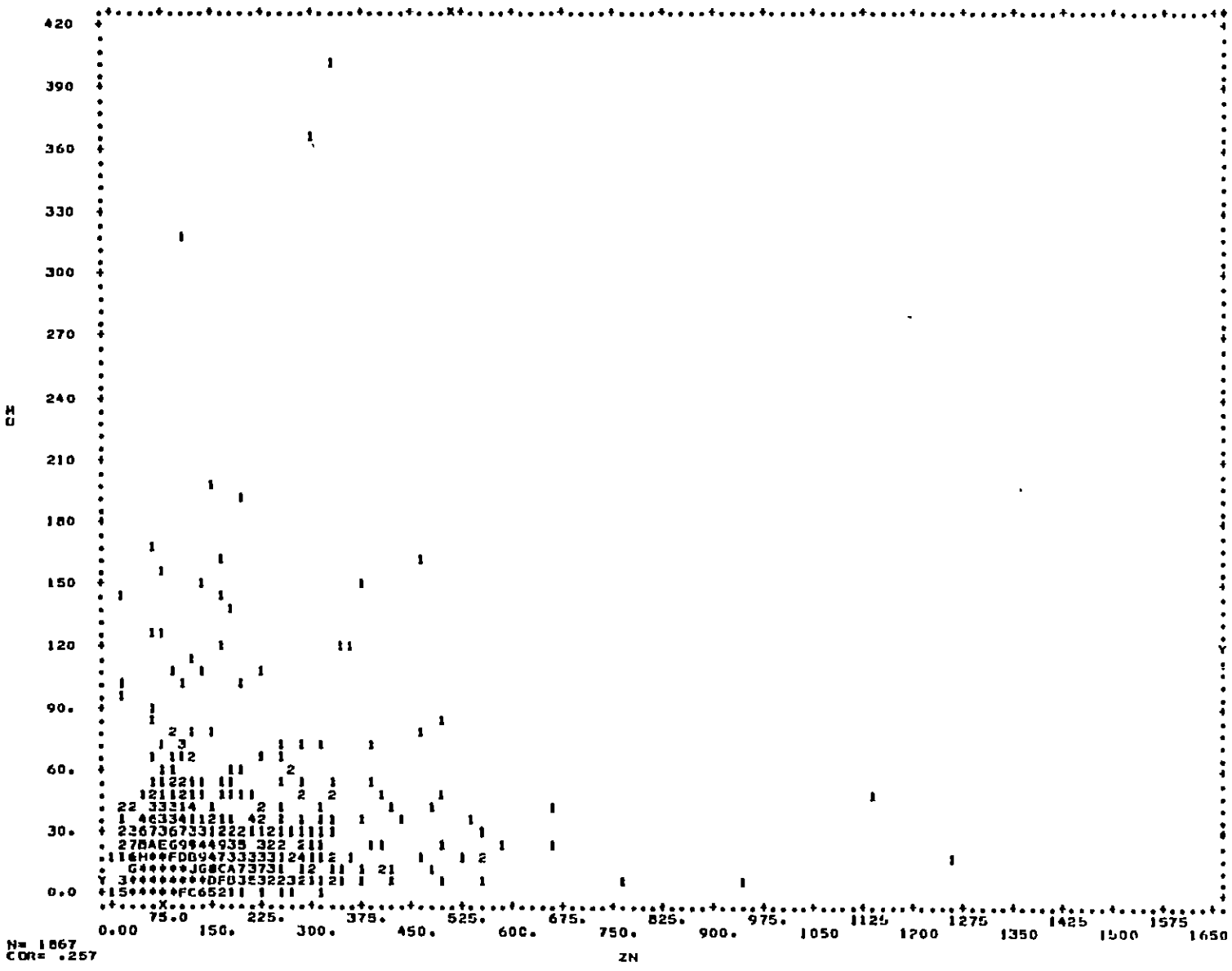

N= 1867
COR= .257

	MEAN	ST.DEV.	REGRESSION LINE	RES.MS.
X	101.26	69.580	X= .97555*Y+ 87.791	7496.5
Y	13.804	23.633	Y= .06793*X+ 6.9257	521.77

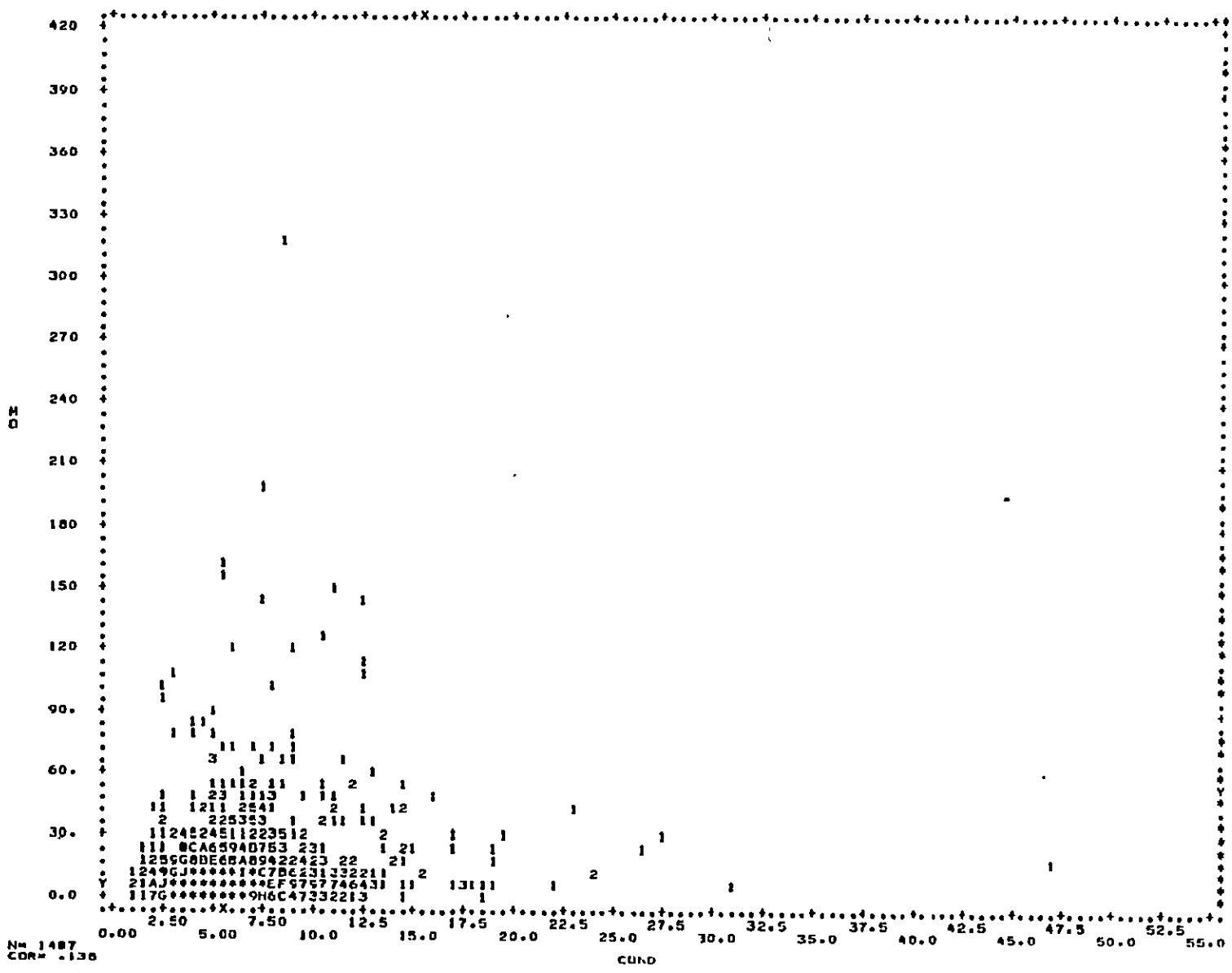

	MEAN	ST.DEV.	REGRESSION LINE	RES.MS.
X	6.0673	3.2664	X= .02320*Y+ 5.7643	10.474
Y	13.058	19.382	Y= .81688*X+ 8.1019	368.78

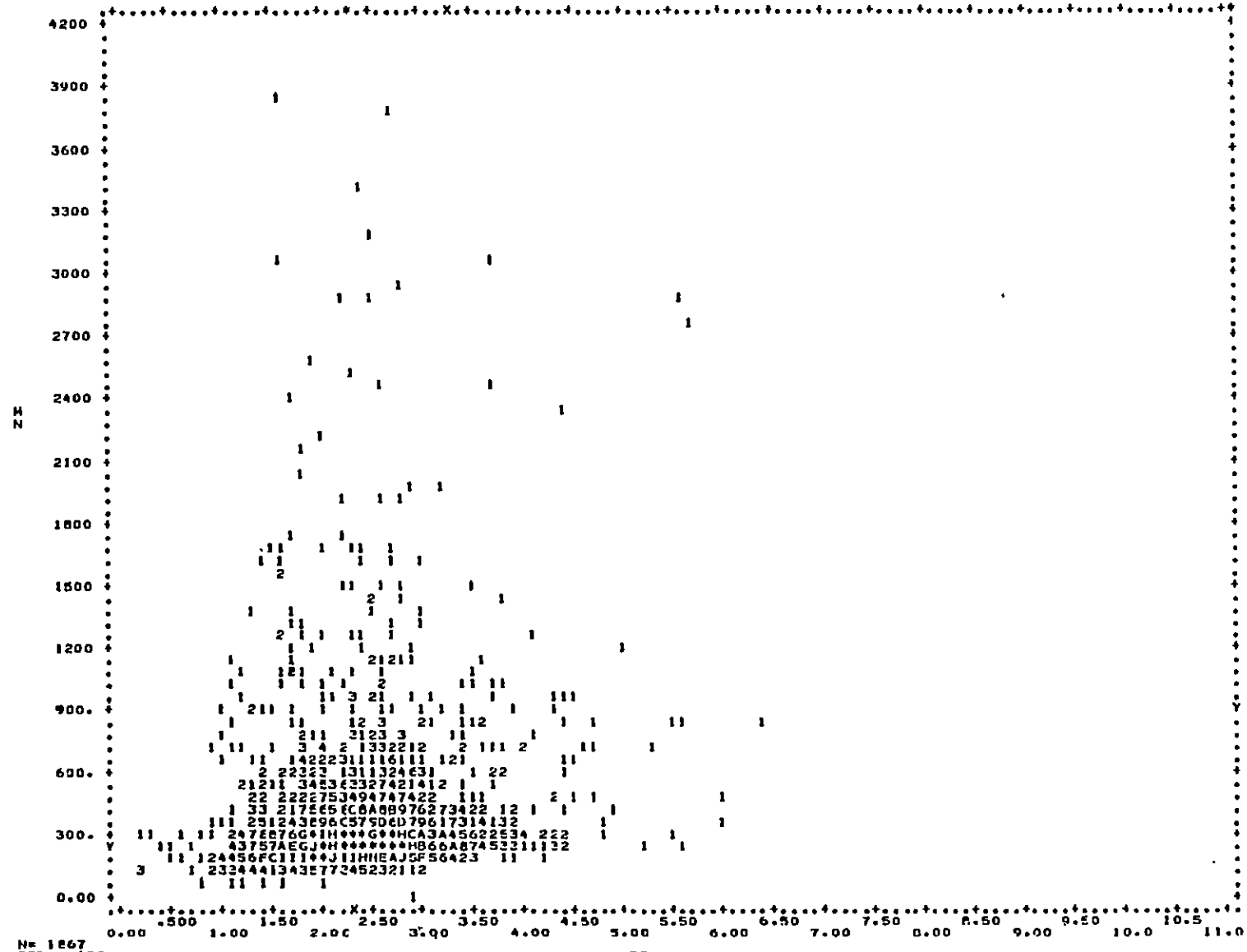

N= 1867
COR= .120

	MEAN	ST.DEV.	REGRESSION LINE	RES.MS.
X	2.4038	.74484	M= 240E-04Y+ 2.3076	.54711

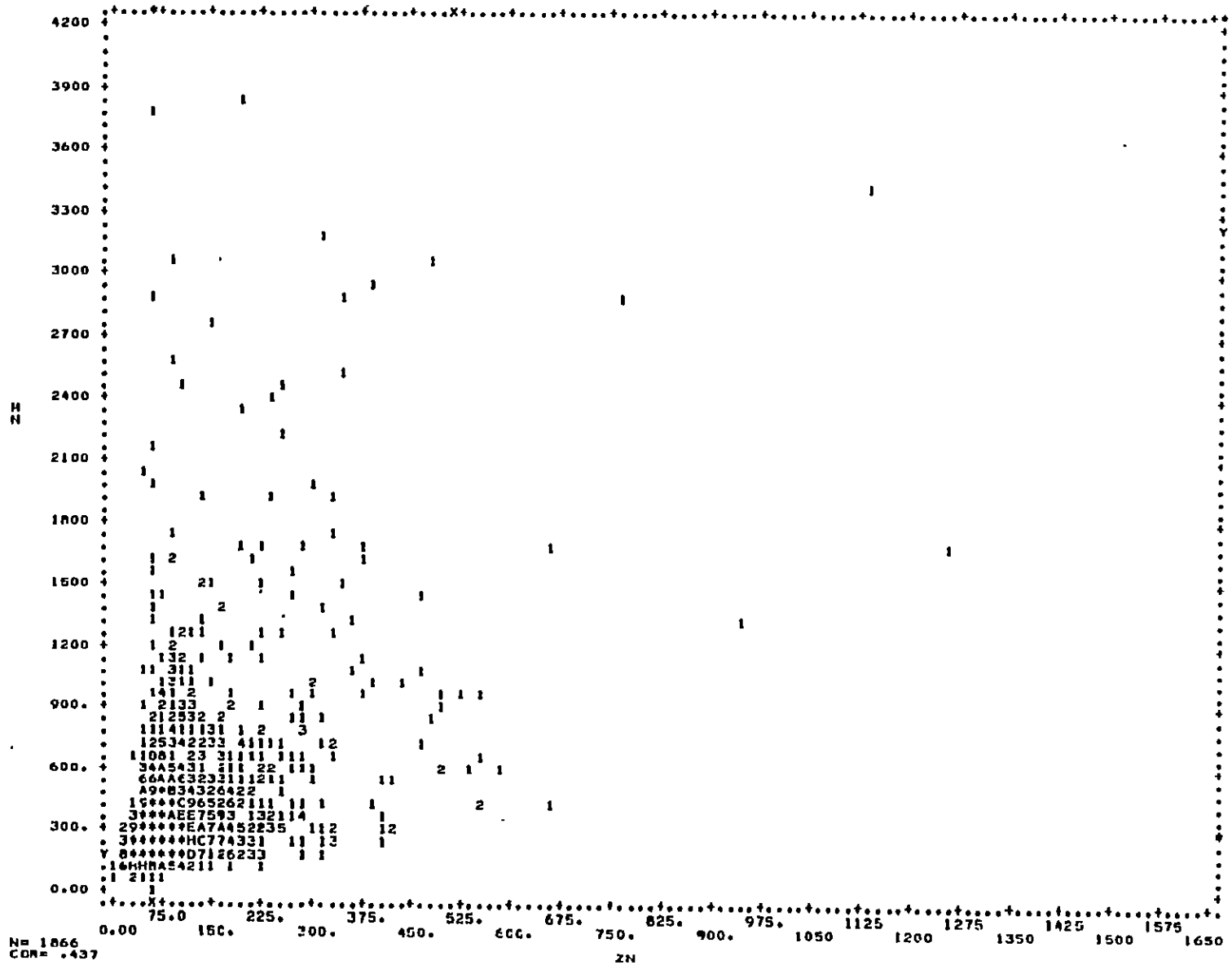

N= 1866
COR= .437

	MEAN	ST.DEV.	REGRESSION LINE	RES.MS.
X	101.29	89.598	X= .105314Y+ 59.084	6496.8
Y	400.75	371.96	Y= 1.8150*X+ 216.92	111967

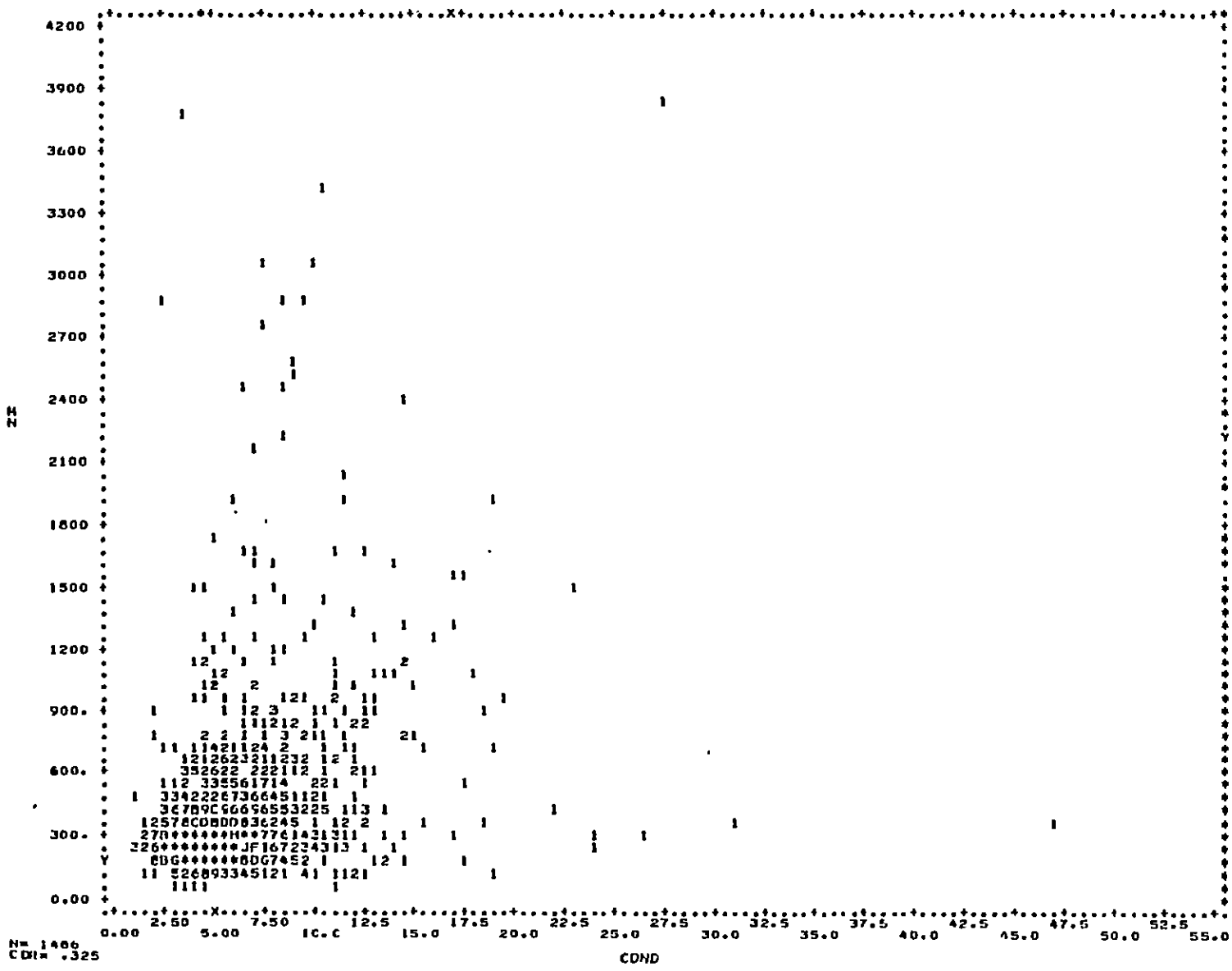

N= 1486
CORR= .325

	MEAN	ST.DEV.	REGRESSION LINE	RES.MS.
X	6.0083	3.2673	X= .00286*Y+ 4.9283	9.5514
Y	398.24	371.42	Y= 36.991*X+ 173.77	123426

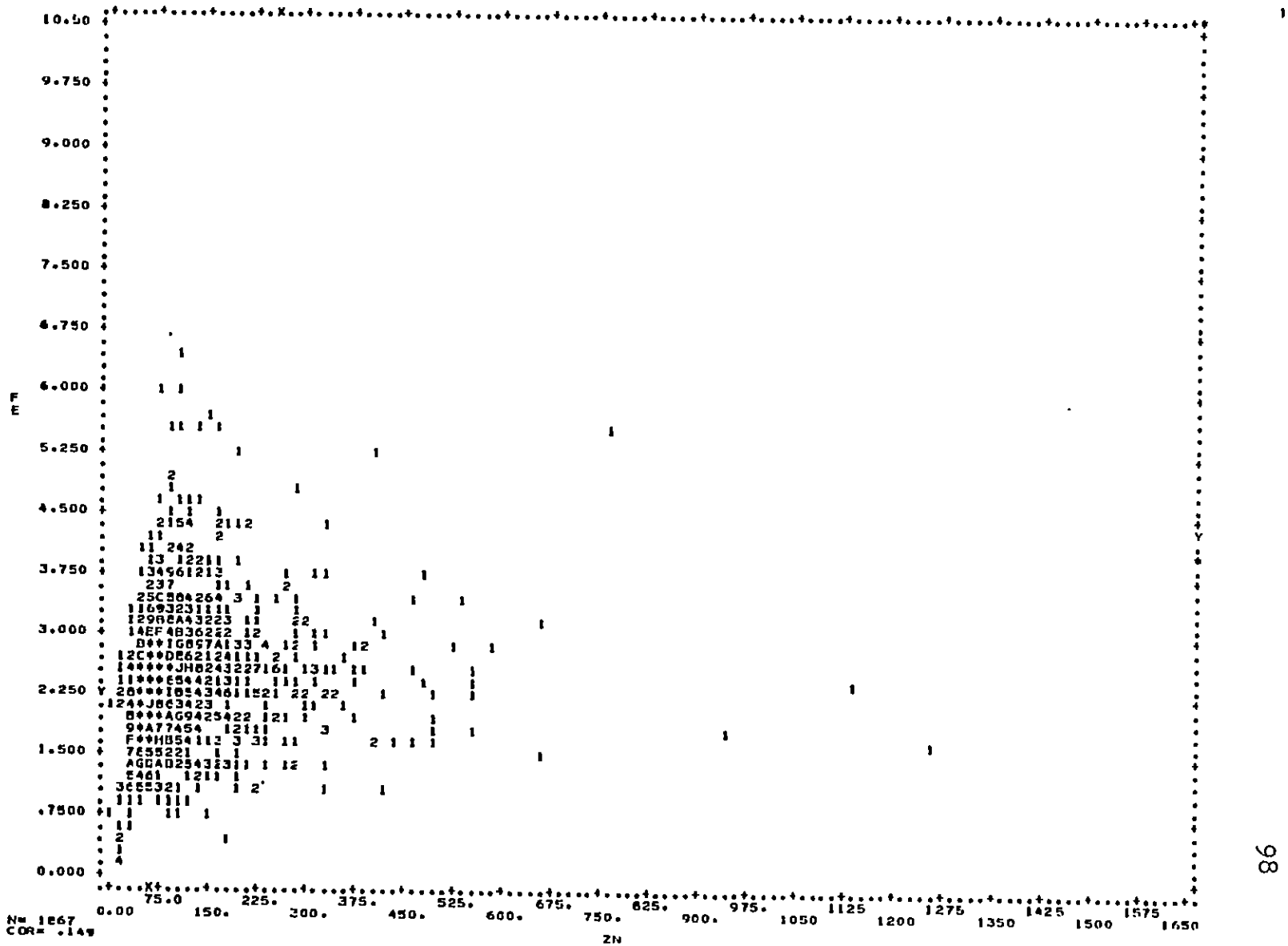

N= 1867
COR= .149

MEAN ST.DEV. REGRESSION LINE RES.MS.

X 101.26 89.580 Y= 17.9724Y+ 58.080 7850.0
Y 2.4029 .74392 X= .001244X+ 2.2774 .54139

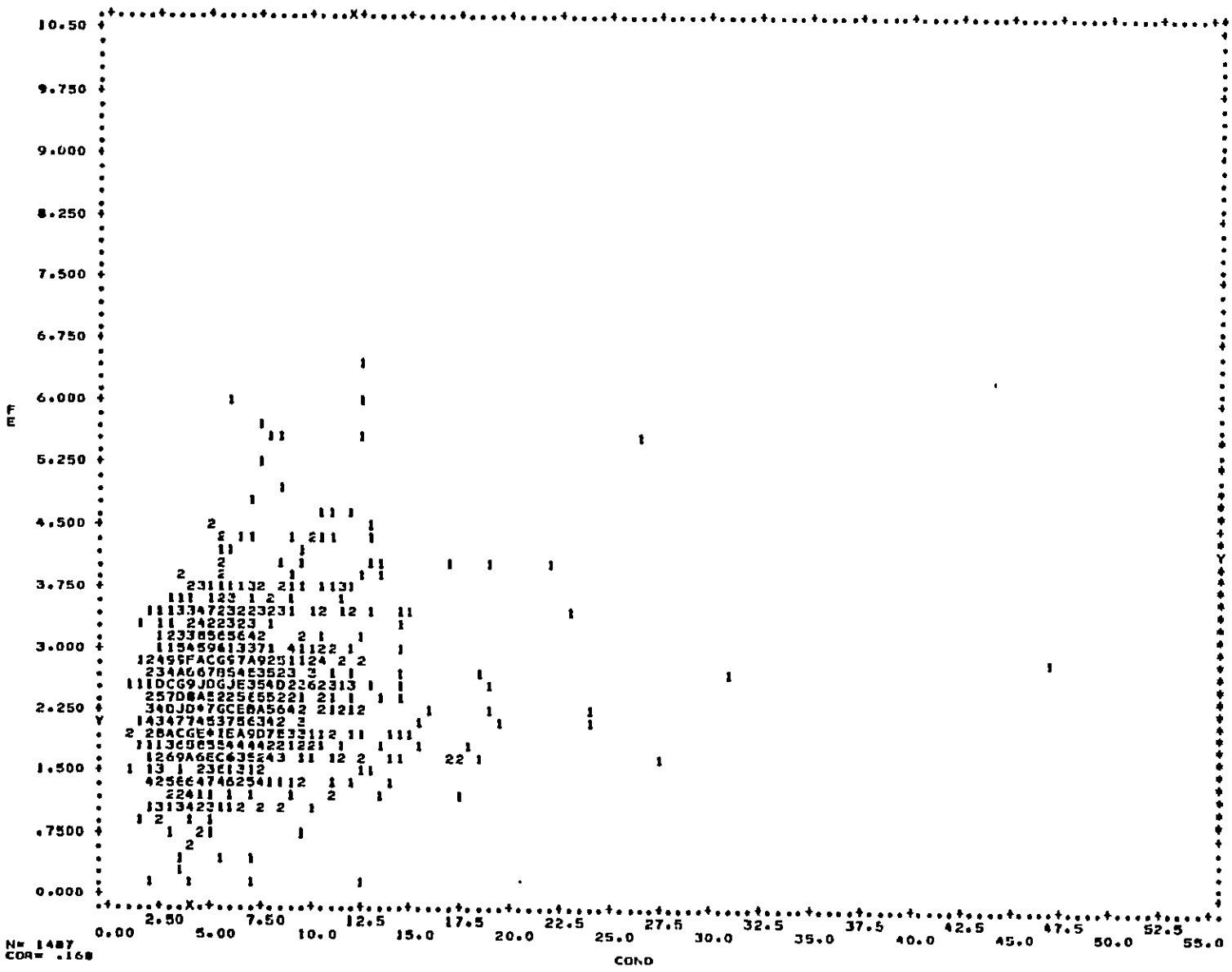

N= 1487
COR= .168

	MEAN	ST.DEV.	REGRESSION LINE	RES.MS.
X	6.0673	3.2664	X= .744234Y+ 4.2900	10.377
Y	2.3082	.73567	Y= .037754X+ 2.1591	.52636

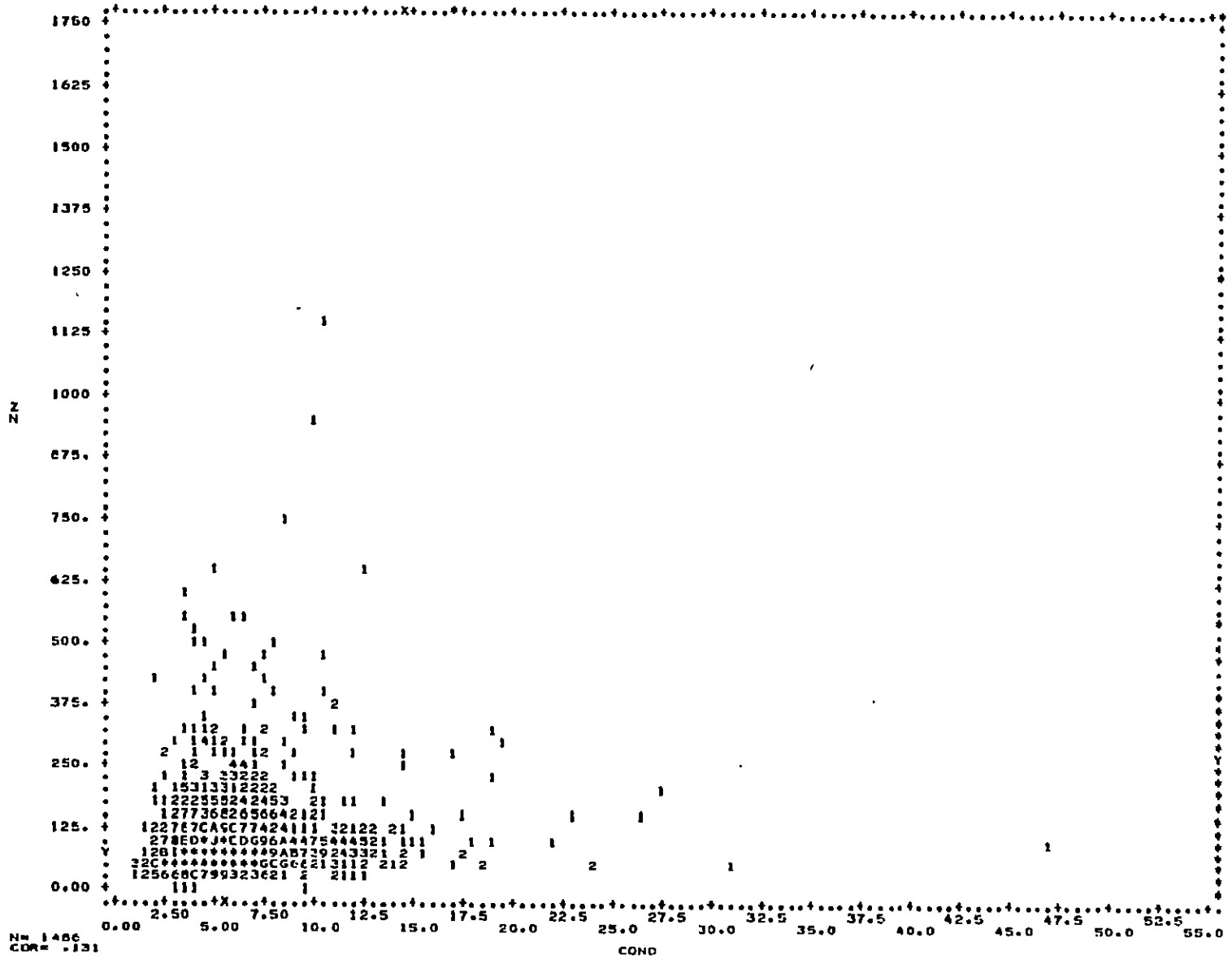

N= 1486
COR= .131

MEAN ST.DEV. REGRESSION LINE RES.MS.

X 6.0599 3.2552 X= .00495*Y+ 5.5689 10.422
Y 99.174 85.952 Y= 3.4521*X+ 78.255 7266.4

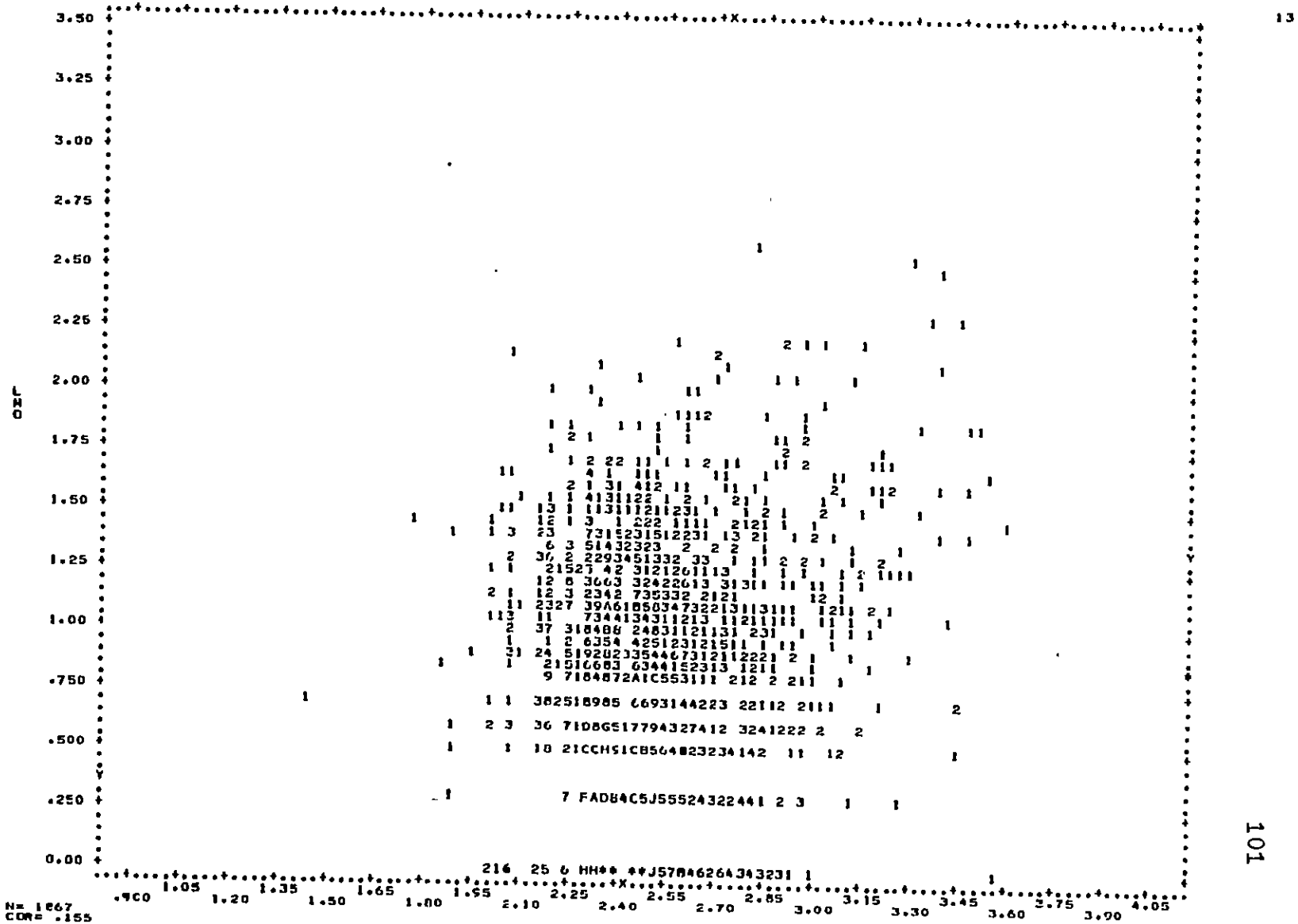

	MEAN	ST.DEV.	REGRESSION LINE	RES.MS.
X	2.5075	.25663	Y= .07995+Y+ 2.4305	.06531
Y	.84960	.60232	Y= .30175+X+ .09297	.24637

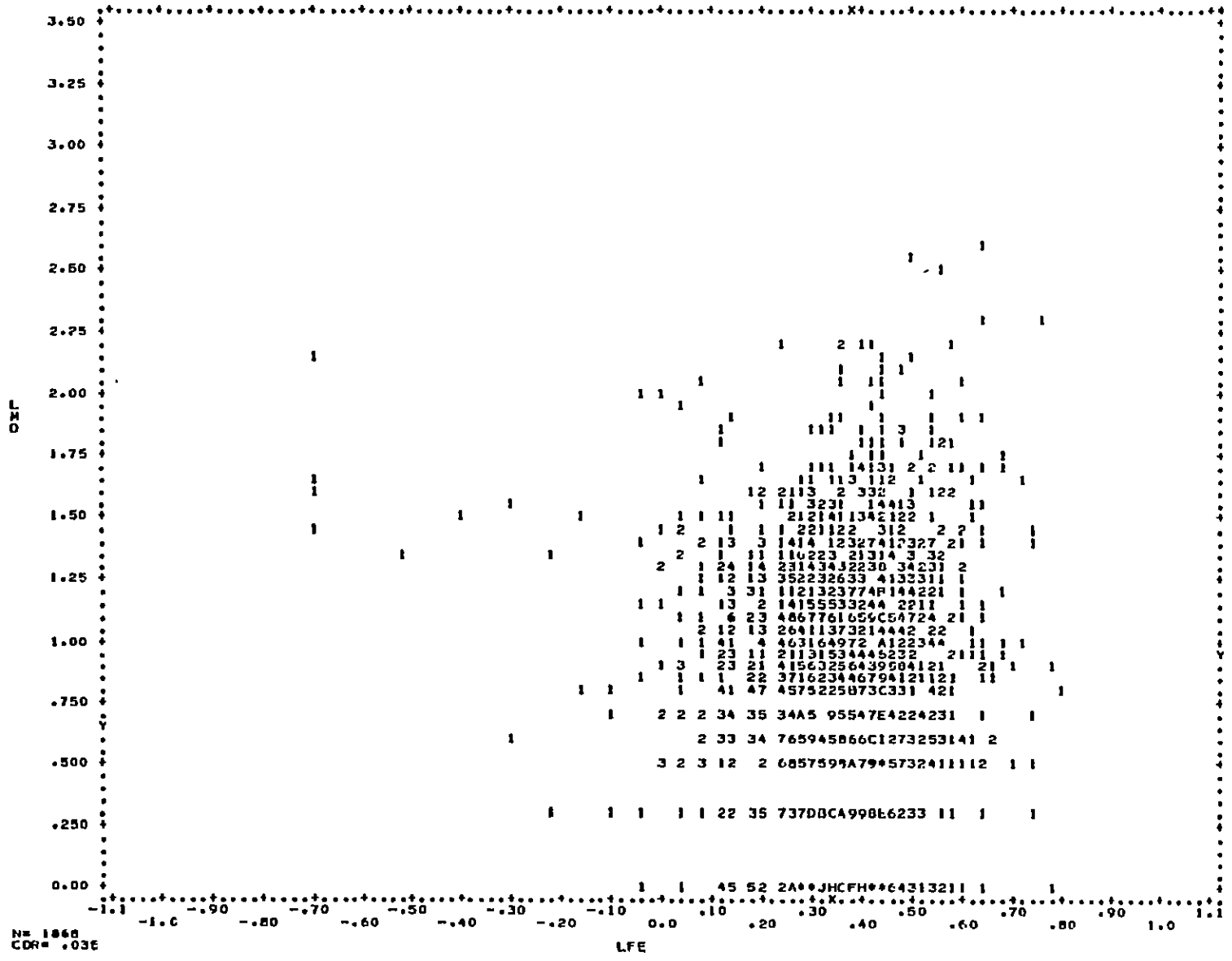

N= 1868
COR= .036

	MEAN	ST.DEV.	REGRESSION LINE	RES.MS.
X	.35857	.14718	X= .01026*Y+ .34983	.02165
Y	.84960	.50219	Y= .11960*X+ .80668	.25201

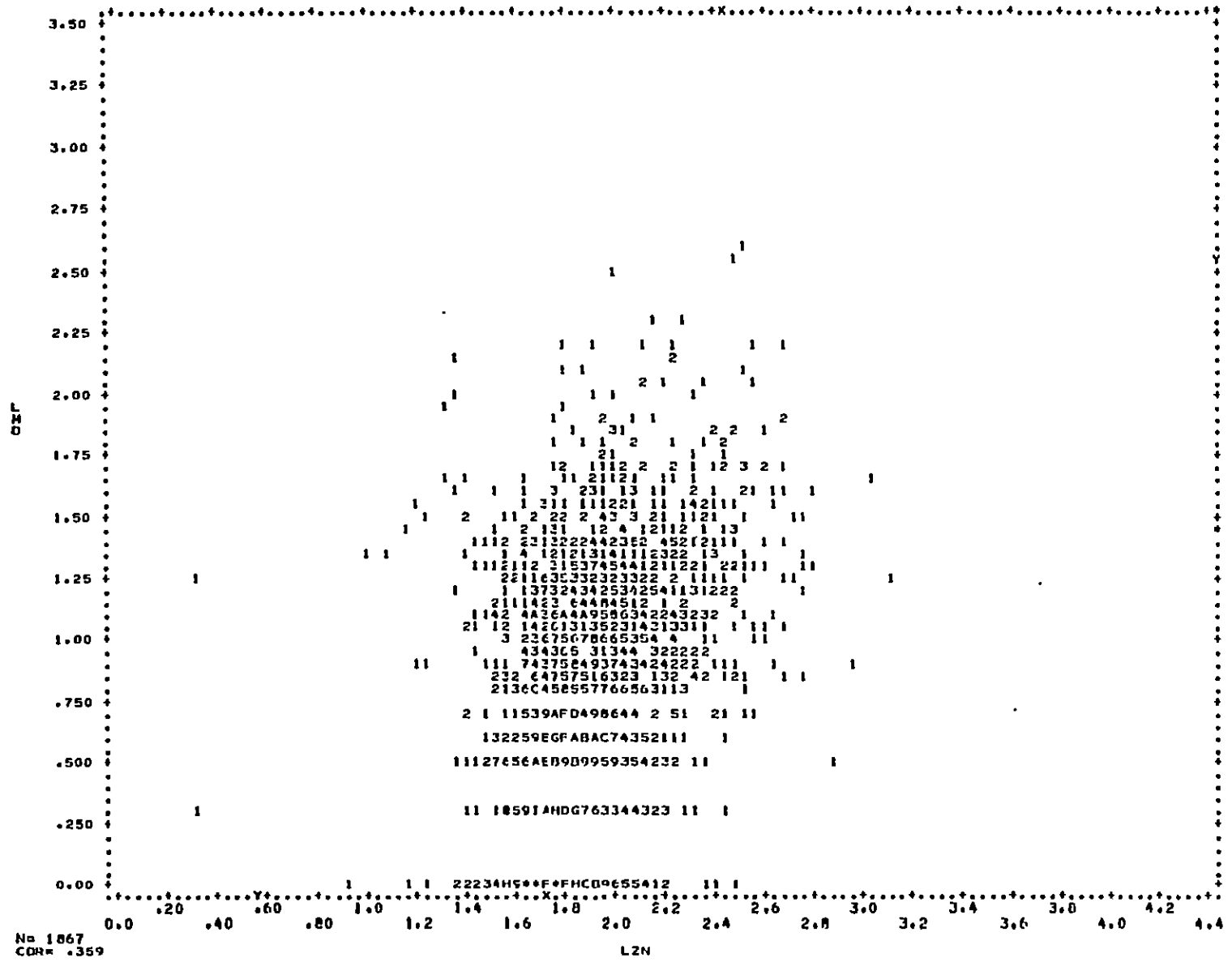

No 1867
COR= .359

	MEAN	ST.DEV.	REGRESSION LINE	RES.MS.
X	1.9096	.27061	X= .19369*Y+ 1.7451	.06381
Y	.84928	.50213	Y= .66686*X-.42418	.21968

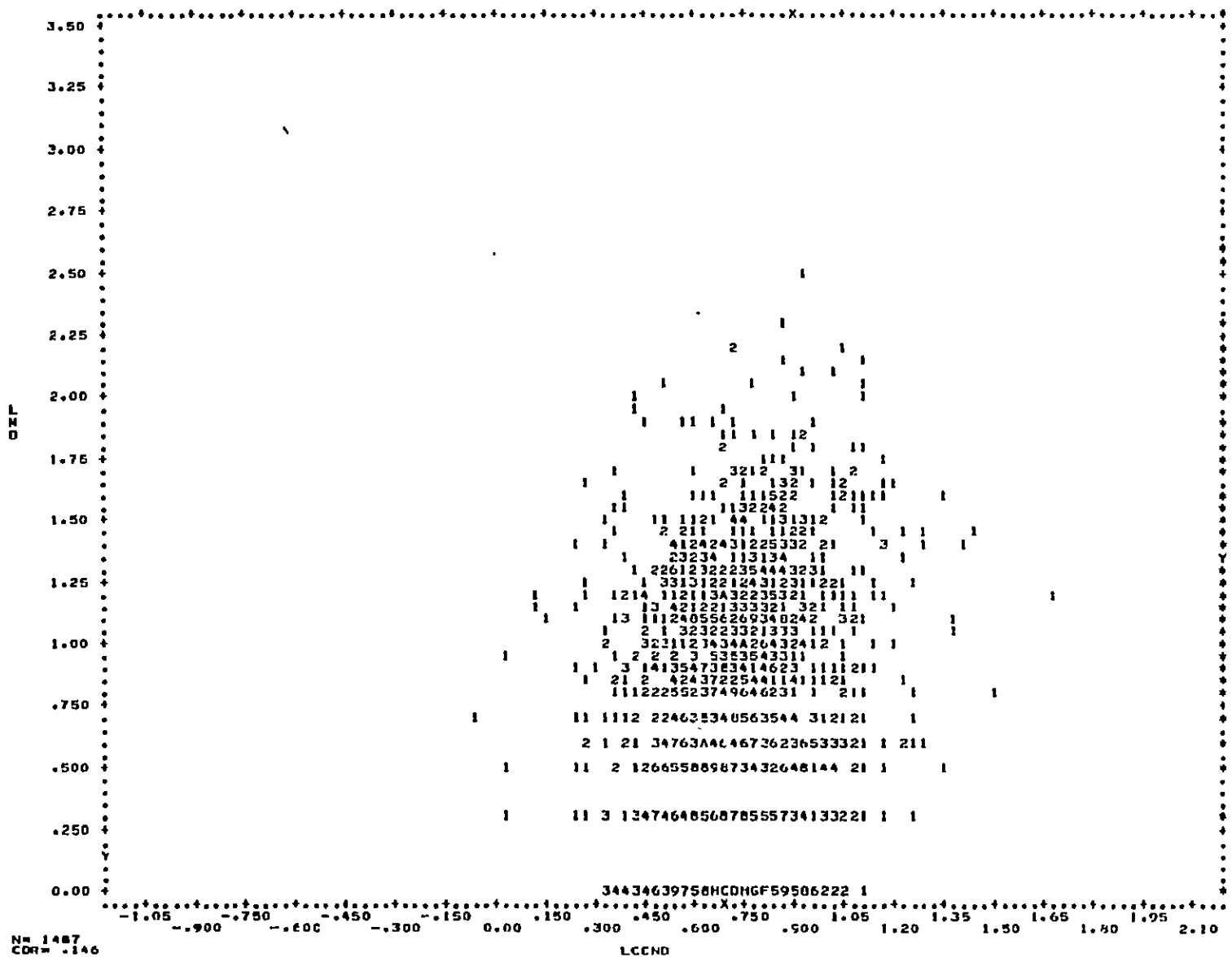

N= 1487
COR= .146

	MEAN	ST.DEV.	REGRESSION LINE	RES.MS.
X	.73474	.20142	X= .05905+Y+ .68516	.03973
Y	.83953	.49655	Y= .36176+X+ .57373	.24341

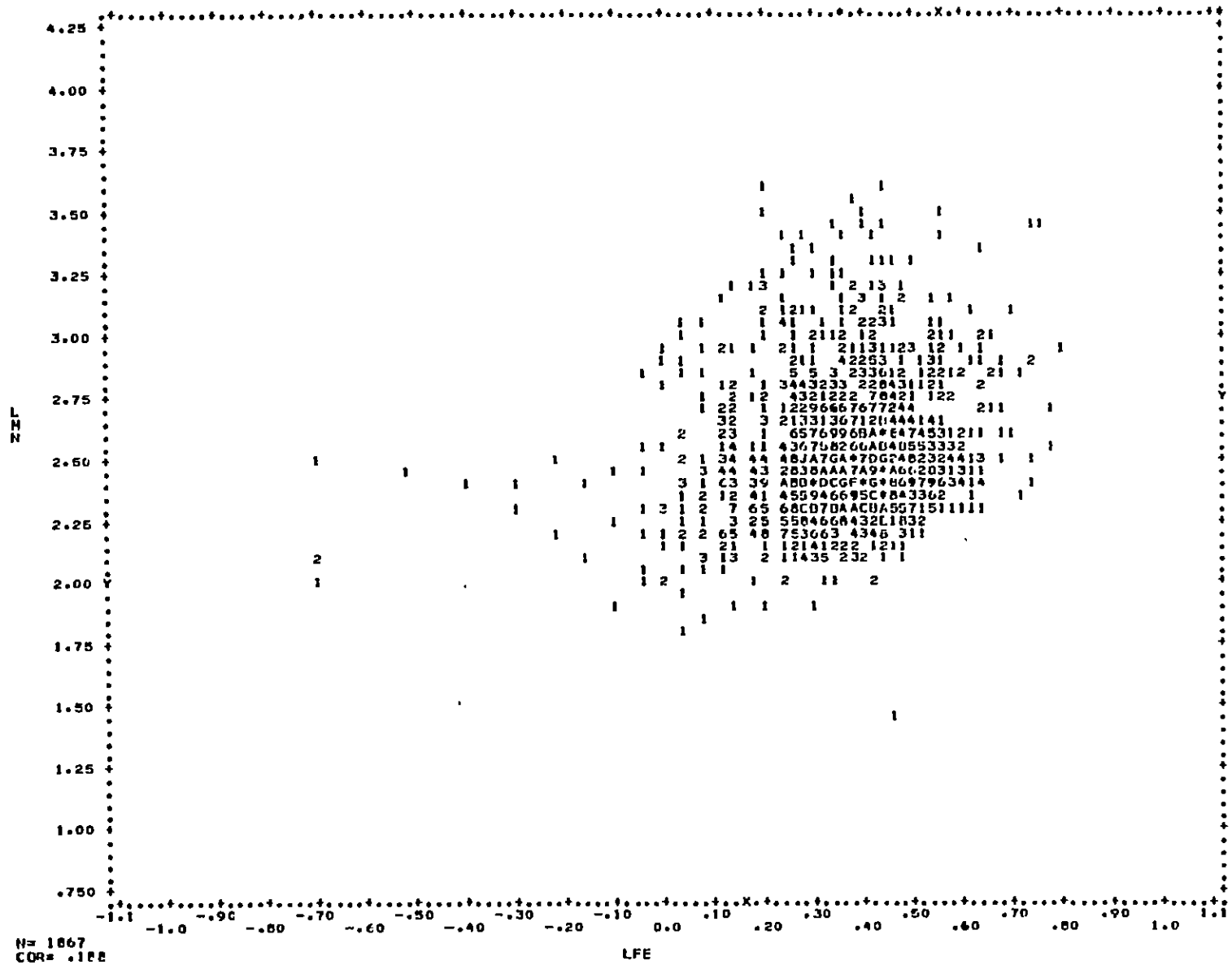

N= 1867
COR= .188

	MEAN	ST.DEV.	REGRESSION LINE	RES.MS.
X	.35856	.14722	Y= .107044*Y+ .09016	.02092
Y	2.5075	.25863	X= .330334*X+ 2.3690	.06456

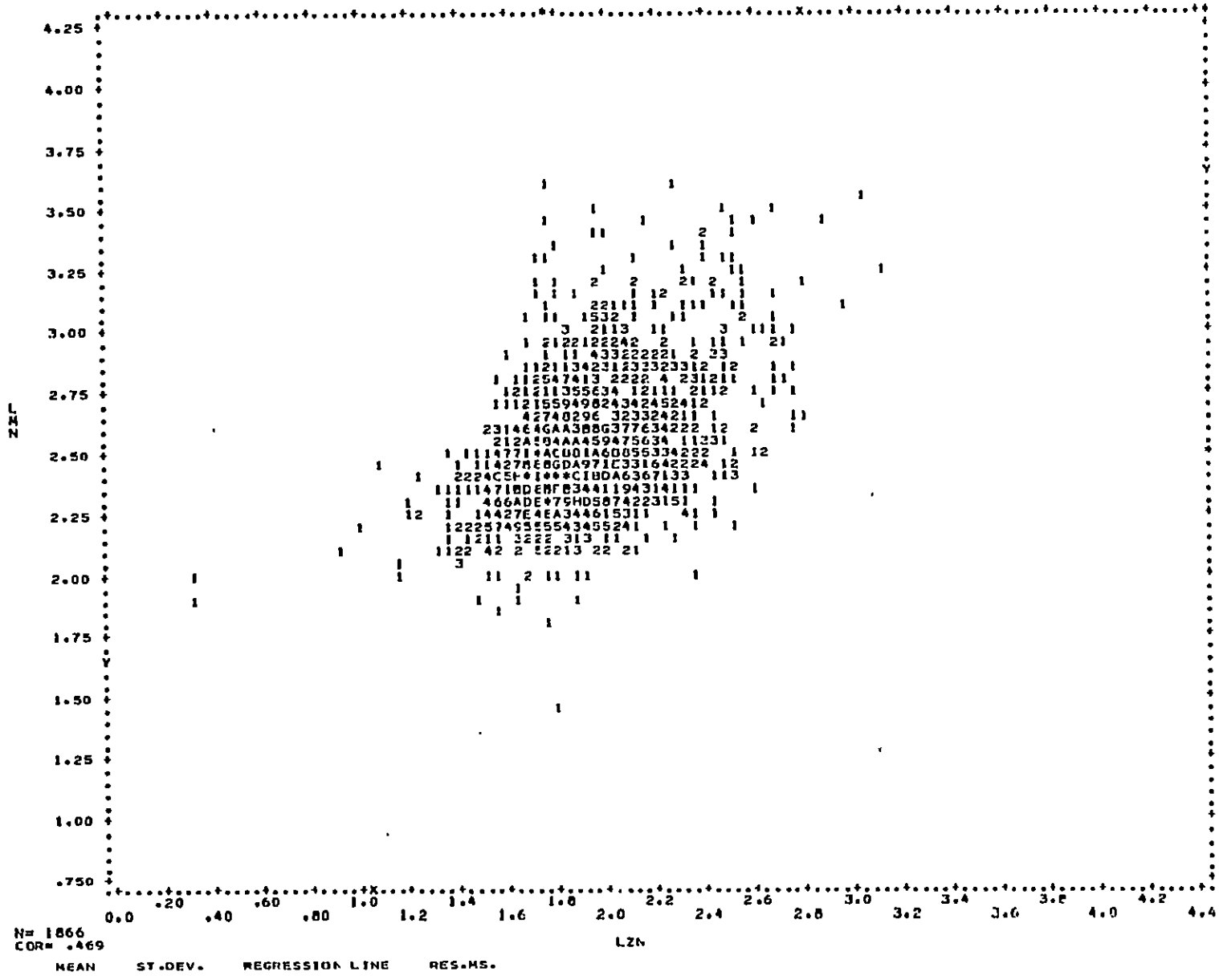

N= 1866
COR= .469

	MEAN	ST.DEV.	REGRESSION LINE	RES.MS.
X	1.9097	.27066	X= .490904Y+ .67875	.05716
Y	2.5075	.25870	Y= .448474X+ 1.6510	.05222

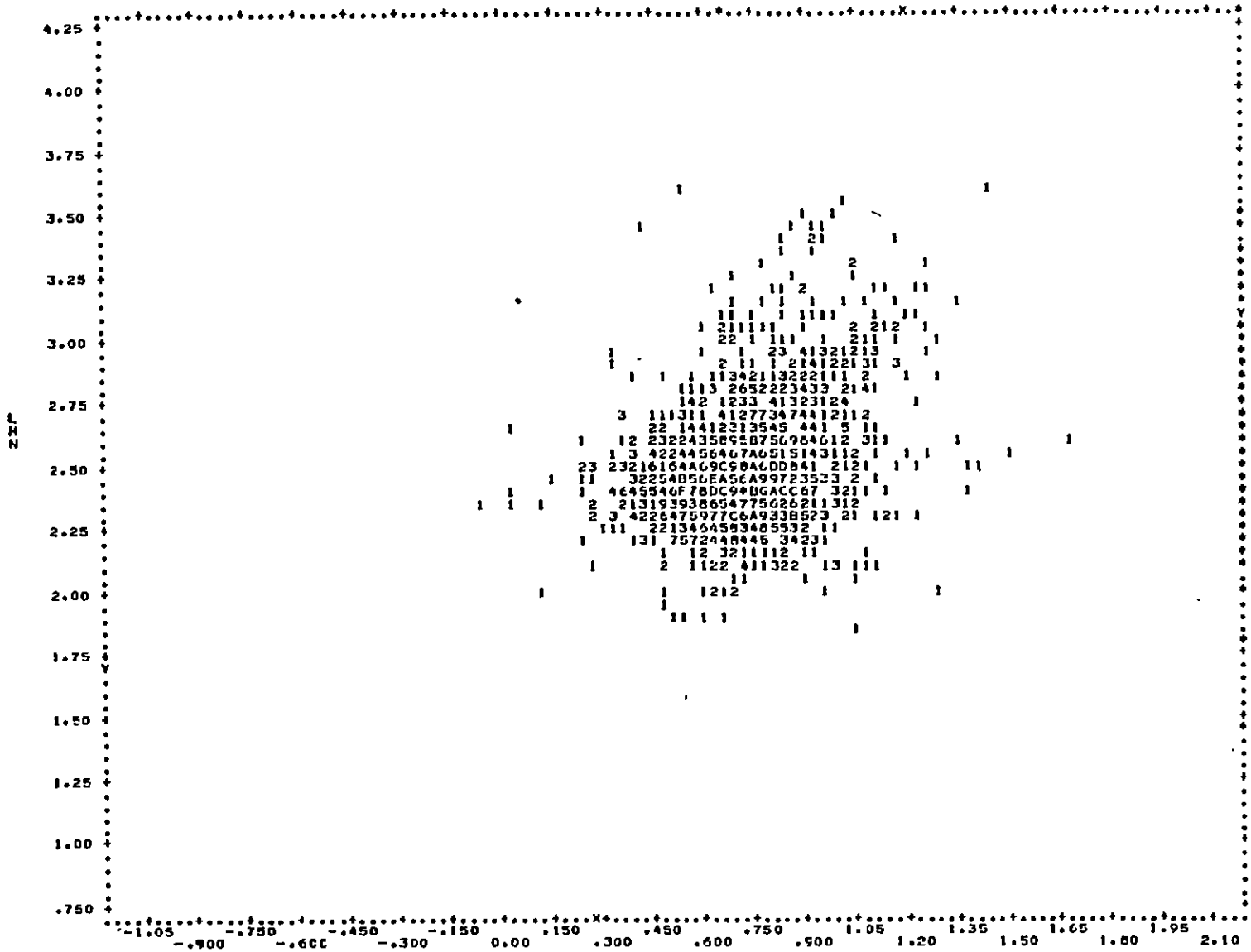

N= 1466
COR= .333

	MEAN	ST.DEV.	REGRESSION LINE	RES.MS.
X	.73479	.20148	X= .26148*Y+ .07957	.03612
Y	2.5058	.25639	Y= .423414*X+ 2.1947	.05850

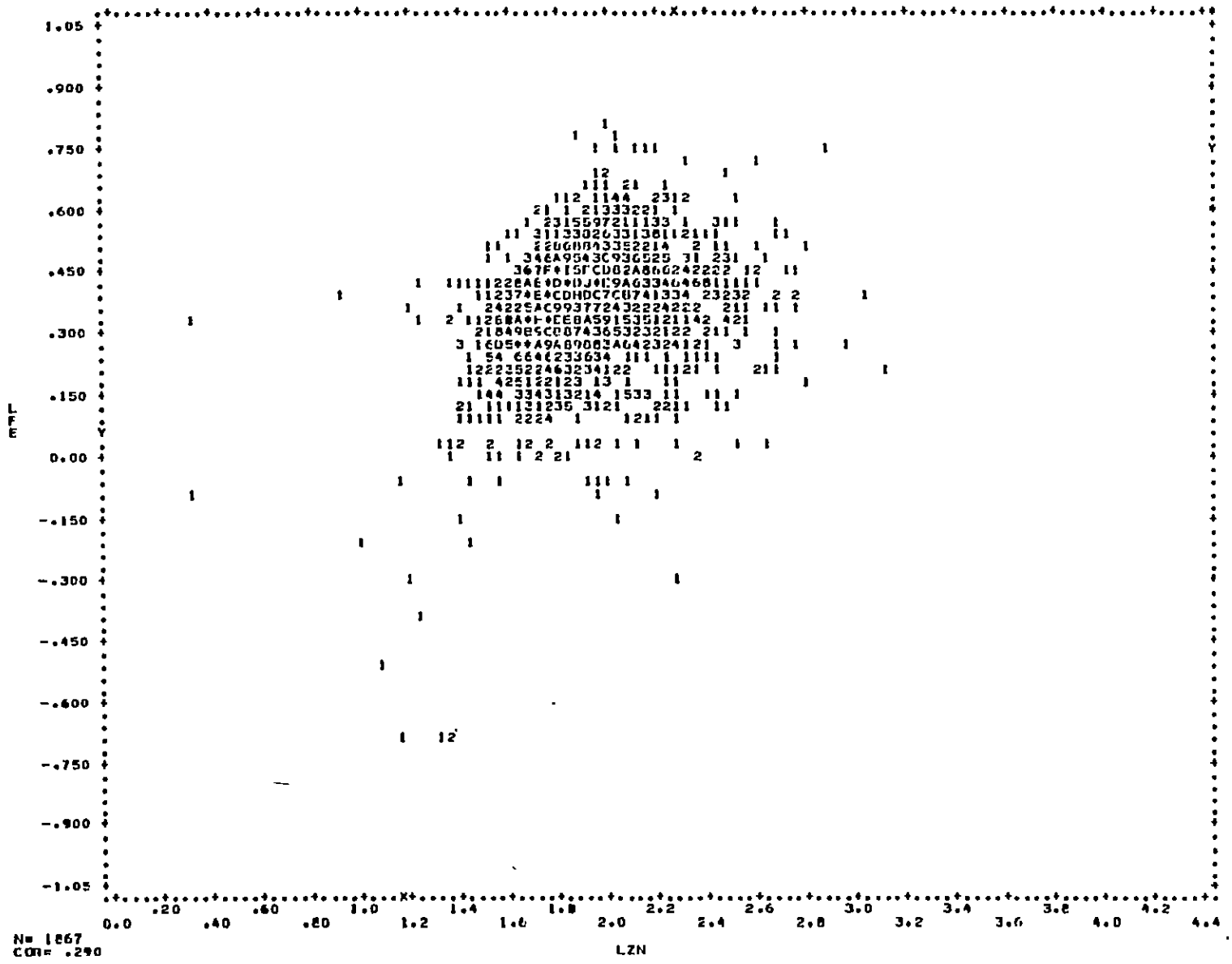

N= 1867
COR= .290

	MEAN	ST.DEV.	REGRESSION LINE	RES.MS.
X	1.9096	.27061	X= .53320*Y+ 1.7185	.06711
Y	.35844	.14711	Y= .15758*X+ .05752	.01983

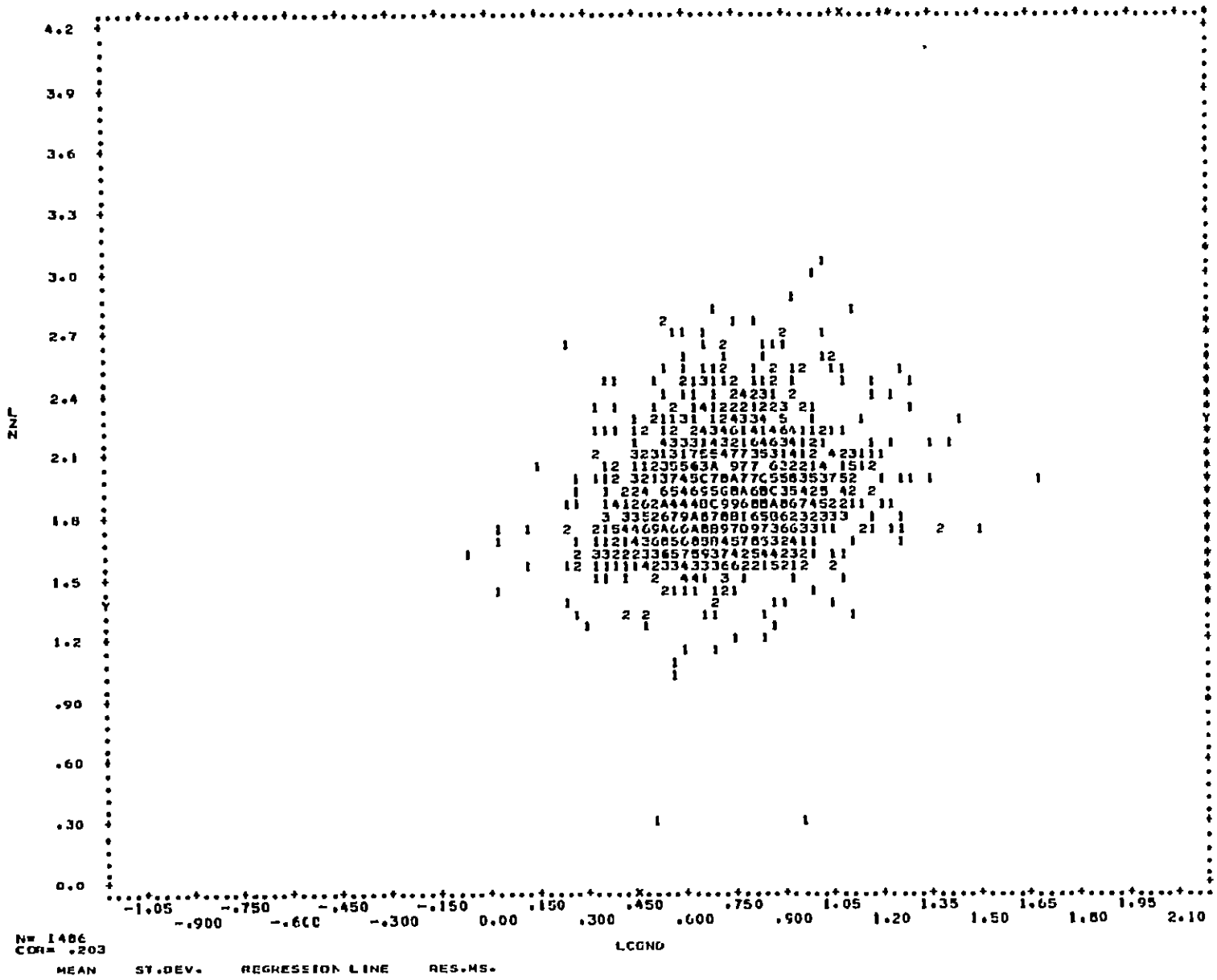

N= 1486
COR= .203

	MEAN	ST.DEV.	REGRESSION LINE	RES.MS.
X	.73440	.20160	X= .15200*Y+ .44520	.03879
Y	1.9026	.26901	Y= .27206*X+ 1.7028	.06942

APPENDIX C

X-Y diagrams and correlation coefficients for the profile A-A'.

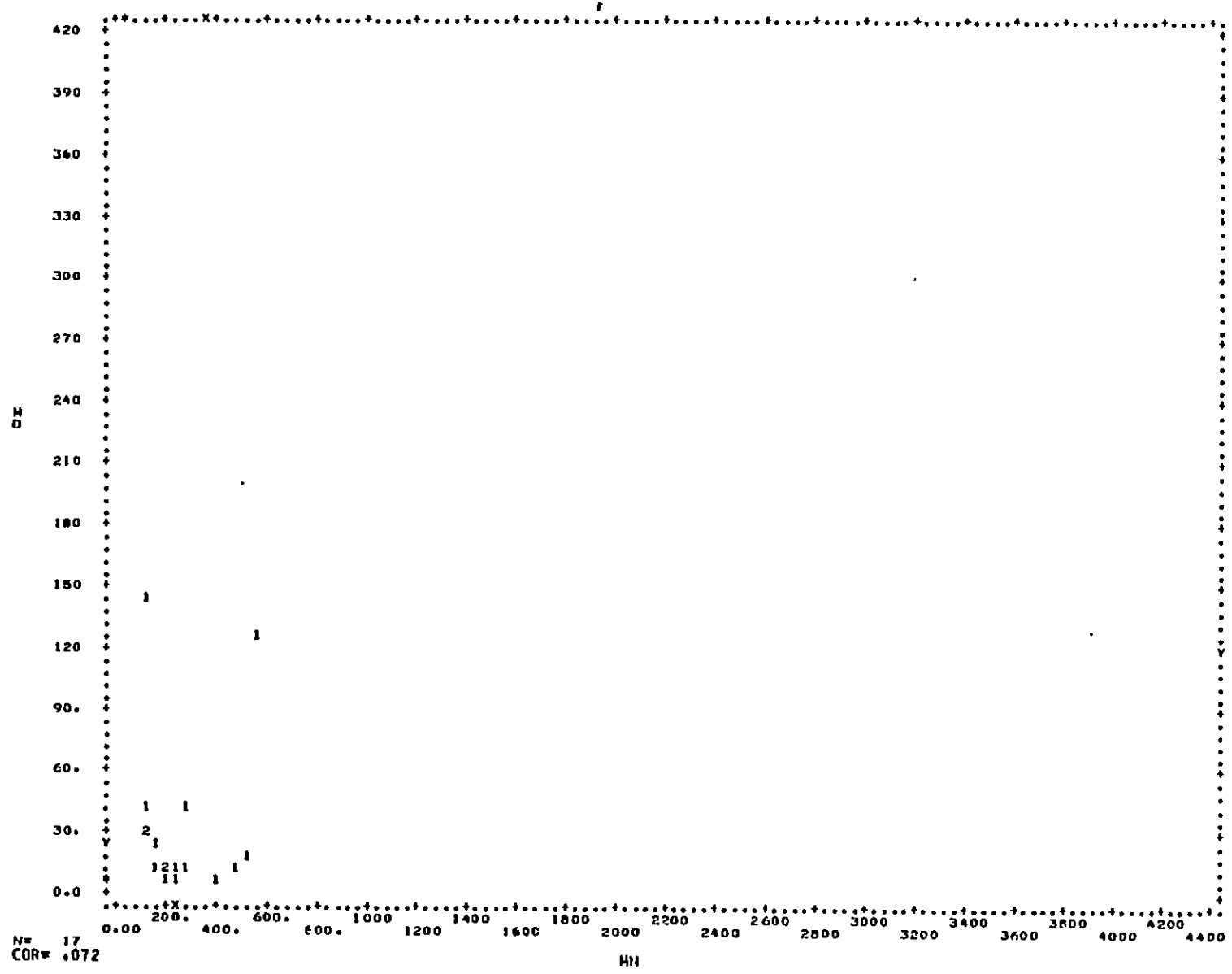

N= 17
COR= .072

	MEAN	ST.DEV.	REGRESSION LINE	RES.MS.
X	251.76	142.84	X= .24836*Y+ 243.08	21651.
Y	31.765	41.267	Y= .02073*X+ 26.546	1807.1

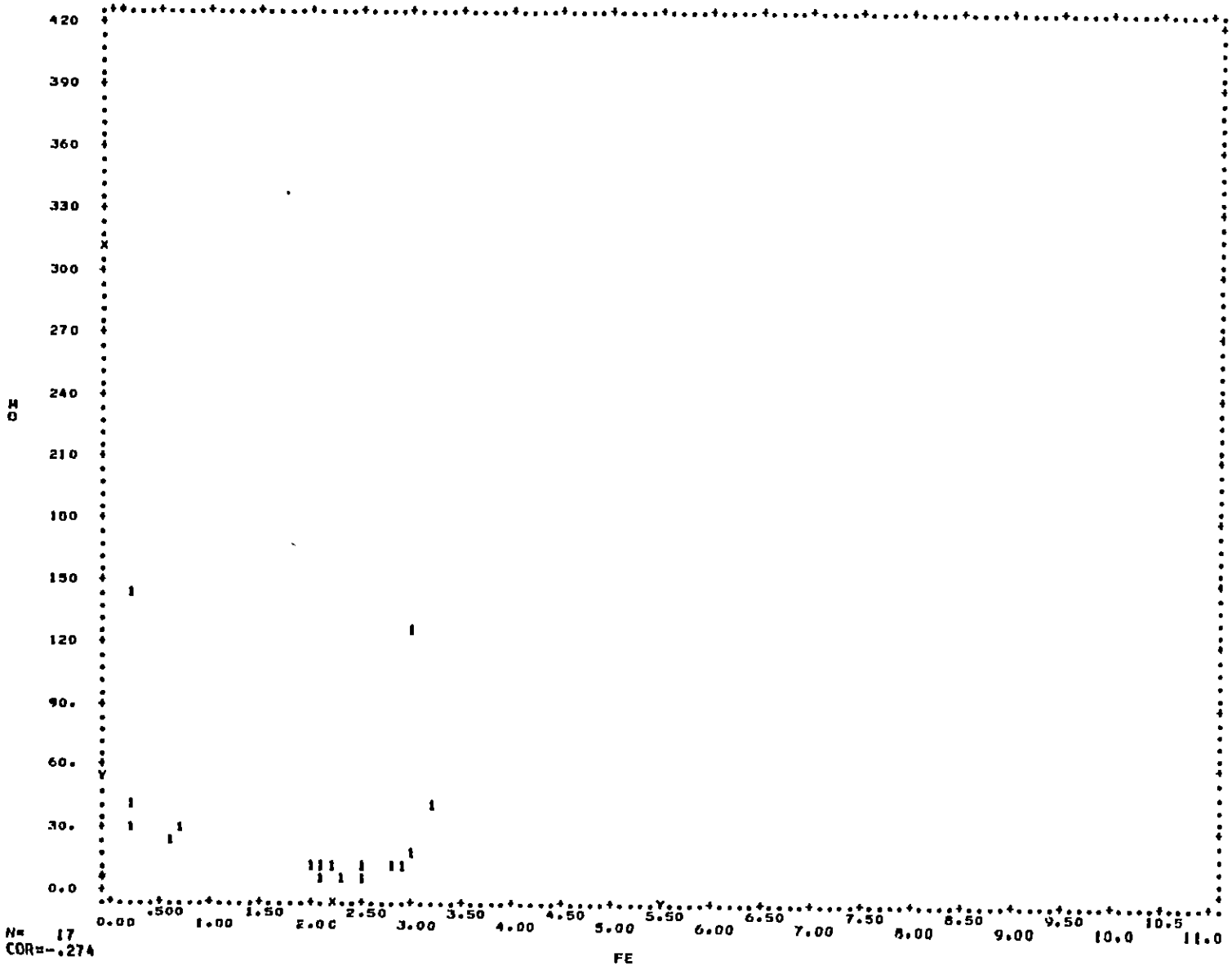

N= 17
COR=-.274

	MEAN	ST.DEV.	REGRESSION LINE	RES.MS.
X	1.9118	1.0833	X=-.007206*Y+ 2.1404	1.1577
Y	31.766	41.267	Y=-10.446*X+ 51.775	1470.6

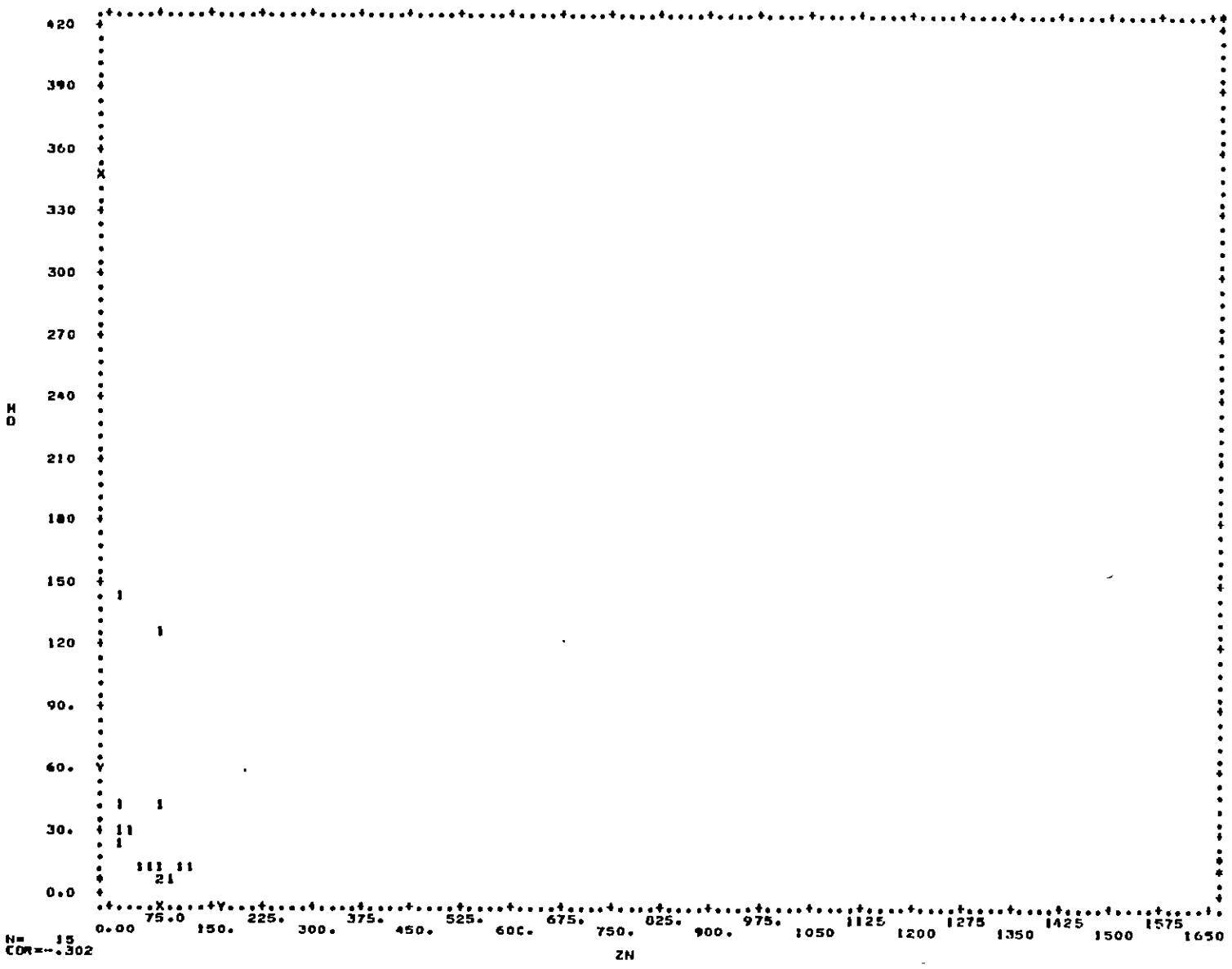

N= 15
COR=-.302

	MEAN	ST.DEV.	REGRESSION LINE	RES.MS.
X	60.400	34.807	X=-.241540*Y+ 68.645	1185.8
Y	34.133	43.507	Y=-.377374*X+ 56.926	1852.6

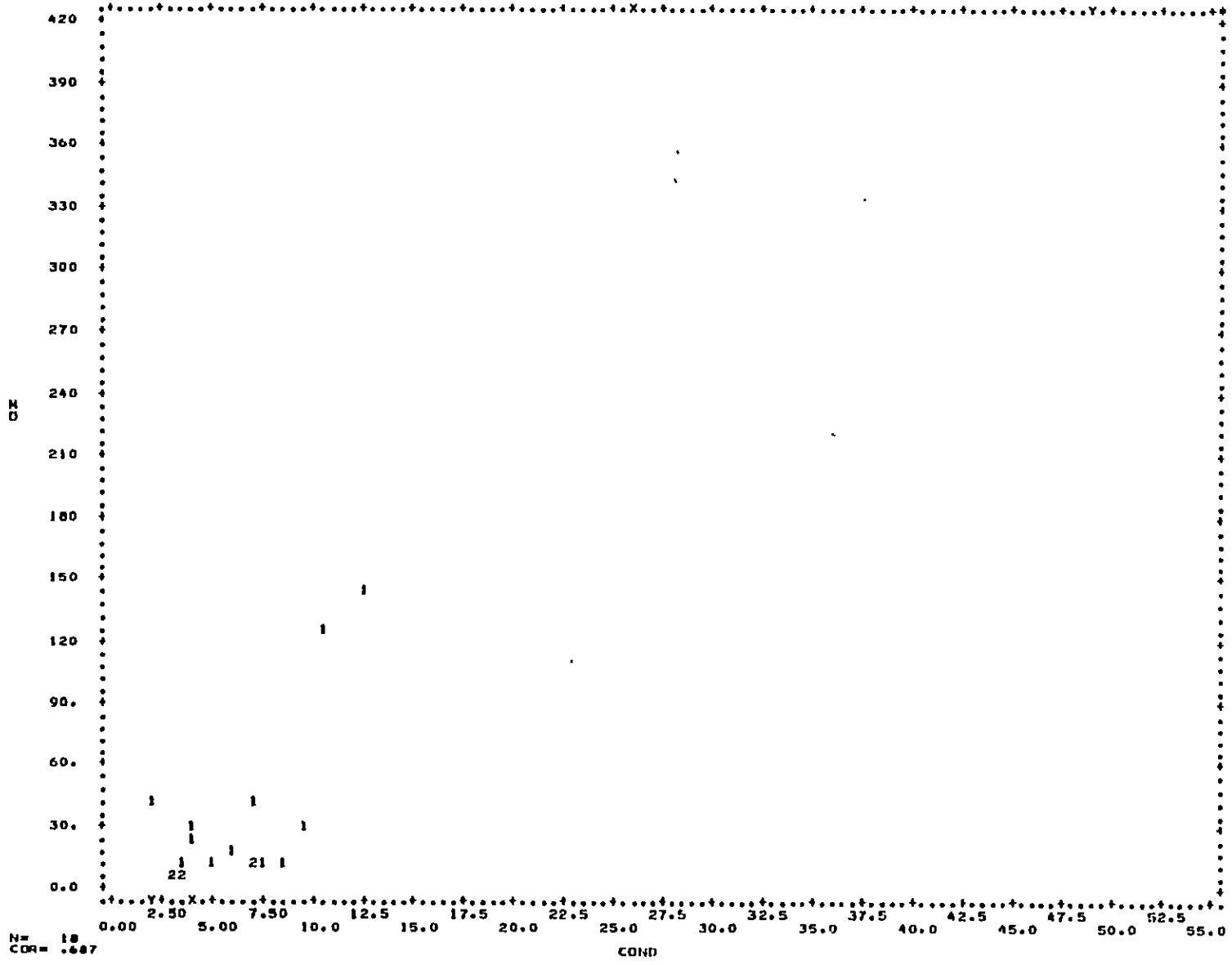

N= 18
COR= .687

	MEAN	ST.DEV.	REGRESSION LINE	RES.MS.
X	5.9150	3.0105	X= .051144Y+ 4.3568	5.0911
Y	30.467	40.412	Y= 5.21544X-24.043	917.37

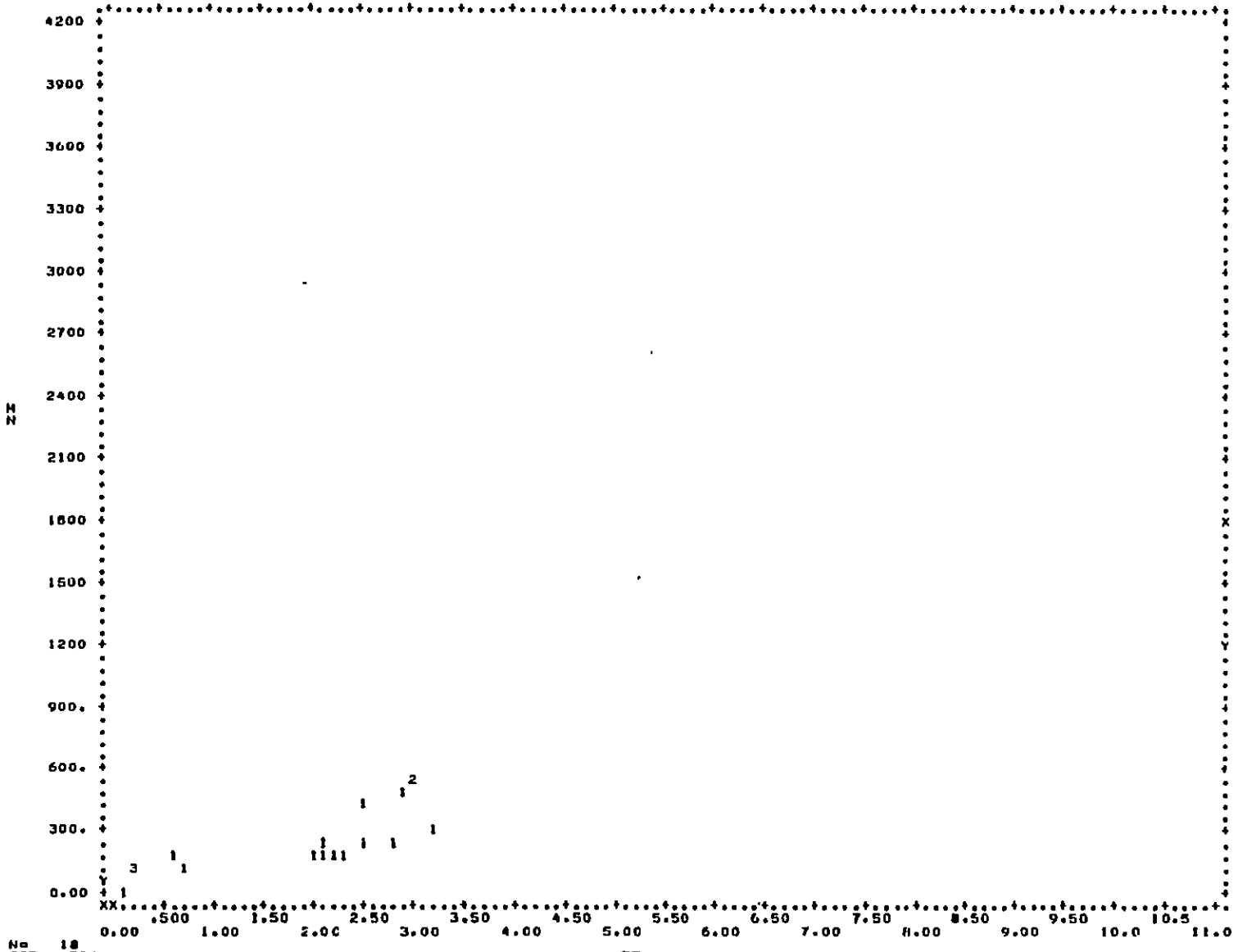

No= 18
COR= .784

	MEAN	ST.DEV.	REGRESSION LINE	RES.MS.
X	1.8111	1.1344	X= .005974Y+ .39464	.52682
Y	238.89	148.95	Y= 102.95*X+ 52.443	9002.5

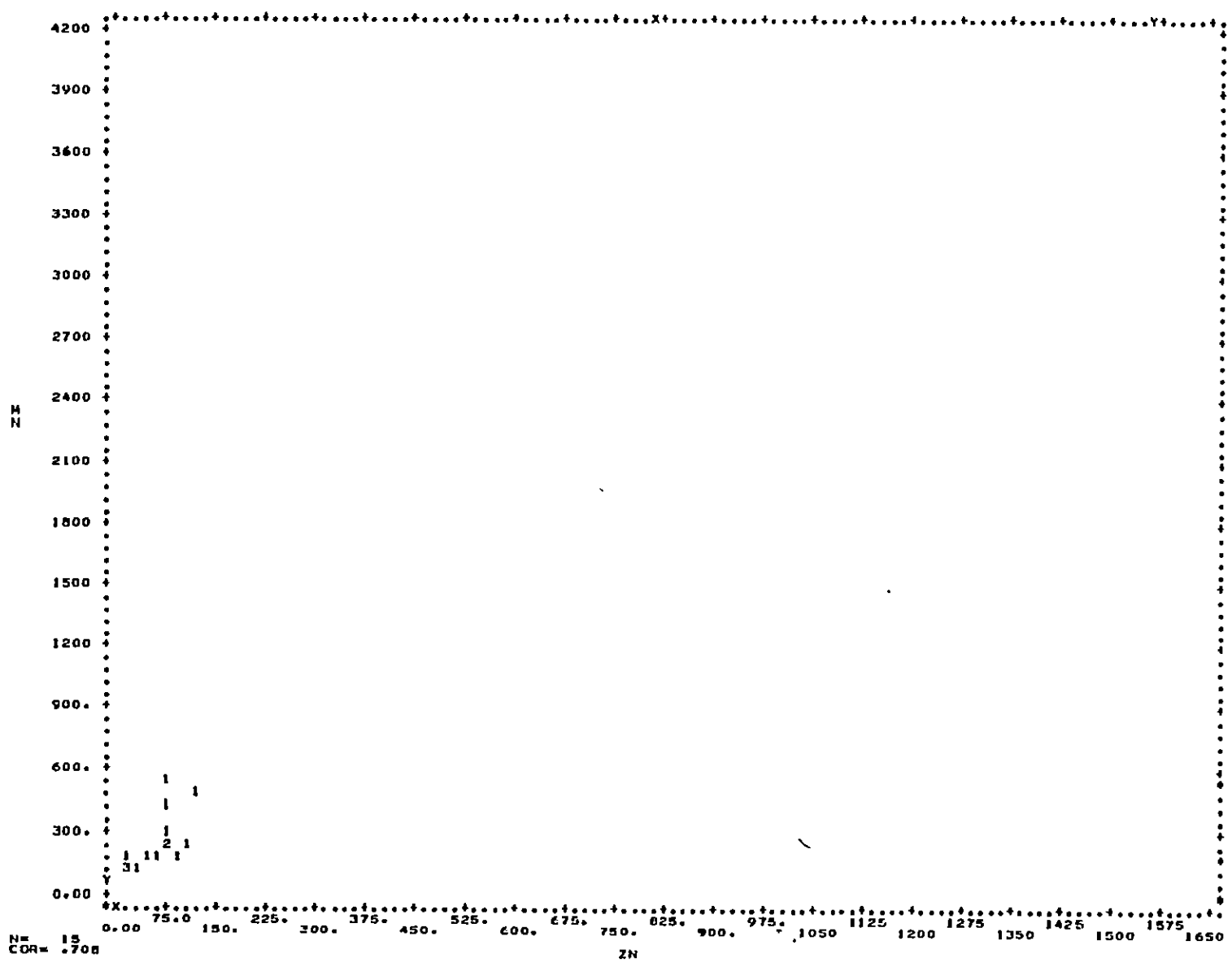

MEAN ST.DEV. REGRESSION LINE RES.MS.

X 60.400 34.867 Y= .186564Y+ 15.626 651.50
Y 240.00 132.02 X= 2.6B376X+ 77.904 9372.1

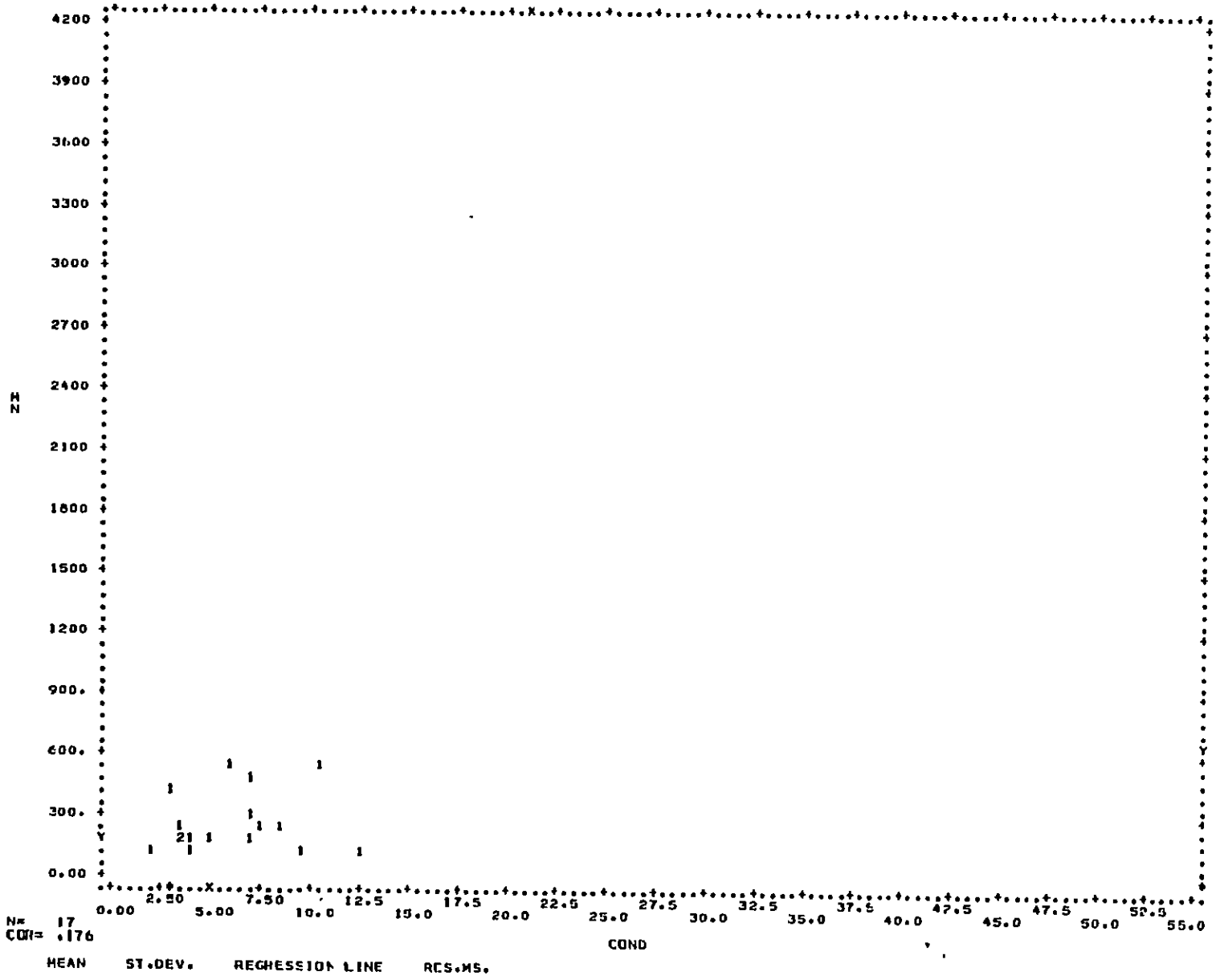

N= 17
COR= .176

	MEAN	ST.DEV.	REGRESSION LINE	RES.MS.
X	6.0865	3.0112	X= .00371*Y+ 5.1530	9.3727
Y	251.76	142.04	Y= 8.3425*X+ 200.99	21090.

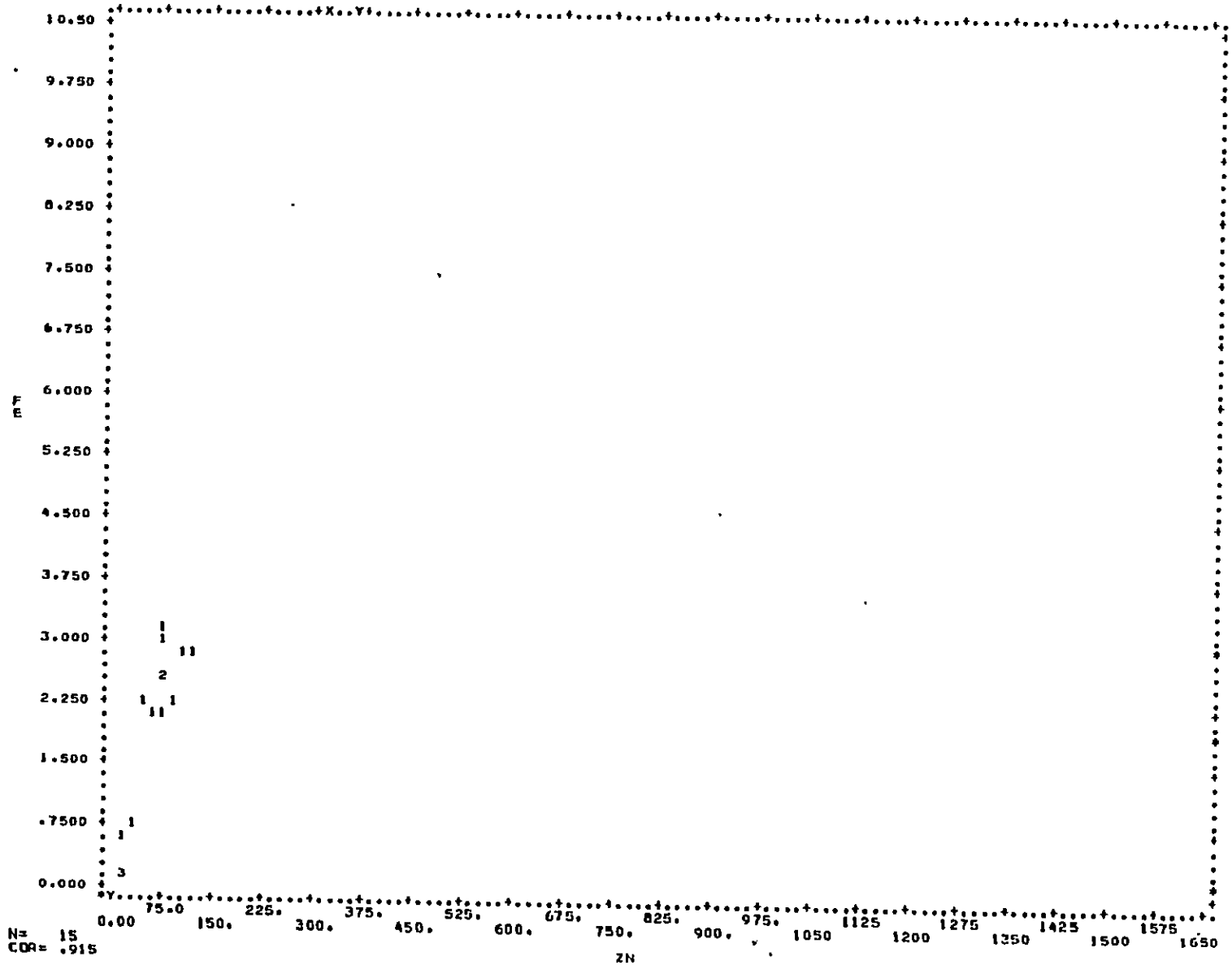

N= 15
COR= .915

	MEAN	ST.DEV.	REGRESSION LINE	RES.MS.
X	60.400	34.807	X= 28.4914*Y+ 8.1669	212.45
Y	1.8333	1.1178	Y= .02936*X+ .05054	.21910

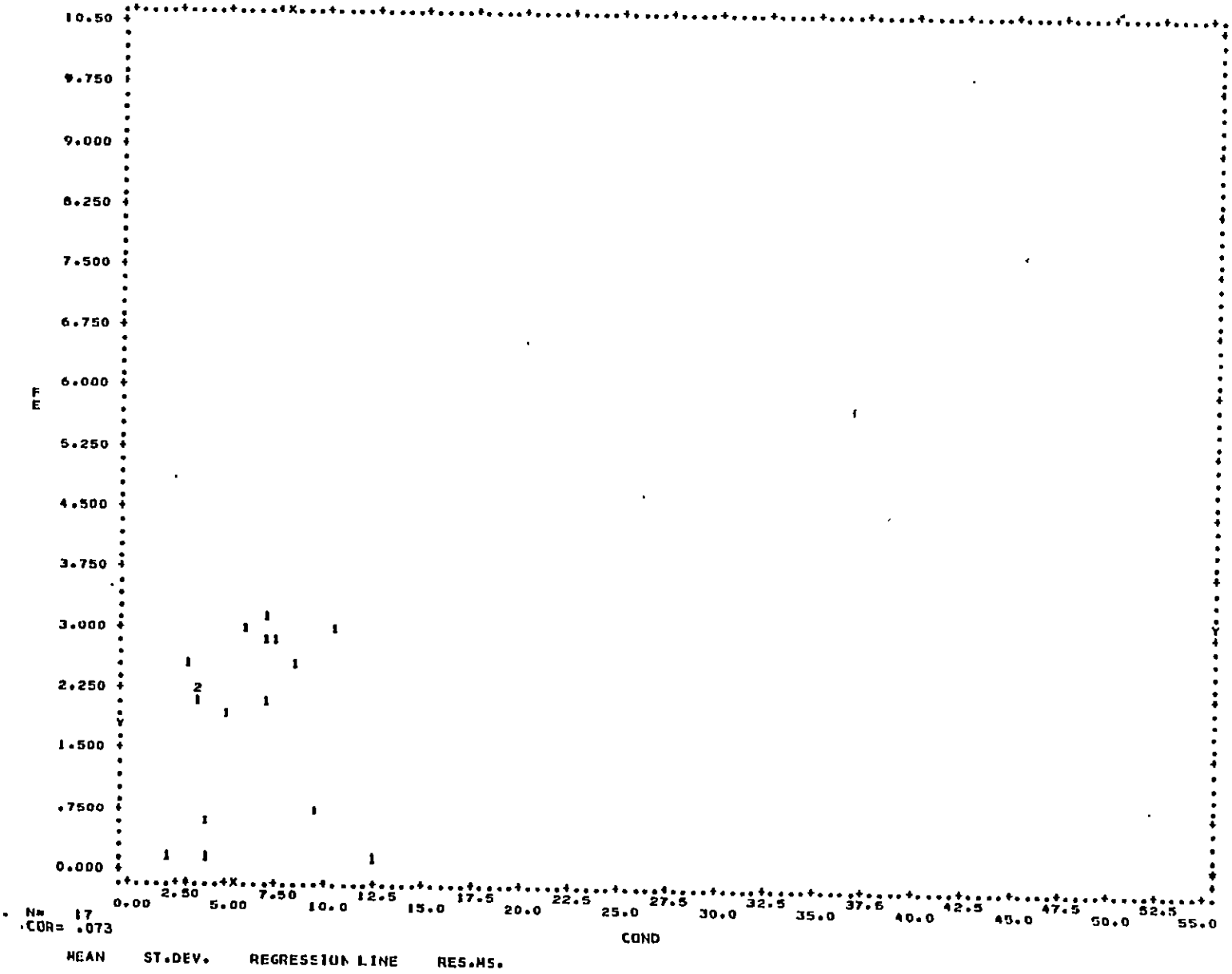

N= 17
COR= .073

	MEAN	ST.DEV.	REGRESSION LINE	RES.MS.
X	6.0865	3.0112	X= .20193*Y+ 5.7004	9.6202
Y	1.9118	1.0633	Y= .026140*X+ 1.7527	1.2452

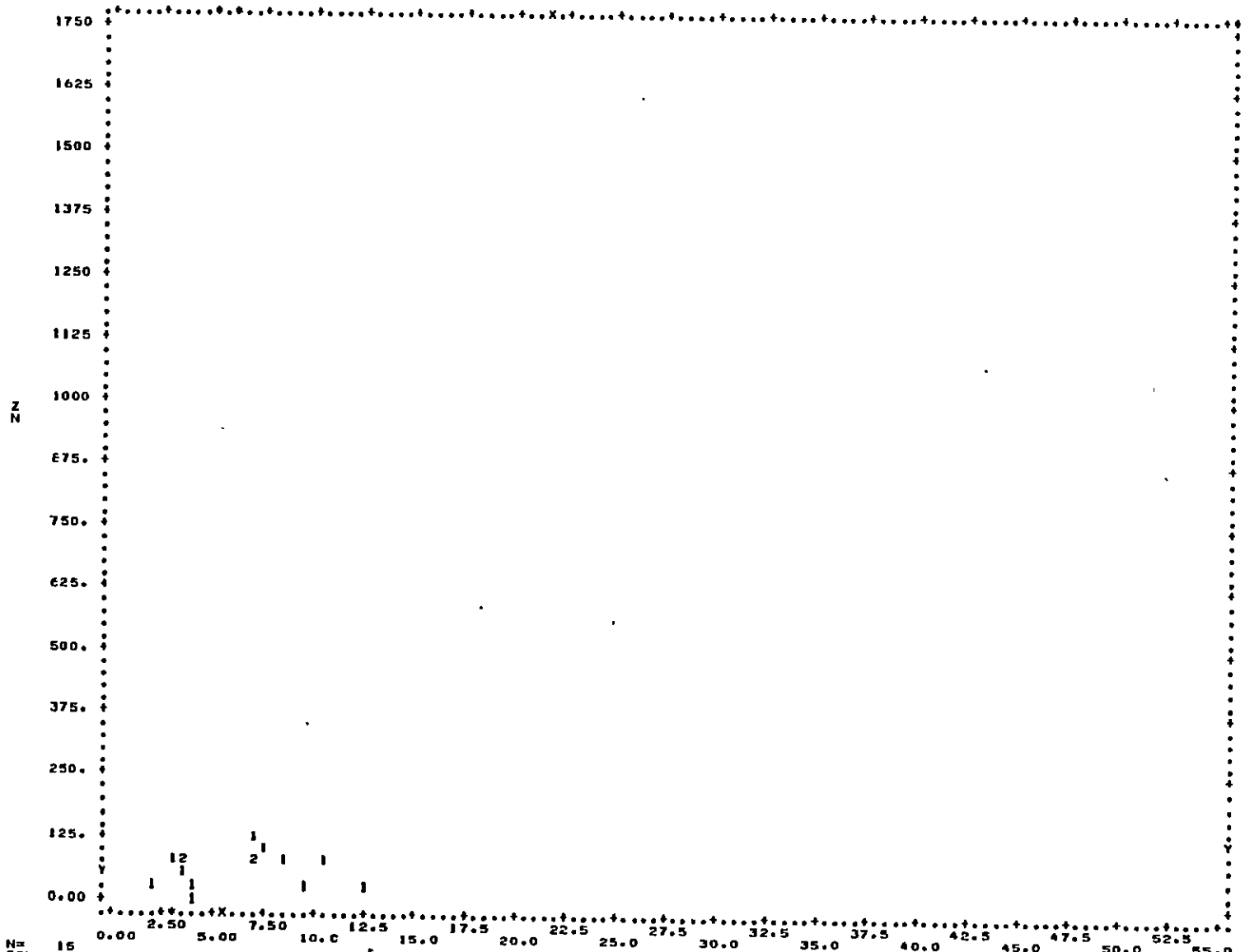

N= 16
COR= .098

	MEAN	ST.DEV.	REGRESSION LINE	RES.MS.
X	6.1447	3.2098	X= .009004*Y+ 5.6011	10.990
Y	60.400	34.807	Y= 1.0582*X+ 53.098	1292.3

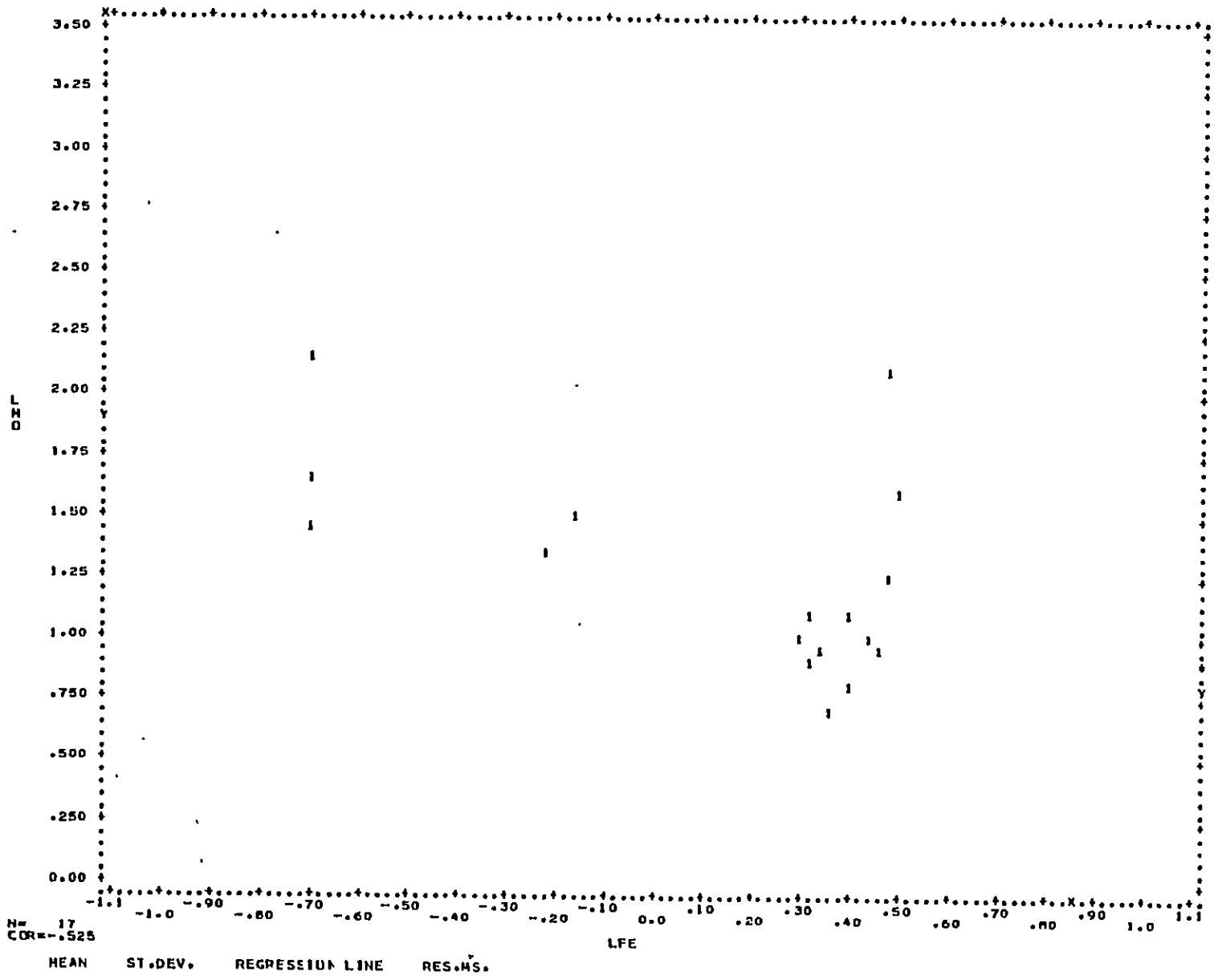

N= 17
COR=-.525

	MEAN	ST.DEV.	REGRESSION LINE	RES.MS.
X	.13769	.44748	X=-.548564*Y+ .83421	.15477
Y	1.2697	.42807	Y=-.502024*X+ 1.3388	.14163

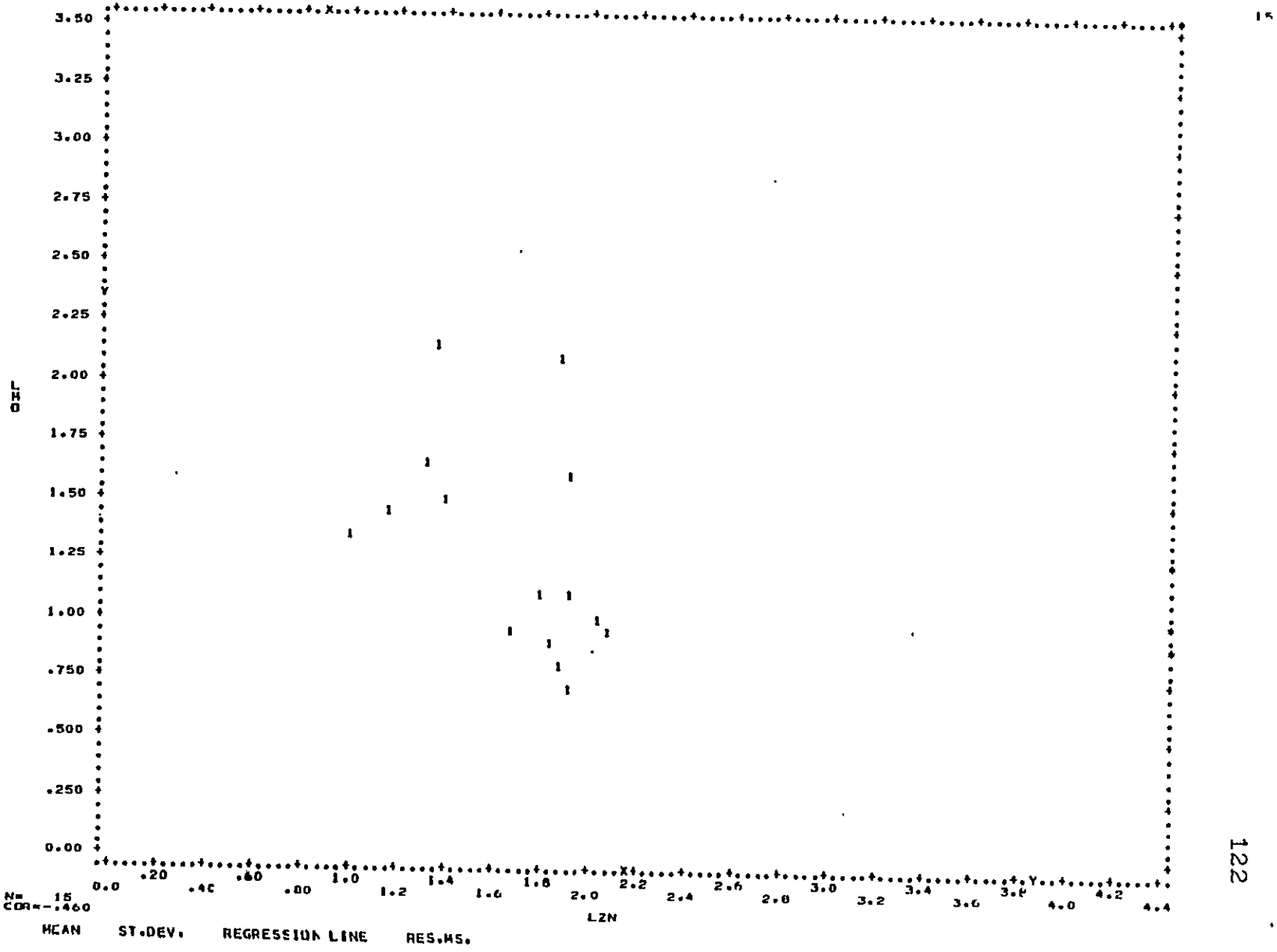

X	1.6757	.34396	X=-.35037*Y+ 2.1312	.10046
Y	1.2686	.45148	Y=-.60365*X+ 2.3025	.17308

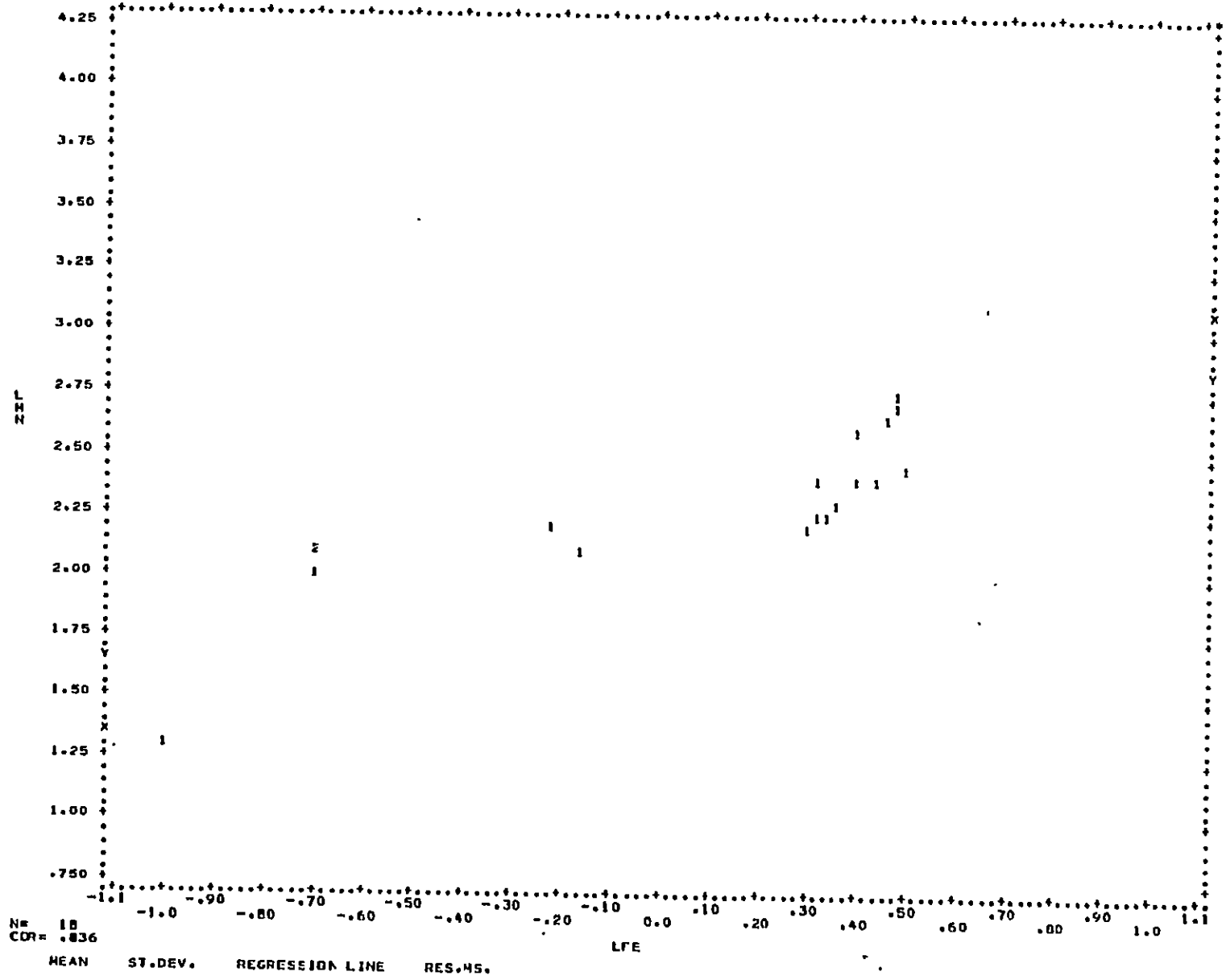

17

N= 18
COR= .836

	MEAN	ST.DEV.	REGRESSION LINE	RES.MS.
X	.07449	.51027	X= 1.2016*Y-2.8513	.08346

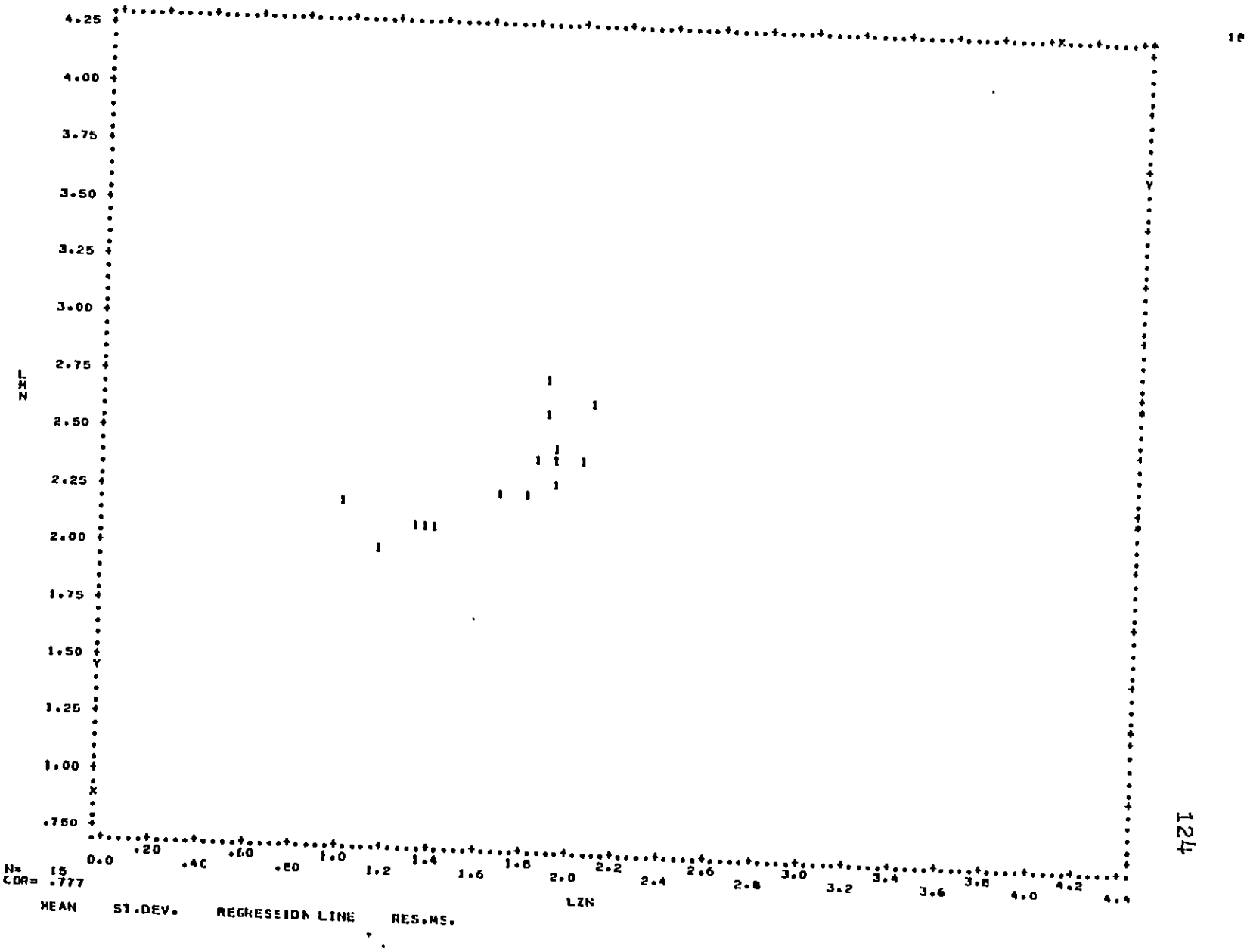

N= 15
COR= .777

	MEAN	ST.DEV.	REGRESSION LINE	RES.MS.
X	1.6797	.34396	X= 1.1976*Y-1.1046	.05043
Y	2.3249	.22325	Y= .50450*X+ 1.4775	.02124

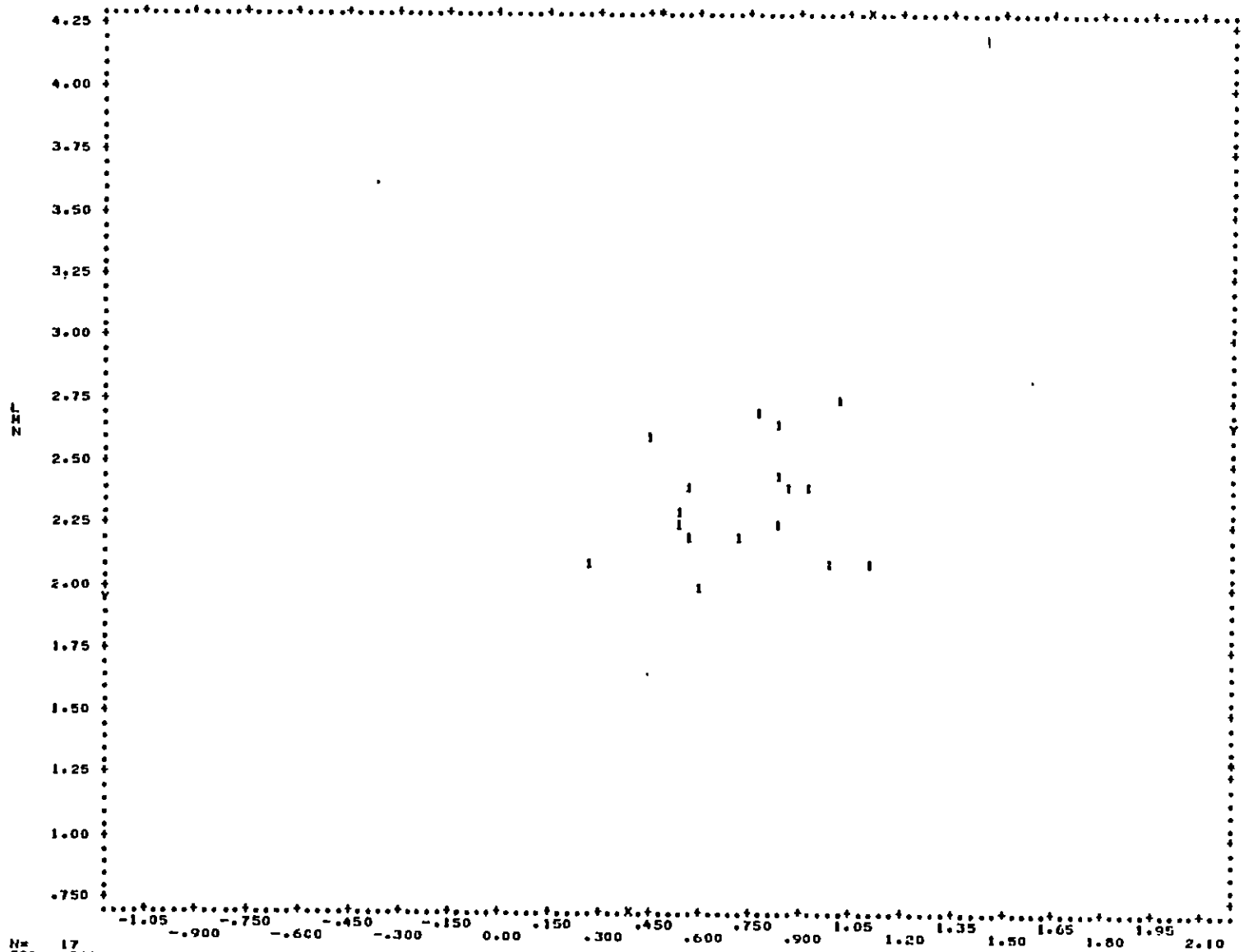

N= 17
COR= .202

	MEAN	ST.DEV.	REGRESSION LINE	RES.MS.
X	.73116	.22827	X= .19914*Y+ .26501	.05330
Y	2.3408	.23158	Y= .20566*X+ 2.1904	.05505

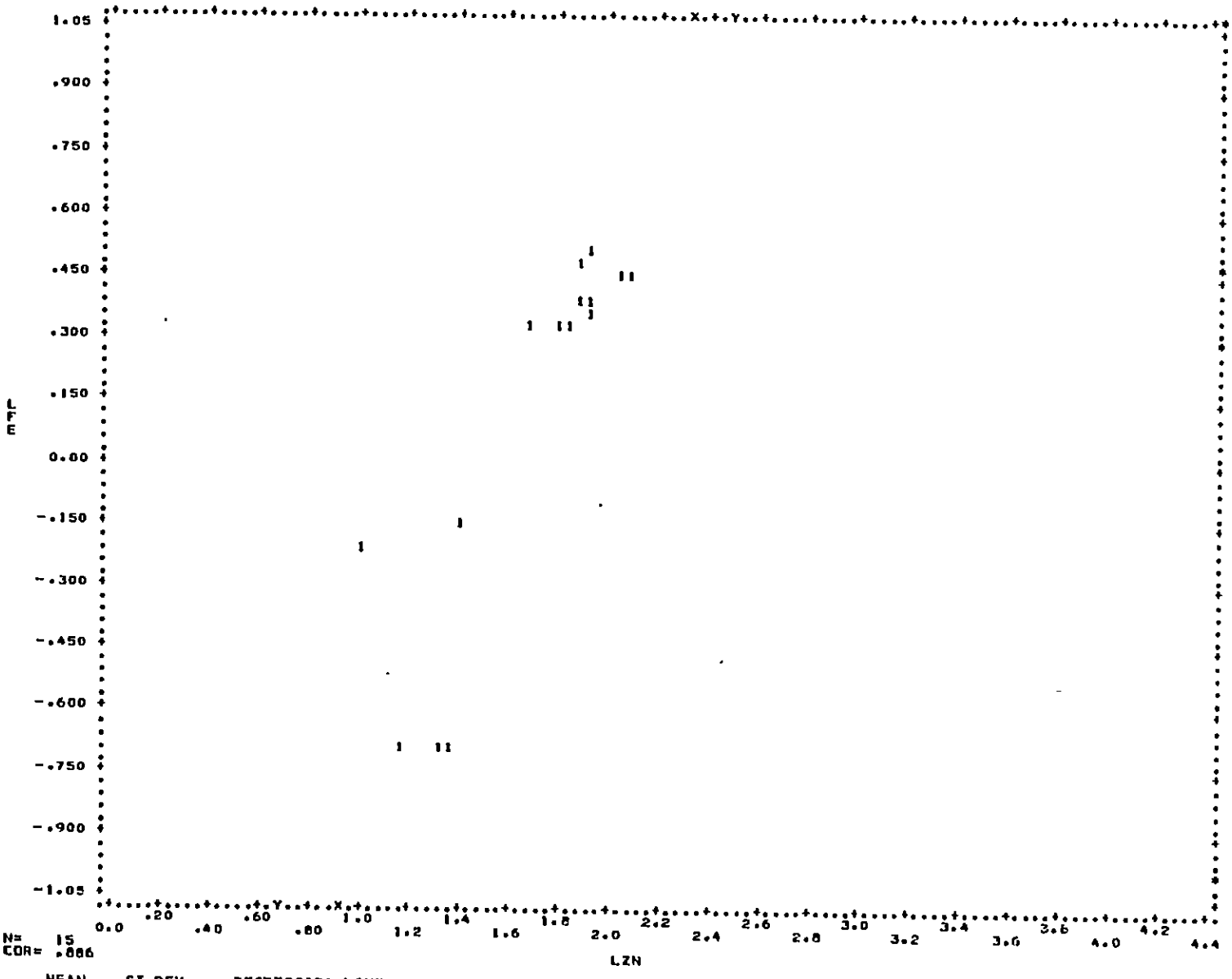

N= 15
COR= .886

	MEAN	ST.DEV.	REGRESSION LINE	RES.MS.
X	1.6797	.34396	X= .65316*Y+ 1.6116	.02748
Y	.10418	.46638	Y= 1.2008*X-1.9128	.05052

21

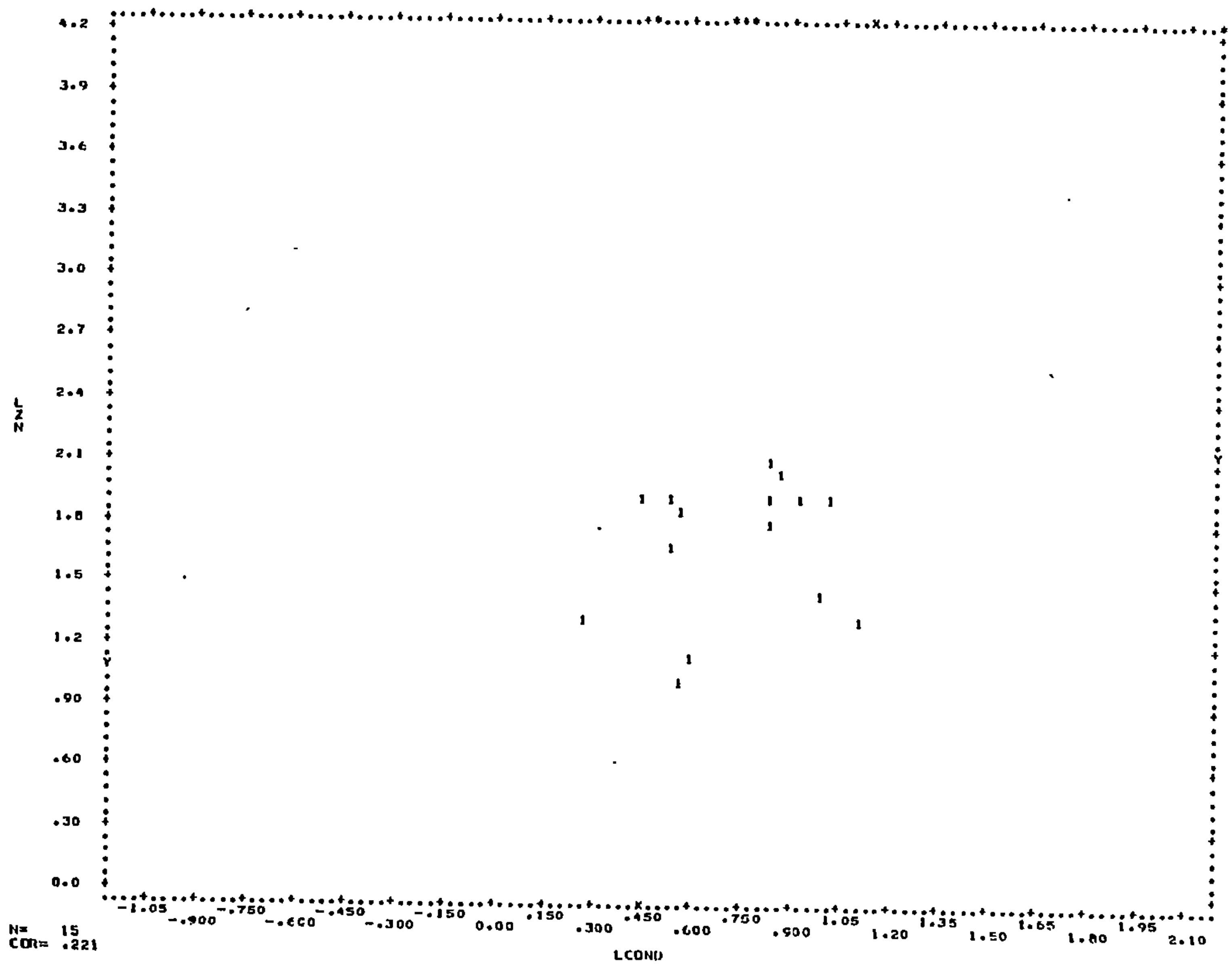

N= 15
COR= .221

	MEAN	ST.DEV.	REGRESSION LINE		RES.MS.
X	.72856	.24355	X= .15660*Y+	.46551	.06076
Y	1.6797	[illegible]	[illegible]	[illegible]	[illegible]

APPENDIX D

X-Y diagrams and correlation coefficients for the profile B-B'.

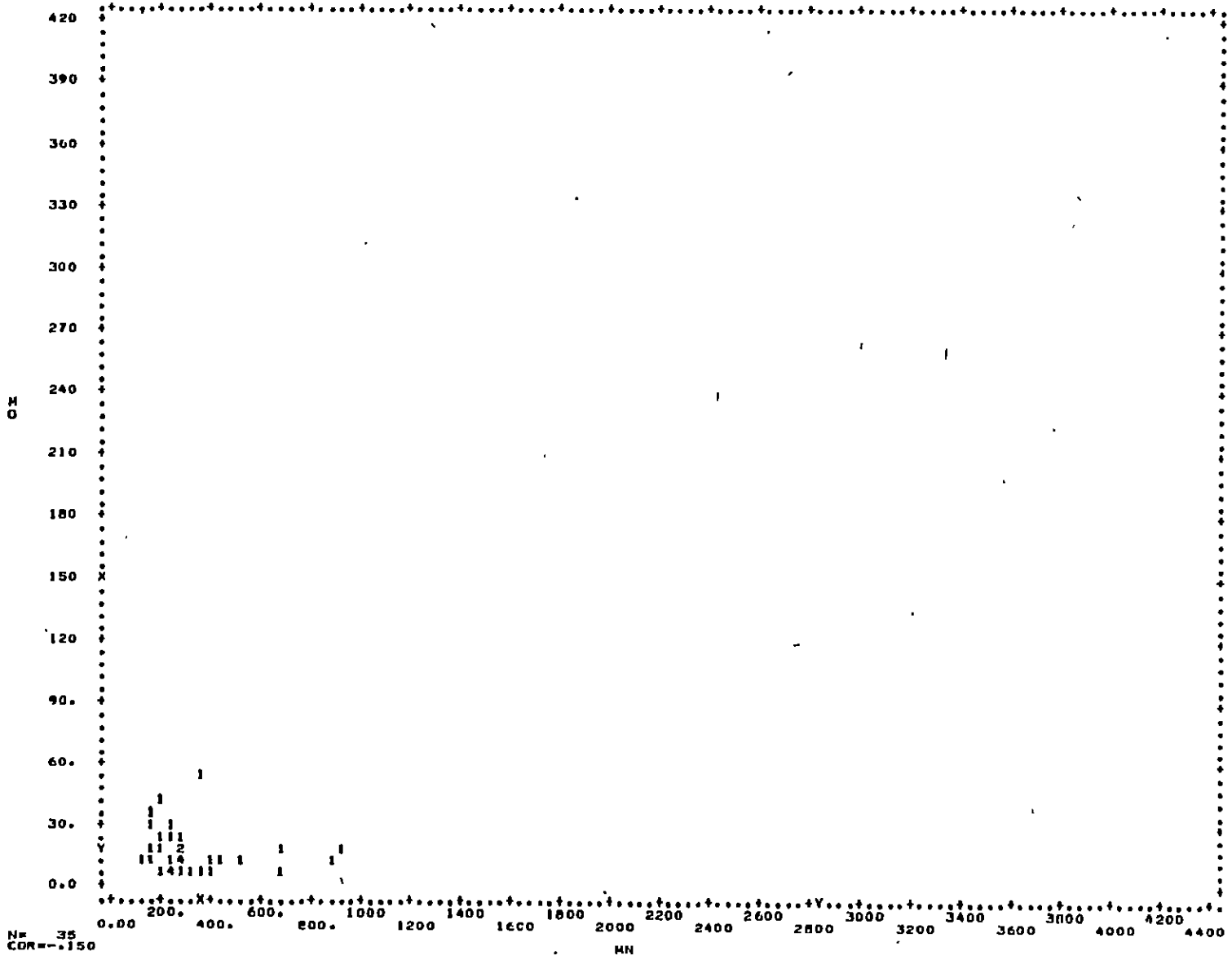

N= 35
COR=-.150

	MEAN	ST.DEV.	REGRESSION LINE	RES.NS.
X	320.00	194.47	X=-2.63024Y+ 361.38	38084.
Y	15.686	11.074	Y=-.006554X+ 18.423	123.50

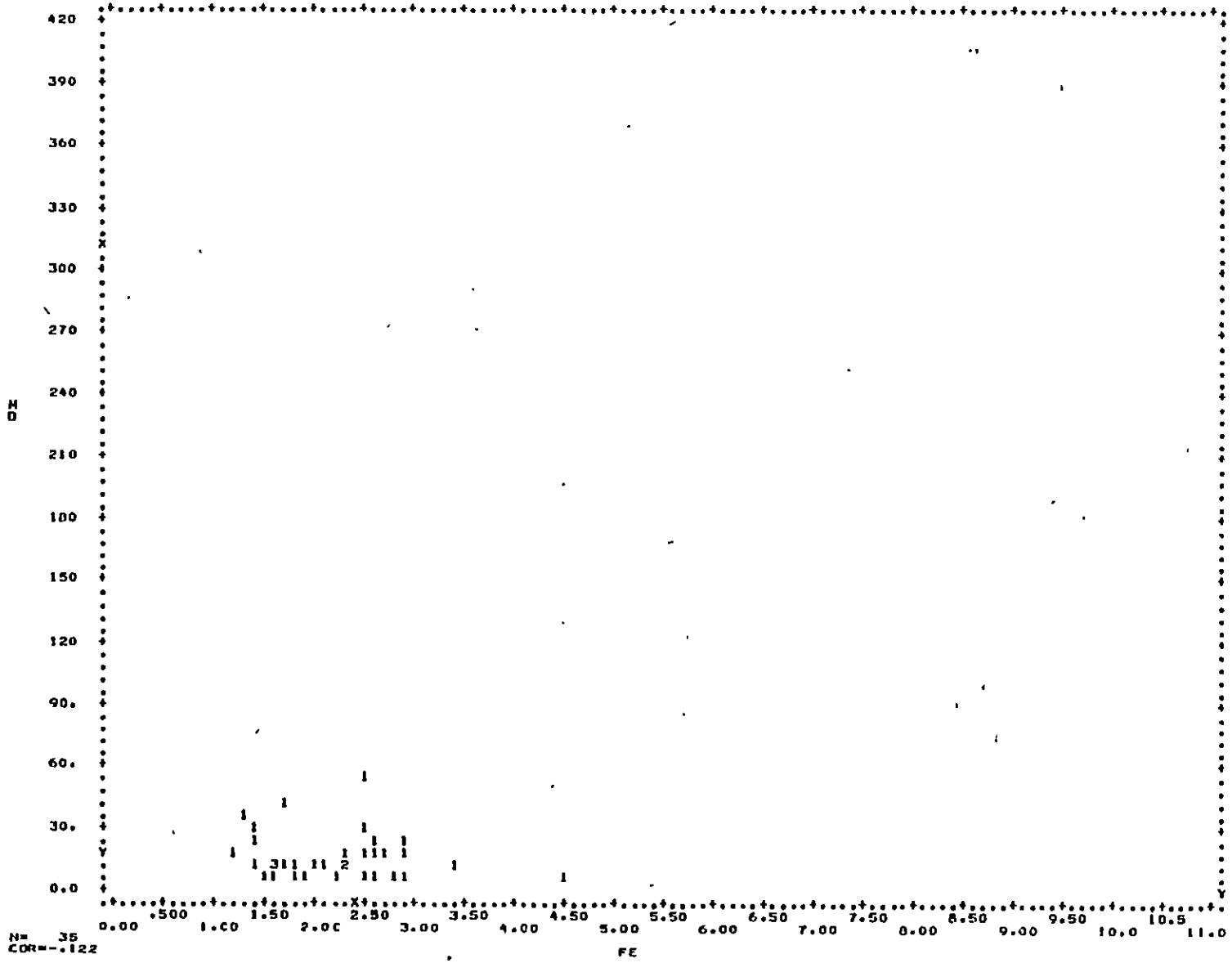

N= 35
COR=-.122

	MEAN	ST.DEV.	REGRESSION LINE	RES.MS.
X	2.1686	.69230	X=-.00766*Y+ 2.3087	.48639
Y	15.686	11.074	Y=-1.9592*X+ 19.973	124.45

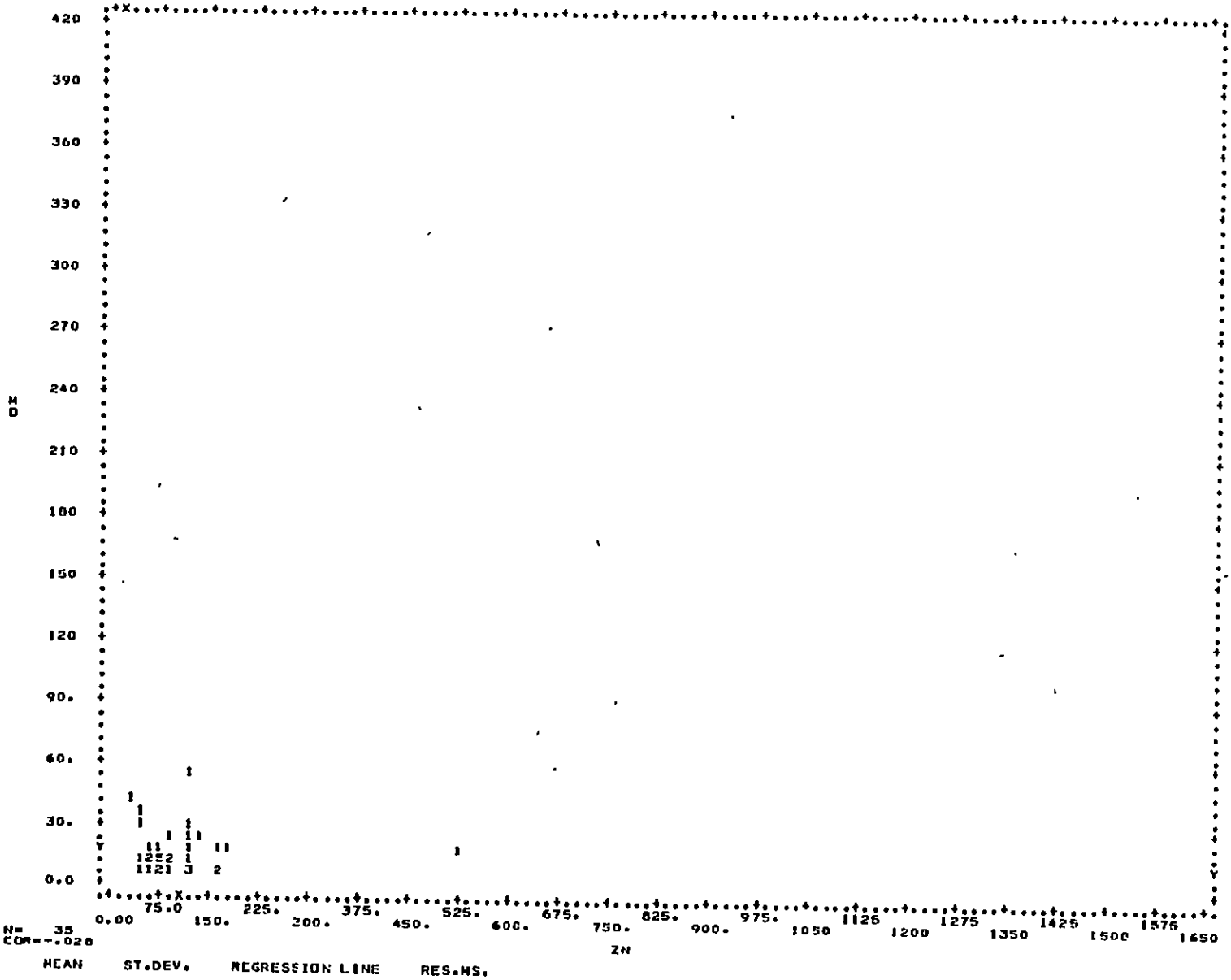

N= 35
COR=-.028

	MEAN	ST.DEV.	REGRESSION LINE	RES.MS.
X	105.94	83.605	X=-.210244*Y+ 109.24	7196.0
Y	15.686	11.074	Y=-.00366*X+ 16.076	126.25

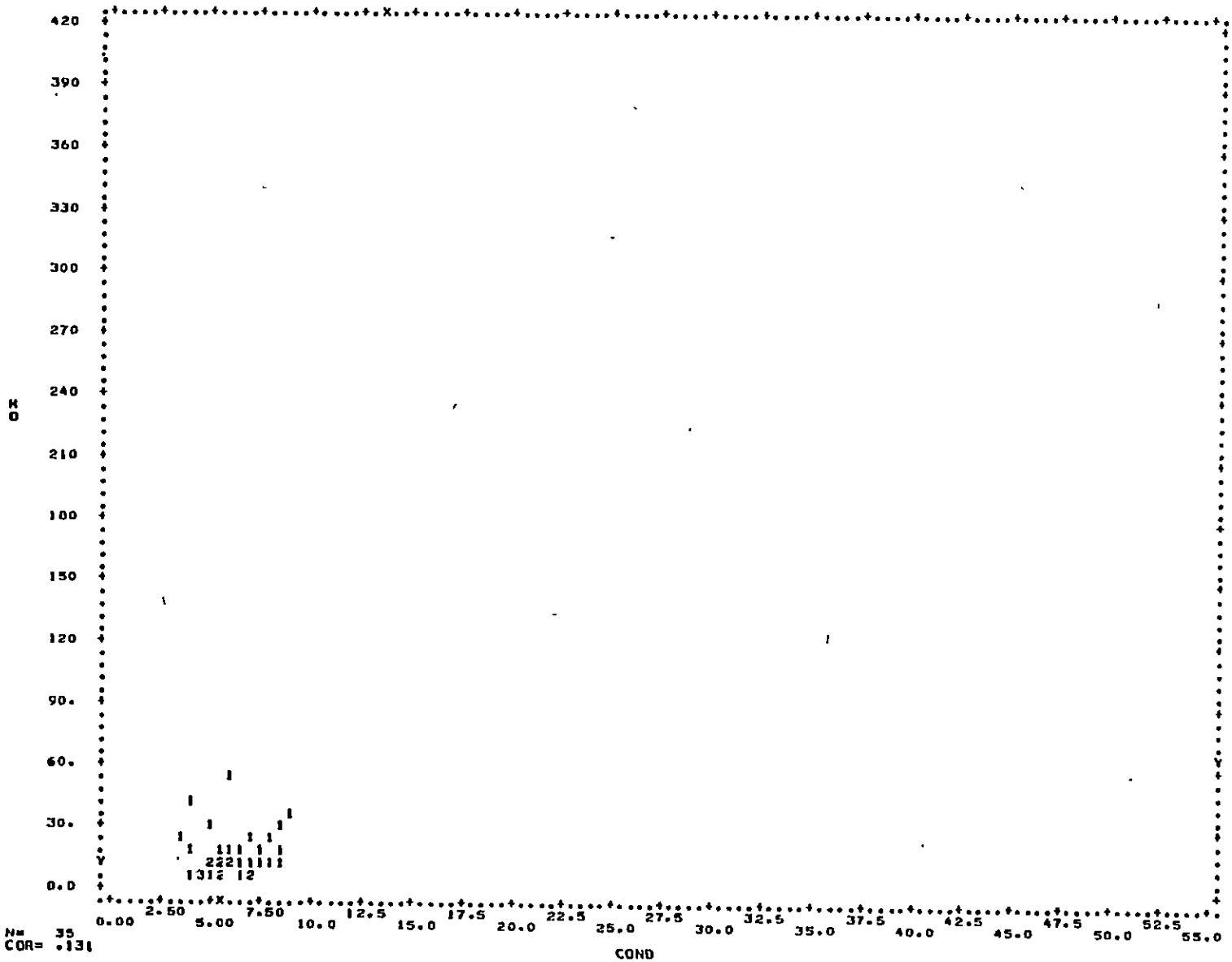

N= 35
COR= .131

	MEAN	ST.DEV.	REGRESSION LINE	RES.MS.
X	6.1286	1.4843	X= .017524Y+ 5.8538	2.2310
Y	15.686	11.074	Y= .975049X+ 9.7101	124.19

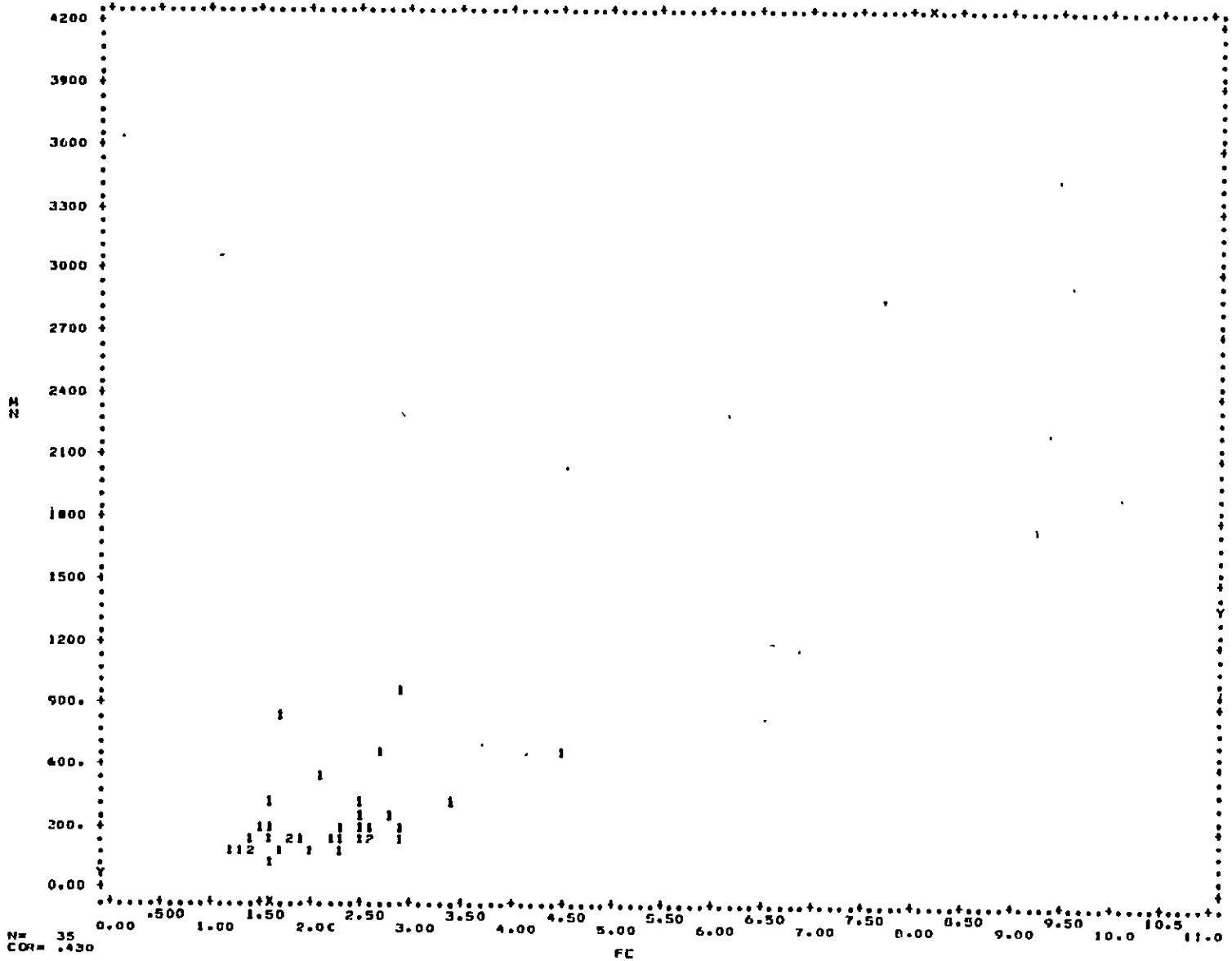

N= 35
COR= .430

	MEAN	ST.DEV.	REGRESSION LINE	RES.MS.
X	2.1686	.69230	X= .00153*Y+ 1.6983	.40234
Y	320.00	194.47	Y= 120.85*X+ 55.416	31747.

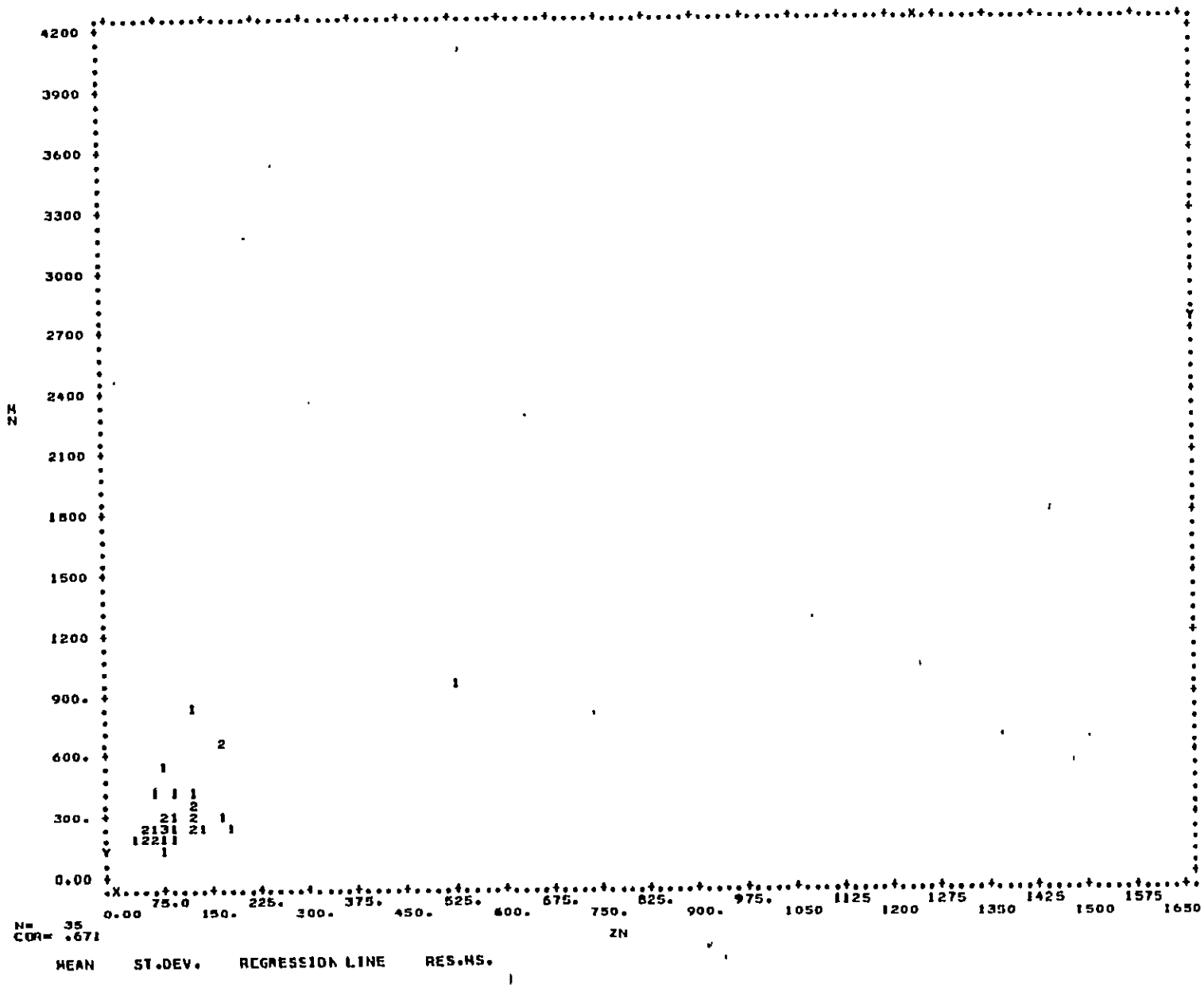

N= 35
COR= .671

	MEAN	ST.DEV.	REGRESSION LINE	RES.MS.
X	105.94	83.605	X= .28829*Y+ 13.691	3963.3
Y	320.00	194.47	Y= 1.5595*X+ 154.75	21443.

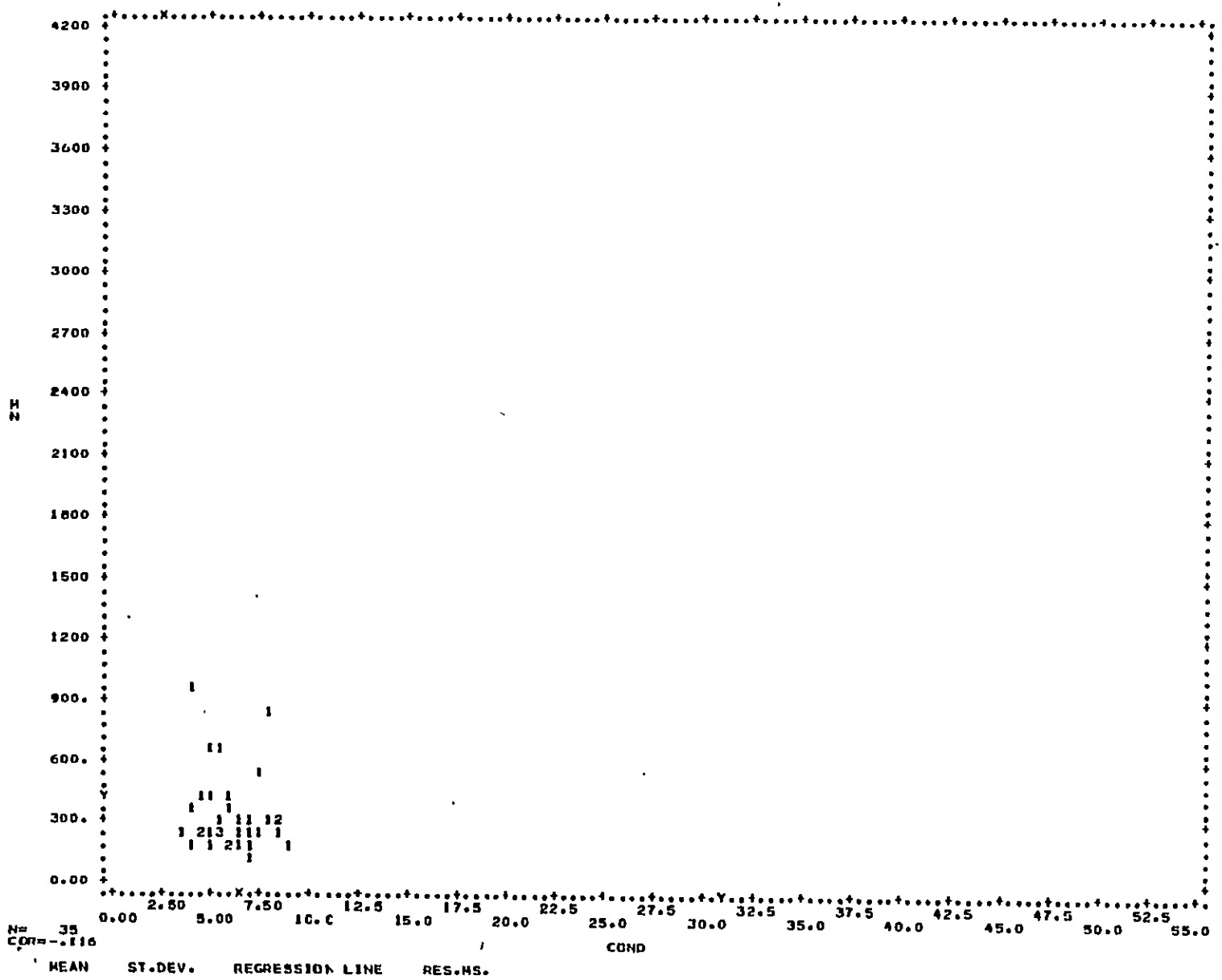

N= 35
COR=-.116

	MEAN	ST.DEV.	REGRESSION LINE	RES.MS.
X	6.1286	1.4643	X=-683E-04Y+ 6.4111	2.2394
Y	320.00	194.47	Y=-15.154X+ 412.87	30442.

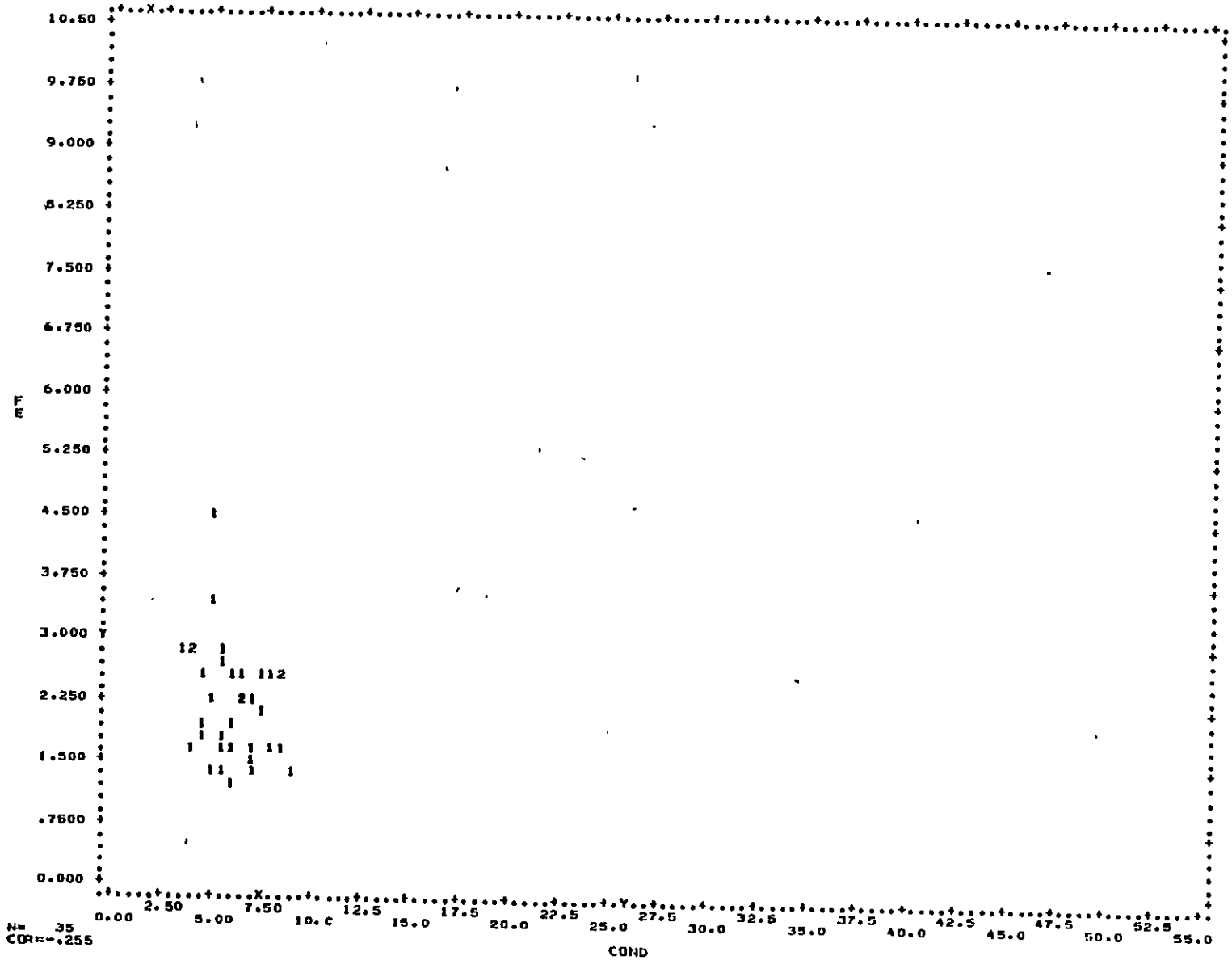

N= 35
COR=-.255

	MEAN	ST.DEV.	REGRESSION LINE	RES.MS.
X	6.1286	1.4843	X=-.64774*Y+ 7.3273	2.1216
Y	2.1886	.69230	Y=-.11916*X+ 2.9109	.46157

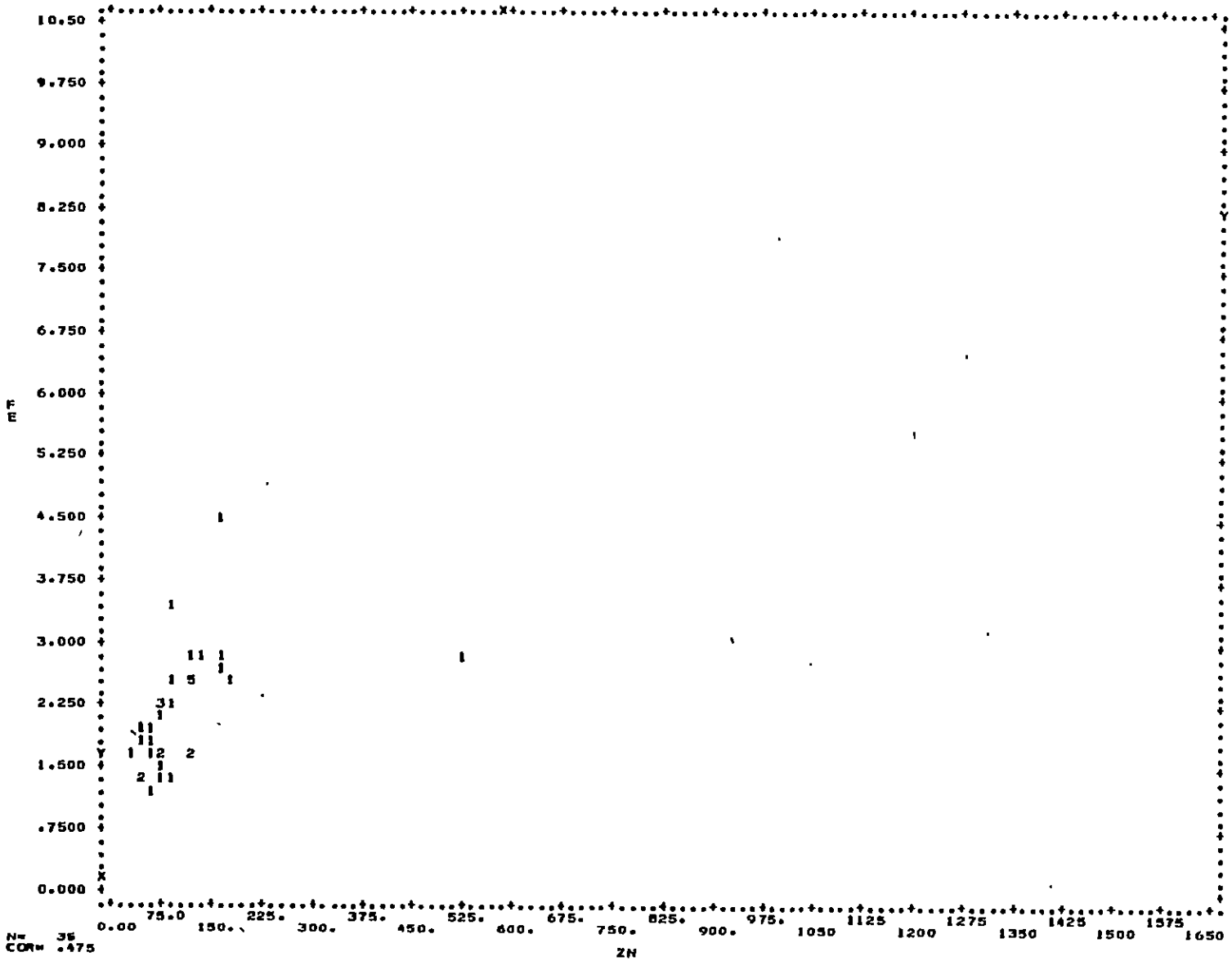

X	105.54	63.605	Y= 57.315*Y-19.496	5579.4
Y	2.1686	.69230	Y= .00393*X+ 1.7722	.30257

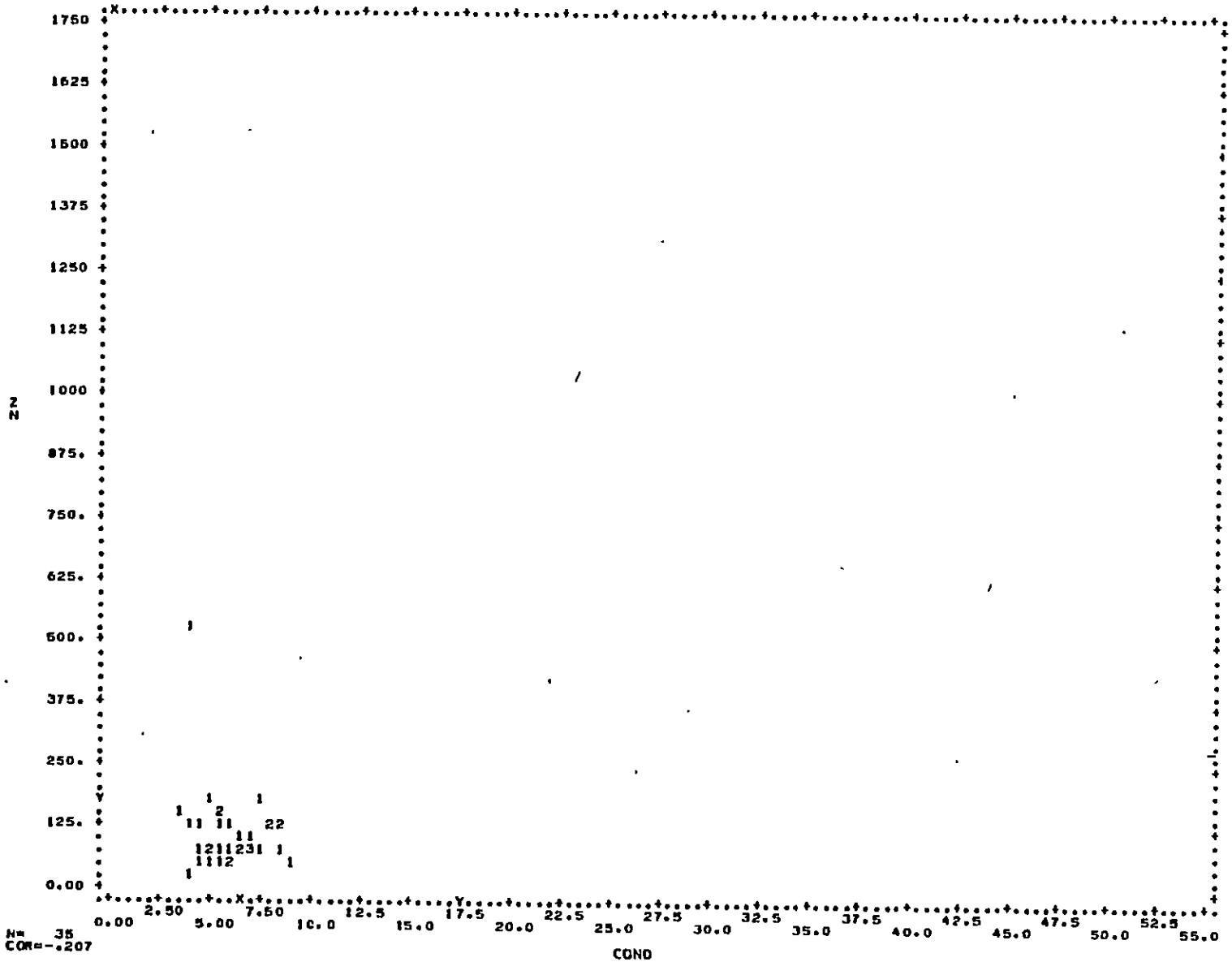

N= 35
COR=-.207

	MEAN	ST.DEV.	REGRESSION LINE	RES.MS.
X	6.1286	1.4843	X=-.00367*Y+ 6.5171	2.1729
Y	105.94	83.605	Y=-11.637*X+ 177.26	6894.2

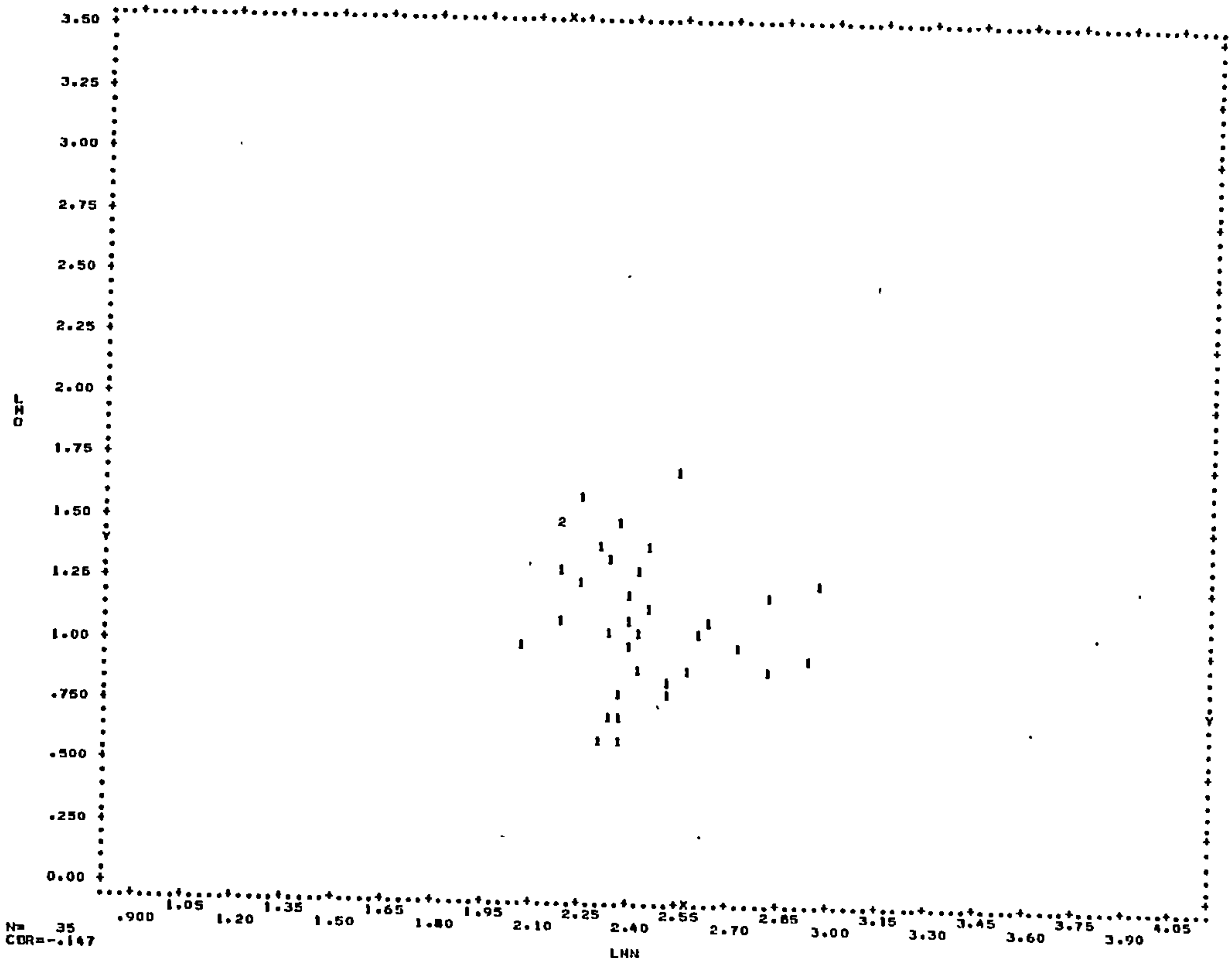

N= 35
COR=-.147

	MEAN	ST.DEV.	REGRESSION LINE	RES.MS.
X	2.4474	.21354	X=-.11030*Y+ 2.5692	.04614
Y	1.1037	.28475	Y=-.1954[illegible]	[illegible]

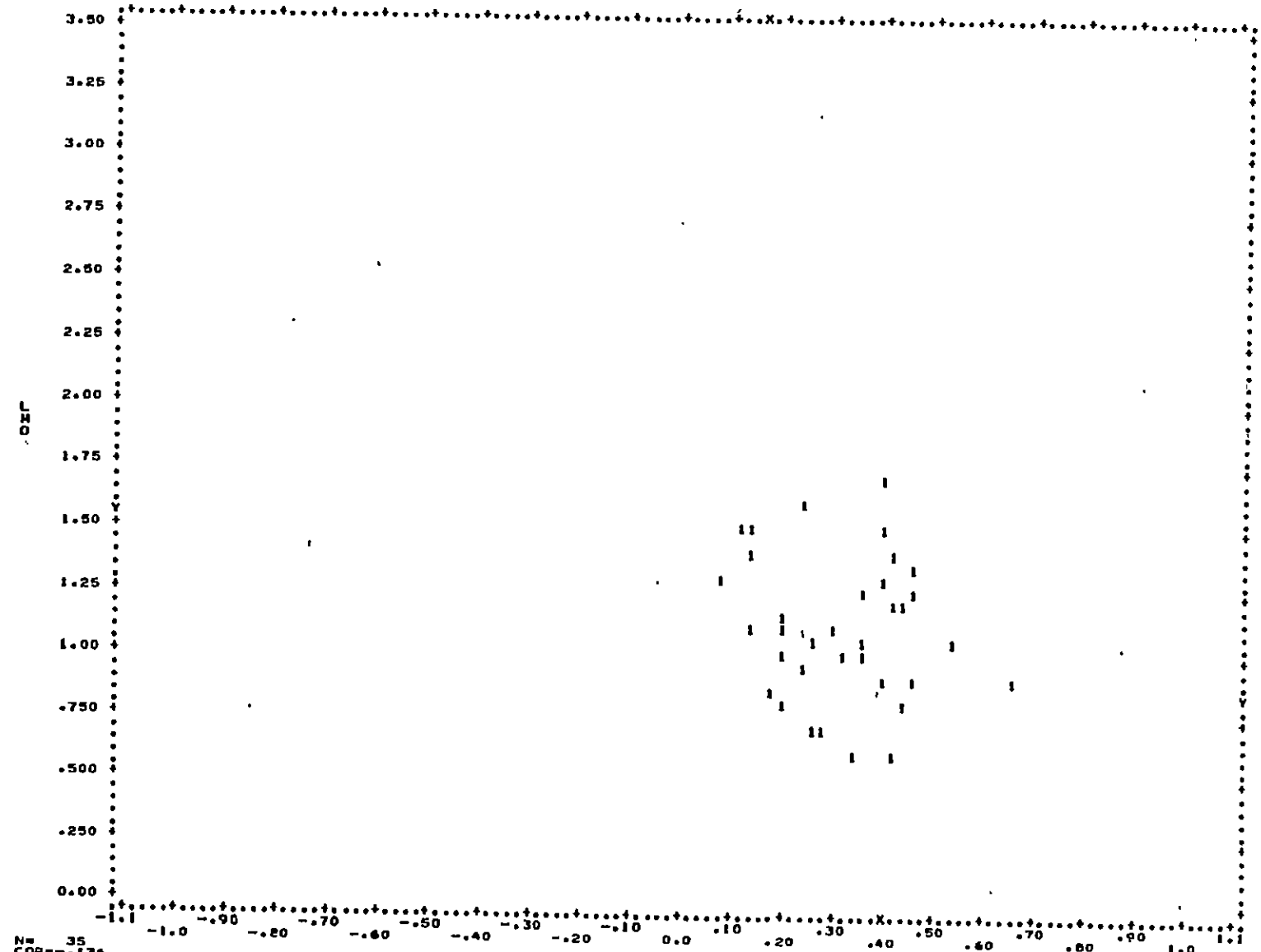

N= 35
COR=-.136

	MEAN	ST.DEV.	REGRESSION LINE	RES.MS.
X	.32035	.13221	X=-.06320*Y+ .39011	.01768
Y	1.1037	.28475	Y=-.29320*X+ 1.1976	.08199

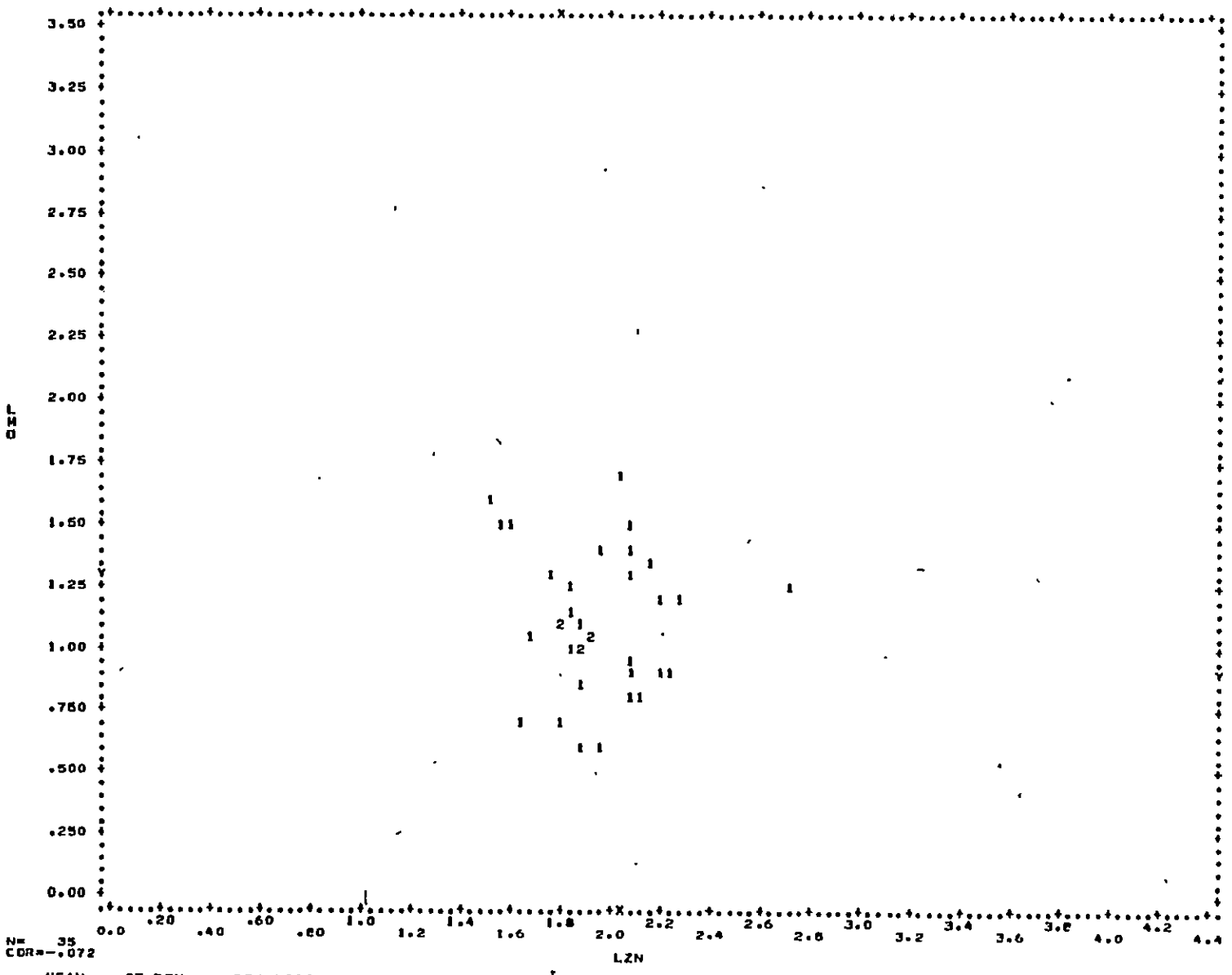

N= 35
COR=-.072

	MEAN	ST.DEV.	REGRESSION LINE	RES.MS.
X	1.9535	.23259	X=-.050644Y+ 2.0184	.05545
Y	1.1037	.28475	Y=-.011818X+ 1.2759	.08311

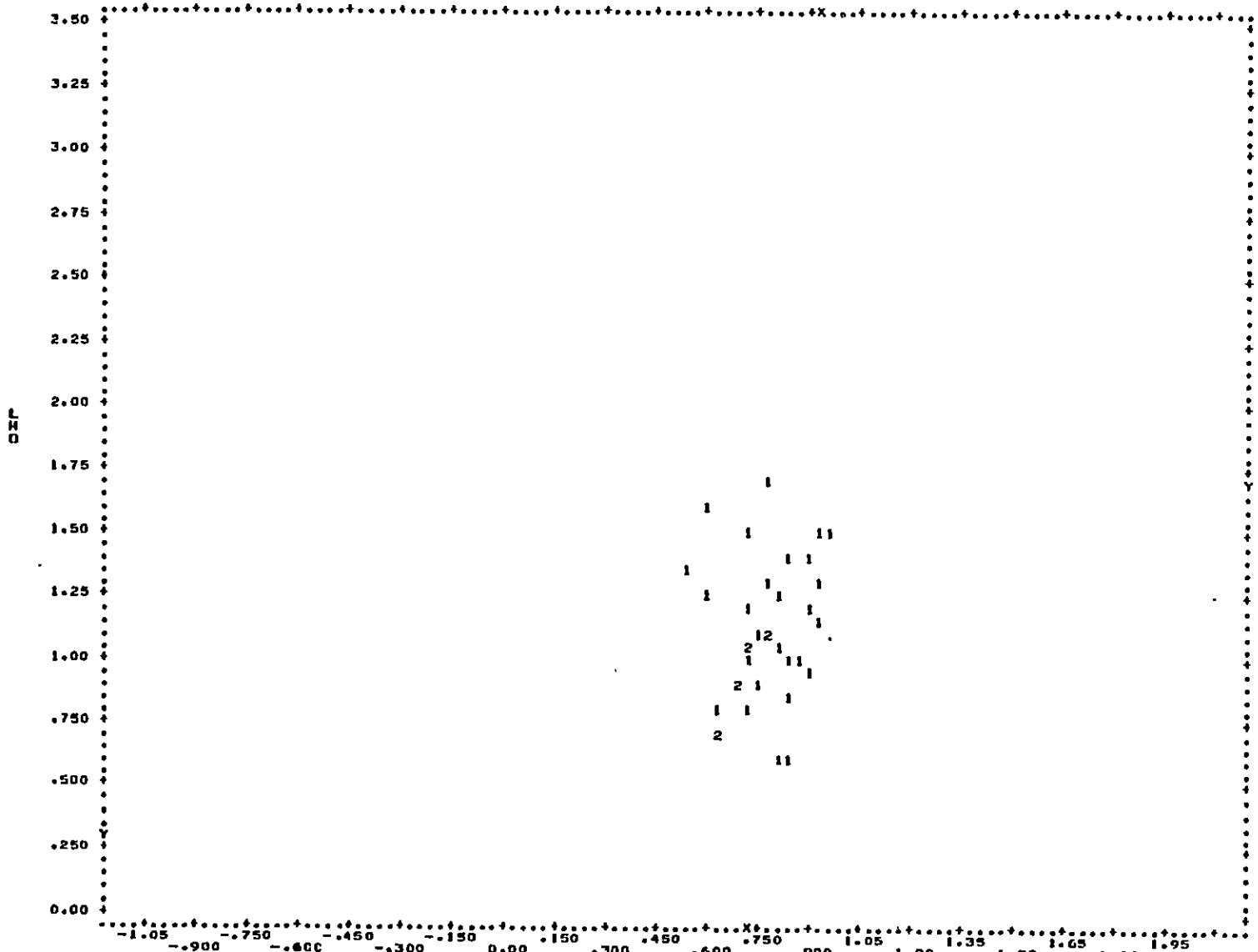

N= 35
COR= .160

	MEAN	ST.DEV.	REGRESSION LINE	RES.MS.
X	.77674	.10702	X= .06003*Y+ .70849	.01150

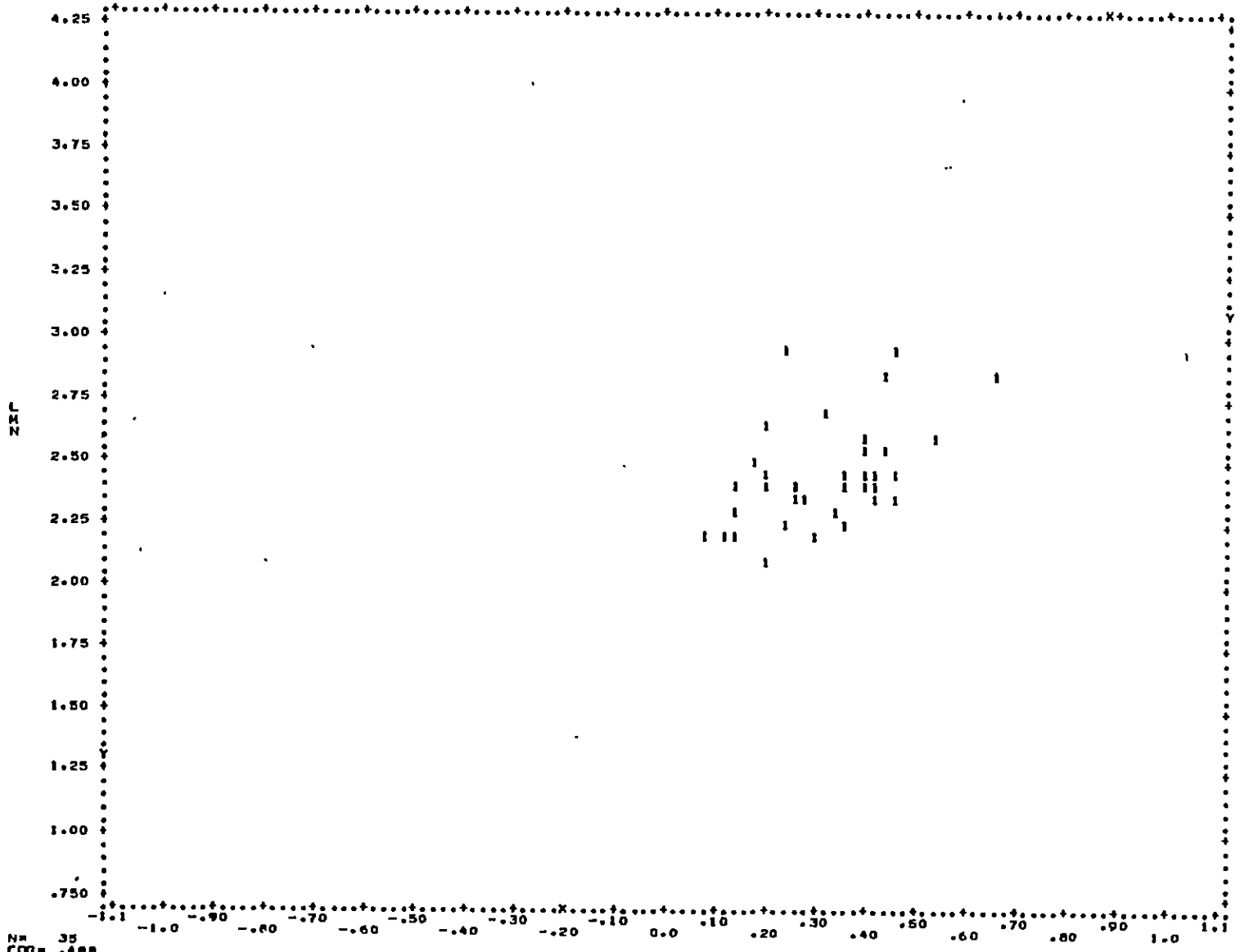

N= 35
COR= .488

	MEAN	ST.DEV.	REGRESSION LINE	RES.MS.
X	.32035	.13221	X= .30165*Y-.41791	.01372
Y	2.4474	.21364	Y= .78990*X+ 2.1944	.03592

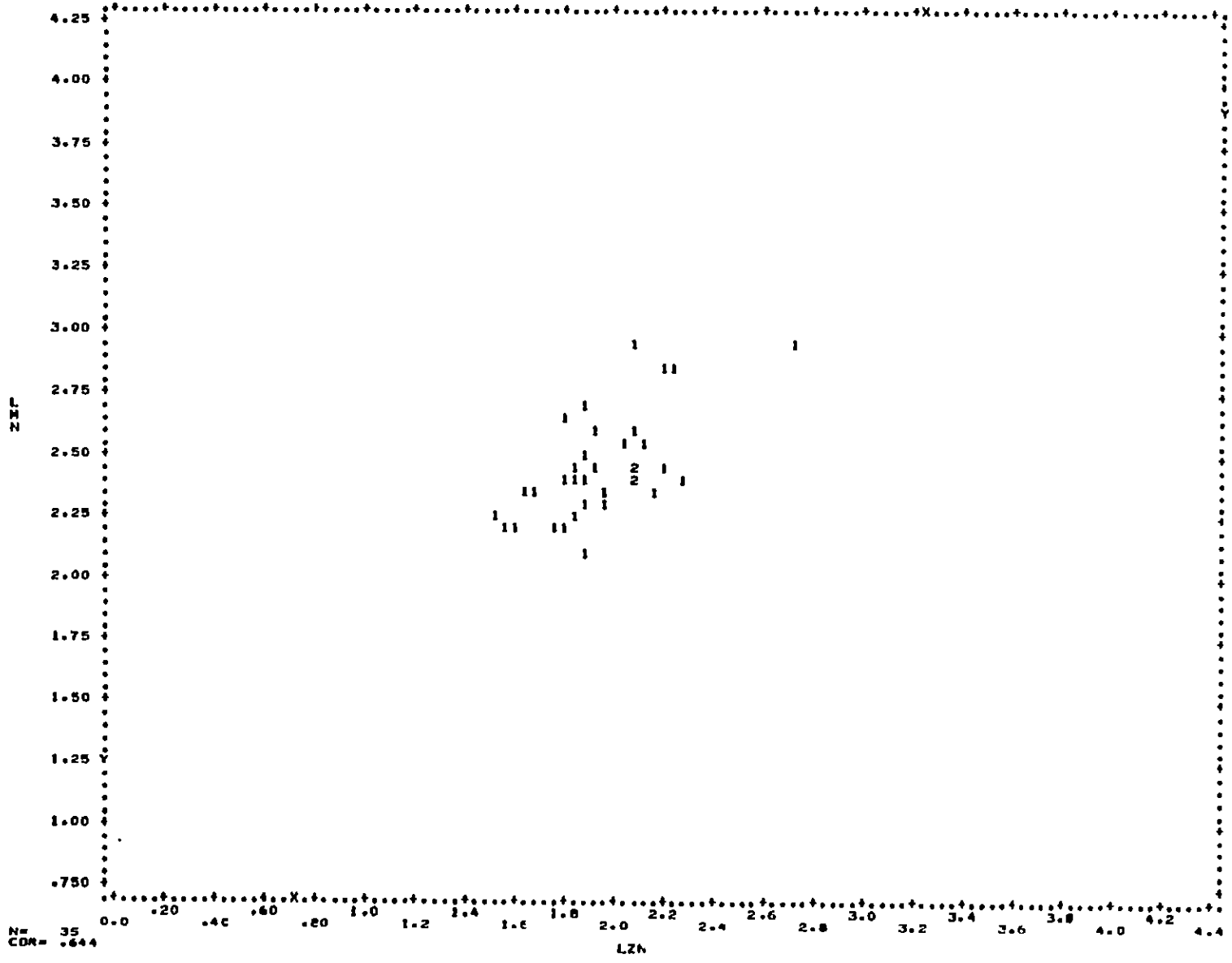

N= 35
COR= .644

	MEAN	ST.DEV.	REGRESSION LINE	RES.MS.
X	1.9535	.23259	X= .69965*Y+ .24114	.03265
Y	2.4474	.21394	Y= .5919C*X+ 1.2910	.02763

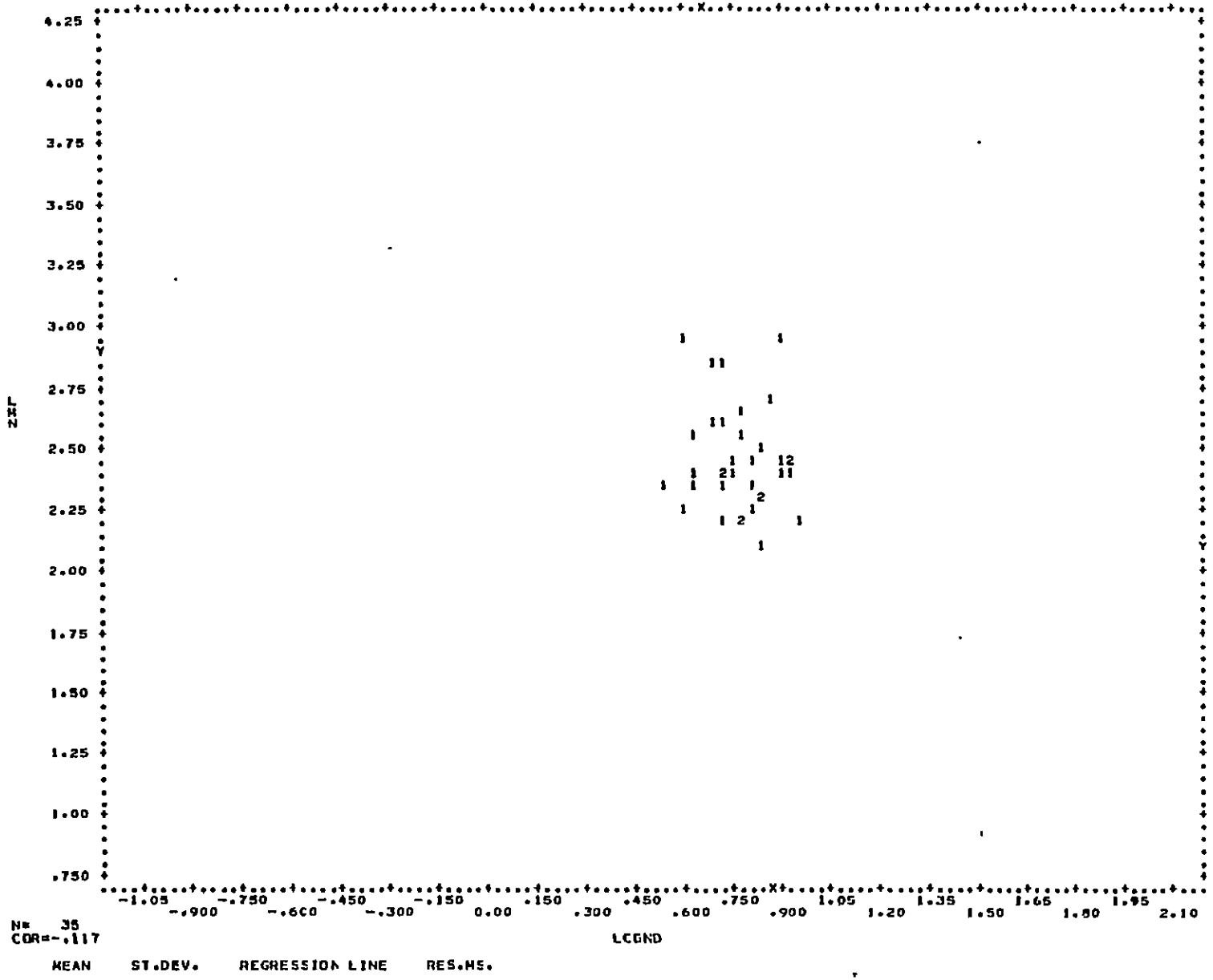

N= 35
COR=-.117

LEGND

	MEAN	ST.DEV.	REGRESSION LINE	RES.MS.
X	.77474	.10702	X=-.0586C*Y+	.91818 .01164
Y	2.4474	.21394	Y=-.2341E*X+	2.6288 .04651

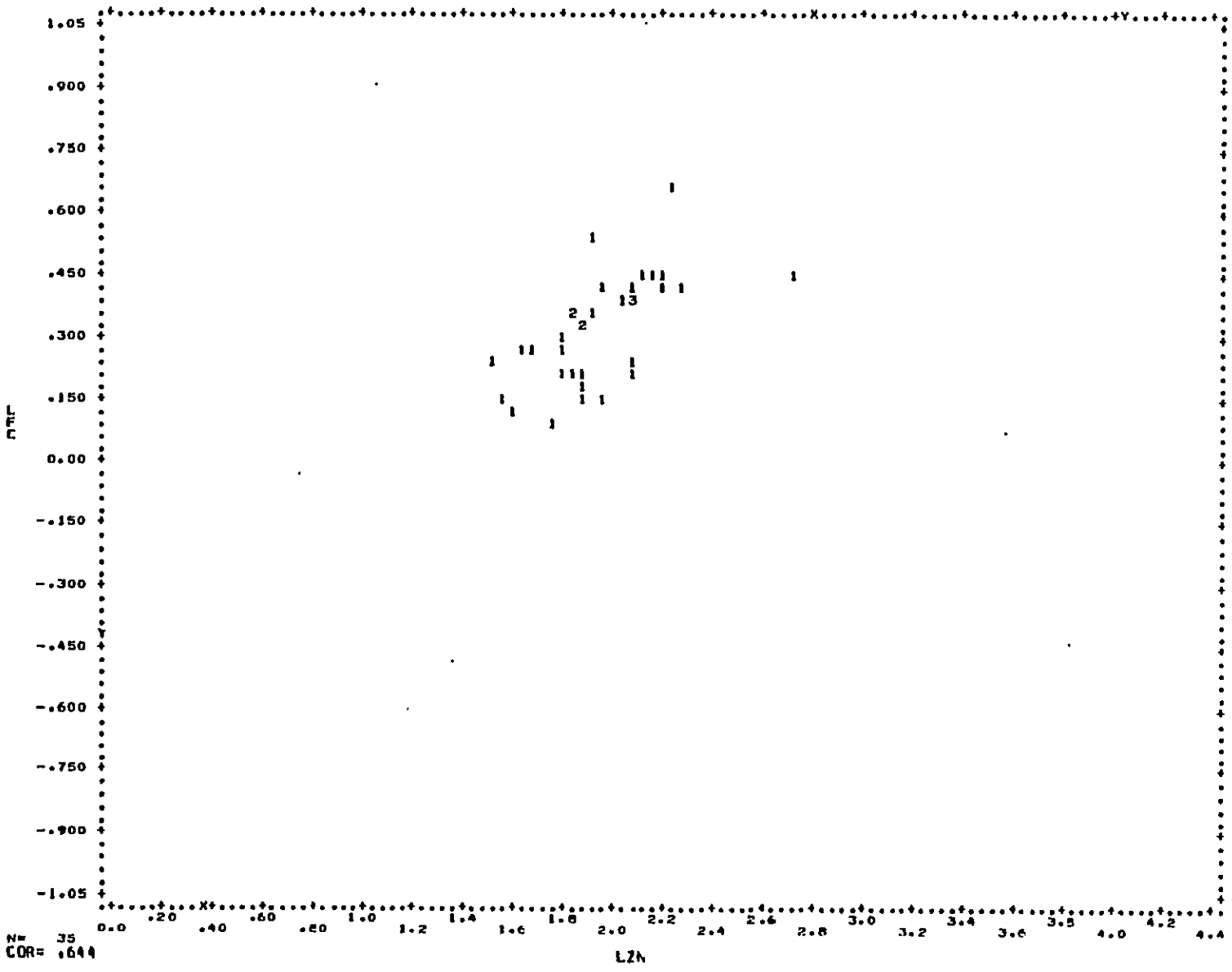

N= 35
COR= .644

	MEAN	ST.DEV.	REGRESSION LINE	RES.MS.
X	1.9535	.23259	X= 1.1327*Y+ 1.5906	.03263
Y	.32035	.13221	Y= .36598*X-.39458	.01054

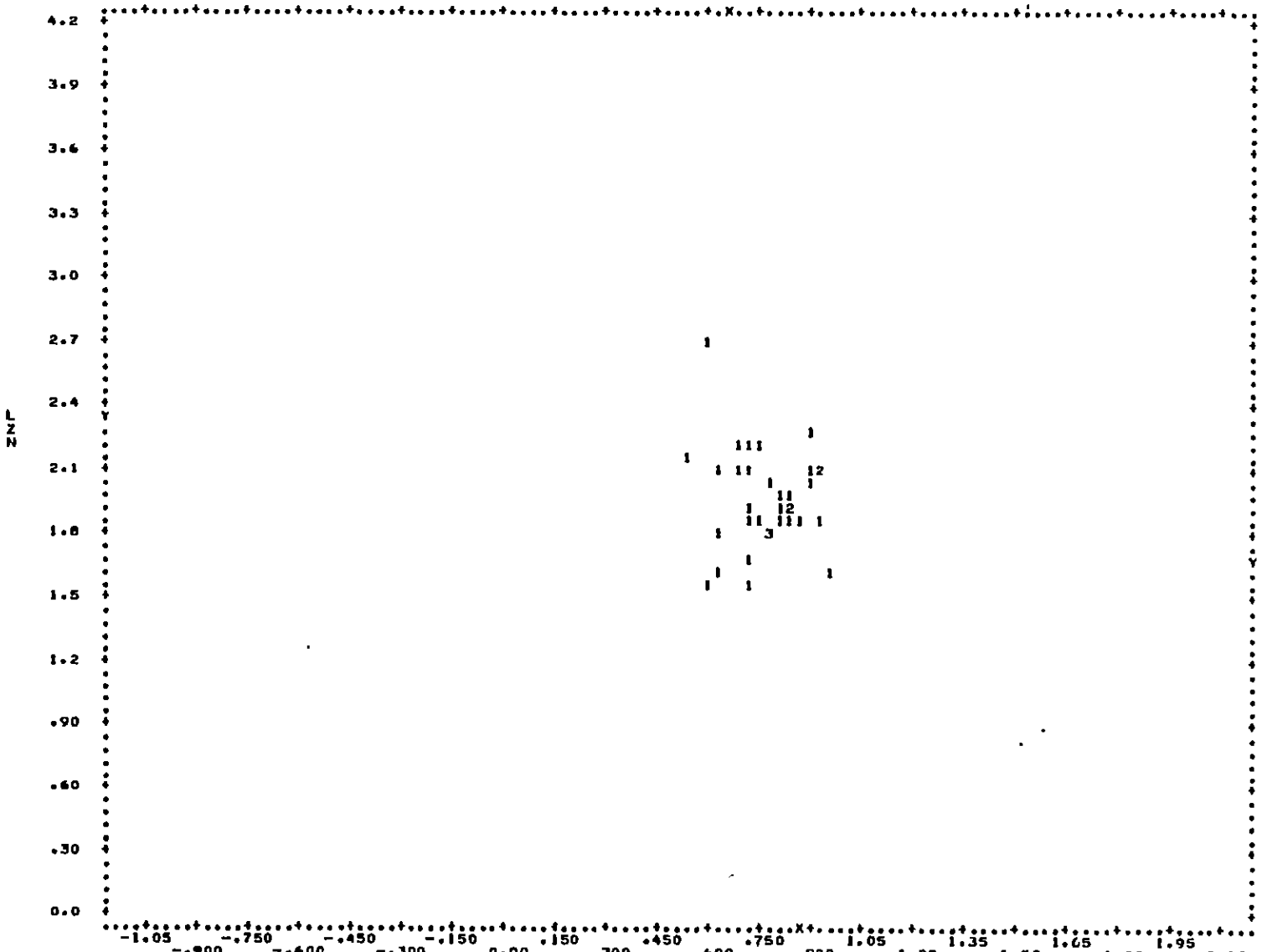

N= 35
CCR=-.097

	MEAN	ST.DEV.	REGRESSION LINE	RES.MS.
X	.77474	.10702	X=-.044660*Y+ .86203	.01169
Y	1.9535	.23259	Y=-.211024*X+ 2.1170	.05521

APPENDIX E

Histograms for all 5 variables based on data for the entire study area.

HISTOGRAM OF VARIABLE 1 MG

SYMBOL X | COUNT 1868 | MEAN 13.812 | ST.DEV. 23.629

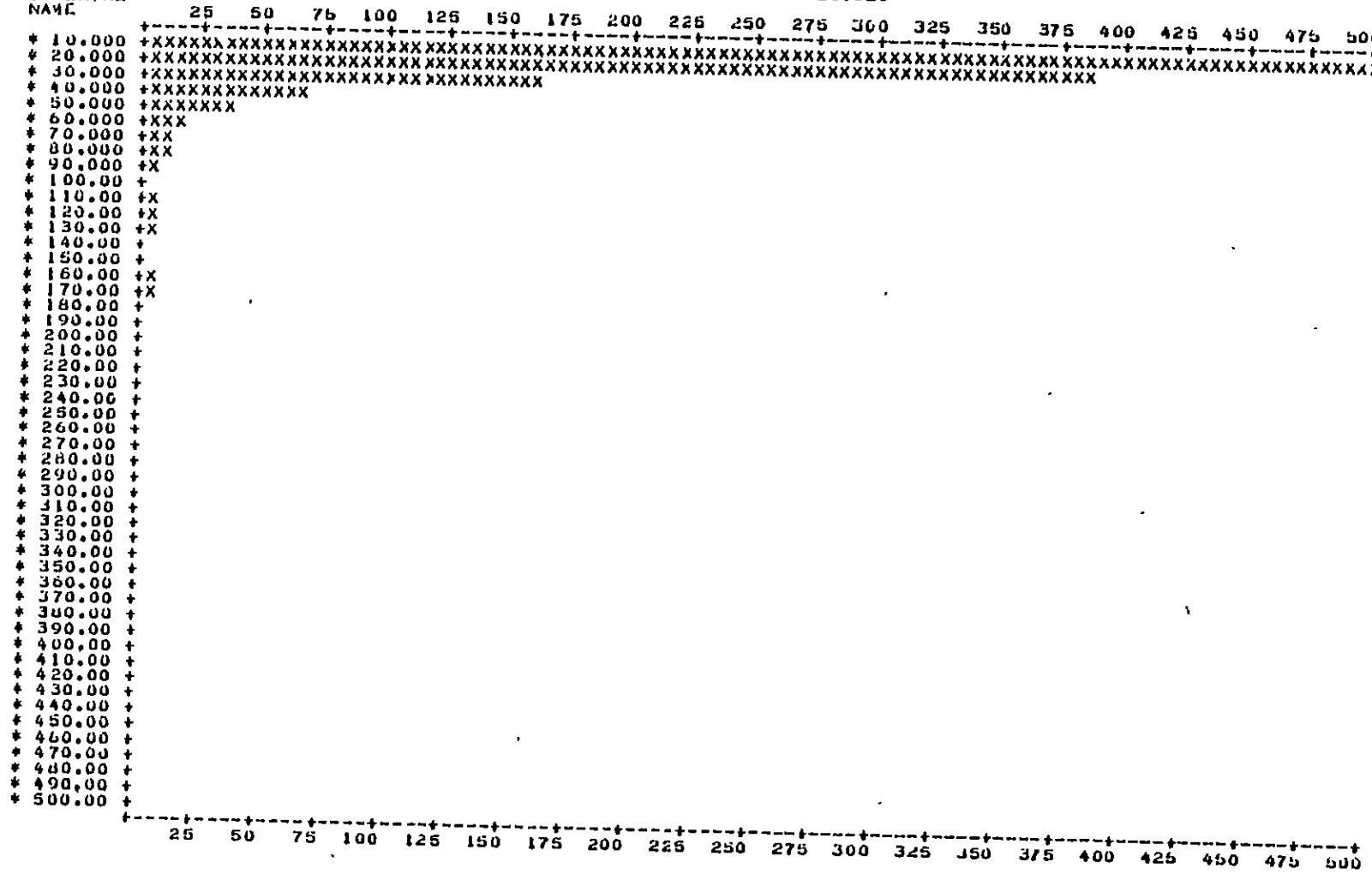

INTERVAL NAME	FREQUENCY INT.	FREQUENCY CUM.	PERCENTAGE INT.	PERCENTAGE CUM.
* 10.000	1147	1147	61.4	61.4
* 20.000	387	1534	20.7	82.1
* 30.000	162	1696	8.7	90.8
* 40.000	67	1763	3.6	94.4
* 50.000	35	1798	1.9	96.3
* 60.000	17	1815	0.9	97.2
* 70.000	11	1826	0.6	97.8
* 80.000	12	1838	0.6	98.4
* 90.000	3	1841	0.2	98.6
* 100.00	2	1843	0.1	98.7
* 110.00	5	1848	0.3	98.9
* 120.00	3	1851	0.2	99.1
* 130.00	3	1854	0.2	99.3
* 140.00	1	1855	0.1	99.3
* 150.00	2	1857	0.1	99.4
* 160.00	3	1860	0.2	99.6
* 170.00	3	1863	0.2	99.7
* 180.00	0	1863	0.0	99.7
* 190.00	1	1864	0.1	99.8
* 200.00	1	1865	0.1	99.8
* 210.00	0	1865	0.0	99.8
* 220.00	0	1865	0.0	99.8
* 230.00	0	1865	0.0	99.8
* 240.00	0	1865	0.0	99.8
* 250.00	0	1865	0.0	99.8
* 260.00	0	1865	0.0	99.8
* 270.00	0	1865	0.0	99.8
* 280.00	0	1865	0.0	99.8
* 290.00	0	1865	0.0	99.8
* 300.00	0	1865	0.0	99.8
* 310.00	0	1865	0.0	99.8
* 320.00	0	1865	0.0	99.8
* 330.00	0	1865	0.0	99.8
* 340.00	1	1866	0.1	99.9
* 350.00	0	1866	0.0	99.9
* 360.00	0	1866	0.0	99.9
* 370.00	0	1866	0.0	99.9
* 380.00	0	1866	0.0	99.9
* 390.00	1	1867	0.1	99.9
* 400.00	0	1867	0.0	99.9
* 410.00	0	1867	0.0	99.9
* 420.00	1	1868	0.1	100.0
* 430.00	0	1868	0.0	100.0
* 440.00	0	1868	0.0	100.0
* 450.00	0	1868	0.0	100.0
* 460.00	0	1868	0.0	100.0
* 470.00	0	1868	0.0	100.0
* 480.00	0	1868	0.0	100.0
* 490.00	0	1868	0.0	100.0
* 500.00	0	1868	0.0	100.0

HISTOGRAM OF VARIABLE 2 MN

SYMBOL	COUNT	MEAN	ST.DEV.
X	1867	400.700	371.864

INTERVAL NAME	FREQUENCY INT.	FREQUENCY CUM.	PERCENTAGE INT.	PERCENTAGE CUM.
* 80.000	7	7	0.4	0.4
* 160.00	161	168	8.6	9.0
* 240.00	528	696	28.3	37.3
* 320.00	453	1149	24.3	61.5
* 400.00	204	1353	10.9	72.5
* 480.00	141	1494	7.6	80.0
* 560.00	84	1578	4.5	84.5
* 640.00	57	1635	3.1	87.6
* 720.00	56	1691	3.0	90.6
* 800.00	25	1716	1.3	91.9
* 880.00	24	1740	1.3	93.2
* 960.00	23	1763	1.2	94.4
* 1040.0	15	1778	0.8	95.2
* 1120.0	14	1792	0.7	96.0
* 1200.0	7	1799	0.4	96.4
* 1280.0	11	1810	0.6	96.9
* 1360.0	5	1815	0.3	97.2
* 1440.0	6	1821	0.3	97.5
* 1520.0	6	1827	0.3	97.9
* 1600.0	4	1831	0.2	98.1
* 1680.0	7	1838	0.4	98.4
* 1760.0	4	1842	0.2	98.7
* 1840.0	0	1842	0.0	98.7
* 1920.0	3	1845	0.2	98.8
* 2000.0	2	1847	0.1	98.9
* 2080.0	1	1848	0.1	99.0
* 2160.0	1	1849	0.1	99.0
* 2240.0	1	1850	0.1	99.1
* 2320.0	0	1850	0.0	99.1
* 2400.0	1	1851	0.1	99.1
* 2480.0	3	1854	0.2	99.3
* 2560.0	1	1855	0.1	99.4
* 2640.0	1	1856	0.1	99.4
* 2720.0	0	1856	0.0	99.4
* 2800.0	1	1857	0.1	99.5
* 2880.0	0	1857	0.0	99.5
* 2960.0	4	1861	0.2	99.7
* 3040.0	0	1861	0.0	99.7
* 3120.0	2	1863	0.1	99.8
* 3200.0	1	1864	0.1	99.8
* 3280.0	0	1864	0.0	99.8
* 3360.0	0	1864	0.0	99.8
* 3440.0	1	1865	0.1	99.9
* 3520.0	0	1865	0.0	99.9
* 3600.0	0	1865	0.0	99.9
* 3680.0	0	1865	0.0	99.9
* 3760.0	0	1865	0.0	99.9
* 3840.0	1	1866	0.1	99.9
* 3920.0	1	1867	0.1	100.0
* 4000.0	0	1867	0.0	100.0

HISTOGRAM OF VARIABLE 3 FE

SYMBOL X COUNT 1868 MEAN 2.404 ST.DEV. 0.745

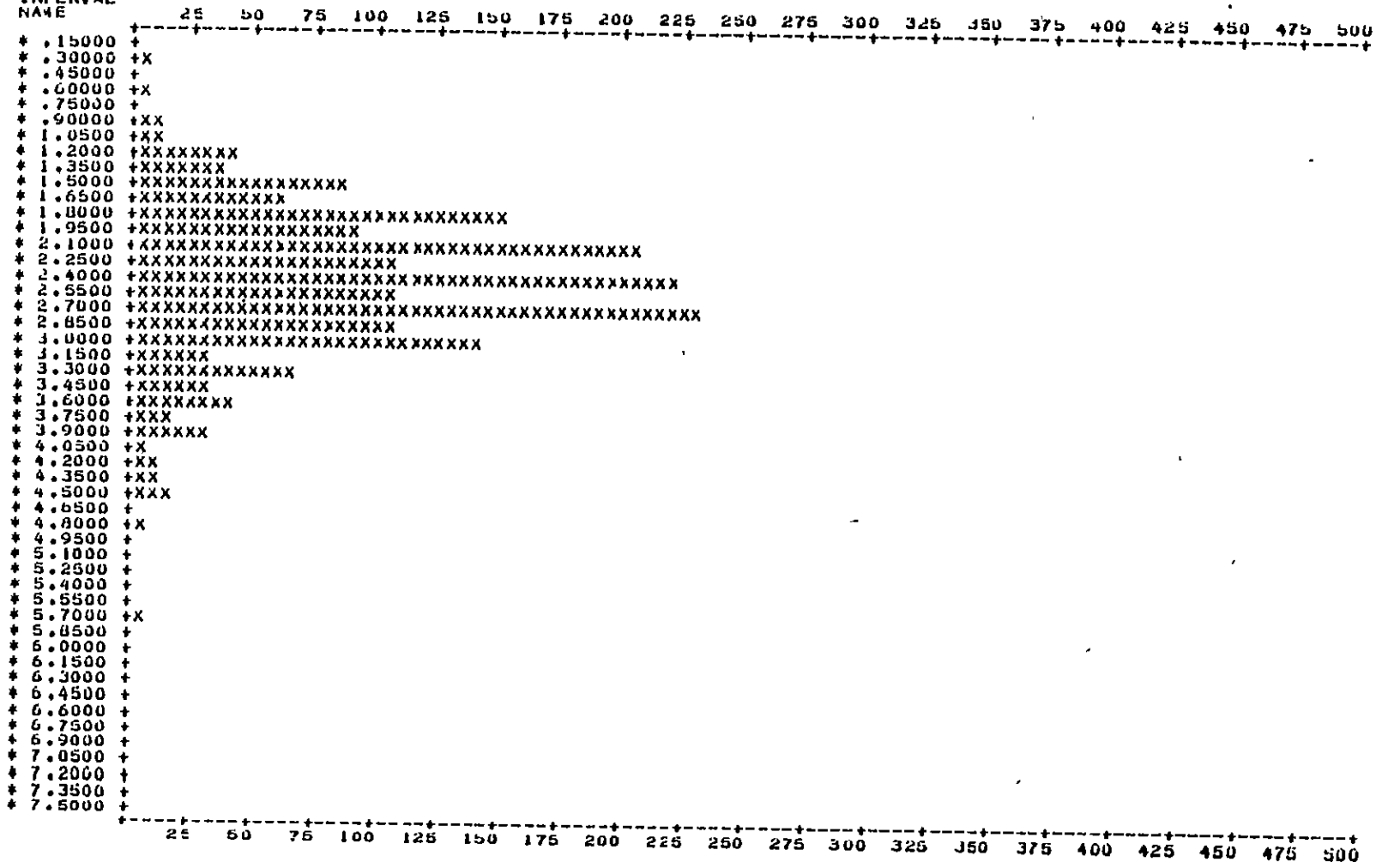

INTERVAL NAME	FREQUENCY INT.	FREQUENCY CUM.	PERCENTAGE INT.	PERCENTAGE CUM.
.15000	0	0	0.0	0.0
.30000	5	5	0.3	0.3
.45000	1	6	0.1	0.3
.60000	4	10	0.2	0.5
.75000	2	12	0.1	0.6
.90000	10	22	0.5	1.2
1.0500	11	33	0.6	1.8
1.2000	42	75	2.2	4.0
1.3500	36	111	1.9	5.9
1.5000	83	194	4.4	10.4
1.6500	58	252	3.1	13.5
1.8000	149	401	8.0	21.5
1.9500	92	493	4.9	26.4
2.1000	204	697	10.9	37.3
2.2500	106	803	5.7	43.0
2.4000	220	1023	11.8	54.8
2.5500	103	1126	5.5	60.3
2.7000	228	1354	12.2	72.5
2.8500	107	1461	5.7	78.2
3.0000	138	1599	7.4	85.6
3.1500	28	1627	1.5	87.1
3.3000	66	1693	3.5	90.6
3.4500	31	1724	1.7	92.3
3.6000	42	1766	2.2	94.5
3.7500	16	1782	0.9	95.4
3.9000	30	1812	1.6	97.0
4.0500	6	1818	0.3	97.3
4.2000	8	1826	0.4	97.8
4.3500	9	1835	0.5	98.2
4.5000	14	1849	0.7	99.0
4.6500	1	1850	0.1	99.0
4.8000	5	1855	0.3	99.3
4.9500	1	1856	0.1	99.4
5.1000	1	1857	0.1	99.4
5.2500	1	1858	0.1	99.5
5.4000	1	1859	0.1	99.5
5.5500	2	1861	0.1	99.6
5.7000	4	1865	0.2	99.8
5.8500	0	1865	0.0	99.8
6.0000	2	1867	0.1	99.9
6.1500	0	1867	0.0	99.9
6.3000	0	1867	0.0	99.9
6.4500	1	1868	0.1	100.0
6.6000	0	1868	0.0	100.0
6.7500	0	1868	0.0	100.0
6.9000	0	1868	0.0	100.0
7.0500	0	1868	0.0	100.0
7.2000	0	1868	0.0	100.0
7.3500	0	1868	0.0	100.0
7.5000	0	1868	0.0	100.0

HISTOGRAM OF VARIABLE 4 ZN

SYMBOL	COUNT	MEAN	ST.DEV.
X	1868	101.264	89.556

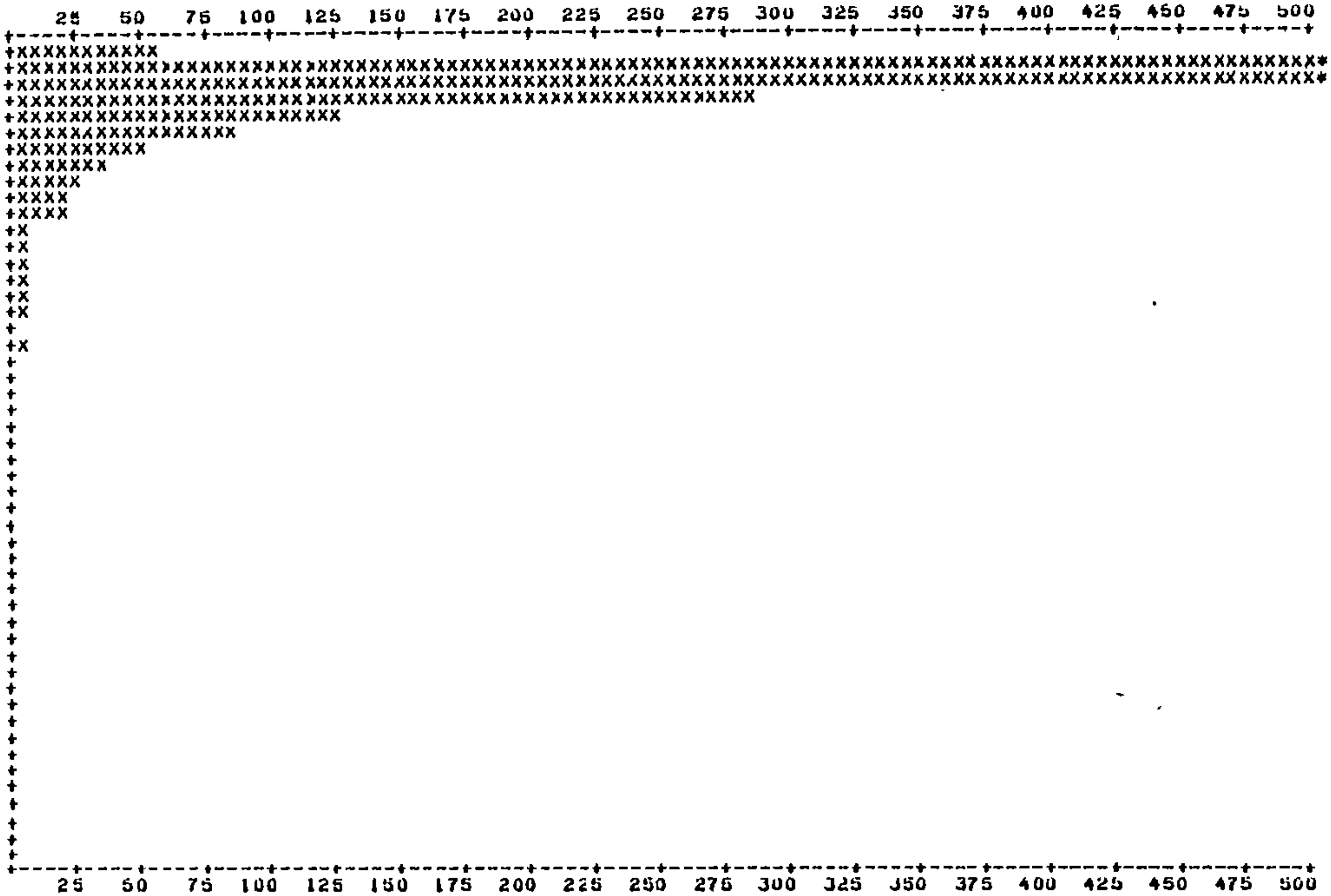

INTERVAL NAME	FREQUENCY INT.	FREQUENCY CUM.	PERCENTAGE INT.	PERCENTAGE CUM.
* 30.000	63	63	2.8	2.8
* 60.000	595	648	31.9	34.7
* 90.000	527	1175	28.2	62.9
* 120.00	283	1458	15.1	78.1
* 150.00	127	1585	6.8	84.9
* 180.00	86	1671	4.6	89.5
* 210.00	51	1722	2.7	92.2
* 240.00	36	1758	1.9	94.1
* 270.00	24	1782	1.3	95.4
* 300.00	21	1803	1.1	96.5
* 330.00	20	1823	1.1	97.6
* 360.00	7	1830	0.4	98.0
* 390.00	7	1837	0.4	98.3
* 420.00	6	1843	0.3	98.7
* 450.00	3	1846	0.2	98.8
* 480.00	4	1850	0.2	99.0
* 510.00	5	1855	0.3	99.3
* 540.00	2	1857	0.1	99.4
* 570.00	4	1861	0.2	99.6
* 600.00	1	1862	0.1	99.7
* 630.00	0	1862	0.0	99.7
* 660.00	2	1864	0.1	99.8
* 690.00	0	1864	0.0	99.8
* 720.00	0	1864	0.0	99.8
* 750.00	0	1864	0.0	99.8
* 780.00	1	1865	0.1	99.8
* 810.00	0	1865	0.0	99.8
* 840.00	0	1865	0.0	99.8
* 870.00	0	1865	0.0	99.8
* 900.00	0	1865	0.0	99.8
* 930.00	0	1865	0.0	99.8
* 960.00	1	1866	0.1	99.9
* 990.00	0	1866	0.0	99.9
* 1020.0	0	1866	0.0	99.9
* 1050.0	0	1866	0.0	99.9
* 1080.0	0	1866	0.0	99.9
* 1110.0	0	1866	0.0	99.9
* 1140.0	1	1867	0.1	99.9
* 1170.0	0	1867	0.0	99.9
* 1200.0	0	1867	0.0	99.9
* 1230.0	0	1867	0.0	99.9
* 1260.0	1	1868	0.1	100.0
* 1290.0	0	1868	0.0	100.0
* 1320.0	0	1868	0.0	100.0
* 1350.0	0	1868	0.0	100.0
* 1380.0	0	1868	0.0	100.0
* 1410.0	0	1868	0.0	100.0
* 1440.0	0	1868	0.0	100.0
* 1470.0	0	1868	0.0	100.0
* 1500.0	0	1868	0.0	100.0

HISTOGRAM OF VARIABLE 5 COND

SYMBOL X COUNT 1487 MEAN 6.068 ST.DEV. 3.268

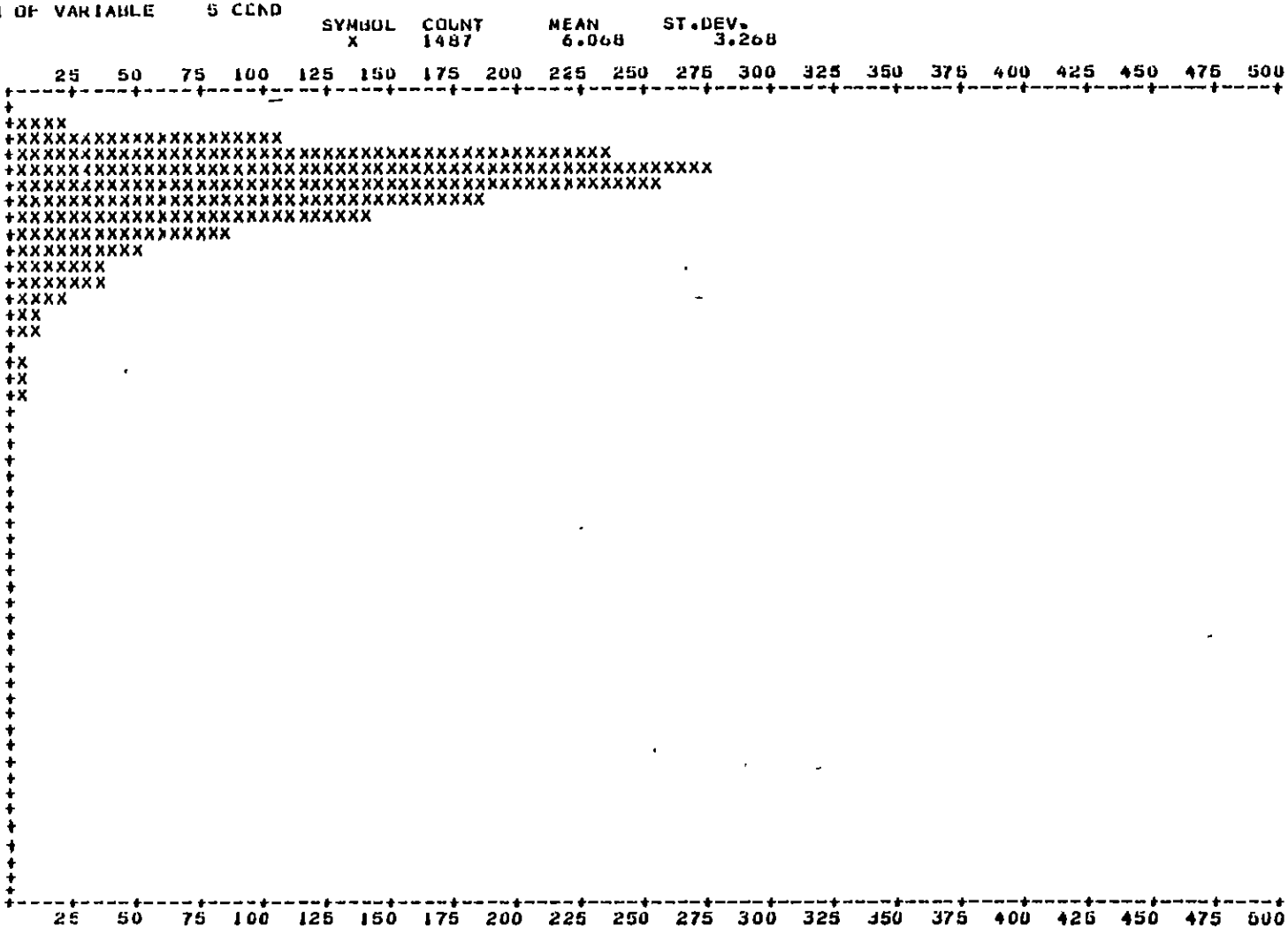

INTERVAL NAME	FREQUENCY INT.	FREQUENCY CUM.	PERCENTAGE INT.	PERCENTAGE CUM.
1.0000	1	1	0.1	0.1
2.0000	22	23	1.5	1.5
3.0000	107	130	7.2	8.7
4.0000	233	363	15.7	24.4
5.0000	274	637	18.4	42.8
6.0000	253	890	17.0	59.9
7.0000	186	1076	12.5	72.4
8.0000	141	1217	9.5	81.8
9.0000	87	1304	5.9	87.7
10.000	50	1354	3.4	91.1
11.000	34	1388	2.3	93.3
12.000	34	1422	2.3	95.6
13.000	22	1444	1.5	97.1
14.000	8	1452	0.5	97.6
15.000	11	1463	0.7	98.4
16.000	2	1465	0.1	98.5
17.000	3	1468	0.2	98.7
18.000	5	1473	0.3	99.1
19.000	5	1478	0.3	99.4
20.000	1	1479	0.1	99.5
21.000	0	1479	0.0	99.5
22.000	1	1480	0.1	99.5
23.000	1	1481	0.1	99.6
24.000	1	1482	0.1	99.7
25.000	1	1483	0.1	99.7
26.000	0	1483	0.0	99.7
27.000	1	1484	0.1	99.8
28.000	1	1485	0.1	99.9
29.000	0	1485	0.0	99.9
30.000	0	1485	0.0	99.9
31.000	1	1486	0.1	99.9
32.000	0	1486	0.0	99.9
33.000	0	1486	0.0	99.9
34.000	0	1486	0.0	99.9
35.000	0	1486	0.0	99.9
36.000	0	1486	0.0	99.9
37.000	0	1486	0.0	99.9
38.000	0	1486	0.0	99.9
39.000	0	1486	0.0	99.9
40.000	0	1486	0.0	99.9
41.000	0	1486	0.0	99.9
42.000	0	1486	0.0	99.9
43.000	0	1486	0.0	99.9
44.000	0	1486	0.0	99.9
45.000	0	1486	0.0	99.9
46.000	0	1486	0.0	99.9
47.000	0	1486	0.0	99.9
48.000	1	1487	0.1	100.0
49.000	0	1487	0.0	100.0
50.000	0	1487	0.0	100.0

HISTOGRAM OF VARIABLE 6 LHC

SYMBOL X COUNT 1868 MEAN 0.850 ST.DEV. 0.502

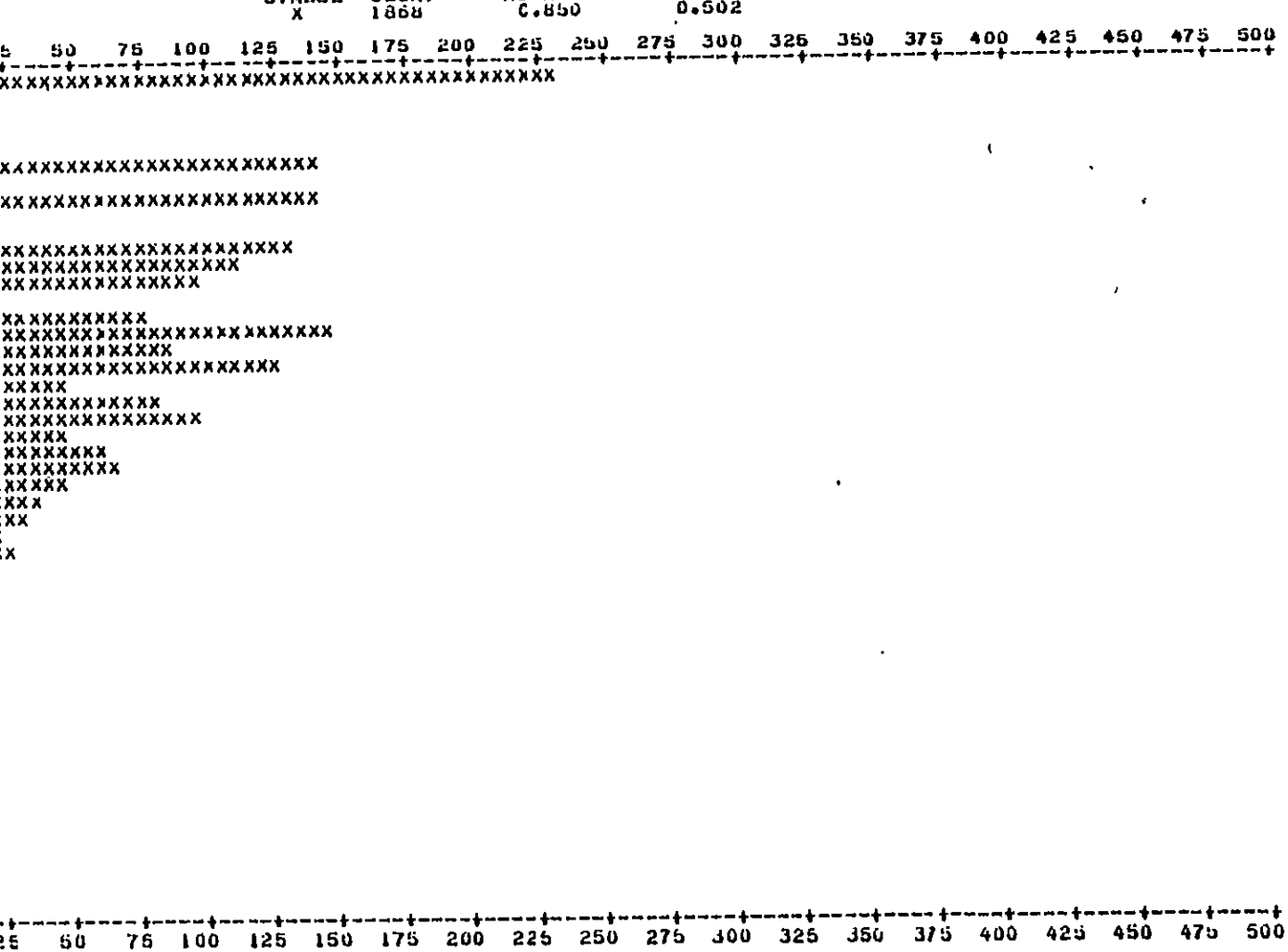

INTERVAL NAME	FREQUENCY INT.	FREQUENCY CUM.	PERCENTAGE INT.	PERCENTAGE CUM.
.06000	232	232	12.4	12.4
.12000	0	232	0.0	12.4
.18000	0	232	0.0	12.4
.24000	0	232	0.0	12.4
.30000	138	370	7.4	19.8
.36000	0	370	0.0	19.8
.42000	138	508	7.4	27.2
.48000	0	508	0.0	27.2
.54000	0	508	0.0	27.2
.60000	132	640	7.1	34.3
.66000	108	748	5.8	40.0
.72000	97	845	5.2	45.2
.78000	0	845	0.0	45.2
.84000	74	919	4.0	49.2
.90000	144	1063	7.7	56.9
.96000	84	1147	4.5	61.4
1.0200	125	1272	6.7	68.1
1.0800	43	1315	2.3	70.4
1.1400	81	1396	4.3	74.7
1.2000	93	1489	5.0	79.7
1.2600	45	1534	2.4	82.1
1.3200	60	1594	3.2	85.3
1.3800	67	1661	3.6	88.9
1.4400	43	1704	2.3	91.2
1.5000	33	1737	1.8	93.0
1.5600	30	1767	1.6	94.6
1.6200	20	1787	1.1	95.7
1.6800	25	1812	1.3	97.0
1.7400	6	1818	0.3	97.3
1.8000	12	1830	0.6	98.0
1.8600	9	1839	0.5	98.4
1.9200	3	1842	0.2	98.6
1.9800	5	1847	0.3	98.9
2.0400	6	1853	0.3	99.2
2.1000	3	1856	0.2	99.4
2.1600	6	1862	0.3	99.7
2.2200	2	1864	0.1	99.8
2.2800	1	1865	0.1	99.8
2.3400	0	1865	0.0	99.8
2.4000	0	1865	0.0	99.8
2.4600	1	1866	0.1	99.9
2.5200	1	1867	0.1	99.9
2.5800	1	1868	0.1	100.0
2.6400	0	1868	0.0	100.0
2.7000	0	1868	0.0	100.0
2.7600	0	1868	0.0	100.0
2.8200	0	1868	0.0	100.0
2.8800	0	1868	0.0	100.0
2.9400	0	1868	0.0	100.0
3.0000				

HISTOGRAM OF VARIABLE 7 LMN

SYMBOL	COUNT	MEAN	ST.DEV.
X	1867	2.507	0.259

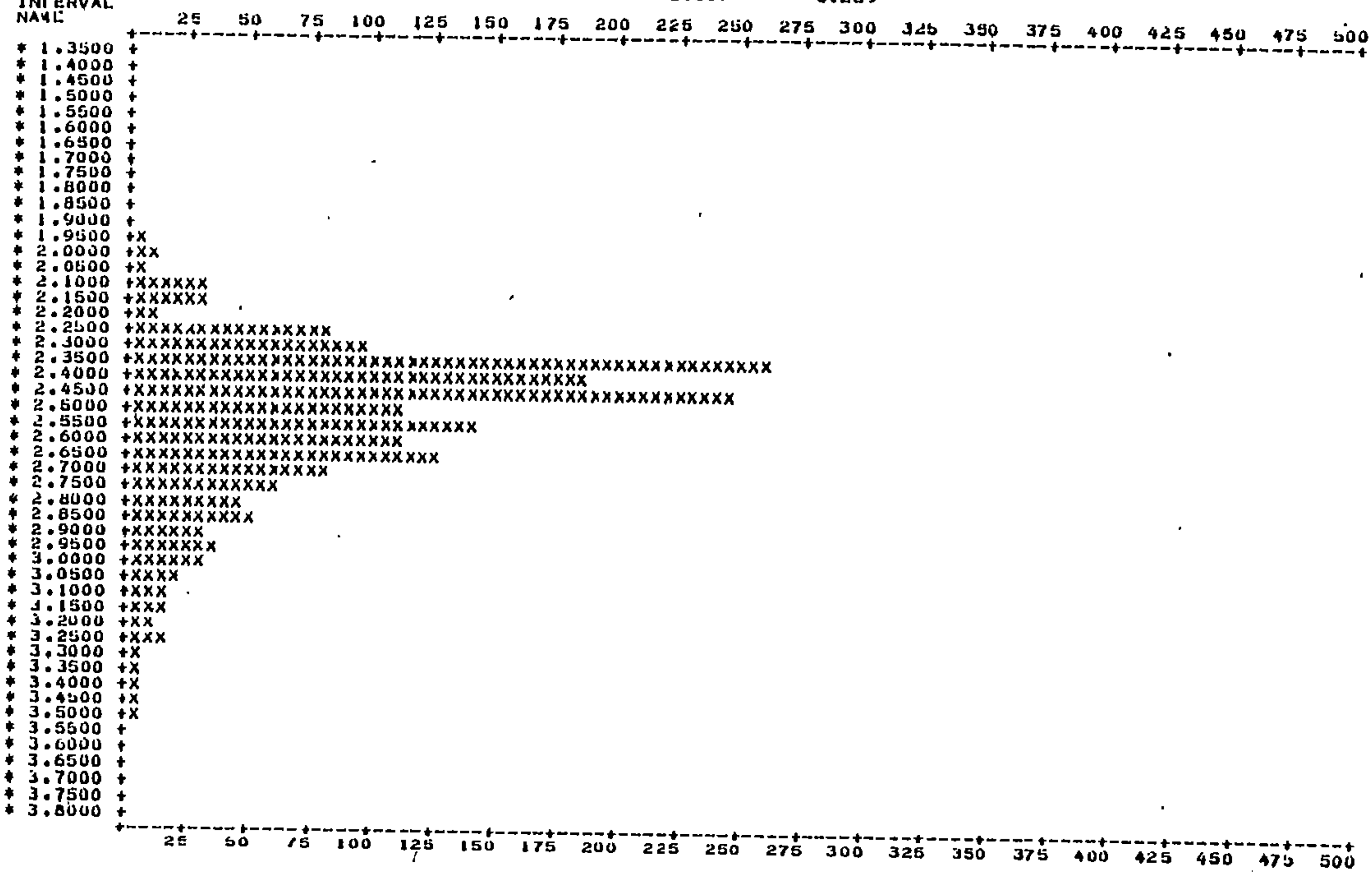

INTERVAL NAME	FREQUENCY INT.	FREQUENCY CUM.	PERCENTAGE INT.	PERCENTAGE CUM.
* 1.3500	0	0	0.0	0.0
* 1.4000	0	0	0.0	0.0
* 1.4500	1	1	0.1	0.1
* 1.5000	0	1	0.0	0.1
* 1.5500	0	1	0.0	0.1
* 1.6000	0	1	0.0	0.1
* 1.6500	0	1	0.0	0.1
* 1.7000	0	1	0.0	0.1
* 1.7500	0	1	0.0	0.1
* 1.8000	1	2	0.1	0.1
* 1.8500	1	3	0.1	0.2
* 1.9000	0	3	0.0	0.2
* 1.9500	4	7	0.2	0.4
* 2.0000	12	19	0.6	1.0
* 2.0500	4	23	0.2	1.2
* 2.1000	32	55	1.7	2.9
* 2.1500	29	84	1.6	4.5
* 2.2000	8	92	0.4	4.9
* 2.2500	82	174	4.4	9.3
* 2.3000	95	269	5.1	14.4
* 2.3500	259	528	13.9	28.3
* 2.4000	183	711	9.8	38.1
* 2.4500	243	954	13.0	51.1
* 2.5000	110	1064	5.9	57.0
* 2.5500	141	1205	7.6	64.5
* 2.6000	109	1314	5.8	70.4
* 2.6500	127	1441	6.8	77.2
* 2.7000	78	1519	4.2	81.4
* 2.7500	59	1578	3.2	84.5
* 2.8000	46	1624	2.5	87.0
* 2.8500	50	1674	2.7	89.7
* 2.9000	31	1705	1.7	91.3
* 2.9500	37	1742	2.0	93.3
* 3.0000	29	1771	1.6	94.9
* 3.0500	21	1792	1.1	96.0
* 3.1000	13	1805	0.7	96.7
* 3.1500	14	1819	0.7	97.4
* 3.2000	10	1829	0.5	98.0
* 3.2500	13	1842	0.7	98.7
* 3.3000	4	1846	0.2	98.9
* 3.3500	4	1850	0.2	99.1
* 3.4000	4	1854	0.2	99.3
* 3.4500	3	1857	0.2	99.5
* 3.5000	7	1864	0.4	99.8
* 3.5500	1	1865	0.1	99.9
* 3.6000	2	1867	0.1	100.0
* 3.6500	0	1867	0.0	100.0
* 3.7000	0	1867	0.0	100.0
* 3.7500	0	1867	0.0	100.0
* 3.8000	0	1867	0.0	100.0

HISTOGRAM OF VARIABLE 8 LFE

SYMBOL X COUNT 1868 MEAN 0.359 ST.DEV. 0.147

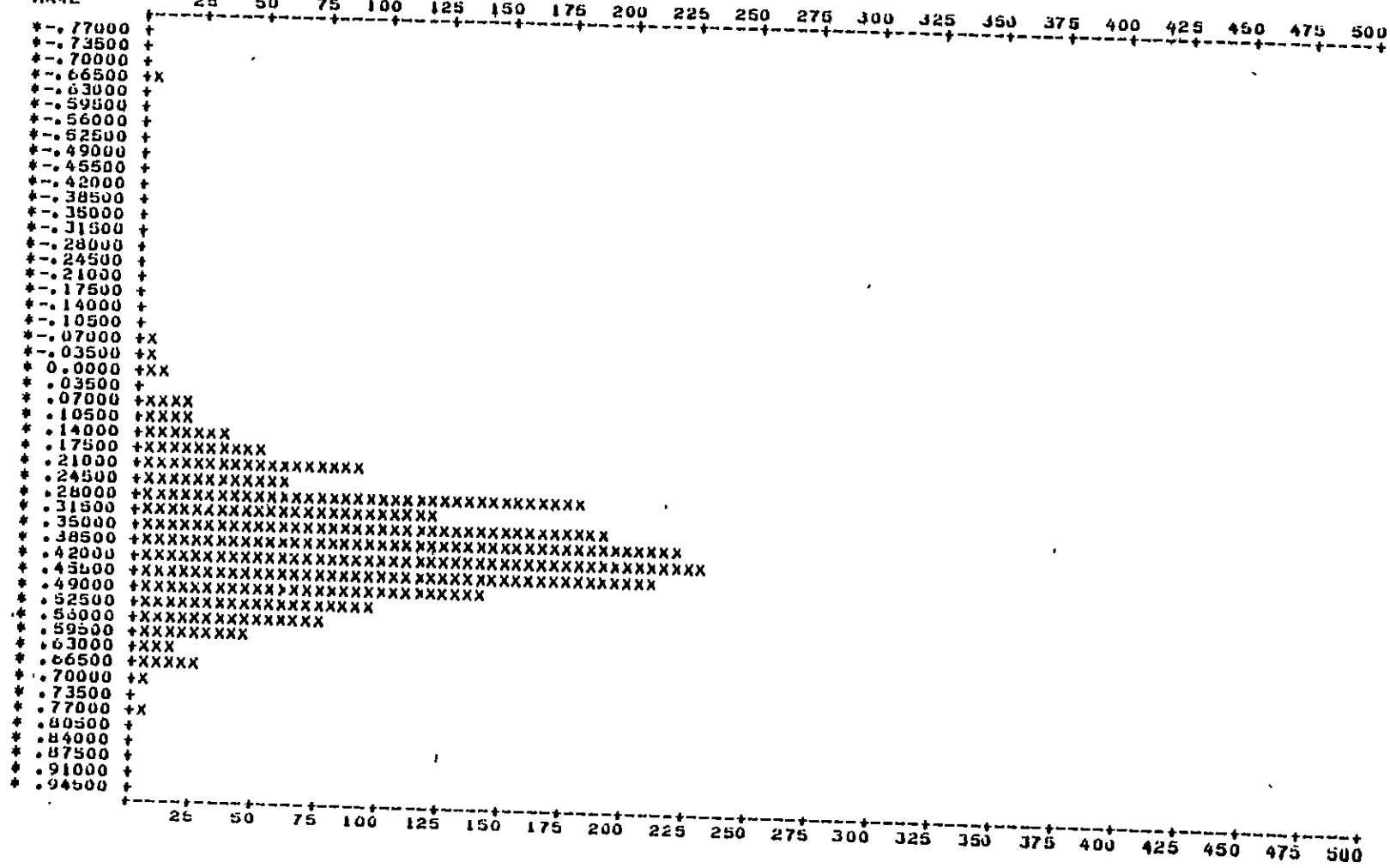

INTERVAL NAME	FREQUENCY INT.	FREQUENCY CUM.	PERCENTAGE INT.	PERCENTAGE CUM.
*-.77000	0	0	0.0	0.0
*-.73500	0	0	0.0	0.0
*-.70000	0	0	0.0	0.0
*-.66500	4	4	0.2	0.2
*-.63000	0	4	0.0	0.2
*-.59500	0	4	0.0	0.2
*-.56000	0	4	0.0	0.2
*-.52500	0	4	0.0	0.2
*-.49000	1	5	0.1	0.3
*-.45500	0	5	0.0	0.3
*-.42000	0	5	0.0	0.3
*-.38500	1	6	0.1	0.4
*-.35000	0	6	0.0	0.4
*-.31500	0	6	0.0	0.4
*-.28000	2	8	0.1	0.4
*-.24500	0	8	0.0	0.4
*-.21000	2	10	0.1	0.5
*-.17500	0	10	0.0	0.5
*-.14000	2	12	0.1	0.6
*-.10500	0	12	0.0	0.6
*-.07000	3	15	0.2	0.8
*-.03500	7	22	0.4	1.2
* 0.0000	11	33	0.6	1.8
* .03500	0	33	0.0	1.8
* .07000	20	53	1.1	2.8
* .10500	22	75	1.2	4.0
* .14000	36	111	1.9	5.9
* .17500	50	161	2.7	8.6
* .21000	91	252	4.9	13.5
* .24500	62	314	3.3	16.8
* .28000	179	493	9.6	26.4
* .31500	121	614	6.5	32.9
* .35000	189	803	10.1	43.0
* .38500	220	1023	11.8	54.8
* .42000	229	1252	12.3	67.0
* .45500	209	1461	11.2	78.2
* .49000	138	1599	7.4	85.6
* .52500	94	1693	5.0	90.6
* .56000	73	1766	3.9	94.5
* .59500	46	1812	2.5	97.0
* .63000	14	1826	0.7	97.8
* .66500	24	1850	1.3	99.0
* .70000	7	1857	0.4	99.4
* .73500	2	1859	0.1	99.5
* .77000	6	1865	0.3	99.8
* .80500	2	1867	0.1	99.9
* .84000	1	1868	0.1	100.0
* .87500	0	1868	0.0	100.0
* .91000	0	1868	0.0	100.0
* .94500	0	1868	0.0	100.0

HISTOGRAM OF VARIABLE 9 LZR

SYMBOL X COUNT 1868 MEAN 1.910 ST.DEV. 0.271

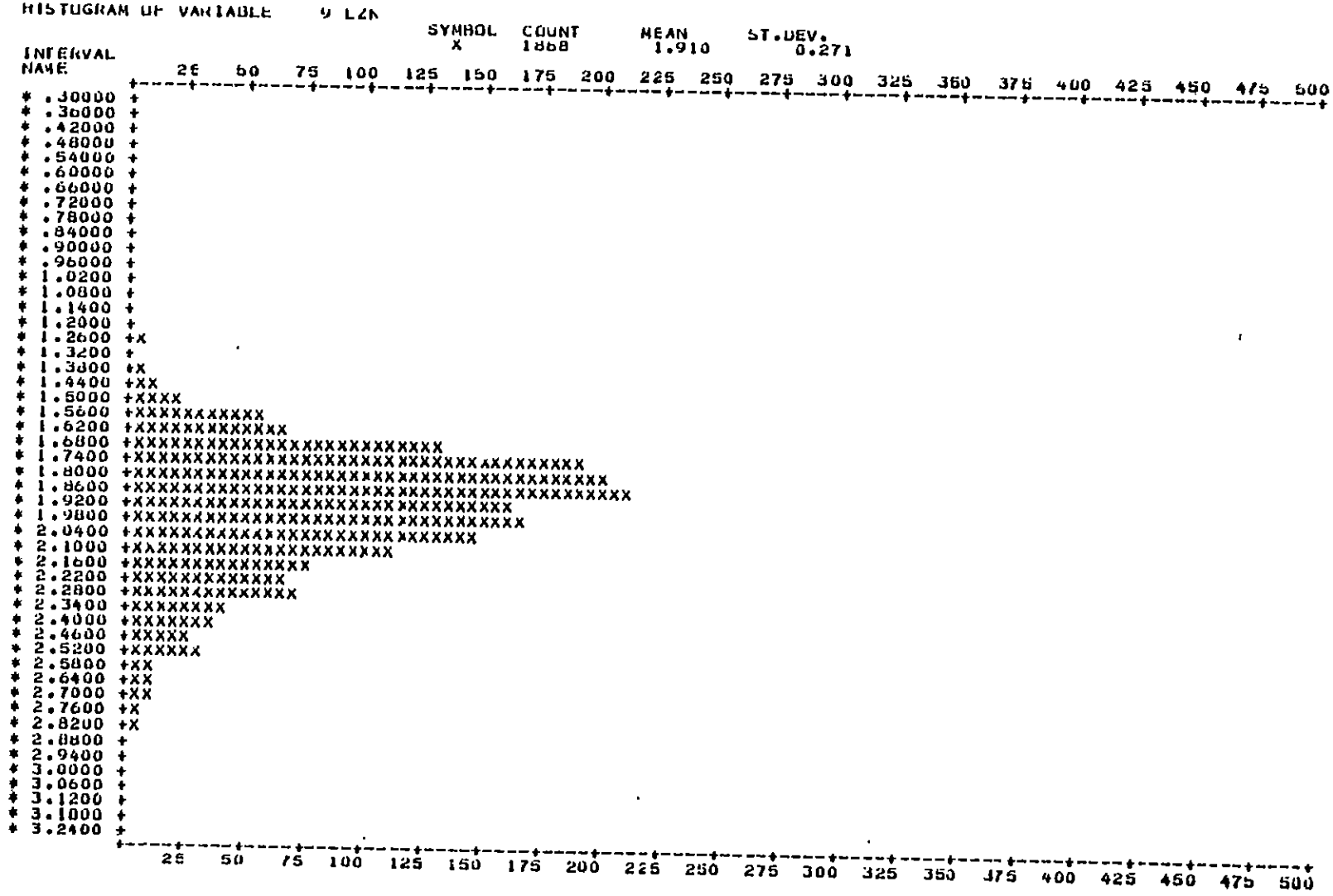

INTERVAL NAME	FREQUENCY INT.	FREQUENCY CUM.	PERCENTAGE INT.	PERCENTAGE CUM.
* .30000	0	0	0.0	0.0
* .36000	2	2	0.1	0.1
* .42000	0	2	0.0	0.1
* .48000	0	2	0.0	0.1
* .54000	0	2	0.0	0.1
* .60000	0	2	0.0	0.1
* .66000	0	2	0.0	0.1
* .72000	0	2	0.0	0.1
* .78000	0	2	0.0	0.1
* .84000	0	2	0.0	0.1
* .90000	0	2	0.0	0.1
* .96000	0	2	0.0	0.1
* 1.0200	1	3	0.1	0.2
* 1.0800	1	4	0.1	0.2
* 1.1400	1	5	0.1	0.3
* 1.2000	0	5	0.0	0.3
* 1.2600	2	7	0.1	0.4
* 1.3200	5	12	0.3	0.6
* 1.3800	2	14	0.1	0.7
* 1.4400	7	21	0.4	1.1
* 1.5000	12	33	0.6	1.8
* 1.5600	20	53	1.1	2.8
* 1.6200	56	109	3.0	5.8
* 1.6800	63	172	3.4	9.2
* 1.7400	131	303	7.0	16.2
* 1.8000	189	492	10.1	26.3
* 1.8600	202	694	10.8	37.2
* 1.9200	211	905	11.3	48.4
* 1.9800	161	1066	8.6	57.1
* 2.0400	163	1229	8.7	65.8
* 2.1000	143	1372	7.7	73.4
* 2.1600	112	1484	6.0	79.4
* 2.2200	75	1559	4.0	83.5
* 2.2800	67	1626	3.6	87.0
* 2.3400	68	1694	3.6	90.7
* 2.4000	38	1732	2.0	92.7
* 2.4600	37	1769	2.0	94.7
* 2.5200	25	1794	1.3	96.0
* 2.5800	29	1823	1.6	97.6
* 2.6400	12	1835	0.6	98.2
* 2.7000	10	1845	0.5	98.8
* 2.7600	10	1855	0.5	99.3
* 2.8200	6	1861	0.3	99.6
* 2.8800	3	1864	0.2	99.8
* 2.9400	0	1864	0.0	99.8
* 3.0000	1	1865	0.1	99.8
* 3.0600	1	1866	0.1	99.9
* 3.1200	1	1867	0.1	99.9
* 3.1800	1	1868	0.1	100.0
* 3.2400	0	1868	0.0	100.0
	0	1868	0.0	100.0

APPENDIX F

STATEMENT OF EXPLORATION EXPENDITURES

Statement of Exploration Expenditures

Geologist (T. Millinoff) 2 days @ $275/diem	$ 550.00
Secretarial	56.00
Drafting Services	78.30
Reproduction	28.60
Air Freight (for sample shipment)	68.70
Telephone	28.40
	$ 810.00

STATEMENT OF QUALIFICATIONS

I, the undersigned, of the City of Calgary in the Province of Alberta, do hereby certify that:

1. I am a consulting geologist with an office at #100, 1300 - 8th St. S.W., Calgary, Alberta;
2. I graduated from the University of Windsor with a B.Sc. in Geology in 1981, and that I have been practising my profession continuously since graduation;
3. I have personally collected and processed the soil samples, and conducted a conductivity survey. This was done under the direction of Dr. A. Turek at the University of Windsor, on behalf of Rockwell Mining Corporation.

Respectfully submitted,

Calgary, Alberta
April 1982

Terri Millinoff

Terri B. Millinoff, B.Sc.

MJM 4

MJM 5

MJM 2

MOLLY 18

MOLLY 17

MOLLY 1

MOLLY 2

MOLLY 3

MOLLY 4

MOLLY 5

MOLLY 6

MOLLY 8

MOLLY 7

MOLLY 10

MOLLY 9

MOLLY 12

MOLLY 11

MOLLY 14

MOLLY 13

MJM 3

MJM 1

DB 4

DB 3

DB 2

DB 1

STREP

STREP 79

NITHI MTN.

"CHRIS" SHOWING

"TERRI" SHOWING

MAP 2 OUTLINE
Scale 1:1000

MAP 3 OUTLINE
Scale 1:1000

54°00'

124°50'

- Road/trench
- Existing access
- Proposed drill sites
- Existing drill sites
- Rock sample sites – Summer program 1980
- Rock sample sites – Winter program 1980

10314

ROCKWELL MINING CORPORATION	
NITHI MOUNTAIN PROPERTY	
NTS 93F/15, 93K/2	MAP 1
PROJECT BC-80-7	ROCK SAMPLE LOCATION MAP
SCALE 1:5,000	50 0 100 200 Meters
TAIGA CONSULTANTS LTD.	

DECEMBER, 1980

N

L15+30W
L14+55W
L14+05W
L13+30W
L10+95W
L9+50W
L7+95W
L7+00W
L0+20E
L1+55E
L3+10E
L4+70E
L6+25E
L7+70E
L9+40E
L10+90E
L12+45E
L13+65E
L15+40E
L16+15E
L16+90E
L17+65E
L19+15E
L19+90E
L20+65E
L21+40E
L22+15E
L22+90E
L23+65E
L24+40E
L25+15E
L25+90E

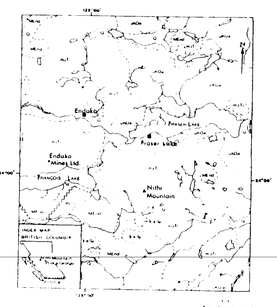

NITHI MOUNTAIN

Nachako Plateau British Columbia
Conductivity Map
Scale 1:5,000 (50 0 100 200 Meters)
Contour Interval 2.0 μmhos⁻¹

Terri Millinoff

10314

ROCKWELL MINING CORPORATION	
NITHI MOUNTAIN PROPERTY	
NTS 93F/15, 93K/2	MAP 2
PROJECT BC-80-7	CONDUCTIVITY MAP
SCALE 1:5,000 (50 0 100 200 Meters)	
TAIGA CONSULTANTS LTD.	